

# Numerical Techniques for Optimising Rail Grinding

Paul Hyde

Submitted for the Degree of Doctor of Philosophy



School of Mechanical and Systems Engineering

September 2011

## **Abstract**

Grinding of rails is a technique widely used within the railway industry to balance the degradation of the condition of the rail with the required performance of the rail. The principal focus of this research is the impact of wear and rolling contact fatigue (RCF) cracks on structural integrity of rails, and how rail grinding affects this relationship.

A numerical model which predicts growth of RCF-initiated cracks in rails has been adapted to take into account periodic grinding of the surface of the rail. The suitability of some of the simplifying assumptions of the adapted model, referred to as the Grinding Model, has been examined with a physical test program, using full scale rail vehicles and track. This test program studied the persistence of the characteristic surface roughness of the rail generated by grinding, and was carried out to determine whether the effect of this roughness on crack growth can be neglected in the Grinding Model.

The Grinding Model has been used to predict crack size, in order to investigate the effect of different grinding strategies, consisting of a depth of grinding applied at a certain interval during a representative pattern of rail vehicle traffic over the rail. The use of the Grinding Model to find grinding strategies which match an optimum criterion has been demonstrated. The applicability of this optimisation technique and the model in its current state of development, to the specification of rail grinding operations, in the context of maximising safe rail life and minimising rail life cycle cost, is discussed.

Dedicated to my family and friends  
in gratitude of their support

## **Acknowledgements**

I gratefully acknowledge the following individuals and organisations for their assistance in this research programme:

- My supervisors, Dr Francis Franklin, Dr. David Fletcher, Prof. Ajay Kapoor, and Prof. Mark Robinson for their guidance.
- NewRail railway research centre, The School of Mechanical and Systems Engineering, Newcastle University, for providing the facilities and resources to conduct this research.
- Engineering and Physical Sciences Research Council for providing funding through a doctoral training account, which was administered through Rail Research UK.
- Barrow Hill Roundhouse Railway Centre for providing the full scale testing facilities.

## Nomenclature

<b>Abbreviation</b>	<b>Description</b>
RCF	Rolling Contact Fatigue
WP	Wheel Pass
GI	Grinding Interval
GD	Grinding Depth
ECWR	Effective Continuous Wear Rate
MGT	Traffic equivalent to one Million Gross Tonnes

### **Roughness**

<b>Parameter</b>	<b>Description</b>
Rz	Average of the peak to trough height range over several sample lengths
Rt	Maximum peak to trough height range over the whole profile
Ra	Arithmetic mean deviation of the assessed profile
Rq	Root-Mean-Square deviation of the assessed profile
Rsk	Skewness (asymmetry) of the assessed profile

<b>Symbol</b>	<b>Description</b>	<b>Unit</b>
$G$	Average Cost of a grinding operation	£/km
$M$	Maximum single pass grinding depth	mm
$R$	Rail Replacement Cost	£/km
$V$	Vertical wear limit of rail	m
$I_i$	Effective grinding interval	WP
$D_i$	Grinding depth	m
$P_i$	Proportion of location type in maintenance section	-
$T$	No. of WP per MGT of the Traffic Pattern	WP/MGT
$W_W$	Effective Continuous Wear Rate	m/WP
$W_T$	Wear per MGT of traffic	m/MGT
$L$	Wear Life of Rail (MGT)	MGT
$C_R$	Replacement Cost/kmMGT of Traffic	£/kmMGT
$I_T$	Grinding Interval in MGT	MGT
$N$	Number of grinding operations over life of rail	-
$O$	Grinding Operation Cost	£/km
$C_G$	Grinding Strategy Cost over life of Rail	£/kmMGT
$C_L$	Rail Life Cost of location type	£/kmMGT
$C_S$	Average Rail Life Cost for Maintenance Section	£/kmMGT
$a$	Constant to fit equation to data	-
$b$	Constant to fit equation to data	-
$c$	Constant to fit equation to data	-
$d$	Constant to fit equation to data	-

<b>Subscript</b>	<b>Description</b>
$i$	Variable denoting location type of parameter
$j$	Variable denoting maintenance section parameter calculated for

<b>Secondary Subscript</b>	<b>Description</b>
$H$	Specific value of subscript $i$ denoting Harringay location type
$S$	Specific value of subscript $i$ denoting Sandy location type

# Contents

Abstract .....	ii
Acknowledgements .....	iv
Nomenclature .....	v
Contents .....	vii
Chapter 1. Introduction .....	1
1.1 Degradation of the Rail Material - Shakedown and Rolling Contact Fatigue ..	2
1.2 Growth of Rolling Contact Fatigue Cracks.....	5
1.3 Vehicle Dynamics - Contact Loads.....	15
1.4 Railway Maintenance - Grinding.....	18
1.5 Scope of the Thesis .....	22
1.6 References .....	25
Chapter 2. Grinding Model Development .....	29
2.1 Grinding Variables .....	29
2.2 Factors affecting grinding specification decision .....	30
2.3 Definition of Crack Size.....	32
2.4 Description of Crack Growth Model.....	32
2.5 Limitations of Crack Growth Model for modelling grinding .....	34
2.6 Grinding Model Development .....	39
Chapter 3. Grinding Roughness Tests .....	46
3.1 Introduction .....	46
3.2 Test Method .....	49
3.2.1 Test site .....	49
Test sample manufacture.....	50
3.2.2.....	50
3.2.3 Installation.....	50
3.2.4 Loading .....	51
3.2.5 Measurement technique .....	53
3.2.6 Test procedure.....	55
3.2.7 Measurement Recording .....	56
3.3 Profile Analysis.....	56
3.3.1 Roughness Parameter Calculation.....	57
3.3.2 Whole Profile Analysis Method.....	58

3.3.3	Selected Section Profile Analysis Method.....	61
3.4	RESULTS .....	64
3.4.1	Whole Profile Roughness Results.....	64
3.4.2	Selected Section Profile Roughness Results.....	66
3.4.3	Summarised Results.....	68
3.5	Discussion.....	75
3.5.1	Scatter.....	75
3.5.2	Location Dependence.....	77
3.5.3	Initial Roughness.....	80
3.5.4	Roughness Trends.....	83
3.5.5	Comparing Test Sample Roughness Trends.....	86
3.6	Conclusions.....	88
3.6.1	Conclusions Made from Test Results.....	88
3.7	Implications of Grinding Roughness Tests for Grinding Model.....	89
3.8	References.....	89
Chapter 4.	Grinding Model Investigation: Optimum Grinding Strategies.....	90
4.1	Introduction to the Grinding Model Case Studies.....	90
4.2	Grinding Model Optimum Grinding Strategy Investigation Method.....	93
4.3	Train Types and Traffic Patterns.....	93
4.4	Wear Rates Determined During Optimum Grinding Variable Investigations.....	94
4.5	Case Study 1: Variable Grinding Interval Investigation.....	96
4.5.1	Variable Grinding Interval Investigation Crack Size Results.....	97
4.5.2	Variable Grinding Interval Investigation Wear Rate Results.....	106
4.5.3	Variable Grinding Interval Investigation Discussion.....	113
4.6	Case Study 2: Variable Grinding Depth Investigation:.....	115
4.6.1	Variable Grinding Depth Investigation Crack Size Results.....	117
4.6.2	Summary of Variable Grinding Depth Investigation Results.....	121
4.6.3	Variable Grinding Depth Investigation Wear Results.....	122
4.6.4	Variable Grinding Depth Investigation Discussion.....	125
4.7	Comparisons Between Case Studies 1 & 2.....	126
4.8	Application of Optimum Grinding Strategies.....	129
Chapter 5.	Grinding Strategy Parameter Error and Sensitivity Analysis.....	131
5.1	Introduction to Grinding Strategy Parameter Error Case Studies.....	131
5.2	Grinding Strategy Parameter Error Results.....	133



5.2.1	Grinding Strategy Parameter Error Conclusions.....	138
Chapter 6.	Trends of Optimum Grinding Strategy Variable Combinations.....	139
6.1	Introduction to Trends of Optimum Grinding Strategy Variable Combinations	
	139	
6.2	Trends of Optimum Grinding Strategy Combinations Results.....	142
6.3	Fitting an Equation to the Trends of Optimum Grinding Strategy Variable	
	Combinations .....	144
6.4	Trends of Effective Continuous Wear Rate Relating to the Trends of	
	Optimum Grinding Strategy Variable Combinations .....	148
6.4.1	Effective Continuous Wear Rate Relating to Optimum Grinding Strategy	
	Variable Combinations.....	148
6.4.2	Fitting an Equation to Trends of Effective Continuous Wear Rate Relating	
	to Trends of Optimum Grinding Strategy Variable Combinations.....	150
6.5	Using the Trends of Optimum Grinding Strategy Variable Combinations to	
	Determine Grinding Strategies to Apply to a Maintenance Section .....	153
6.5.1	Example Maintenance Sections A and B.....	154
6.5.2	Determining the Most Suitable Grinding Strategy Combinations for the	
	Example Maintenance Sections Considered in Isolation.....	155
6.5.3	Determining the Most Suitable Grinding Strategy Combinations for	
	Maintenance Sections within a Wider Network.....	162
6.6	References .....	165
Chapter 7.	Estimating Grinding Strategy Effect on Rail Life Cost.....	166
7.1	Method of Estimating Effect of Grinding Strategies on Rail Life Cost.....	166
7.1.1	Definition of the Parameters for Estimating the Effect of Grinding	
	Strategies on Rail Life Cost .....	167
7.1.2	Calculation of Rail Replacement Cost of a Kilometre of Rail for Each	
	Million Gross Tonnes of Traffic Carried .....	169
7.1.3	Calculation of the Cost of Grinding Each Kilometre of Rail for Each	
	Million Gross Tonnes of Traffic Carried .....	170
7.1.4	Calculation of the Rail Life Cost for Individual Locations and Maintenance	
	Sections .....	172
7.2	Rail Life Cost Estimates for Example Grinding Strategies .....	173
7.3	Rail Life Cost Estimate Results for Example Grinding Strategies .....	175
7.4	Rail Life Cost Trends .....	175

7.5	Determining the Most Suitable Grinding Strategy Combinations to Apply from the Estimated Rail Life Cost Results.....	182
7.6	Summary of the Use of Estimations of Rail Life Cost for Specifying Grinding Strategies .....	186
7.7	References .....	187
Chapter 8.	Comparing Grinding Model Predictions and Rail Life Cost Estimates with UK Railway Network Practice.....	188
8.1	Introduction to the Comparison of the Grinding Model Predictions and Rail Life Cost Estimates with UK Railway Network Practice. ....	188
8.1.1	Current UK Rail Grinding Policy for Rolling Contact Fatigue Damage Management.....	188
8.2	Comparison of UK Rail Grinding Policy with the Variable Grinding Interval Investigation Results .....	189
8.3	Comparison of UK Rail Grinding Policy and Grinding Strategies Suggested from the Trends of Optimum Grinding Strategy Variable Combination Results .....	191
8.4	Comparison of Cost Estimates for UK Rail Grinding Policy and Grinding Strategies Suggested from Modelling .....	196
8.5	References .....	201
Chapter 9.	Conclusions and Further Work .....	202
9.1	Conclusions from the Initial Stages of Developing the Grinding Model and Investigating the Effects of Different Grinding strategies on Crack Growth .....	202
9.2	Conclusions from the Trends of Optimum Grinding Strategy Variable Combinations .....	204
9.3	Conclusions from the Rail life Cost.....	206
9.4	Conclusions Derived from the Comparison of Grinding Strategies Developed using the Grinding Model and those of the UK Network Policy.....	207
9.5	Conclusions Regarding the Suitability of the Grinding Model for Investigating Effects of Rail Grinding on Crack Growth and Specification of Railway Network Grinding Strategies.....	208
9.6	Further Work.....	209
9.6.1	Investigations with the Grinding Model .....	209
9.6.2	Further Development of the Grinding Model .....	211
9.6.3	Further Grinding Roughness Testing.....	212
Appendix A.	Rail Life Cost Estimate Calculation.....	213

Appendix B.	Proposed Modifications to Grinding Roughness Test Procedure .....	214
B.1	Introduction to Proposed Modifications to Grinding Roughness Test Procedure.....	214
B.2	Proposed Modifications to Test Procedure .....	214
B.3	Proposed Test samples Specifications .....	217
B.4	Proposed Roughness Measurement Procedure Modifications.....	219
B.5	Issues Affecting Implementation of Modified Grinding Roughness Test Procedure.....	220

## **Chapter 1. Introduction**

Railways enable heavy loads and high speed vehicles to travel efficiently by distributing the mass of the vehicles and their contents over a relatively large ground area through a system of, typically, steel wheels running on two parallel steel rails, which not only provides the support but also the guidance of the vehicles. The loads that can be supported, without significant bulk deformation, by the contact between a steel wheel and rail are much greater than between a solid or pneumatic wheel and most types of ground surface, such as earth, gravel, tarmac, or concrete, for a given contact area. Due to the low levels of deformation at the contact the rolling resistances of the rail vehicle can be much lower than road vehicles, requiring less energy to be expended in moving the load. The strength of the steel rail enables the loads from the rail vehicle to be supported and distributed over the rail supporting structure. The supporting structure, as well as distributing the load over the ground, also serves the purpose of maintaining the correct separation between the rails.

The low levels of deformation at the contact patch between the wheel and the rail which contributes to the efficiency of the system results in the contact patch being small in comparison, for example, to the contact patch resulting from a pneumatic tire deforming to match a road surface at the contact patch. This, coupled with the high loads typically transmitted through the contact, leads to high stresses at the contact patch to which the rails are resilient. However, the repeated application of these high contact stresses by wheels over many thousands and millions of cycles leads to the degradation of both the wheel and the rail, although it is the rail which is of primary concern in this work. There are various mechanisms and types of degradation of the wheel-rail contact system, which require maintenance to be carried out on the wheel and rail to keep the system within operating limits. Failure to maintain the wheel and rail effectively, for the operating conditions concerned, can lead to sub-standard performance of the system, the failure of components, or the requirement to replace the components prematurely to avoid failure. The repeated cyclic loading of the rail causes damage to the material at the contacting surface; this leads to two main types of degradation of the rail, the wearing away of the rail and the formation of cracks in the rail. The wear alters the shape of the rail; this can develop to the extent that the rail does not guide the vehicle effectively, and the cracking can potentially threaten the structural integrity of the rail,

preventing it from carrying the loads transmitted from the vehicle. Both of these types of degradation of the rail can be treated by maintenance processes which include grinding the rail to give the contact surface of the rail the required shape, and to remove the damaged material which can lead to cracks and the cracks themselves.

The significant operational mechanisms of degradation of the rail, and the numerical techniques used to represent them, are introduced in the following subsections, as are the maintenance techniques employed to mitigate their effects. The properties, behaviour and management of the wheel-rail contact are complex issues with many interrelated and peripheral factors. This introduction is limited to dealing with the principal factors affecting the behaviour and modelling of the wheel-rail contact, the effect of repeated contact cycles on the rail, and the maintenance of the rail, which is the focus of this work. There is also particular focus on the principles and modelling of the particular wheel-rail contact related issues which have been applied to the study of specific locations in previous projects. The results of which were available to be applied in the work described in this thesis to enable the effects of grinding on the degradation mechanisms to be studied.

### **1.1 Degradation of the Rail Material - Shakedown and Rolling Contact Fatigue**

The high strength of the steel rails and wheel allows large loads to be carried with low resistance due to low levels of bulk deformation at each contact. However, the low levels of deformation results in the contact patch being very small compared to that of a pneumatic tire deforming to match a road surface; this, coupled with the high loads typically transmitted through the contact, leads to extremely high contact pressures. Where the normal and shear stresses within the contact remain within the elastic limits of the material, it is able to carry loads without permanent localised deformation at the contact, and repeated contacts have little effect. If the contact pressure is greater than this, and the elastic limits of the material involved in the rolling contact are exceeded then the "elastic shakedown limit" of the material is said to have been exceeded and a process known as "shakedown" commences. In this process, the first contact at which the shakedown limit is exceeded causes the material to deform plastically and start to flow. At the boundary between the plastically deformed material and the material which hasn't exceeded its elastic limits, the layer that has plastically flowed prevents the

neighbouring material from returning to its original shape, resulting in residual stress within the material after the contact is unloaded. These residual stresses reduce the tendency for the material where the stresses exceed the elastic limits to flow in subsequent contacts. Provided there is sufficient material away from the contact where the elastic limits are not exceeded, then after a number of contacts a steady state condition will develop with a layer of plastically deformed material supported by the surrounding material with residual stresses. This state is steady in that repeated contacts which would exceed the elastic limits of the original material by the same amount do not cause further material to flow plastically; this state persists until the conditions change, either by the removal of material from the surface by wear or flow away from the contact, or an increase in the contact stresses. The development of these protective residual stresses coupled with the strain hardening of the plastically deformed material enables the material to support much higher loads than the elastic limit of the material.

The plastic flow of material at locations where the 'shakedown limit' is exceeded does not cease with the establishment of residual stresses in the material to contain the extent of material undergoing plastic flow. Repeated contacts cause further plastic flow and the material accumulates strain; where this strain is unidirectional the process is known as ratchetting. The unidirectional strain accumulates until ductility of the material is exhausted and it loses integrity and fails. This ratchetting failure of the material does not occur uniformly, it occurs at different locations within the highly strained region at any given point in the degradation process. The exact point of failure is related to the material property variations within the microstructure material. This process of ratchetting failure is described more fully by Kapoor and Franklin et al [1.1, 1.2].

The ratchetting process of strain accumulation leading to ductility exhaustion and material failure, can lead to the removal of material from the surface of the rail as wear debris, or areas of failed material which remain in the rail can form initiation sites for micro cracks. These micro cracks can propagate by the action of the contact loads either towards the surface, in which case the failed material and isolated un-failed material detaches as wear, or into the rail, potentially beyond the highly strained material into the rest of the rail. The micro-cracks can be removed by the wearing away of the adjacent material through which they propagate; additionally the cracks can also be effectively extended by the continued strain of the adjacent material. That is, even if the crack tip

does not propagate into un-cracked material, the faces of the crack can grow longer through the straining of the material.

A computer model of this process, the "Dynarat" model, has been developed by Franklin et al [1.3] which can predict the wear rate and the depth of initiating cracks. This model has been developed to take into account the 3D nature of the contact and the different strain rates of the different elements within the microstructure of the rail steel. The scale of the elements of material used in this model can be varied, however the elements used to produce the wear rates predictions used in this work had sides of one micron. This model has also been used by Vasic et al [1.4] to predict the effect of different traffic patterns on the initiation of cracks at the locations studied in this thesis. However in the work of Vasic et al there is only one case where the representation of the pattern and types of vehicles making up the traffic which passes over the rail, is similar to the traffic pattern represented in the work described in this thesis. This case is that in which the traffic represented in the modelling consists solely of a single type of high speed train.

This process of crack initiation is termed Rolling Contact Fatigue (RCF) and hence cracks initiated in this manner are referred to as Rolling Contact Fatigue Cracks. On a scale of thousands of contact cycles, the rate at which the material wears from the surface is in competition with the rate at which any initiated RCF cracks tend to propagate into the rail. Whether RCF cracks develop beyond the initial micro-crack size is determined by whether the crack growth rate is higher than the wear rate. Some rail systems are designed to operate with contact conditions below the shakedown limit, and this design philosophy can be of benefit in reducing the severity, rate and chances of RCF crack formation. However, in practice plastic ratchetting is found to occur even in such systems, and RCF cracking does still occur in certain instances. This was investigated by Franklin et al [1.5], and it was found that whilst the predictions of the stresses within the contact material derived from Hertzian models would be expected to be within the elastic limit of the material, the surface roughness of the contacts results in the pressures below the asperities of the contact exceeding the shakedown limit and leading to plastic flow.

As well as in the wheel and rail, RCF occurs in other analogous situations, such as in roller bearings; this work is principally concerned with the effects of repeated loading of the rail by the wheel and its effect on the structure of the rail.

## **1.2 Growth of Rolling Contact Fatigue Cracks**

Having introduced the theory and modelling of the initiation of Rolling Contact Fatigue Cracks, consideration is now given to how these cracks can propagate to threaten the integrity of the rail. The region in the rail at which the contact load conditions result in stresses in excess of the shakedown limit, and hence the highly strained region where ductility exhaustion damage can occur, is typically limited to the material within the first couple of millimetres of the contacting surface. Therefore the ratchetting failure mechanism cannot cause cracks to develop deep into the rail material by itself. The modelling of RCF cracks in rails up to failure is represented by three mechanisms which are dominant for different sizes of the crack, and hence the modelling is divided into three phases where each mechanism is primarily responsible for the total crack growth rate. The first phase is the crack initiation phase and initial growth which is determined by the ratchetting mechanism, in the second phase the crack growth is driven by the wheel contact stress, and in the third phase crack growth is driven by rail bending. Fletcher et al [1.6] introduce and illustrate the division of the crack growth phases, and proceed to discuss the modelling of the third phase in more detail. Figure 1.1, which is reproduced from [1.6], illustrates schematically the relationship between the rate of crack growth predicted for each of the mechanisms which dominate during each of the crack growth phases. It is not proposed to go into more detail regarding the third phase of crack growth modelling here, other than to state that this crack growth mechanism starts to become significant in the overall crack growth rate when length of the crack reaches the size of around 10mm. When the crack exceeds this size, the risk that the bending of the rail under the action of wheel contacts interacting with the rail support system will propagate the crack rapidly to threaten the integrity of the rail becomes significant, and this is a condition which should be avoided when maintaining a rail.



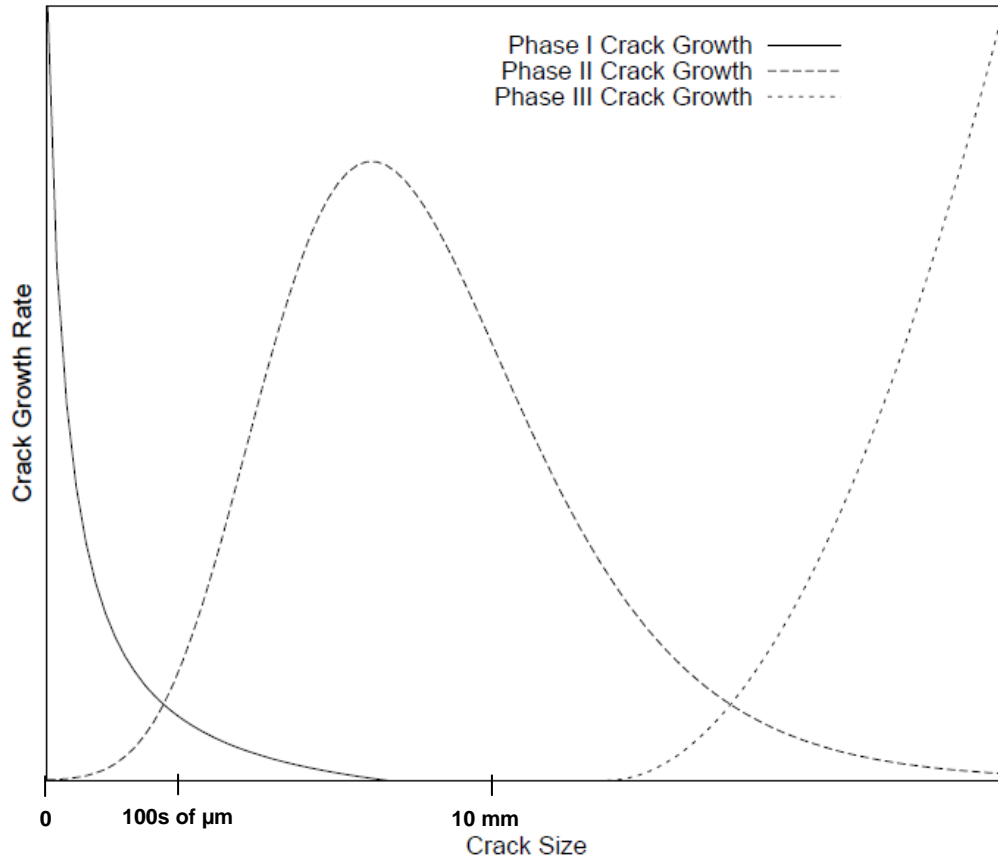


Figure 1.1: Sketch of crack growth rate versus crack size curves for the crack growth mechanisms which operate during Rolling Contact Fatigue crack growth. Phase I Crack Growth is driven by ratchetting and failure through ductility exhaustion. Phase II Crack Growth is shear mode crack growth driven by contact stresses. Phase III Crack Growth is driven by bending stresses.

The curves of crack growth versus crack size in Figure 1.1 represent the crack growth rate predicted for each mechanism operating in isolation. The crack growth rate curves for each mechanism would be affected by various factors such as the wheel loads, contact conditions, operating conditions and other factors. The combination of these factors might affect the crack size at which each crack growth mechanism is predicted to be the dominant mechanism, and hence the crack size at which the transition between the phases of crack growth takes place. However whilst these factors might affect the crack size at which the transition between the phases of crack growth takes place, the same general relationship between the curves would be expected for all commonly occurring conditions within the context of conventional railway operations. The crack growth rate curves produced by certain combinations of factors could lead to the situation where the crack growth rate at the transition between Phases I and II is such that the rate at which the crack tip is advancing into the material is less than the rate at

which the wear process is reducing the crack size. This situation would prevent the crack developing to a size at which Phase II crack growth could begin, therefore the crack would remain stable at a small size unless the conditions changed. Examples of the factors which could affect the precise values of the crack growth rate curves for each mechanism, but not the general trend, include:

- Vehicles of different weights affecting the wheel load.
- The geometry of the track formation affecting, the suspension characteristics of the vehicle and the speed of the vehicles altering the wheel load and contact location, and therefore affecting the contact conditions.
- Different wheel and rail profiles altering the contact conditions.
- Different weather conditions altering the level of adhesion at the wheel rail contact as well as temperature variations affecting the tensile stress in the rail.

In order for a crack to continue to grow to a size which threatens the integrity of the rail the crack growth curves for each mechanism must overlap, as occurs in Figure 1.1, indicating that more than one mechanism can drive crack growth at certain crack lengths. The approach to modelling the growth of a crack of any particular size which has been adopted is to apply the crack growth mechanism which has the highest crack growth rate, and can be considered to dominate the growing of the crack. This approach is considered suitable for the modelling of rolling contact fatigue initiated cracks in rails subject to the crack growth mechanisms described above, as each of the crack growth mechanisms has a discrete range of crack size over which they have a significantly higher crack growth rate than the others and can be considered dominant. Also the transition between which mechanism is dominant (i.e. the transition between phases of crack growth) occurs when the crack growth rates of both mechanisms are at the lower ends of their range. The approach of only considering the crack growth due to the dominant mechanism is particularly suitable for the work which is presented later in this thesis, since the initial size of the cracks which are of primary interest are in the range of crack sizes where the crack growth rate of the mechanisms associated with Phase II of crack growth is much greater than that of the other mechanisms (i.e. considered dominant). Therefore this approach was considered appropriate so long as it was applied with an appreciation of the changing significance of the effects of the other crack

growth mechanisms as the crack size changed according to the predictions of a crack subject to the mechanism which dominates Phase II of crack growth.

It is the second phase of crack growth mentioned above which is of principal concern in this work; in this phase the crack growth is driven by the contact stresses, the levels of which are both within and in excess of the elastic limit of the material. The mechanism by which the initial crack is grown to larger sizes in the second phase is by the normal and longitudinal traction loads on the rail surface driving coplanar shear crack growth. This mechanism of crack growth is thought to dominate for a range of crack sizes. The start point of the range being the size at which the crack is at a depth where the failure of material due to ratchetting is unlikely, the mechanism associated with Phase I being unable to drive crack growth beyond a few hundred microns below the surface. The end of the range is when the crack size is a few tens of millimetres, this is where the crack is getting too far from the contact to grow rapidly, however this size of crack is where it is getting deep enough for propagation by rail bending to become dominant. The cracks which initiate in the first phase tend to occur between the sheared planes of the deformed material and hence typically form at an angle of about 30 degrees below the surface. This roughly coincides with the plane of maximum shear stress that occurs during the stress cycle generated by the passage of the wheel, this stress cycle in the area below the contact predominantly consists of compressive and shear stresses. The work of Bold and Brown [1.7cXX] investigated the problem of using fracture mechanics to predicting crack growth rate under these stress regimes associated with the rolling contact between the wheel and rail. It had previously been observed that the stress system throughout a contact did not appear to contain a cycle of tensile stresses sufficient to drive the observed growth of RCF cracks. However alternating shear stress could be found that appeared to be sufficient to cause crack growth, but reproducing cracks, the growth of which was controlled by shear stresses, in order to obtain the crack growth rate proved difficult. Bold and Brown found that the then conventional assumption that cracks grow perpendicular to the maximum tangential stress did not apply in the case of RCF cracks in rails, the cracks were found to be growing in the plane of maximum shear stress. They succeeded in reproducing stress conditions representative of rolling contact in samples of rail steel, this allowed them to grow cracks representative of RCF cracks in rails and apply fracture mechanics to the prediction of the growth of cracks under these loading conditions.

In integral part of using the crack growth law applicable to RCF cracks developed by Bold and Brown to convert the stress intensity factors into a crack growth rate, is the calculation of the stress intensity factors. The method used to calculate the stress intensity factors for the crack is that method developed by Fletcher et al [1.8 & 1.9], this method is a Green's function based approach it allows the contact loads to be converted into stress intensity factors for the types of crack and loading conditions representative of RCF cracks below the wheel-rail contact. Although the model is of coplanar shear mode crack growth, both shear mode (Mode II) and crack opening mode (Mode I) of crack growth play a part in growth of cracks. Separate Green's functions to convert the stresses in the rail due to the contact into Mode I and Mode II stress intensity are required to take account of the forces normal and tangential to the crack faces. The use of Green's functions provides a means to sum up the Mode I and Mode II stress intensity factors throughout the stress cycle of a wheel contact passing into an equivalent stress intensity factor, it is this equivalent stress intensity factor that is applied to the crack growth law developed by Bold and Brown to predict the crack growth rate. This method of determining the stress intensity factor is rapid, as the distribution of stresses in the rail as a wheel contact passes only has to be calculated once (for each set of contact conditions) these calculations are carried out as if the crack is not present. The Greens function uses the stresses calculated for the uncracked rail at the location where the crack lies, which it treats as a series of point forces along the crack face, to find and combine the stress intensity factors for Modes I and II into an equivalent stress intensity factor. The stresses in the uncracked rail used to calculate the crack growth rate data used in the work described here, were generated using conventional finite element modelling techniques.

In summary the method of predicting the coplanar shear crack growth rates relevant to this work was:

1. Calculate the contact forces using vehicle dynamics (this is discussed in the next section).
2. Calculate the stress distribution in the rail bellow a passing wheel contact using finite element techniques
3. Use a Green's function based method to calculate an equivalent stress intensity factor for a crack of a certain size.

4. Apply the equivalent stress intensity factor to the crack growth law developed by Bold and Brown to obtain the crack growth rate prediction.

This process of generating crack growth rate data for RCF cracks, that is, the calculation of crack growth rates for a series of crack lengths for several the contact conditions (combinations of vehicles and track locations) had been carried out by a project team in previous work, to that described here, the development of the process extends beyond that project to the initial work by Brown and Bold. This previous work, further details of the process, its development and the conditions for which the crack growth data applied in the work described in this thesis can be found in the relevant sections of the appendix of the report on that project [1.10]. This report includes details of the combination of crack growth and wear modelling for each contact cycle to, predict the overall effect on the crack for each contact cycle. It also details a study of the minimum initial crack size which would have to be generated by the first phase of crack initiation and growth, in competition with wear, for the cracks to be predicted to grow by the second phase mechanisms.

During all three phases of crack growth, the wear process is removing material from the surface of the rail, effectively shortening the length of the crack, if at any point the combined crack growth rate of the three mechanisms is less than the wear rate then the crack will reach a stable length or reduce in length and not propagate further. Therefore if, for a certain set of conditions, the crack growth rate of either the first or second mechanism reduces as the crack grows to a value which is less than the rate at which the crack length is being reduced by wear, before the crack is long enough for the crack growth mechanism of the subsequent phase to grow it, then the crack will reach a stable size and not propagate further unless there is a change of conditions.

Many of the papers reviewed and the work described therein (including those pertaining to the development of the Crack Growth Model used to represent shear mode crack growth), concern not only the initiation and growth of RCF cracks with respect to the loads at the contact the geometry of the contact, but also the effect on the development of RCF cracks, of the coefficient of friction at the wheel-rail contact and between the faces of the crack. For a rail in service the coefficients of friction can alter gradually as the wheel, rail and crack surfaces develop, and they can alter abruptly due to a change in

conditions, such as the presence of a contaminant in the contact, most commonly water from the environment. Changes in the friction within the wheel-rail contact can affect the development of RCF cracks in two principal ways, it can alter the traction forces transmitted through the contact and the dynamic behaviour of the vehicles. Both of these effects of variation in the friction at the wheel-rail contact can affect the loads transmitted to the rail which drive RCF damage and hence can affect the development of RCF cracks. In the work described here the wheel-rail contact friction is taken into account when determining the contact loads using vehicle dynamics modelling, as described in the next section. A good summary discussion of the theories concerning the effect of crack face friction is included in the work by Fletcher et al [1.6] in which tests were conducted to prove that fluid does penetrate the RCF cracks in the tests, and describes models developed to take fluid (and its effect on crack face friction) into account when predicting RCF crack growth rates. A Crack Face Friction parameter is included in the calculation of contact driven shear mode crack growth, to take account of the presence of fluid in the crack. The treatment of stresses as point forces along the crack face in the Green's functions allows the regions where the crack faces are sliding relative to each other or the friction locks the faces, restricting crack growth, to be determined. The crack face friction is set at 0.18 throughout the work presented here.

The behaviour of cracks is different in different materials and hence specific crack growth laws for each material are required to predict the crack growth accurately. The crack growth law used here was determined from laboratory crack growth studies using material, pearlitic rail steel, and loading conditions representative of those of a rail undergoing rolling contact. Therefore the predictions of coplanar shear crack growth should be suitable for rail steel. The strain accumulation and hardening that accumulates during the ratchetting process would affect the crack growth behaviour of the material. However the most significant alteration of the material properties by repeated rolling contacts is limited to the surface region immediately involved in the contact and the crack modelled is growing away from this area. Therefore it is considered suitable to use crack growth law determined for pearlitic rail steel which has not undergone ratchetting in the crack region, however further refinement of the crack growth law to take into account material variability could be beneficial.

There are alternate models for predicting the development of Rolling Contact Fatigue initiated cracks, one such model is the “Rolling Contact Fatigue Damage Function”, this is based on the energy dissipated in the contact patch and therefore the energy available to cause damage to the rail. The energy dissipated in the wheel-rail contact is calculated from the product of traction forces and creepage, in both the longitudinal and lateral directions, in contact patch, obtained from vehicle dynamics simulation. This represents energy expended in contact patch through creepage and forms a parameter known as the Wear Number (commonly given the symbol  $T_\lambda$ ), the relationship between this parameter and wear rates has been established through experiment and observation is commonly used to describe wear rates [1.10]. The “Rolling Contact Fatigue Damage Function” is based on the hypothesis that the energy dissipated in the contact could also be the source of RCF damage, crack initiation and crack growth, therefore that the Wear Number could be related to RCF damage. Since the wear number is also related to wear rates, then the Wear Number could be used to describe the competition between the damage being done to the material causing RCF cracks, and the removal of material by wear, including any material containing RCF damage, preventing the development of RCF cracks. If wear is predicted to be dominant then no RCF cracks are expected to initiate and if damage is predicted to be dominant then RCF cracks are expected to initiate and develop.

The “Rolling Contact Fatigue Damage Function” describes the relationship between wear and damage and is used to determine which is expected to be dominant for the specific energy dissipation calculated for a set of conditions. The “Rolling Contact Fatigue Damage Function” is an empirical function, the relationship between the wear number and RCF damage being developed by comparing the observed occurrence of RCF (or lack thereof) with the Wear Number parameter, noting the correlation, and producing a function which expresses this relationship [1.10]. The “RCF Damage Function” describes three regions, a threshold region at low energy levels (low Wear Numbers) the predicted damage is zero, a second region where increasing energy results in increasing damage, and a third region where predicted damage reduces with increasing energy levels, the predicted damage passing through zero to negative values in this region. Where the predicted damage is above zero RCF cracks are expected to develop, with the severity increasing as damage increases, where the predicted damage is zero, no RCF cracks are expected to initiate. In the first region where wear is low,

there appears to be insufficient energy input to initiate RCF cracks therefore damage is zero, in the second region and initial part of the third region the increase in energy promotes RCF cracks more than it does wear, resulting in RCF cracks developing. In the second part of the third region the predicted damage becomes negative and the increase in energy levels, is predicted to promote wear more than it does the development of RCF cracks, therefore wear becomes dominant prevent the development of RCF cracks. It should be noted that the empirical “Rolling Contact Fatigue Damage Function” has a different definition of crack initiation than the fundamental models based on material failure and crack growth, it defines crack initiation as development of cracks that are detectable by detailed examination in the field (around 1mm surface length). According to the fundamental models, such a crack must have already experienced crack initiation through material failure due to ductility exhaustion and some degree of crack growth. The definition of crack initiation in fundamental models being the failure of material due to ductility exhaustion generating micro cracks.

Statistical models of rail defects take a different approach to modelling rail defects and failures. An example of a statistical modelling approach to rail defects and failures is the work by Zhao et al [1.11], which is concerned with the relationship between maintenance, rail failures and the costs and risks associated with those maintenance procedures and failures. It is particularly concerned with rail failures associated with alumino-thermetic welds. In general statistical models are based on the analysis of large amounts of data, which can cover a wide range of conditions and combinations of conditions. Statistical models have the advantages that they generally allow calculations to be performed very quickly which give results for large segments of a railway network, and give a broad overall view, provided sufficient data is available concerning the issues being examined. However they tend to have the effect of aggregating the effects of numerous factors and are not based on fundamental principles, their predictions are based on what has happened before. Therefore they might be able to predict effects for general variables, such as an increase in the amount of traffic, which can be useful, they are less suitable when considering new situations and for taking into account variation in more detailed conditions separately, which the fundamental based models can predict and statistical information is unlikely to be available for. An example of a new situation might be a new type of vehicle that behaves differently, so that whilst it might weigh the same as previous vehicles, therefore represent the same



weight of traffic (which might have the parameter associated with the collected data, it might have a different effect on the track due the different combination of contact load and conditions, which fundamental based models could potentially predict.

The prediction of Rolling Contact Fatigue crack initiation and growth rates, using a fracture mechanics based approach consisting of coplanar shear crack growth and the “Dynarat” wear model, was selected for the investigations into the effects of different grinding strategies on crack growth described in this thesis, as opposed to the other methods discussed here or full Finite Element or Boundary Element modelling. The advantages of the selected approach are that unlike, some aspects of the contact energy criterion model, and particularly a statistical model approach, all aspects of it are based on fundamental principles of material behaviour and physical phenomenon. Therefore there is a specific parameter which can be varied at one stage or another to represent a specific change in conditions. The statistical models are more suited to predicting general trends rather than specific values for different cases. The contact energy criterion model comes closest to the selected method for having a fundamental basis for the crack growth predictions, since they both use similar vehicle dynamics modelling to generate the contact loads, and the energy dissipated in the contact is based on fundamental principles. However both the wear and crack damage predictions derived from the energy input to the rail are derived from empirical relationships, that are less firmly linked to the mechanisms thought to be operating. This is not to say that it would necessarily be inappropriate to use an energy based criterion to investigate and predict the effect of grinding on the development of RCF cracks, providing it was conducted with the appropriate awareness of the models limitations, just as the limitations of any model should be acknowledged. The main reason that the more fundamentally based selected method retains an advantage, is that the work conducted in this thesis is based on an understanding of fundamental principles and which might be extended in future work, allowing other principles to be added logically. The reason that Finite or Boundary element models were not used to obtain the stress intensity factors to apply to the crack growth law, is that they are significantly more complex and time consuming to carry out, a new model would be required for every load condition and every crack length combination. To generate the crack growth rates for the same range of 120 crack sizes for one vehicle at one location would require 120 models to be set up and solved, whilst certain elements of the models, such as the geometry could be re-used for other

conditions, the boundary conditions would have to be changed and each model solved. Adopting a Finite/Boundary element approach rather than using the crack growth rate data and model that was already established and suitable for the investigation would have resulted in very little new work being carried out to investigate the effect of grinding on the growth of Rolling Contact Fatigue initiated cracks.

### **1.3 Vehicle Dynamics - Contact Loads**

In the preceding sections, the loads carried at the contact between the wheel and the rail which are applied to the modelling of wear and crack initiation and growth have been mentioned. However, how they arise from the interaction between vehicles and the rail, and how the contact loads are determined has not been covered in detail; this will be introduced in this section.

The contact between the wheel and the rail, in addition to supporting the loads imparted by the wheel to the rail, also provides the forces necessary for the guidance of a vehicle along the track. Indeed a significant proportion of the loads transmitted through the contact patch are attributable to the mechanism of guiding the wheels and hence the vehicle, particularly through curves, in addition to supporting the vehicle's weight. In conventional railway systems, the guidance of the vehicle as it runs along the rails is provided by the wheels having a conical profile, and additionally by flanges on the wheels that prevent them moving off the rails. The principle that allows the conical wheels to provide guidance is that they are arranged in pairs on a fixed axle, with the larger diameter of each wheel being towards the centre of the axle, a set distance apart that coincides with the separation of the rails. As the centre of the axle is displaced from the centreline of the rails, then the radius of the wheel at the point of contact with the rail becomes larger on the wheel in the direction of displacement; similarly the radius at the point of contact becomes smaller on the other wheel. Since the wheels are fixed to the same axle they rotate at the same rate, therefore the one with the larger rolling radius has a tendency to travel further. On straight track this results in the wheel of the wheelset which has the larger rolling radius advancing ahead of the other wheel, skewing the wheelset in relation to the normal of the centreline, steering it so that it tends to roll towards the centreline. When negotiating a curved section of track there is a rolling radius difference that matches the difference in length of rail around the inside

and outside of the curve, this location is known as the equilibrium rolling line [1.12] and is offset radially from the centreline. Deviation of the wheelset from the equilibrium rolling line changes the rolling radius difference, this steers the wheelset back to the equilibrium rolling line in a similar way to a difference in rolling radius steering a wheelset on straight track back to the centreline.

The acceleration of a vehicle either around a curve, or to maintain its position relative to the track in spite of disturbances, is achieved the generation of steering forces at the wheelset. These steering forces are generated by the displacement of the wheels of the vehicle from the position where the wheels would run in the equilibrium position (the equilibrium position is co-incident with the centreline on tangent track). These steering forces overcome the resistances of the suspension system and are transmitted to the vehicle guiding it towards the centreline of tangent track or around a curve. Forces transmitted to wheelset arising from the acceleration of the vehicle, either around a curve, or to maintain its position relative to the track in spite of disturbances, are resisted by radial displacement of the wheelsets from the equilibrium position. The radial displacement of the wheelsets from the equilibrium position results in creep taking place at the contact. The forces generated by the creep of the contact steers the wheelset around the curve, balancing the acceleration forces of the vehicle and the resistance of the suspension system. The levels of creep force that can be generated to steer the wheelset are limited by the level of adhesion between the wheel and the rail. These creep forces exert lateral and longitudinal tractions at the wheel-rail contact, generating shear stresses in the rail, in addition to the stress systems from the compressive load of the vehicle.

When the maximum rolling radius difference of the wheelset or level of adhesion between the wheel or rail are insufficient to generate the necessary steering forces then the flange on the inner edge of one of the wheels comes into contact with the rail and presents an obstacle for the wheel moving off of the rail and this contact normal to the direction of the steering force provides the necessary steering force until the lateral forces become excessive and derailment occurs. It is desirable for flange contact to be avoided since this contact always has a major sliding component rather than being predominantly rolling, and therefore it increases the force required to move the vehicle. There is significant wear associated with flange contact, both to the gauge corner of the

rail and the wheel flange; in severe cases this wear can significantly reduce the operational lives of these components.

Increasing the conicity of the wheelset increases the rolling radius difference that can be generated for a given wheel width and flange clearance, and reduces the radius of curve which can be negotiated with the wheelset in perfect curving. However, when a wheelset steers back to its equilibrium rolling line, it arrives with a steering angle and so tends to overshoot the equilibrium rolling position and then has to steer back the other way. This behaviour is known as hunting, and the greater the conicity of the wheels the lower the speed at which the oscillation of the wheelset from one side of the track to the other reaches a magnitude at which the flanges make contact with the rail to limit the lateral travel of the wheelset and becomes unstable. Therefore the angle of conicity in the wheelset is a compromise between the minimum radius of curve at which the wheelset can roll in equilibrium position and the maximum speed at which the behaviour of the wheelset is stable.

To reduce the lateral loads in curves and avoid flange contact the outer rail is often raised above the inner; this cant results in some of the lateral forces required to accelerate the vehicle around the curve being generated by the wheel-rail contact patch in the direction normal to it rather than laterally. The ideal amount of cant to assist with the passage of a rail vehicle around a curve depends upon the speed at which it passes through the curve. If there is too much cant or the speed is too low, the flange on inner wheel contacts with the inner or "low rail", if there is too little cant or the speed is too high then the flange on outer wheel contacts with the outer or "high rail". Where there are different vehicles expected to pass through a curve at different speeds, the amount of cant used in the curve is a compromise between the ride quality required for each type of vehicle, the amount of wear on the rails and wheels, and safety.

The load and contact patch data required as the inputs to RCF wear and crack growth models which are the critical drivers of the first two stages of the RCF damage modelling are difficult to measure directly. Therefore the characteristics of the vehicles and the measured track geometry at the locations represented were used as the inputs to extensively validated and reliable vehicle dynamics simulation techniques to predict the load and contact patch data required. The characteristics of the vehicles and track used

as inputs can be either idealised cases used to study certain aspects of the system, such as changing the suspension stiffness or discrete track anomalies or, as in the context of this work, the characteristics can be representative of real situations. The vehicle dynamics techniques model the vehicles as a network of bodies connected by flexible elements and contact elements, the dynamic interaction of the bodies being represented by equations of motion. The structure of the track can also be modelled in a similar way depending on the complexity of the model. The equations of motion can then be solved in a range of ways of varying complexity, ranging from determining the natural frequencies of the system, through quasi static 'steady state curving' analysis, to full 'dynamic analysis' requiring time stepping integration of the equations of motion. Routines of varying sophistication in the software packages calculate the shape and size of the contact along with the normal and tangential forces acting at the contact.

More detail on vehicle dynamics, and the modelling processes used to generate the inputs for the RCF damage models use in this work, can be found in [1.13]. The effect on RCF of various different characteristics of the wheel-rail contact, such as curve radius, vehicle design, the traction and braking applied by the vehicle, wheel and rail profiles, contact friction and lubrication, the level of cant, and the track gauge, have been examined by Evans et al [1.12]. One of the points that it is worth drawing out of this work is that the forces required in curving to steer a vehicle generate higher levels of shear stress in the contact. This is one of reasons, alongside issues such as variation in contact shape, why shakedown limit is more likely to be exceeded in curves, and hence curves are typically more prone to RCF damage.

#### **1.4 Railway Maintenance - Grinding**

This section of the introduction looks at the use of rail grinding as a rail maintenance technique to manage the performance of and safety of the rail as part of the railway system. An overview of the history and development of the use of rail grinding to maintain the rail is provided by Magel et al [1.14], from early development of grinding machines capable of grinding the rail in a single fixed plane in the 1960's, to the modern sophisticated multi stone production grinding machines able to grind the rail to specific railhead profiles. Their work also describes the development of the understanding of the effective management of the wheel-rail contact conditions and rail defects through rail

grinding. The overall aim of carrying out grinding maintenance is to keep the rail within its operational specification and extend its safe working life. To do this cost-effectively, the performance of the system, the cost of maintaining the rail and the cost of replacing the rail at the end of its life must be balanced.

Rail grinding is carried out for a variety of reasons and often one grinding operation will be targeted at the maintenance of several parameters of the wheel-rail contact and hence the performance of the vehicles and rails. The principal reasons for carrying out grinding operations are:

- To prevent and control the development of defects which occur at or near the surface of the rail which develop as a result of the high contact stresses between the wheel and the rail, or to remove them once if they develop. Such defects are RCF cracks (also known as head checks), the formation of which has been described in previous sections, and also squats and spalling.
- To manage the transverse profile of the rail: Repeated contacts wear the rail to a different transverse profile altering the contact conditions which has implications for the contact stresses and the dynamic performance of the vehicles (including the risk of derailment). Grinding is used to remove different amounts of material from around the rail profile to maintain the profile within operational limits. This profile can either be the original as-produced rail profile, or a different profile intended to alter the contact conditions to those which represent a better compromise between reducing the contact stress between the wheel and the rail, the dynamic behaviour of the vehicles and the maintenance requirement. Some of the factors to be considered in designing the transverse profile to apply during grinding have been discussed by Magel and Kalousek [1.15], this paper also includes a schematic representation of the feedback loop relationship between contact geometry, rail degradation and vehicle dynamics.
- To remove corrugations: Corrugations are short wave length (10-200mm) regular variations in the longitudinal profile of the rail head, generally resulting from differential wear or plastic deformation of the rail head. This differential wear or plastic deformation of the rail head is related to variations in the normal and/or tangential loads at the contact associated with the excitation of resonant frequencies of the vehicle and/or the rail. An overview of the specific

mechanisms for each type of corrugation formation and how they can interact with each other is given by Grassie [1.16] and the preceding work referred to therein. Grinding is used as a treatment to remove, in so far as possible, the short wavelength variation in the longitudinal rail profile; additionally it may be used to alter the transverse profile of the rail to one which reduces the propensity for the corrugations to re-occur. When carrying out grinding to remove corrugations, consideration should be given to ensuring (as far as is practicable) that a periodic grinding signature is avoided, or at least has a different frequency to the characteristic frequency of the corrugations at a particular location, to avoid excitation of the contact interaction at that frequency.

- To reduce the noise emitted by the wheel rolling on the rail: The noise emitted by the wheel rolling on the rail, for particular traffic conditions, is related to the roughness of the wheel and the rail, and can be lowered by reducing their roughness; this issue is of particular concern in built up areas. Therefore grinding might be carried out to reduce noise emissions before other parameters reach their maintenance limits. As an example, the work of Dings et al [1.17] considers the noise reduction which can be achieved by grinding to reduce the roughness of the rail (including corrugations).

One side effect of grinding, of which certain aspects will be considered in more detail later and hence requires introducing briefly here, is that the ground surfaces of the rail exhibit a surface finish characteristic of the grinding process. The surface finish of the rails immediately after grinding exhibits increased roughness at wavelengths less than a millimetre, caused by the abrasive action of the grinding stones. The wavelength of this 'grinding' roughness is less than the size of the contact patch, and hence will affect the contact conditions, notably the contact stress (as will be appreciated from section 1.1), the level of adhesion between the wheel and the rail, and the noise emitted from the wheel rolling along the rail. A distinction should be made, particularly with regard to noise emission, between roughnesses with wavelengths greater than the contact patch size, including corrugation (which can be classified as a roughness), which grinding is used to remove in order to reduce noise and dynamic effects, and roughnesses with wavelengths less than the contact patch size. Here we are concerned with the roughnesses with wavelengths less than the contact patch size, so whilst grinding

increases the noise emission from roughnesses with wavelengths less than the contact patch size, it can simultaneously reduce noise emission from roughnesses with wavelengths greater than the contact patch size. Work has been carried out by Lundmark et al [1.18 & 1.19] to study the 'grinding' roughness, both on a Swedish heavy haul railway and in laboratory tests representing those conditions. The results of the site tests in between service trains of rail surface roughness after grinding indicated that in the heavy haul environment the roughness of the rail tended towards the steady state operating value after one day of traffic.

Another side effect of grinding relates to the fact that the strains which develop in the rail steel in the immediate vicinity of the contact region of a rail in service work harden the material. Therefore the material properties of the rail steel vary significantly with distance from the contact region. The removal of the rail surface material by grinding exposes a different layer of material to the wheel contact altering the material properties of the rail at the contact. The changes in material properties at the rail surface affects the rails rolling contact fatigue and wear response until the newly exposed contact layer experiences a number of contact load cycles and develops the same steady state level of plastic strain, i.e. work hardening, as existed before grinding. The work of Tyfour et al [1.20] measured the development of the hardness profile and plastic strain profiles within the contact region and establishment of steady state wear of rail steels in their initial stress state, subjected to a rolling sliding contact representative of the wheel on rail contact. Using the values obtained and comparing them to a given depth of material removed by grinding, the material properties at the surface of the ground rail can be inferred. Also the development of those properties and wear rate, and the number of load cycles before the steady state is reached can also be inferred.

The effective maintenance of the rail reduces loads and therefore the rate of degradation of other elements involved in the wheel-rail contact system, elements such as sleepers, the track support system and vehicle suspension systems. Also effective maintenance of the other elements involved in the wheel-rail contact system reduces the loads and generally reduces rate of degradation of the rail (there may be exceptions, such as where a reduction in wear rate allows RCF cracks to develop in wheels or the rail). Therefore the development of effective strategies to utilise rail grinding to maintain the rail should consider the impact of the maintenance of the rail profile and the control of the



degradation of the rail on the other elements involved in the wheel-rail contact system. Similarly the operation and maintenance of the rest of the elements involved in the wheel-rail contact system should be carried out with consideration for its effect on the maintenance requirements of the rail. All of the elements involved in the wheel-rail contact system influence one another to some extent, with feedback between them, which can result in vicious circles forming which results in rapid degradation of the system. As stated by Magel and Kalousek [1.15] "*These same "vicious" circles can be turned into "virtuous" circles—an improvement in the profiles reduces stress and creepage that reduces further profile deterioration, etc. Understanding and exploiting these virtuous circles is the key to the most economically appropriate grinding interval and achieving the optimal w/r interface.*" One approach to overcome the complexity of deciding the optimal interval at which to carry out rail grinding operations has been proposed by Chattopadhyay et al [1.21]. The work of Chattopadhyay et al involved the identification of the factors influencing rail degradation, development of models for rail failures, and the analysis of the cost of various grinding intervals as part of a statistical approach to setting economic grinding intervals. However, in the work described in this thesis a different approach to inform the decision as to the optimum grinding strategy to employ is developed. That approach is to use the modelling techniques described in the previous sections to represent the effect of rail grinding on the growth of RCF cracks to find the grinding strategy which is predicted to give the maximum safe rail life and to investigate the effect of the cost of different grinding strategies over the life of the rail. To do this, grinding will be represented in the models as an additional contact cycle in traffic pattern with extremely high wear rate.

## **1.5 Scope of the Thesis**

The aim of the work described in this thesis is to develop investigative modelling tools and techniques which could be useful in specifying grinding strategies required to control the development of Rolling Contact Fatigue (RCF) cracks, so that the safe operating life of the rail can be maximised or the cost of the rail over its life (note: this Rail Life Cost, is different from a full economic rail life cycle costing, see Chapter 7 for definition), including the cost of maintenance, can be minimised. The methodology employed involved the adaptation of an existing, established, Crack Growth Model without fundamentally altering the principles behind it, to allow it to represent the

application of occasional rail grinding operations within a pattern of frequently changing vehicle types which represent the traffic pattern over section of track. This pre-existing Crack Growth Model and its use in conjunction with other modelling techniques to predict the growth of RCF cracks in rails is described in a report for the Railway Safety and Standards Board (UK) by Burstow et al [1.10]. The adapted model, termed the Grinding Model, is used to investigate the effect of grinding on RCF cracks and the grinding strategies required to control the growth of RCF cracks. Techniques are developed which could enable the use of the model to assist with the specification of the grinding to control RCF cracks efficiently, and provide estimates of the effect of different grinding strategies on the cost of the rail over its life. Examples as to how these techniques could be used to improve the specification of the grinding applied to manage RCF cracks at specific locations are given, and the crack growth predictions for these examples are compared with the real locations they represented. The aim of this comparison is to put the crack growth predictions and grinding strategy recommendations into context with respect to their accuracy at predicting the behaviour of RCF cracks in real situations.

The description of the work outlined above is broken down into the following sections:

- In Chapter 2 the factors affecting rail grinding are introduced and the principal variables to be considered in the modelling selected. The limitations of the Crack Growth Model when predicting the growth of RCF cracks in rails with traffic patterns of frequently changing train types with occasional rail grinding operations are demonstrated. The process of developing the Grinding Model is described, and modelling runs conducted to demonstrate that it overcomes limitations of the Crack Growth Model for representing the effects of grinding on the crack growth for a traffic pattern of frequently changing vehicle types.
- In Chapter 3 the validity of the simplifying assumption that the characteristic roughness of the rail which results from grinding would not significantly affect the crack growth predictions, due to it being removed by the passage of rail vehicles within a relatively short period of time compared to the interval between grinding operations, is investigated. This is done with a program of tests using full scale railway equipment to study the development of grinding roughness within the first tens of wheel passes after grinding.

- To investigate how the grinding model could be used to specify grinding strategies based on the predicted crack size trend, a set of example optimum criteria is established against which the predicted crack size trends could be assessed. A technique for using the Grinding Model to find grinding strategies which produce a crack size trend which match the optimum criteria is developed; these grinding strategies are termed *optimum grinding strategies*. This technique is then used to find the optimum grinding strategies for a number of different train types and combinations of train types. As part of this process, a traffic pattern with a mix of frequently changing vehicle types is used to represent high speed and commuter train traffic over a primary route. This is described in Chapter 4.
- The sensitivity of the predicted crack size trend is examined in Chapter 5, particularly its sensitivity to variations in the values of the grinding strategy equivalent to the error which could reasonably be expected to occur in applying a grinding strategy.
- The relationship between the values of the two principal variables of the grinding strategy which form an optimum grinding strategy is examined in Chapter 6. The trend of this relationship was established to allow the optimum grinding strategies across the range of grinding strategy variable values to be predicted quickly, without having to conduct an investigation manually. Techniques for the use of these trends for making subjective judgements about the most suitable grinding strategies to apply to a section of track are developed and are discussed with examples.
- Chapter 7 describes work carried out to develop a method for estimating and examining the effect of different grinding strategies on the cost of a rail over its life. Also in Chapter 7 the development of a technique for the use of the results of the cost estimation method to select grinding strategies against the objective criteria of minimising the cost of the rail over its life, including the effect of grinding on that cost, is described and discussed, with examples.
- Chapter 8 concerns the comparison of the crack growth predictions of the Grinding Model with site observations of the locations they represent to put the modelling results in context with respect to their accuracy.

- Finally the conclusions and recommendations for future work are presented in Chapter 9.

It is recognised that grinding is carried out for reasons other than the control of RCF cracks, such as rail profile management, and acoustic emission, and that grinding to control RCF takes place within the context of these practices. However, the specification of the grinding relating to these other aspects of rail maintenance is beyond the scope of this thesis. It would be intended that where the techniques developed here were used to assist the specification of the grinding required to control RCF cracks, those specifications would be compared with those for the grinding and maintenance requirements for other factors, and whichever specification requires action soonest or most frequently is applied. In situations where grinding is applied according to the requirements of factors other than the control of RCF, it is intended that the techniques developed here could assist in specifying the aspects of that grinding which are aimed at controlling RCF cracks.

## 1.6 References

- 1.1. Kapoor A. (1994) A Re-Evaluation of the Life to Rupture of Ductile Metals by Cyclic Plastic Strain. *Fatigue & Fracture of Engineering Materials & Structures*, **17**, 201–219.
- 1.2. Kapoor A., Beynon J.H., Fletcher D.I., Loo-Morrey M. (2004) Computer simulation of strain accumulation and hardening for pearlitic rail steel undergoing repeated contact. *Journal of Strain Analysis* **39**(4), 383-396.
- 1.3. Franklin F.J., Kapoor A. (2007) Modelling wear and crack initiation in rails. *IMechE, Part F: J. Journal of Rail and Rapid Transit* **221**, 23-33.
- 1.4. Vasic G., Franklin F.J., Fletcher D.I., Kapoor A. (2010) ‘Effect of traffic on crack initiation in rails.’ *Journal of Mechanical Systems for Transportation and Logistics* **3**(1), 100–109.

- 1.5. Kapoor A., Franklin F.J., Wong S.K., and Ishida M. (2002) Surface Roughness and Plastic Flow in Rail Wheel Contact, *Wear* **253**, 257–264.
- 1.6. Fletcher D.I., Hyde P., Kapoor A. (2004) Growth of Multiple Rolling Contact Fatigue Cracks Driven by Rail Bending Modelled Using a Boundary Element Technique. *IMechE, Part F: J. Journal of Rail and Rapid Transit* **218**, 243-253.
- 1.7. Bold P.E., Brown M.W. (1991) Shear mode crack growth and rolling contact fatigue. *Wear* **144** 307-317.
- 1.8. Fletcher D.I., Beynon J.H. (1999) A simple method of stress intensity factor calculation for inclined fluid-filled surface-breaking cracks under contact loading. *IMechE, Part F: J. Journal of Rail and Rapid Transit* **213**, 299-304.
- 1.9. Fletcher D.I., Kapoor A. (2006) Rapid method of stress intensity factor calculation for semi-elliptical surface breaking cracks under three-dimensional contact loading. *IMechE, Part F: Journal of Rail and Rapid Transit* **220**, 219-234.
- 1.10. Burstow M.C., Fletcher D.I., Franklin F.J., Kapoor A. (2008) Management and Understanding of Rolling Contact Fatigue: WP1 Mechanisms of Crack Initiation - Final Report.  
*[http://www.rssb.co.uk/SiteCollectionDocuments/pdf/reports/Research/T355\\_rpt\\_final\\_wp1.pdf](http://www.rssb.co.uk/SiteCollectionDocuments/pdf/reports/Research/T355_rpt_final_wp1.pdf)*
- 1.11. Zhao J., Chan A.H.C., Roberts C., Stirling A.B. (2006) Assessing the economic life of rail using a stochastic analysis of failures. *IMechE, Part F: Journal of Rail and Rapid Transit* **220**, 103-111.
- 1.12. Evans J., Iwnicki S.D. (2002) Vehicle Dynamics and the Wheel/Rail Interface, Rail Technology Unit, Manchester Metropolitan University, From: Wheels on Rails – An update. *Understanding and managing the Wheel/Rail Interface, IMechE Seminar, London, April 2002.*

- 1.13. Iwnicki S. (2003) Simulation of Wheel-Rail Contact Forces, *Fatigue & Fracture of Engineering Materials & Structures* **26**, 887-900.
- 1.14. Magel E., Roney M., Kalousek J., Sroba P. (2003) The Blending of Theory and Practice in Modern Rail Grinding. *Fatigue & Fracture of Engineering Materials & Structures* **26**, 921-929.
- 1.15. Magel E., Kalousek J. (2002) The Application of Contact Mechanics to Rail Profile Design and Rail Grinding. *Wear* **253**, 308–316.
- 1.16. Grassie S.L., Rail (2009) Corrugation: Characteristics, Causes, and Treatments. *IMechE, Part F: Journal of Rail and Rapid Transit*. **223**, 581-596.
- 1.17. Dings P., Verheijen E., Kootwijk-Damman C. (2000) A Traffic-Dependent Acoustical Grinding Criterion. *Journal of Sound and Vibration* **231**(3), 941-949.
- 1.18. Lundmark J., Höglund E., Prakash B. (2006) Running-in Behaviour of Rail and Wheel Contacting Surfaces. *Proceedings from the 5<sup>th</sup> International Conference on Tribology AITC-AIT 2006. Parma, Italy in September 2006*. ISBN: 978-88-902333-0-2.
- 1.19. Lundmark J., Kassfeldt E., Hardell J., Prakash B. (2007) Influence of Initial Surface Topography on Tribological Performance of the Wheel/Rail Interface During Rolling/Sliding conditions. *Proceedings from the conference IHHA STS 2007. Kiruna, Sweden in June 2007*. ISBN: 978-91-633-0607-5.
- 1.20. Tyfour W.R., Beynon J.H., Kapoor A. (1995) The Steady State Wear Behaviour of Pearlitic Rail Steel Under Dry Rolling-Sliding Contact Conditions. *Wear* **180**, 79-89.

- 1.21. Chattopadhyay G., Reddy V., Larsson-Kraik P.O. (2005) Decision on Economical Rail Grinding Interval for Controlling Rolling Contact Fatigue. *International Transactions in Operational Research* **12**, 545-558

## **Chapter 2. Grinding Model Development**

In this chapter the main variables of the process of rail grinding as a maintenance technique are introduced. Of these variables, those that are considered the most significant to scheduling grinding based on crack propagation, and therefore were considered necessary to include in a simplified model, are identified. The factors that are significant to a considered decision of grinding scheduling are introduced and the relevance to the grinding scheduling decision making process of a crack growth model that includes the effects of grinding is discussed. The Crack Growth Model on which the grinding model is based is described, and its limitations discussed with regards to the modelling of the effects of different grinding strategies on the predicted rolling contact fatigue crack length. The Grinding Model is described, and example results presented, to show that the Grinding Model has overcome some of the limitations of the Crack Growth Model when used to investigate the effect of grinding operations on the development of rolling contact fatigue crack length.

### **2.1 Grinding Variables**

There are several main variables when carrying out grinding operations that it would ideally be desirable to have the capability of modelling, some of these are outlined below:

- The amount of material removed, that is the difference in the whole rail head cross section between that before and that after grinding, with respect to some common datum such as the base of the rail.
- The original, resultant and specified profile of the rail, and their effects on the propagation of RCF cracks are variables that it would be desirable to consider in a grinding model.
- The frequency with which grinding operations are carried out, or the interval between each operation.
- The maximum material removal rate of the grinding machine, the relationship between the material removal rate and the vehicle speed. This will give the number of passes of the grinding machine required to achieve the specified material removal, and how long it would take to achieve this for a given length of rail.



- The roughness of the rail surface in the region that is contacted by the wheels of passing vehicles throughout the interval between grinding operations and the relationship between this roughness and the rate of RCF crack propagation.

The type and pattern of traffic that passes over sections of track, and the variation in associated crack growth and wear rates, is also a significant variable that should be considered when determining the appropriate grinding strategy to use. Also the track geometry at a particular location significantly affects the crack growth rate, wear rate and wear pattern and hence the appropriate grinding strategy.

The original crack growth model has both been used, as far as its limitations allow, and adapted to remove some of those limitations, in the form of the Grinding Model, to model the effects of selected key variables. The selected variables are the interval between grinding operations, the depth of material removed normal to the surface at the location of the maximum depth of the crack and the types and pattern of vehicles using a particular section of track. The geometry of the track at the selected location is a variable of the vehicle dynamics modelling process that is used to create the input crack growth rate data. The use of vehicle dynamics results for different track geometries in the Crack Growth and Grinding Model allows the effect of grinding strategies on crack length development at locations with similar geometries to be investigated.

These are considered the main variables of the grinding operations that it is necessary to represent in order to study the effect of grinding operations on RCF crack propagation. The development of the roughness of the rail resulting from grinding operations was investigated experimentally; these experiments and the significance of their results to the grinding model are discussed separately in Chapter 3. The effect of the variation of rail surface roughness between grinding operation is not modelled in the current version of the Grinding Model.

## **2.2 Factors affecting grinding specification decision**

Currently network guidelines that break the network down into sections based on ranges of track curvature are used to schedule grinding operations to control RCF cracks in the UK. Grinding may also be scheduled based on rail inspections to maintain the rail cross sectional and longitudinal profiles within tolerances and to remove any surface defects.

Other factors that may affect the specification of grinding operations are the availability of grinding machines and associated personnel; if a grinding machine is scheduled to a section of line on a regular basis then the flexibility in the system is the depth of material removed during grinding. Other considerations may be the availability of traffic paths to get grinding machines to the work site, and in which to take possession of track sections, i.e. remove them from service to carry out maintenance work, to carry out grinding.

The aim of adapting the crack growth model to include the effects of grinding on crack growth was to investigate the effect of different grinding strategies on crack length. This would allow the grinding strategy to be found that was predicted controlled the crack size whilst having the minimum effect on the wear life of the rail, such a grinding strategy would be the optimum compromise to obtain the maximum safe working life of the rail. The definition of what constitutes crack size control would be determined by the network operator. Grinding strategies which maintained the crack below a specified size, or resulted in the crack being removed after a specified number of wheel passes, would be examples of grinding strategies which are defined as controlling crack size. Whilst outside of the scope of the work described in this thesis, the potential eventual outcome of future further work in this area could be the use of the Grinding Model to specify grinding strategies to be used on a railway network. The aim would be to specify optimum grinding strategies which would maximise the safe operational life of the rail and minimise the expenditure on grinding operations. To use a further developed Grinding Model in this way would require the application of suitable factors of safety and field trials to calibrate and validate the model.

The grinding model only aims to represent the effects of varying the intervals between grinding operations and the depth of material removed on the predicted crack length. Other factors such as altering the cross sectional profile might affect the predicted crack length. In addition to controlling crack length grinding might be scheduled for other reasons, such as track inspections revealing that the cross sectional profile or the extent of corrugation are, or are about to become, outside specified limits. The modelling of the development and treatment of these modes of degradation of rail condition is beyond the scope of this work, it would be expected that when all reasons for scheduling grinding are considered, the reason that requires the most immediate

treatment would be used for scheduling and a strategy developed that satisfied the requirements to treat the other rail defects as well. The grinding model could then be used to investigate what effect the grinding strategy developed would have on the predicted crack size.

### **2.3 Definition of Crack Size**

The term "crack size" is used throughout the work described in this thesis, where this refers to a value in the Crack Growth Model or Grinding Model, it has a specific meaning. It is used to indicate the value of the defining characteristic dimension of the crack modelled to represent RCF cracks in rails. This representative crack is semi-circular in shape with the straight edge being open at the running surface of the rail. It is orientated with the straight edge in the transverse direction, with the plane of the crack at 30 degrees below the surface of the rail. The term "crack size" refers to the radius of the semi-circle normal to the straight edge, that is, the length of the crack at its deepest point below the surface of the rail. The models make the simplifying assumption that the crack always remains semi-circular and that any changes to the shape due to wear or grinding, which in practice would only affect the dimensions of the crack at the surface of the rail, are compensated for by crack growth which is assumed to restore the crack shape. Part of the simplifying assumption is that this occurs without affecting the growth rate of the crack in the direction of the characteristic dimension.

### **2.4 Description of Crack Growth Model**

A modelling run of the Crack Growth Model is initiated by the inputting of a file which contains the sets of contact data, initial crack size and other parameters of the modelling run. Each set of contact data represents either, a different type of vehicle or a grinding operation. The contact data for vehicles contains the crack growth rate predictions calculated using the fracture mechanics based model of the second phase of crack growth described in section 1.2, it also contains a fixed wear rate prediction calculated using the "Dynarat" model described in section 1.1. The crack growth predictions consist of crack growth rate values for a large number of discrete crack sizes, approximately 120 crack sizes in the range 0-35mm. When the Crack Growth Model requires the crack growth rate of a crack of a particular size, due to a wheel pass of a

particular vehicle in order to calculate the change in crack size, caused by that wheel pass, it interpolates the crack growth from the crack growth prediction data for cracks larger and smaller than the required size. The crack growth and wear rate data for each vehicle has been calculated for the specific characteristics, such as curvature, rail profile and cant of the location being modelled in the modelling run, modelling a different location requires the Crack Growth Model to be run with data generated for that location. After reading in the data and parameters for the modelling run, the Crack Growth Model progresses through a modelling run by applying the net crack size change calculated for each wheel pass to, at first the initial crack length, and then the crack size after the previous wheel pass, changing between sets of contact data as specified in the input file to represent the traffic pattern. The net crack growth calculated for each wheel pass is based on the combined effects on the crack size, of the extension of the crack at the tip (crack growth), and the truncation of the crack by wear at the mouth, taking into account that the angle of the crack to the rail surface and that the wear is measured vertically. The Crack Growth Model progresses through each set of contact data in turn, applying the specified number of wheel passes of that set to the current crack size, representing the number of wheels of that vehicle type that pass over the crack in sequence. When the Crack Growth Model has applied the last of the specified wheel passes of the last set, it repeats the process from the first set. The Crack Growth Model finishes either when the total number of wheel passes specified in the modelling run parameters have been applied, or the crack size reaches a value of less than zero. A simplified representation of the Crack Growth Model is given in Figure 2.1.

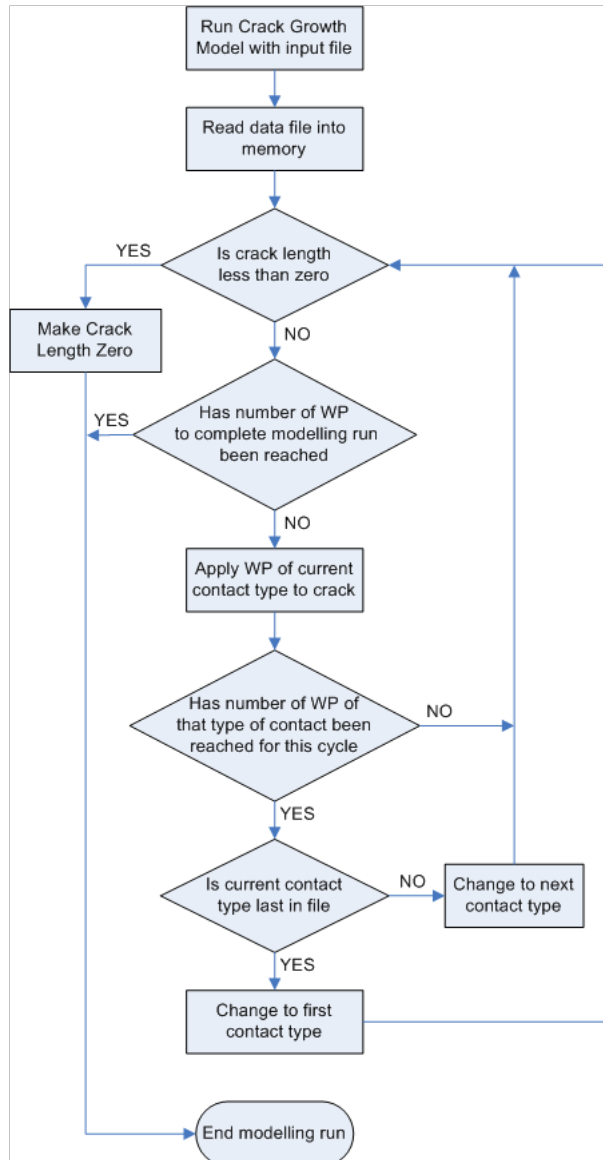


Figure 2.1. Simplified representation of the Crack Growth Model.

## 2.5 Limitations of Crack Growth Model for modelling grinding

The crack size prediction results from the use of the Crack Growth Model with a single wheel-rail contact type and single grinding operation were acceptable. This is because with one vehicle type the number of wheel passes of the type of vehicle modelled could be applied in the order which they would occur in the traffic pattern, followed by the grinding operation. This represents a traffic pattern that consists of multiple passes of a single vehicle type with grinding operations of fixed interval and depth. The result of the Crack Growth Model run with a single contact type, representing Class 365 units and a grinding operation that removes 0.2mm from the head of the rail, carried out after

every  $1 \times 10^6$  wheel passes of are shown in Figure 2.2. The downward trend of the crack size shows that cracks smaller than the initial crack size are reduced by repeated contacts which are modelled to be representative of a Class 365 unit. This is because, for a crack of less than the initial crack size, the predicted crack growth rate due to a wheel contact is less than the crack size worn away by each wheel contact; hence the crack size reduces with each wheel contact. This results in a gradual reduction of the crack size until the first grinding operation, removes the remaining crack length. It should be noted that due to the crack being modelled as being inclined at 30 degrees below the rail surface, then entire remaining crack size immediately before the grinding operation (0.36mm) lies within the 0.2mm thick surface layer of the rail that it removed during the grinding operation.

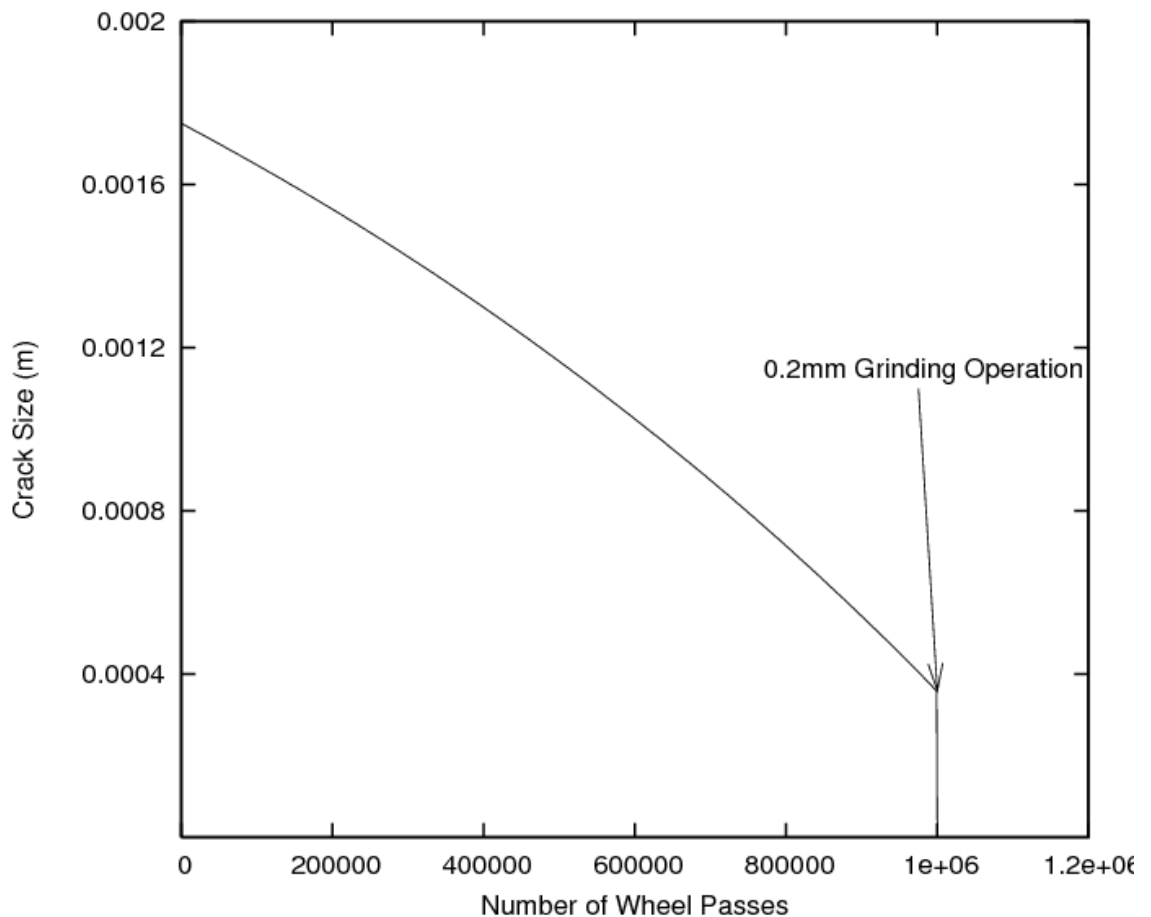


Figure 2.2. Predicted crack size results from the Crack Growth Model for Class 365 multiple units with grinding applied.

With multiple types of wheel-rail contact, representing different vehicles, the data for the different types of contact is written in the input file, the original model can only

apply wheel passes of each set of contact data once between applications of the data for the grinding operation, there are a limit to the number of sets of data that the original model can read in and process efficiently. This means that all of the contacts of each type that occur within each grinding interval are modelled consecutively before switching to the next contact type. That is that each set of contact data can only be applied for its specified number of times once in each recurrence of the outer loop in figure 2.1, at least one of the contact data sets must represent a grinding operation in order for the effects of grinding to be studied. For instance if the grinding interval was  $1 \times 10^6$  wheel passes and there were two different contact types representing equal numbers of two different types of vehicles running over the rail, then  $5 \times 10^5$  wheel passes of one contact type would have to be applied followed by  $5 \times 10^5$  wheel passes of the second type followed by one pass of the grinding operation, if the resultant crack growth rates of the two rail vehicle contact types are different then the order in which the different contact types are applied significantly affects the change in crack length between grinding intervals.

The crack growth trend and effects of applying multiple vehicle types in different orders can be seen in Figures 2.3 and 2.4. These are plots of the results from the Crack Growth Model of modelling runs specified in the manner described above. They represent the passage of trains consisting of four vehicle multiple units and trains formed of two locomotives and eight passenger vehicles in fixed formations. Using the Crack Growth Model to model the passage of these trains without grinding allowed the type of vehicle contact data applied to be alternated after numbers of wheel passes representative of the number of that type of vehicle in that train, or the number of each type of train that occur consecutively within the traffic pattern. The ratio of trains represented in Figures 2.3 and 2.4 are five Class 365 units to two HSTs, this works out at  $5 \times 10^6$  Class 365 wheel passes to  $5 \times 10^6$  HST wheel passes, the HST wheel passes are a combination of  $4 \times 10^6$  passenger vehicle (Mark III coaches) and  $1 \times 10^6$  locomotive (Class 43) wheel passes.

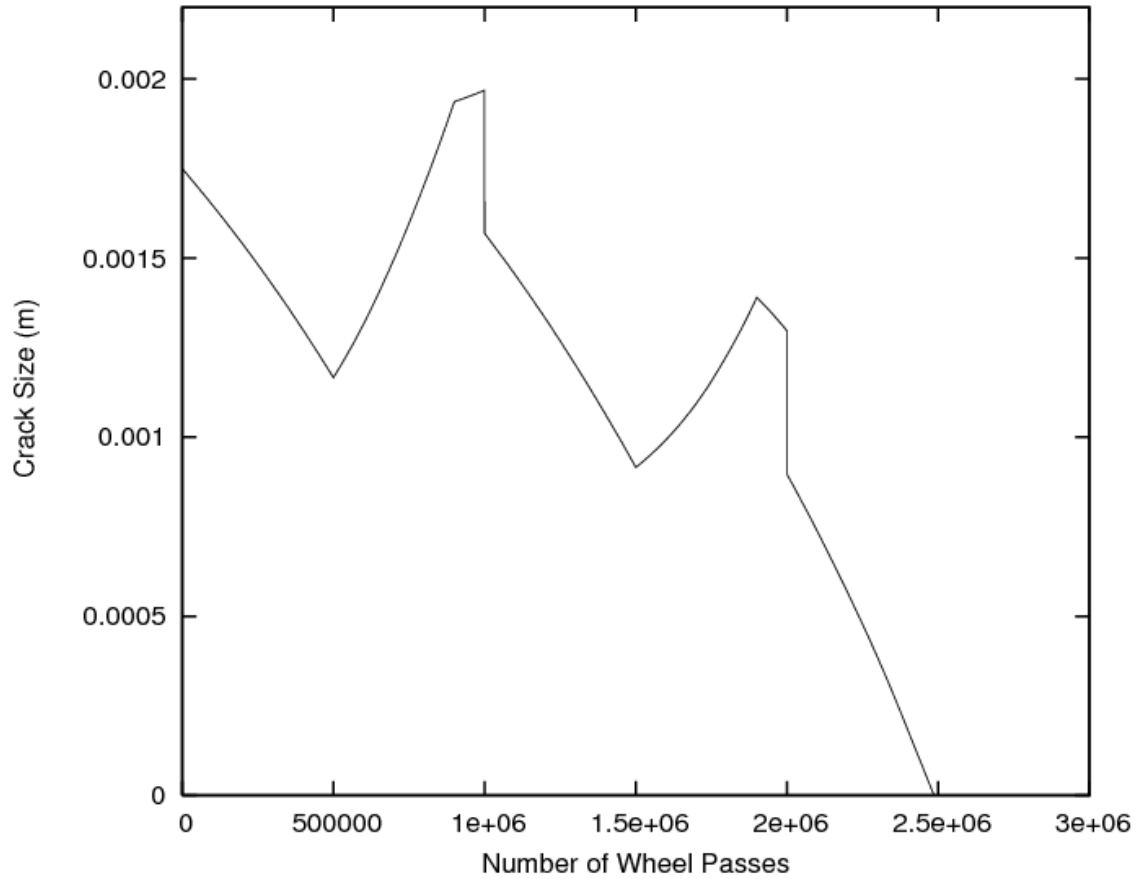


Figure 2.3. Predicted crack size results for a modelling run with the Crack Growth Model. Ratio of vehicle type wheel passes, 5 Class 365 to 4 Mark III to 1 Class 43, applied in that order between grinding operations of 0.2mm depth at  $1 \times 10^6$  wheel passes.



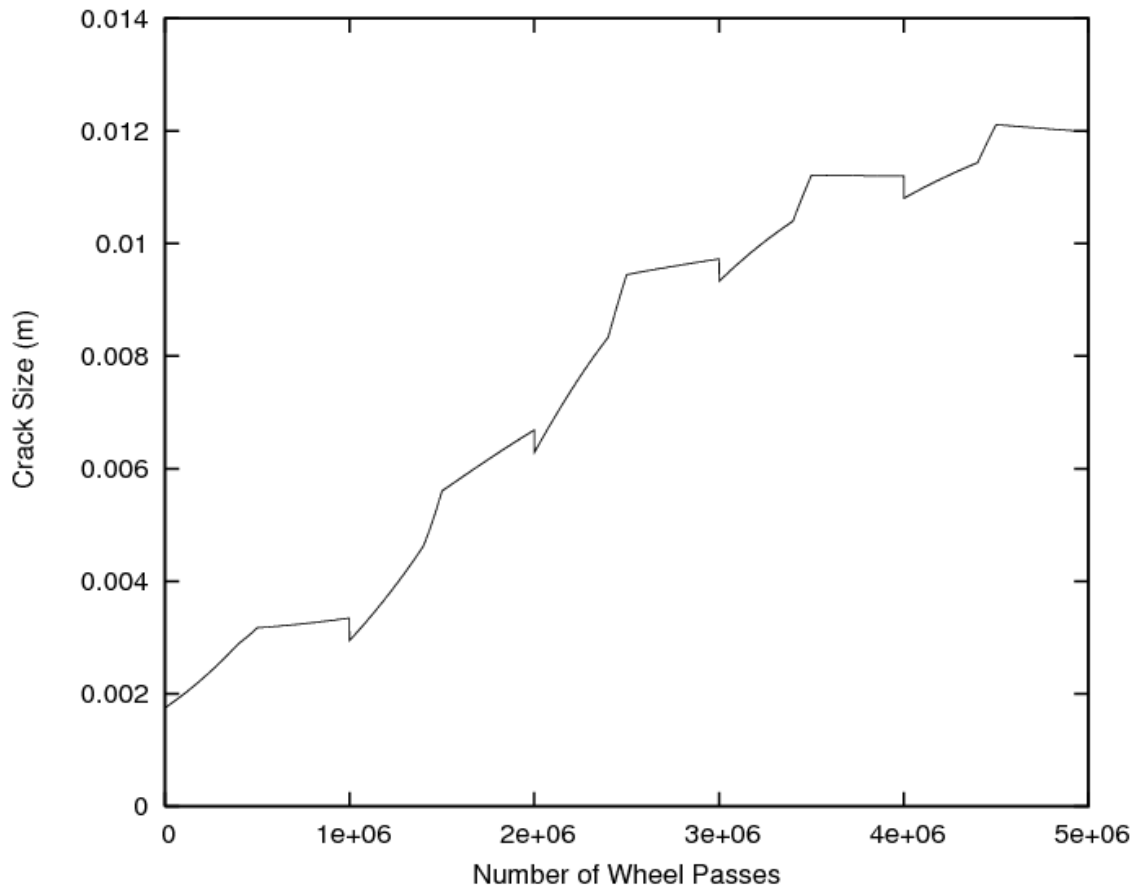


Figure 2.4. Predicted crack size results for a modelling run with the Crack Growth Model. Ratio of vehicle type wheel passes, 4 Mark III to 1 Class 43 to 5 Class 365, applied in that order between grinding operations of 0.2mm depth at  $1 \times 10^6$  wheel passes.

Figure 2.3 shows the result of a modelling run of the Crack growth model with grinding operation of 0.2mm depth after each  $1 \times 10^6$  wheel passes of traffic. The wheel passes of the different types of vehicles within the grinding interval are grouped together and applied in the following order, Class 365, Mark III and Class 43. That the crack length tends to zero after approximately  $2.5 \times 10^6$  wheel passes indicates that the crack would be expected to wear out with this traffic pattern and grinding strategy. Figure 2.4 also shows the result of a modelling run of the Crack growth model with grinding operation of 0.2mm depth after each  $1 \times 10^6$  wheel passes of traffic. In this case the wheel passes of the different types of vehicles within the grinding interval are grouped together and applied in the following order, Mark III, Class 43 and Class 365. That the general trend of crack length tends to a value greater than 10mm indicates that the crack would be expected to grow to an unsafe size, since above 10mm other crack propagation

mechanisms, which could grow the crack until failure of the rail and which are not included in the model, start to dominate.

In reality where there is a mixture of vehicle types using a section of track, the types of vehicles change much more frequently between grinding operations than it is feasible to specify with the Crack Growth Model. For example the type of vehicles in a traffic pattern can alternate between different trains of 8 axles and less, or there can be different types of vehicles within trains, rather than the different types of vehicles being grouped together between each grinding operation. The original model was not suitable for applying wheel passes in sequences representative of typical traffic patterns since although the contact data for different vehicles could be repeated in the sequence between grinding operations, it did not allow for enough repetitions between grinding operations to represent alternating train types and other representative traffic patterns. As figures 2.3 and 2.4 show, when the wheel passes of the different types of vehicles between grinding operations are grouped together, the order in which they are applied significantly affects the result and can even affect whether the crack is predicted to grow to unsafe levels or be worn away. That there is such a difference in the predicted behaviour of the crack length depending upon the order in which the grouped wheel passes of different types of vehicles are applied means that the Crack Growth Model is not suitable for modelling the effects of different grinding strategies with realistic traffic patterns consisting of multiple vehicle types.

## **2.6 Grinding Model Development**

The method of implementing grinding operations in the Crack Growth Model means their interval and depth are fixed and repeated cyclically, once the traffic contact type and grinding type had been set they were repeated until the required number of wheel passes had been modelled or the crack was worn out. This does not allow for the modelling of situations where the grinding interval, or the depth of material removed, is changed for the different grinding operations within a modelling run. This precluded investigations being carried out into grinding strategies that involved either, more regular grinding or the removal of a greater depth of material, or both, at the start of the modelling run followed by less severe grinding once the crack size has been reduced to size that grows at a lower rate.

Considering the limitations of the original model, the enhancements that it was felt would be useful and feasible to make were to separate the application of traffic wheel passes from the application of grinding operations, so that the contact types could be changed at a frequency representative of realistic traffic patterns. It was also decided to make the specification of grinding operations within the modelling run flexible so that interval between each grinding operation, and depth of material removed, could be varied.

The grinding model has two input files, one contains the different types of contact data including how often (in terms of wheel passes) the model should switch between applying wheel passes of the different types, to represent different traffic patterns. The other input file specifies after how many wheel passes each grinding operation takes place (total number as opposed to the number since the last grinding operation) and the depth of material to be removed.

The Grinding Model progresses through a modelling run by reading in the traffic data (which includes the initial crack size and other parameters of the modelling run), and the grinding data, from the input files. The grinding model then applies the net crack length change calculated for each wheel pass to, at first the initial crack length, and then the crack length after the previous wheel pass, changing between contact types as specified in the traffic file. When the number of wheel passes applied reaches one of the values specified in the grinding data file the change in crack length due to the wheel pass is applied as usual, followed by the change in crack length due to the specified grinding depth for that operation is subtracted from the current crack length. A simplified representation of the Grinding Model is given in Figure 2.5.

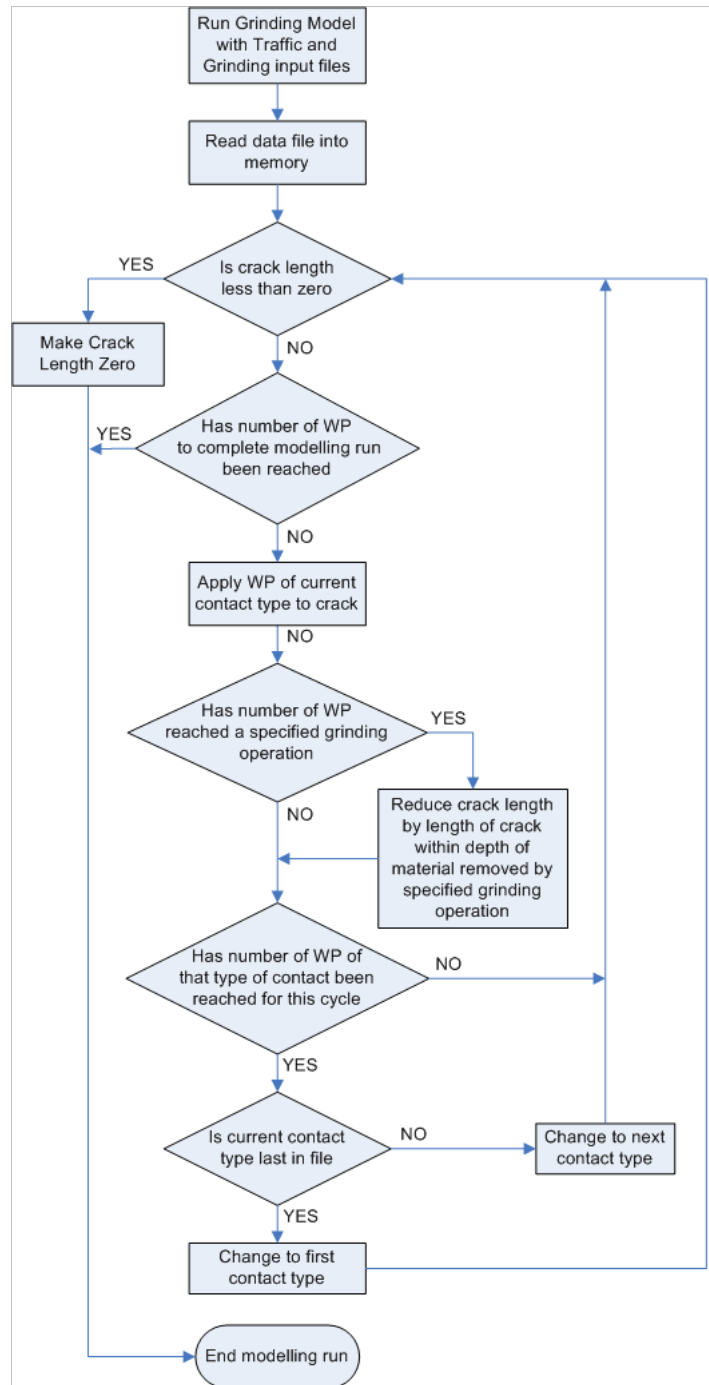


Figure 2.5. Simplified representation of the Grinding Model.

The results for the grinding model show that the plots of crack length are smooth between grinding operations, irrespective of whether single, or multi-contact type traffic data has been used. Modelling runs have been carried out in which the only difference was that the different contact types specified for application within the cycle were applied in different orders, the number of wheel passes of each type being representative of a small number of trains each cycle. The results for these runs were virtually identical

and the trends were the same with respect to a scale showing millions of wheel passes. Figure 2.6 shows the results of three of modelling runs with the Grinding Model, in all of the runs the contact data for Class 365 units, Class 43 locomotives and Mark III passenger vehicles are applied 32, 8 and 32 times respectively. For each modelling run the different types of contact data is applied for the specified number of wheel passes in the order they are listed in the key. The number of wheel passes of each type applied represents the application of a traffic pattern each cycle that consists of two four-vehicle Class 365 units and a High Speed Train (HST) made up of eight Mark III passenger vehicles and two Class 43 locomotives.

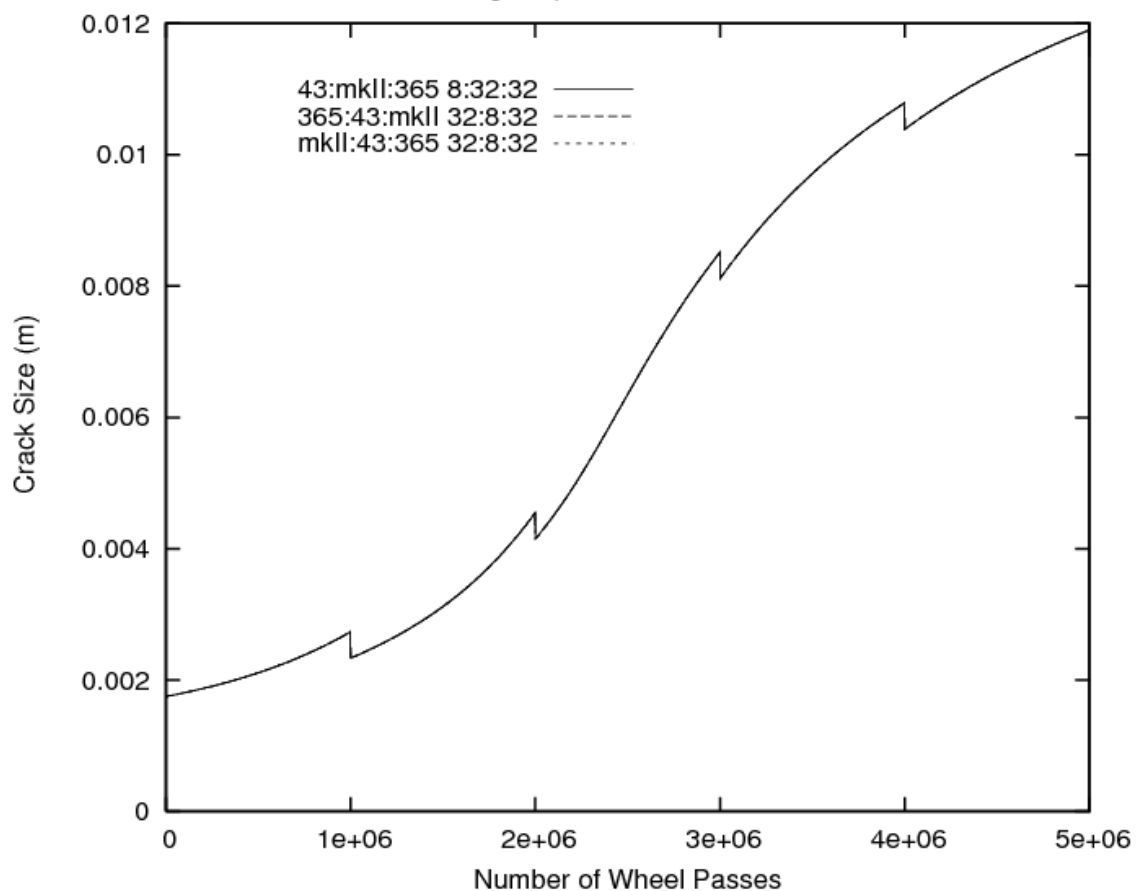


Figure 2.6. Crack size results for three modelling runs with the Grinding Model. Ratio of vehicle type wheel passes, 4 Mark III to 1 Class 43 to 4 Class 365, applied in different orders between grinding operations of 0.2mm depth at 1x10<sup>6</sup> wheel passes.

Figure 2.7 shows a selected section of the same results as shown in figure 2.6 on a scale of a few tens of thousands of wheel passes. The predicted crack size results do exhibit minor differences, however these do not appear to be cumulative and the results cross over and re-converge on the same or similar values so that the predicted trends in the

crack size are virtually identical on the millions of wheel pass scale as shown in figure 2.6. Figure 2.7 also shows that at the zoomed scale there results appear to be made up of sections of straight lines rather than a smooth curve. This is because whilst the predicted crack size is calculated for every wheel pass and is stored in the computer memory to be used when calculating the effect of the next wheel pass, the crack size value is only written to the output file every 1000 wheel passes, or when the modelling run ends. This was done in order to keep the process time and file sizes down as it was felt that the recording of the result of the crack size after every wheel pass was an unnecessary level of precision for plotting the trend in crack size over millions of wheel passes.

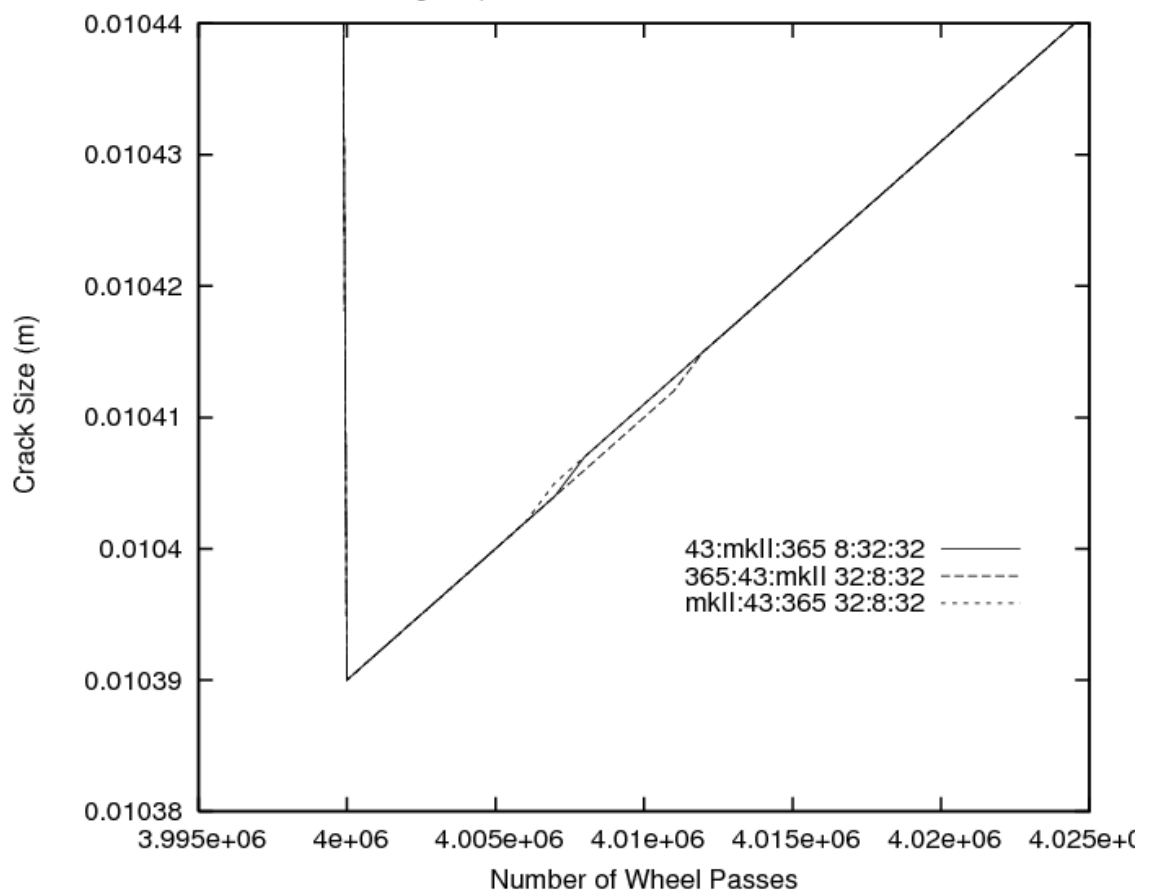


Figure 2.7. A selected section of crack size results for three modelling runs with the Grinding Model. Ratio of vehicle type wheel passes, 4 Mark III to 1 Class 43 to 4 Class 365, applied in different orders between grinding operations of 0.2mm depth at  $1 \times 10^6$  wheel passes.

The similarity of the results for the three runs in figures 2.6 and 2.7 shows that the application of contact types in one order representing interspersed trains is representative of the results for alternative ordering. This in turn meant that only one

order of applying the vehicles in a traffic pattern needed to be considered, since it was expected that the results for other traffic data file orders would be indistinguishable. It has not been considered necessary, to represent the different types of vehicle wheel passes, in the exact order that occurs within the formation of the trains in the traffic pattern for, since it has been shown that the effect of the order in which the vehicle types are applied in the cycle of contact data application is negligible. The effect of applying the contact types in different orders that represent trains of different types, has only been investigated for representations of traffic patterns where the type of train changes after a small number of trains. There may be a cut-off point after which the order that the contact types are applied in the data file cycle does have a detectable effect on the predicted crack size after millions of wheel passes, however it is not expected that this would be the case for traffic patterns representing, for example, an hourly cycle of train types.

An additional development of the Grinding Model over the Crack Growth Model is that it includes a parameter for the cumulative total of the wear applied to the rail, either from rail vehicle traffic or grinding. The wear or grinding applied at each modelling step is added to the cumulative total wear value, and this value is recorded in the output file throughout the modelling run along with the crack size and number of wheel passes modelled. The cumulative total wear is not used during the modelling process, only the current wear rate for each step is used, however it is a useful additional result as it allows comparisons to be made between the vertical wear for different traffic patterns and grinding strategies. This is significant as if a rail does not require replacement due to cracks threatening its structural integrity, then the replacement criteria is usually related to a wear limit, this will be discussed further in subsequent sections.

For various traffic cases and grinding strategy combinations the crack size might reach zero at different points in the traffic pattern, or continue growing, however the wear would continue to accumulate throughout the modelling run regardless. Therefore in order to obtain the cumulative total wear for a whole modelling run, the Grinding Model was altered to continue to the end of the specified modelling run even after the predicted crack size reaches zero. The cumulative total wear only records vertical wear at the centre of the running surface of the rail due to rolling contact or grinding as included in the model. It does not take into account side wear from wheel flanges or other wear

events such as wheel slip which might also affect the wear life of the rail, these are separate wear processes and would have to be considered separately on a railway network.

The Grinding Model has been developed from the Crack Growth Model and run with contact data representing traffic patterns of frequently changing train types and occasional grinding operations. The results of these runs shows that some of the limitations of the Crack Growth Model when used to represent traffic patterns of alternating multiple vehicle types with occasional grinding have been overcome and that the Grinding Model appears to be suitable for modelling these situations. In the subsequent chapters the effects of different combinations of traffic patterns and grinding operations on predicted crack size will be investigated.



## Chapter 3. Grinding Roughness Tests

### 3.1 Introduction

In this section a program of full scale testing is described, these tests were carried out to evaluate the effect of the wheel-rail contact on the rougher rail surface that results from grinding operations. Specifically how long the rougher rail surface resulting from grinding persists in the initial stages after grinding, which in turn determines how long the increased roughness effects rolling contact fatigue crack generation and propagation, as well as the wear rate. The Grinding Model described in Chapter 2 uses fixed values for the wear rates and the crack growth rates are calculated assuming that the roughness is the steady state value that develops over a period of time after rolling contact has taken place. The stress distribution within the contact patch is dependent upon the roughness of the contacting surfaces, the greater the roughness the higher the local stresses within the contact patch. Therefore both the wear and the crack growth and initiation, when the crack is small, caused by each wheel pass is affected by the surface roughness of the rail. In this instance a small crack is one of a length such that the crack tip is in the region where the high stresses in the material surrounding the contact vary in relation to the peaks and troughs in the rail surface resulting from grinding, and are not gradually dissipated into the rail head. The rougher surface that results from rail grinding operations is characterised by sharp ridges and furrows, typically running transversely across the rail head with a slight curve to them. The horizontal distance between the tops of two neighbouring ridges, and the vertical distance from the tops of two ridges to the bottom of the furrow between them are similar, both being visibly discernible, but less than a millimetre. These distances mean that the area involved in the contact between the wheel and the rail will involve several ridges. The surface of a test sample which has been ground to represent the surface resulting from grinding with a large production rail grinder and hasn't had a wheel pass over it can be seen installed in the test site in figure 3.1 in section 3.2.3.

For the Crack Growth Model that didn't include grinding it was considered that modelling the wear rate as constant and the crack growth to be the same as calculated for the steady state rail roughness were valid simplifying assumptions. In the Grinding Model the effects of grinding on crack size are incorporated into the model, but again

the effect of increased roughness on crack growth and wear rate are not modelled. The validity of ignoring the possible effects of the roughness caused by grinding on wear and crack growth needed to be considered. It was considered that the same simplifying assumptions would remain valid if the wear rate and the rolling contact fatigue crack growth rate associated with the steady state roughness level that dominates throughout the interval between grinding operations, could be considered to be representative of the whole period between grinding operations. That is, if the proportion of wheel passes between grinding operations, for which the contact surface of the rail would be expected to exhibit roughness above the steady state level (due to grinding), is low enough for the expected effects on crack length predictions to be within acceptable error levels. Then the simplifying assumption to ignore the possible effects of the roughness caused by grinding on wear and crack growth could be considered to be valid.

Studies have been carried out into how long the grinding roughness on the contact band of the rail head persists after the grinding operation, the one that provides the most relevant information for the Grinding Model is described in a paper by Lundmark et al [3.1]. The results in this work came from measurements of rail surface roughness taken in between service trains after rail grinding had taken place. They indicated that in the Swedish heavy haul environment the roughness of the rail tended towards the steady state operating value after one day of traffic. However in that study the trend in roughness values was not obtained due to the limited number of readings that could be taken as a result of the railway being operational. Also it was carried out on a Swedish heavy haulage line, where the contact conditions would be different from those on a British mixed traffic line, due to factors such as the different weight and suspension characteristics of the vehicles. Therefore it is conceivable that the rate at which the roughness due to grinding is reduced to a steady state operating value by traffic, could be significantly different for the contact conditions represented in the modelling using the Crack Growth Model and Grinding Model, compared to the rate observed with contact conditions present during the study by Lundmark et al [3.1]. The aims of the present work were to obtain more information on the persistence of grinding roughness under known and controllable contact conditions representative of a British mixed traffic route, particularly the full roughness trend resulting from the initial contacts. In particular the aim was to capture the roughness values from the first tens of contacts, to get the full roughness trend of the early stages after grinding, since it was expected that

the roughness would change rapidly under the first few contacts. Also the previous work had shown that the roughness could be expected to approach the steady state operating value within a number of wheel passes of the order of magnitude of the number that occur in one day's worth of traffic. The present work aims to determine whether this true for harder premium grade rail steels and vehicles more representative of a UK mixed traffic route.

To study the initial stages of the trend in rail surface roughness immediately after grinding a program of tests in the full scale rail environment, with control of the number of wheel passes that the rail experienced between measurements, was designed and carried out. The test site consisted of a fishplated rail joint where the gap between the rail ends was sufficient to insert a 15mm long rail test sample; the test samples were ground in situ using a rail profile grinder. Roughness measurements were taken on the rail surface before and after, between one and 100 wheel passes of a locomotive, the locomotive being stopped to allow measurement to take place.

The specification for the test was that the contact conditions should be representative of a British mixed traffic line, as used for the inputs to the Grinding Model, and that the surface roughness of the rail should be representative of that which results from grinding operations on the rail network. Also it was required that the tests could be stopped at various stages after low numbers of wheel-rail contacts to enable roughness measurements to be taken, this would require the traffic over the test site to be a controlled part of the test procedure. In addition it was decided to test five different grades of rail steels from two different manufacturers to compare the trends in roughness for different rail steels. To meet this specification, a test site on a section of full-scale railway, dedicated to the tests, was selected such that 15mm long test samples, manufactured from specimens of each rail steel, could be inserted into the gap at the joint between two rails. The test samples were then installed in turn into the test site and ground in situ with a Rail Profile Grinder to a profile that exceeded that of the worn test site rail by approximately 1mm. For each test in turn the test sample was installed into the test site and a dedicated locomotive driven over it. Roughness measurements were taken on the rail surface before and after, between one and 100 wheel passes of a locomotive dedicated to the tests, the locomotive being stopped to allow measurement to take place. The locomotive selected for the test, an ex-British Railways Class 33

locomotive, was chosen as it was considered the most suitable of those available. This was because it is mounted on two twin axle bogies in the same basic arrangement as the vehicles modelled in the grinding model, and has a static axle loading between that of the, Class 43 and 91 locomotives represented in the modelling.

## **3.2 Test Method**

### *3.2.1 Test site*

A joint between two rails was selected as the test site, this joint consists of two rail end which are more than 15mm apart, kept in alignment by two plates, known as fishplates, fitted in the web recess bearing on the inner faces of the rail head and foot, and clamped in position by bolts that pass through the plates and rails. The greater than 15mm gap between the ends of the rails in the joint selected as the test site, which makes it suitable for inserting test samples, is greater than the specification for such joints. The gap should be just sufficient to allow for the thermal expansion and contraction of the lengths of the rail without putting the rails in sufficient compressive stress to cause buckling of track. The gap in the test site joint is above this specification, and is the exception with regard to the rest of the test track, however it is acceptable for the test track which is only rated for low speed and experiences low densities of traffic. Due to the relatively low temperatures during the testing, the gap between the rail ends in the joint was significantly more than 15mm due to the thermal contraction of the rails; this required a significant degree of packing material to constrain the test sample longitudinally. Ideally a larger sample would have been used to increase the contact length for roughness measurement and reduce the clearance between the rails; however such a test sample would possibly be too long to fit in the test site if the temperature was at the upper end of the temperature range that could be expected. The use of a pre-existing rail joint capable of accepting a test sample was chosen as the best compromise achievable for testing the effects of wheel contacts on grinding roughness on different rail materials. The installation of full lengths of specimens of rail or the design, certification and manufacture of a structure, to hold test sample and allow rail vehicles to pass across them were both beyond the resources available for the testing program.

### 3.2.2 *Test sample manufacture*

The roughness trend after grinding was tested for five types of rail steel, these were Corus grades 260, 350 and 400 and VoestAlpine grades 350 and 400. Test samples 15mm long were cut from each of the specimens of rail steel. The test samples had the foot and part of the web of the rail profile removed so that they could be slotted into the gap between the rails and fishplates. The underside of the railhead was machined, so that the rail head profile of the samples would be left protruding above the running surface of the test site by approximately 1mm, when the machined underside of the head was sitting on the fishplates. The machining of the test samples was required to achieve this alignment between the test track rails and sample, because the test track rail was heavily worn.

Final profiling of the test samples to match the test site, the generation of the surface roughness on the running surface of the test samples was carried out with a Rail Profile Grinder. Each test sample was installed in the test site for grinding in turn. The Rail Profile Grinder was used as it was the closest suitable representation of production grinding available and was capable of applying the required profile to the test samples. The use of a large production rail grinding machine was beyond the resources of the testing program. The Rail Profile Grinder was considered a suitable alternative as they are used on the U.K. rail network for the treatment of localised rail head defects and the localised re-profiling of rails, such as after the welding of joints, also the Rail Profile Grinder uses similar grinding stones to a large production rail grinding machine. The main differences between the processes are that the contact angle around the longitudinal axis, the depth of cut and the grinding pressure of the Rail Profile Grinder, are determined by the operator according to their judgement, and is therefore variable between test samples. The test sample were ground to a profile to match the test site rail, but exceeded it to a sufficient extent to ensure that the wheels of vehicles passing over the test sample made full contact with it.

### 3.2.3 *Installation*

Each test sample was installed in the test site in turn by inserting the test sample into the test site so that the machined undersides of the rail head were resting on top of the fishplates. The test samples were installed with one vertical face against the end of one

of the rails of the test site, and the gap between the other face and the other test site rail packed firmly with packing material. The packing material used is cut down track components that are fitted between rail fasteners and the rail and made from PA66 (Polyamide (Nylon) 66), which had a suitable resistance to compression and was easily shaped to fit the gap. The installed test sample can be seen in Figure 3.1.

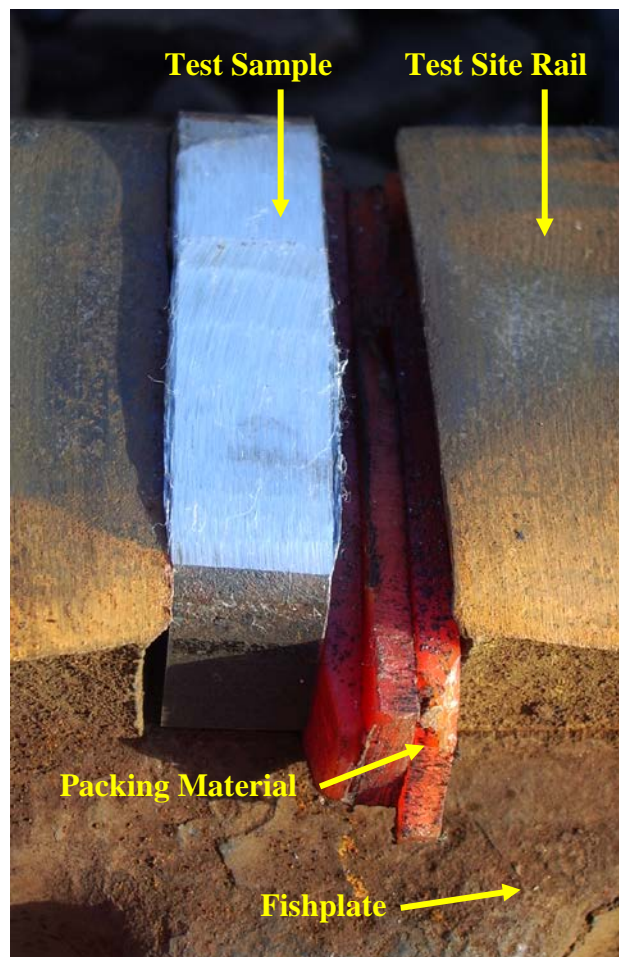


Figure 3.1. Photograph of a ground test sample installed in the test site.

#### 3.2.4 *Loading*

The test samples for each type of rail steel were tested separately, for each test the sample was installed in the test site as at the grinding preparation stage. Once installed the sample was subjected to 100 wheel passes with an ex-British Rail Class 33, four axle Diesel locomotive, the locomotive was stopped at prescribed intervals and measurements of the sample taken. The measurements taken from the sample, the measurement regime, and intervals at which the measurements were taken, are described in the next section. The wheels of the Class 33 locomotive are arranged in two

two-axle bogies, and it has an axle loading of approximately 19.5tonnes. The locomotive was driven in both directions over the test site, the direction alternating every pass of the locomotive (four wheel passes). Most locomotive passes over the test site were conducted in one movement at a speed of 10m.p.h. The exception to this was where the locomotive was stopped in mid-pass for measurements to be taken after one wheel pass, and restarted in the same direction, for the remaining three wheel passes of the first locomotive pass; in this case the braking and traction loads were kept to a minimum.

That the test sample length of 15mm and the profile of the test sample exceeding that of the test site, will have resulted in the loads and the shapes of the contact patch between the wheel and the rail, differing from those between wheels and long continuous rails of the same profile. These differences were minimised by the test sample length being as long possible and its profile matching the test site as closely as possible. The test sample profile was made such that it only exceeding that of the test site, by the minimum required to reliably ensure that the contacting wheel made full contact with the test sample. This was to ensure that all of the load was transferred through the test sample, and did not bridge the gap from one test site rail to the other. As a result of the testing being carried out when the ambient temperature was at the lower end of the expected temperature range, the thermal contraction of the test site rails meant that a longer test sample could have been used, however this would have been at the risk of the test sample being too long if the temperature had been higher. It was not possible to predict the expected rail temperature or the actual rail temperature when the test sample length was specified, so a length was selected that would fit the test site under all but exceptional circumstances. The edges of the sample would be expected to experience high contact pressures, due to the shape of the contact and load that result from the wheel having to climb onto the test sample. These contact pressures at the edges of the sample are not expected to be representative of those that a continuous length of rail would be subject to, this effect will be more pronounced on the edge of the sample next to the packing material. However it is felt that whilst the contact conditions over the centre of the test sample might not be exactly the same as for the test locomotive on long lengths of rail of the profile of the test site, they would be representative of the contacts on a mixed traffic railway network.

### 3.2.5 *Measurement technique*

The surface roughness of the test samples was recorded in three ways. The principal measurement technique was the use of a surface profiler to record the surface profiles of the test samples which were subsequently analysed to calculate the surface roughness parameters. In addition to the surface profiles, the surface of the test samples were photographed at every measurement interval and replicas made at selected measurement intervals of selected test samples.

The surface profiles were recorded using a Surtronic 25 surface profiler has a resolution of  $0.01\mu\text{m}$ . It was mounted on a removable bracket attached to the test site rail, as shown in figure 3.2, and linked to a laptop computer for profile storage and analysis. The profiles were saved unfiltered and the analysis was conducted after all of the tests had been completed, the roughness parameters generated by the profiler after each measurement were not recorded, and only used as a rough guide to the development of the surface roughness of the samples as the test were carried out. At each measurement interval five 8mm longitudinal profiles were taken, one at each of the five locations distributed transversely 10mm apart, with the middle profile coinciding with the centreline of the rail. The 8mm longitudinal profile was selected as the majority of the grinding roughness was aligned with the groves and ridges running in a general transverse direction. Taking profiles across these grinding marks ensured that the full severity of the roughness was recorded, rather than a transverse profile that might run along the features for the majority of its path. Also the minimum radius of curvature that the profiler could cope with was greater than that at the outer measurement locations, even for profiles of 4mm in length. Longitudinal profiles of 8mm were recorded from the centre of the 15mm long samples, rather than using a longer profile. This was because trials of the test procedure, indicated that the profiles beyond the 8mm centre region, exhibited a more rapid change in longitudinal surface profile, that was not consistent with that in the centre and, at the outer edges, bulk plastic flow. These differences were attributed to the unrepresentative contact conditions at the ends of the sample, and the wheel contact climbing onto the test samples at the unsupported edges of the sample respectively. Therefore the measurements were concentrated on the 8mm centre region which was felt to be representative of a mixed traffic railway wheel on rail contact.





Figure 3.2. Surtronic 25 Surface Profiler, mounted on the rail head, taking a profile reading from the test sample. The five lateral locations are marked (A to E) on the test site rail next to the test sample. Location A being nearest the gauge corner (furthest from camera).

A photograph of the test sample was taken at each measurement interval, these were taken looking vertically down on the test samples using a hand held compact digital camera. These photographs provide a record of the visual appearance of the test samples surface roughness associated with the recorded profiles, and features, such as the locations of the running band(s), to be identified. The photographs also act as a useful reference that allows the possible causes of any step change in the roughness trends to be identified, such as the shifting of the test samples position or surface contamination on the test sample and adjoining test site rail.

Replicas of the test samples surface roughness were taken using Microset 101 Replicating Compound. This two-part compound was mixed and applied to the running surface of certain test samples at certain measurement intervals and allowed to cure. The surface of the test samples was cleaned in a non-abrasive manner, before the application of the compound to remove any contamination. The viscosity of the compound is sufficiently high that its application did not require any forming to keep it in place on the test samples while it cured, the curing time varied with temperature and was between 5 and 15 minutes. The curing time of the replicating compound precluded replicas being taken at every measurement interval, and for all of the test samples and

within the test program. The cumulative contact loads on each test sample through the test program mean that, once the roughness profile is recorded at each measurement interval, the opportunity to get more information from the test sample at that stage of the test is lost as subsequent wheel passes alter the surface of the test sample. Taking replicas of the test samples allows the surface roughness information at that stage of the tests to be saved for later analysis. The analysis of the replicas can be of the whole running surface, and can take place in more detail than is possible in the field during the testing program.

### 3.2.6 *Test procedure*

In addition to the measuring equipment, the test procedure required the dedicated use of the test site and adjacent track, the locomotive and its driver, and two test personnel. One of the test personnel was principally responsible for the taking of measurements, and the other was principally responsible for the test, including the coordinating between the operation of the locomotive and the taking of measurements, to ensure safety. All of the measurements were taken with the test samples installed in the test site; this ensured that the initial and final measurements were taken under the conditions as the intermediate measurements of each test. At the start of each test the test sample being tested was installed and the first set of measurements taken, then the locomotive was driven over the sample at a crawl until the first wheel had passed over the test sample, and stopped before the second wheel made contact. Measurements were then taken, the locomotive being secured and its diesel engine shut down so that the vibrations from it didn't interfere with the surface profiler. After these measurements had taken place the locomotive was re-started and continued in the same direction over the test sample at a crawl, applying a further three wheel contacts to it, making a total of four contacts for the test. At this stage the locomotive was driven away from the test sample further along the track adjoining the test site to wait whilst measurements were carried out. Once the measurements following the application of four wheel contacts had been taken further wheel contacts were applied by the locomotive passing fully over the test sample with all wheels (on the rail containing the test sample) in one movement at about 5 m.p.h.. After the required number of wheel passes had been applied to reach the next measurement interval, with the locomotive reversing its direction of travel every four wheel passes where necessary, the locomotive was stopped away from the

test site, and the measurements taken. Table 3.1 below shows the types of measurements and the intervals at which they were taken, the units of the measurement interval are the number of individual wheel passes applied to the test samples. The measurement regime was weighted towards the early stages of roughness development, that is, the measurement operations were concentrated towards the initial wheel passes.

Table 3.1. Measurement Regime.

Measurement Interval (No. of wheel passes over sample)	0	1	4	8	12	16	32	64	100
	Initial state								
Profile Measurements	X	X	X	X	X	X	X	X	X
Photographs	X	X	X	X	X	X	X	X	X
Replica (Corus grades 260, 350 and 400 Only)	X	X	X		X		X		X

### 3.2.7 *Measurement Recording*

To ensure that the numerous measurements taken during the tests were recorded and correctly associated with the information identifying which measurements they were, the following procedures were adopted. The profiles that the surface profiler output to the laptop were each saved with a file name that incorporated a code, indicating which test sample, measurement interval and transverse location it was recorded from. The digital camera numbered each photograph sequentially and a log was kept of which photograph number corresponded to which test sample and measurement interval. Only one replica was formed at a time, once it had cured, it was removed from the test sample and placed in a sealed sample bag, which was marked with the test sample and measurement interval that it came from.

## 3.3 **Profile Analysis**

Studying the raw surface profiles generated by the surface profiler only allows general visual comparisons to be made between different measurements. To allow quantitative comparisons to be made between measurements, that quantify the trend in roughness for each test sample, the profiles need to be analysed. To do this the raw profile results need

to be filtered to separate the roughness from the waviness of the profiles and the roughness parameters calculated.

### 3.3.1 *Roughness Parameter Calculation*

The roughness parameters calculated from the roughness profiles are described below as are the reasons that the Rz, Ra and Rsk values were selected to compare the roughness of the samples throughout the tests:

- Rz, Average of the peak to trough height range over several sample lengths.
  - Selected to study the change in height of the roughness.
- Rt, Maximum peak to trough height range over the whole profile
- Ra, "Arithmetic mean deviation of the assessed profile"
  - Selected as it is a commonly used roughness parameter and would allow for direct comparison between the results of this study and those of other studies that calculated it. Also this parameter is often used in standards, guidelines and contracts to specify the required tolerances for grinding roughness. Therefore it is important to calculate this parameter to compare the roughness of the test samples with network specifications.
- Rq, "Root-Mean-Square (RMS) deviation of the assessed profile"
- Rsk, "Skewness (asymmetry) of the assessed profile". Is used as a measure of the skewness of the roughness profile, that is what proportion of the roughness is above or below the mean line of the profile, the more negative the value the more of the roughness below the mean line deviates from the mean line relative to the roughness above the mean line.
  - The expected initial pattern of roughness modification was that the peaks of the grinding roughness would be removed by wear and plastic deformation to a greater extent than the troughs. This would result in the trend of the value tending towards a negative minimum, with more wheel passes. Following the negative minimum it would be expected that, as the material that contained the grinding roughness was worn away completely, the value would tend towards its characteristic steady state value. It was not expected that the test procedure would apply sufficient wheel passes to remove the grinding marks completely. Therefore this parameter was selected to monitor this expected trend.

### 3.3.2 Whole Profile Analysis Method

The techniques employed in the analysis of the whole profile are described below, with example profile measurements. An example of the profiles recorded during the test is shown in (figure 3.3), this shows the recorded profile for the initial measurement (i.e. before any wheels pass over sample) taken at location A on the Corus grade 260 sample.

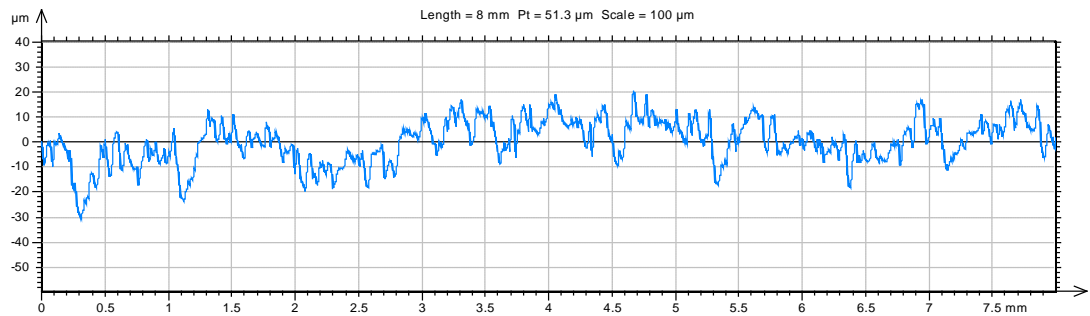


Figure 3.3. Recorded profile taken at location A, Corus grade 260 sample, initial measurement.

Recorded profile filtered to separate the waviness and roughness profiles (Figures 3.4 and 3.5 respectively) from the measured profile, using a Robust Gaussian filter with a cut off of 0.8mm. The Robust Gaussian filter was selected since it is less affected by local features (such as valley/scratches), so that the mean line remains representative of the trend. The cut off value of 0.8mm was used since this was most effective at separating the roughness from the waviness and the length of the measured profile was long enough to include several samples.

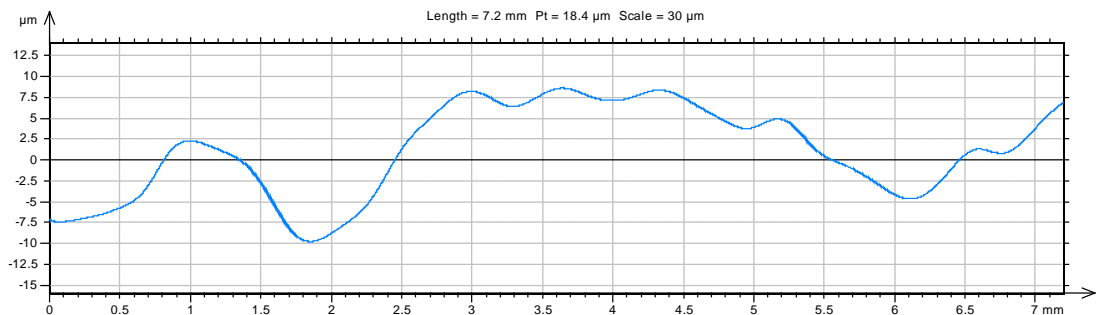


Figure 3.4. Waviness profile filtered from recorded profile taken at location A, Corus grade 260 sample, initial measurement.

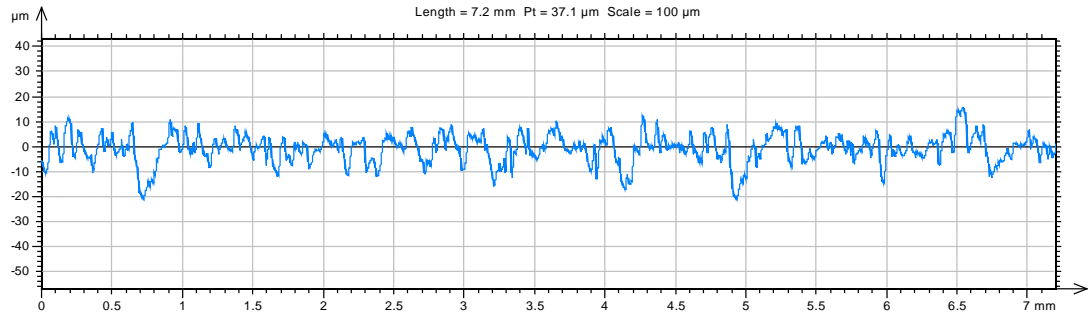


Figure 3.5. Roughness profile after filtering out of waviness from recorded profile taken at location A, Corus grade 260 sample, initial measurement.

The roughness parameters, defined in section 3.3.1, were then calculated from the roughness profile using the same filtering as the waviness and roughness separation operation for the same reason. Table 3.2 shows the roughness parameter results calculated from the roughness profile in figure 3.5. The filter and cut off selected were applied to all of the filtering operations and parameter calculations so that the results were comparable.

Table 3.2. Roughness parameter values calculated from, roughness profile filtered from recorded profile (Figure 3.5), for initial measurement (no wheel passes) of Corus 260 grade sample, at location A.

ISO 4287			
Amplitude parameters - Roughness profile			
Roughness parameter	Value	Units	Parameters Filter
Rz	24.7	µm	Robust Gaussian Filter, 0.8 mm
Rt	36.1	µm	Robust Gaussian Filter, 0.8 mm
Ra	4.31	µm	Robust Gaussian Filter, 0.8 mm
Rq	5.62	µm	Robust Gaussian Filter, 0.8 mm
Rsk	-1.13		Robust Gaussian Filter, 0.8 mm

Figures 3.6-3.8 and Table 3.3 illustrate the same analysis process as described previously, for the same sample and location after been subjected to 100 loco wheel passes. Comparison with figures 3.1-3.3 and table 3.2 gives an example of the changes that occurred in the roughness of the samples between the start and end of the tests.

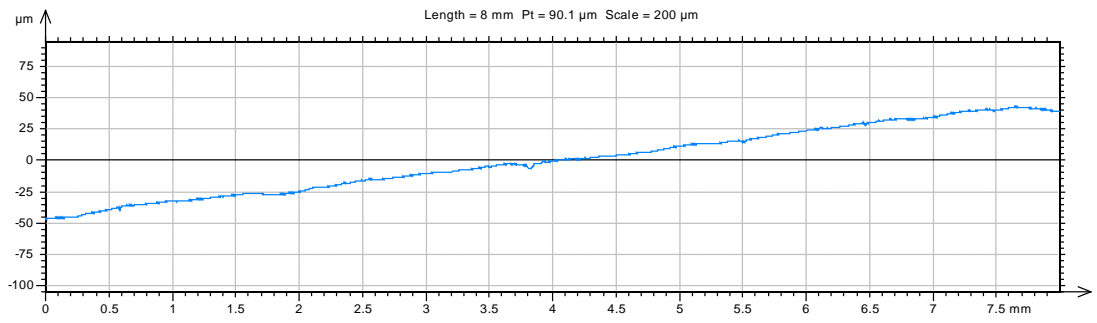


Figure 3.6. Recorded profile taken at location A, Corus grade 260 sample, measurement taken after 100 wheel passes.

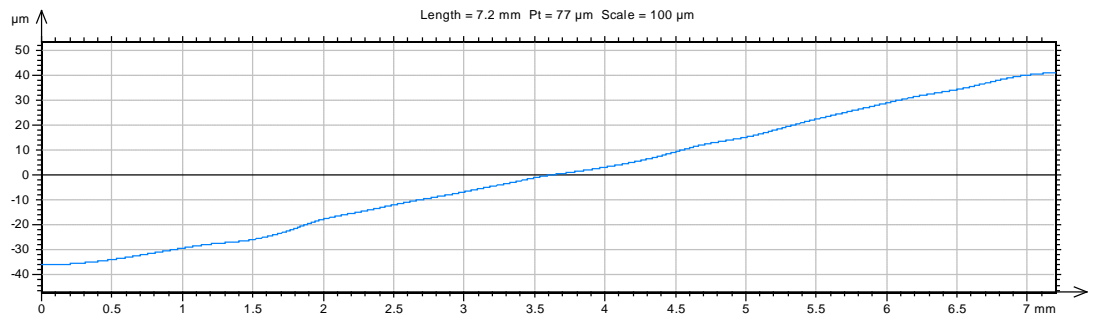


Figure 3.7. Waviness Profile filtered from recorded profile taken at location A, Corus grade 260 sample, measurement taken after 100 wheel passes.

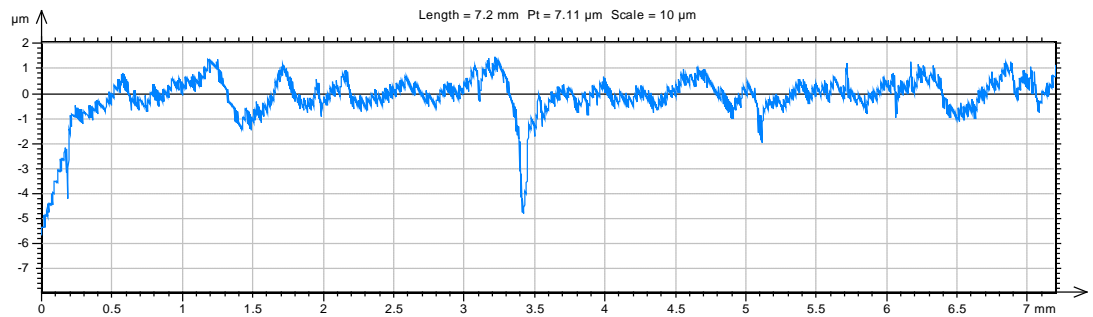


Figure 3.8. Roughness profile after filtering out of waviness from recorded profile taken at location A, Corus grade 260 sample, measurement taken after 100 wheel passes.

Table 3.3. Roughness parameter values calculated from, roughness profile filtered from recorded profile (Figure 3.8), for measurement taken at location A, after 100 wheel passes over Corus 260 grade sample.

ISO 4287			
Amplitude parameters - Roughness profile			
Roughness parameter	Value	Units	Parameters Filter
Rz	2.54	μm	Robust Gaussian Filter, 0.8 mm
Rt	6.39	μm	Robust Gaussian Filter, 0.8 mm
Ra	0.373	μm	Robust Gaussian Filter, 0.8 mm
Rq	0.521	μm	Robust Gaussian Filter, 0.8 mm
Rsk	-4.21		Robust Gaussian Filter, 0.8 mm

### 3.3.3 Selected Section Profile Analysis Method

The configuration of the test sample installation was such that the test samples were higher than the test site rail. This arrangement of the test samples was to ensure that the wheels of the test locomotive would be in contact with only the test samples as they passed over the middle portion of the test samples, and that the contact would not be divided between the middle portion of the test samples and the test site rails (which might have occurred if the test samples were lower than the test site rails). The situation where the wheel contact was divided between the test site rails and the test samples will have occurred at the leading and trailing edges of the test samples as the wheels transitioned to and from the test sample, and this will have resulted in the contact conditions at these locations on the test samples being different to those between a wheel and a continuous rail. Therefore the effects of the wheel contacts on the surface roughness at the leading and trailing edges of the test samples will not have been representative of wheel contacts with a continuous rail. A section approximately 4mm in length was selected from the centre of each measured profile for the roughness parameters to be calculated from. This was done to remove the influence, of the contact conditions at the leading and trailing edges of the samples not being representative of a continuous rail, on the roughness parameter calculations.

In the example case shown in Figure 3.9 the section selected for the roughness profiles of all measurement intervals taken of that sample and location was between 2mm and



5.5mm (as denoted by the section between the two vertical marks). The measured profile used for this example is the same as that used in the first example of the analysis of the whole profile (initial measurement of the Corus grade 260 sample at location A); this allows a comparison between the results of the two analysis methods to be made, to show the effects of the different analysis methods. The selected section is shown in Figure 3.10. The start and end points of the section selected was determined by a set of criteria that included the elimination of end effects evident in the full profile of all of the profiles taken at each measurement interval for that test sample and location. The same range of the measurement profile was selected for all measurement intervals for each test sample and location to ensure that the length of the selected profile section would be the same in all cases so that the trend in the calculated roughness parameters between measurement intervals was not affected by a difference in profile length that the parameters were being calculated upon. Also the limits of the selected section was kept constant so that the development of the roughness could be studied for a specific section of the sample and thus the trend in roughness of that section of the sample could be established. The measurement device was placed in the same longitudinal position on the rail for each measurement, in so far as was practicable, however there will have been some error in the placing of the measurement device and therefore the start and end points of the full profile, we estimate that this error was  $\pm 1$ mm. The end effects of the profile that were eliminated as far as possible from the selected section of profile (whilst retaining a long enough sample and taking into account the error in the start and end points of the profile relative to the test sample) were indicated by the waviness profile sloping down towards the ends of the full measurement range, or significantly reduced roughness at the ends of the full measurement range indicating increased contact pressure at the ends of the sample. It was felt that it was important to remove the edge effects from the results, in so far as it was possible, so that the results would be more representative of the conditions in long sections of rail and the conclusions that were drawn from them would be more transferable to regular railway operations.

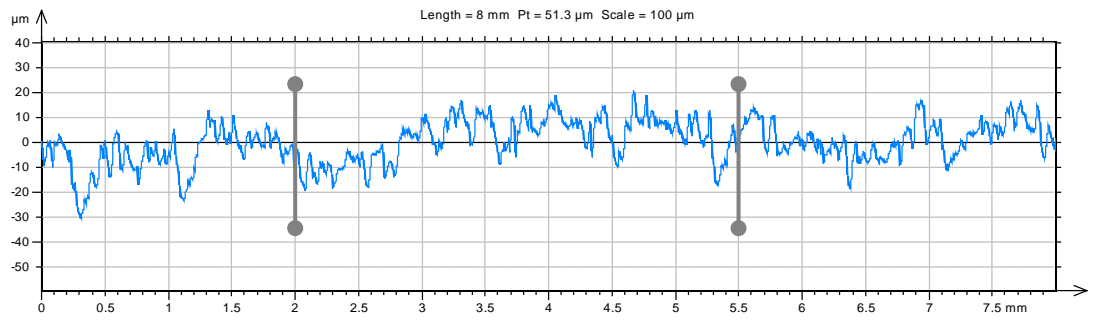


Figure 3.9. Recorded Profile, taken at location A, Corus grade 260 sample, initial measurement. Section of profile selected for roughness analysis between vertical lines.

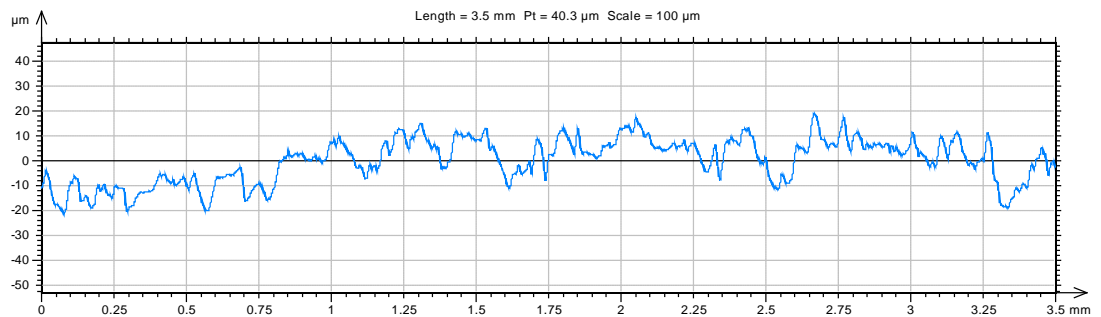


Figure 3.10. Selected section of the recorded profile shown in Figure 3.9, range of selection 2-5.5mm.

The roughness was then separated from the waviness of the selected section, using the same filtering operation as for the whole profile. Figure 3.11 shows the roughness profile that results from the filtering of the selected section of profile shown in Figure 3.10. The roughness parameter values, defined in section 3.3.1, were calculated from the roughness profile in Figure 3.11 and are shown in Table 3.4.

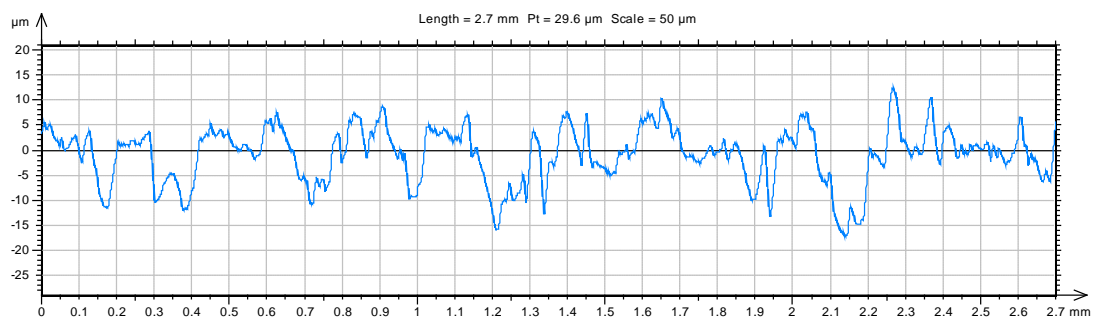


Figure 3.11. Roughness profile filtered from selected section of recorded profile (Figure 3.10)

Table 3.4. Roughness parameter values calculated from, roughness profile filtered from selected section of recorded profile (Figure 3.11), for initial measurement (no wheel passes) of Corus 260 grade sample, at location A.

ISO 4287			
Amplitude parameters - Roughness profile			
Roughness parameter	Value	Units	Parameters Filter
Rz	22.7	μm	Robust Gaussian Filter, 0.8 mm
Rt	29.2	μm	Robust Gaussian Filter, 0.8 mm
Ra	4.07	μm	Robust Gaussian Filter, 0.8 mm
Rq	5.04	μm	Robust Gaussian Filter, 0.8 mm
Rsk	-0.336		Robust Gaussian Filter, 0.8 mm

The roughness parameters values were calculated from both the whole and selected section of the filtered roughness profile for each profile recorded. The presentation of the results of is discussed in the next section.

### 3.4 RESULTS

#### 3.4.1 *Whole Profile Roughness Results*

The results of Rz, Ra and Rsk, for all test samples at each location, were plotted against the number of wheel passes, on separate graphs for each parameter to enable a comparison to be made of how each of the steels responded to the wheel passes at a particular location. Figures 3.12-3.14 show the roughness parameter results calculated from the whole profile at location A for all steels, Rz is plotted on Figure 3.12, Ra is plotted on Figure 3.13, and Rsk is plotted on Figure 3.14.

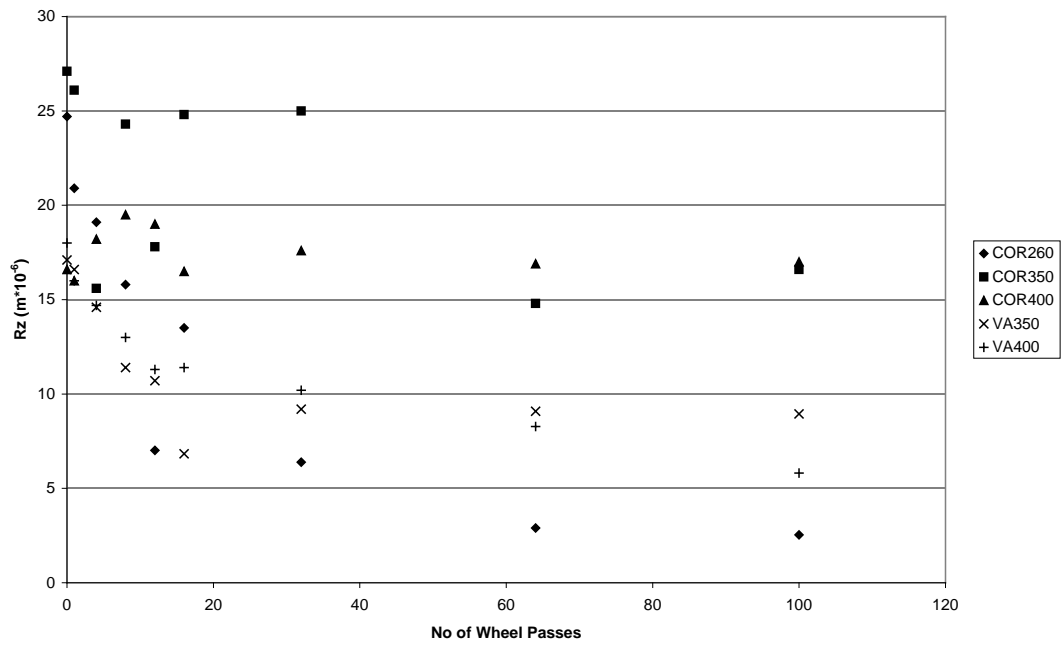


Figure 3.12. Rz roughness values calculated from the whole profile measured at location A, plotted against the number of wheel passes that had taken place when the measurements were taken, for all the different rail steels tested.

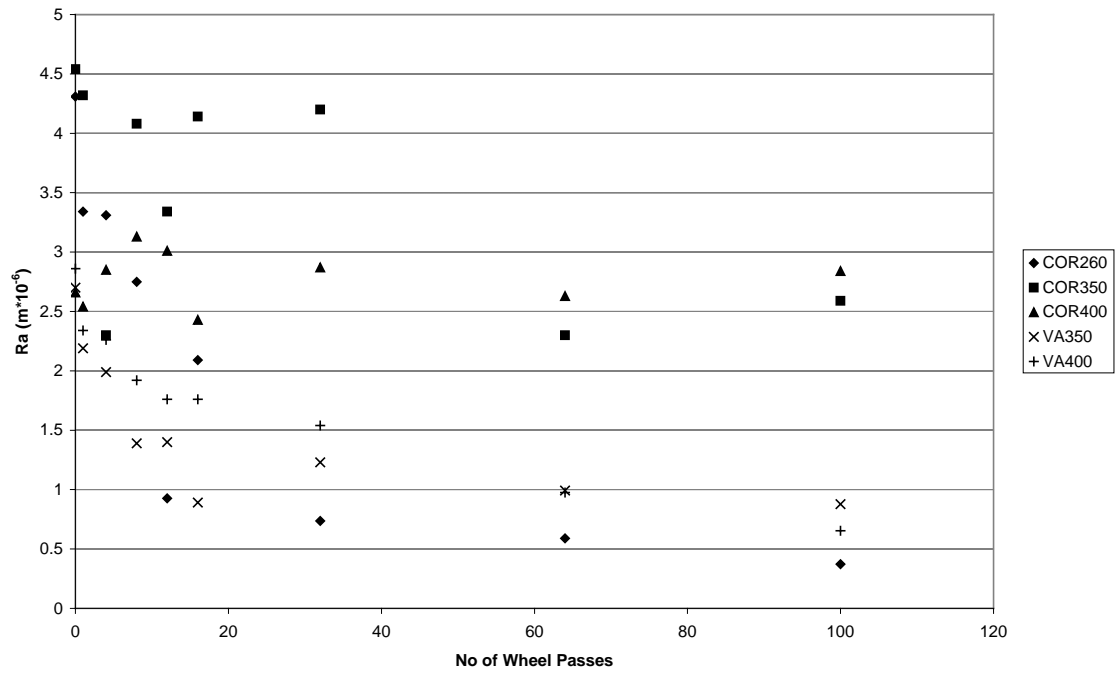


Figure 3.13. Ra roughness values calculated from the whole profile measured at location A, plotted against the number of wheel passes that had taken place when the measurements were taken, for all the different rail steels tested.

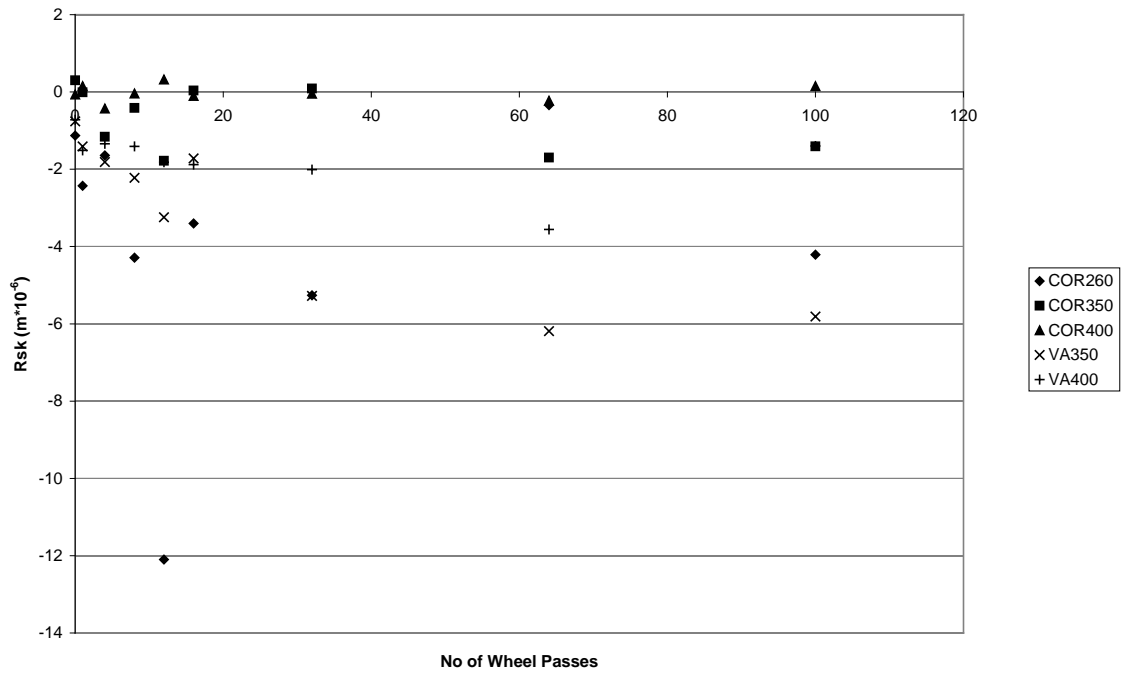


Figure 3.14. Rsk roughness values calculated from the whole profile measured at location A, plotted against the number of wheel passes that had taken place when the measurements were taken, for all the different rail steels tested.

### 3.4.2 Selected Section Profile Roughness Results

Figures 3.15-3.17 show the roughness parameter results calculated from the selected sections of the profiles taken at location A for all steels, Rz is plotted on Figure 3.15, Ra is plotted on Figure 3.16, and Rsk is plotted on Figure 3.17.

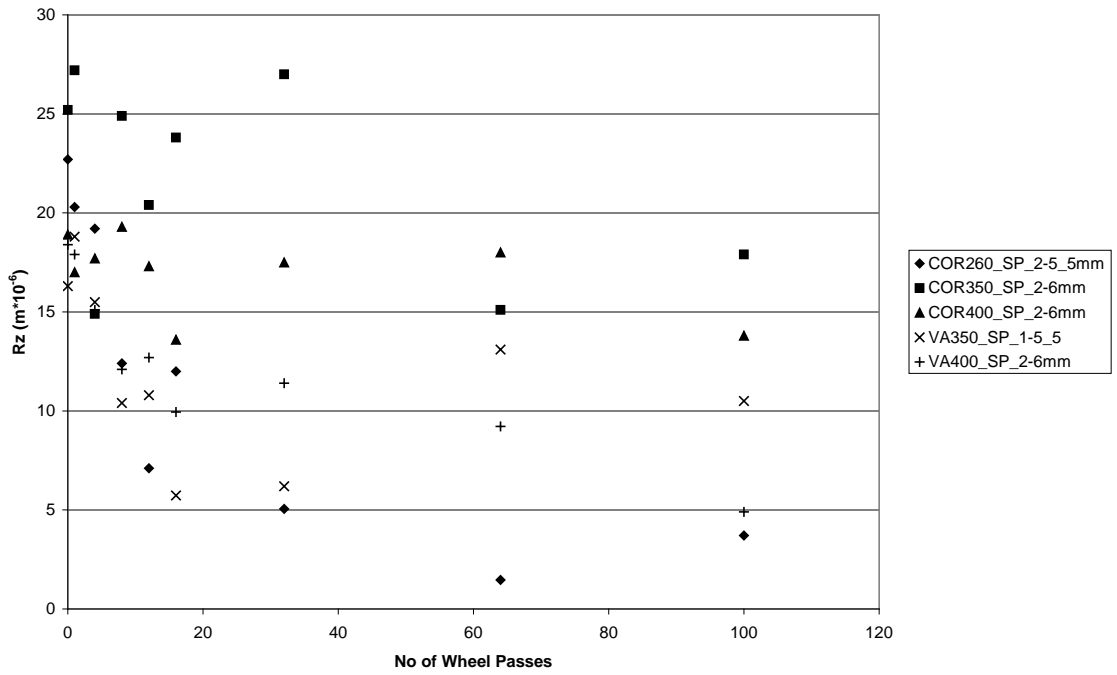


Figure 3.15. Rz roughness values calculated from the selected sections of the profile measured at location A, plotted against the number of wheel passes that had taken place when the measurements were taken, for all the different rail steels tested.

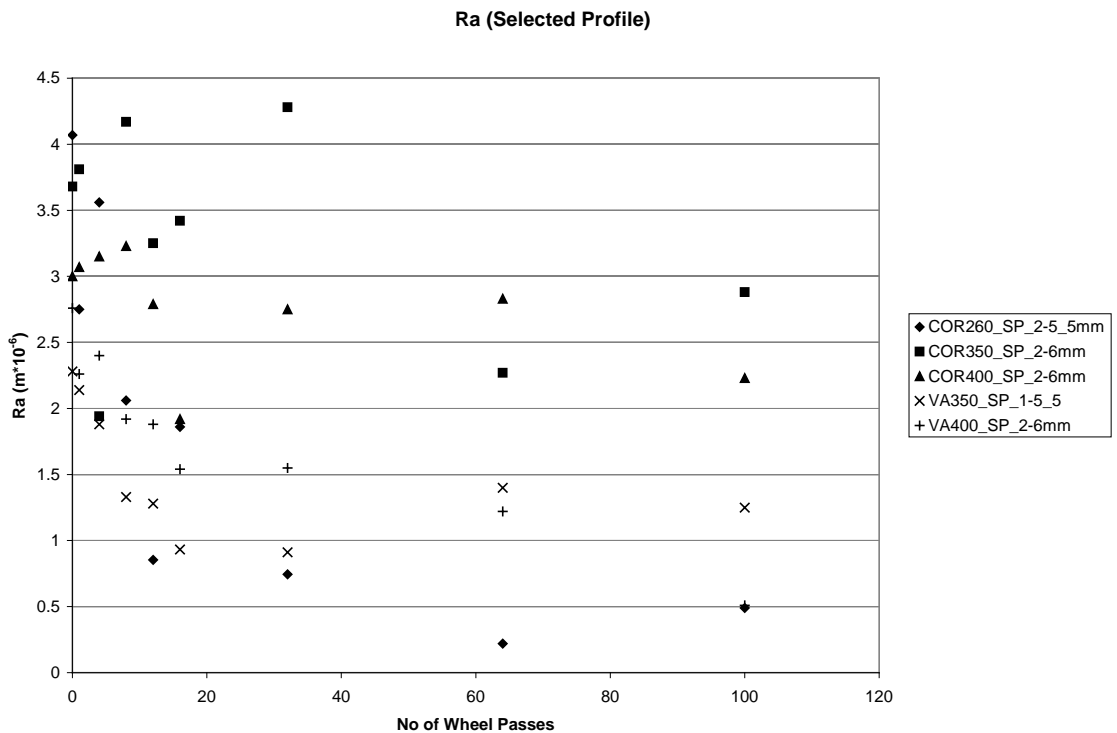


Figure 3.16. Ra roughness values calculated from the selected sections of the profile measured at location A, plotted against the number of wheel passes that had taken place when the measurements were taken, for all the different rail steels tested.

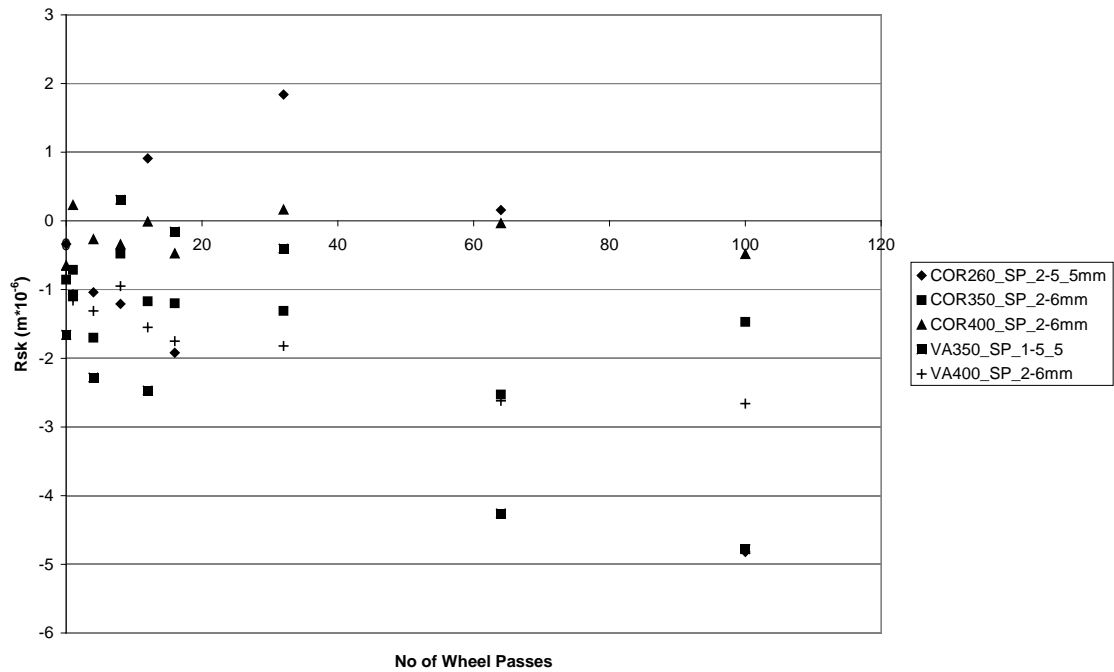


Figure 3.17. Rsk roughness values calculated from the selected sections of the profile measured at location A, plotted against the number of wheel passes that had taken place when the measurements were taken, for all the different rail steels tested.

The results from the selected section of the profile appeared to be more consistent and less susceptible to influence and variation generated by the experimental technique. This is due to the contact conditions of the selected section being more representative of those between a wheel and a continuous rail, as the selection omits the sections of the profile where the wheels of the locomotive were in the process of transitioning from the test site rail to the test sample. Therefore for the further analysis of the results, it is the results from the selected section of the profile that will be used from this point onwards to analyse the effect of the wheel contacts on the roughness of the test samples.

### 3.4.3 Summarised Results

Direct comparison of the results taken at the same location from the different test samples, is not the most informative way of analysing the results, to gain insight into the response of the roughness on each test sample to the wheel contacts, or compare the responses of the different test samples. This is because each test sample was not expected to have the same contact history at each measurement location and the significance of any lateral variation in the measurement location. The reasons for these variations, and their significance, are described in the following section. To gain an

overview of the effect of the wheel contacts on the roughness of the test samples, the average of the roughness parameter results at all locations where calculated for each combination of measurement interval and test sample, these are plotted in figures 3.18-3.20 below.

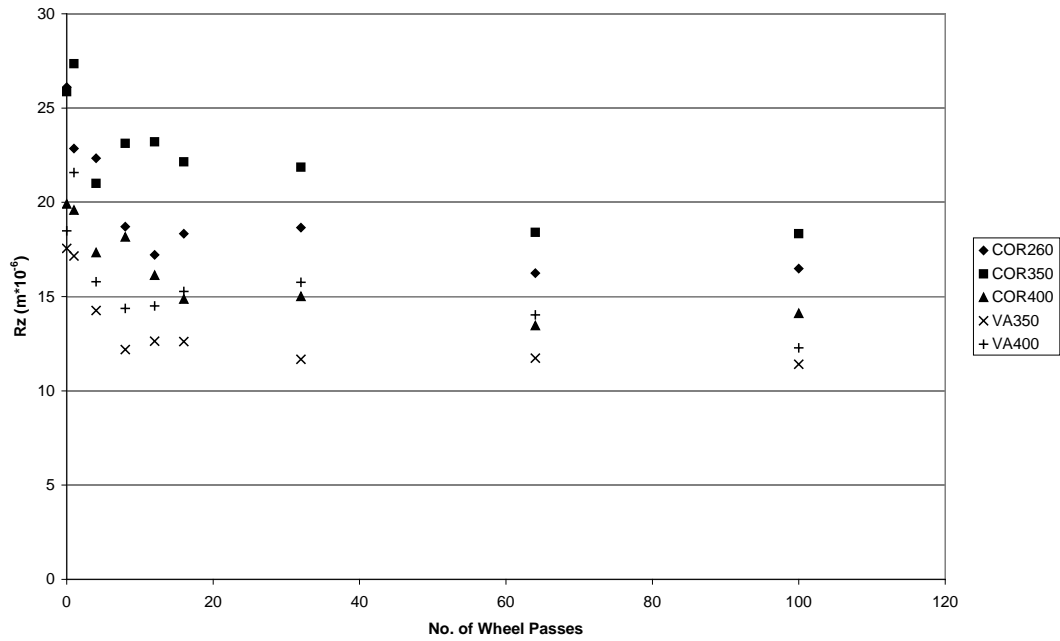


Figure 3.18. Average of Rz parameter values at all measurement locations plotted against measurement interval for all test samples.



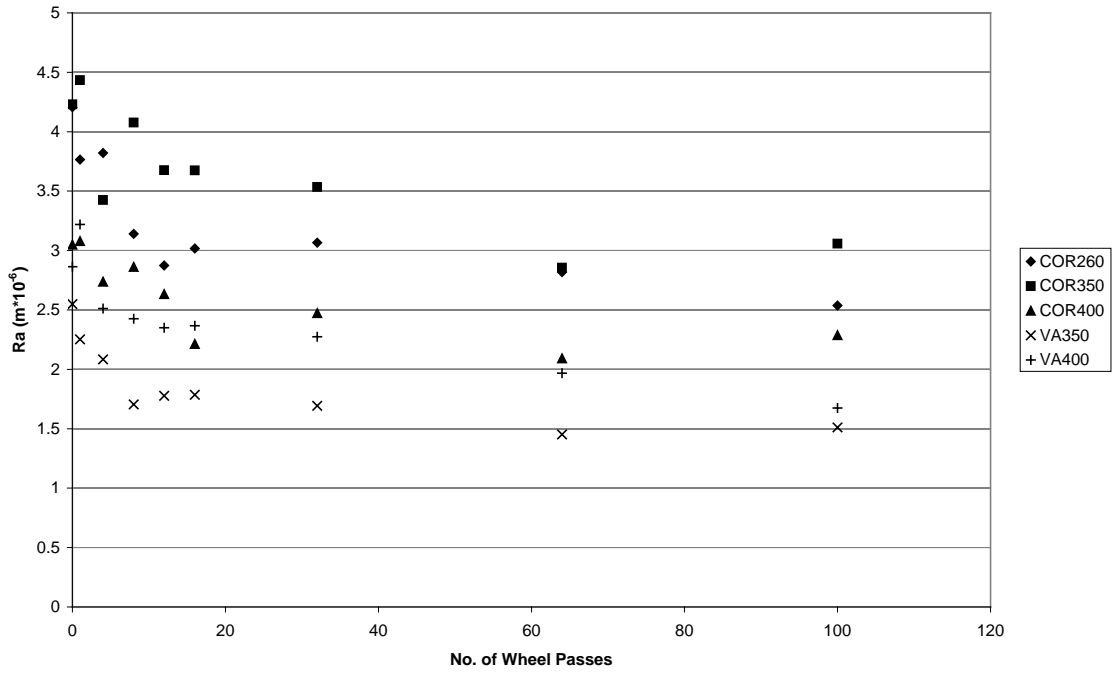


Figure 3.19. Average of Ra parameter values at all measurement locations plotted against measurement interval for all test samples.

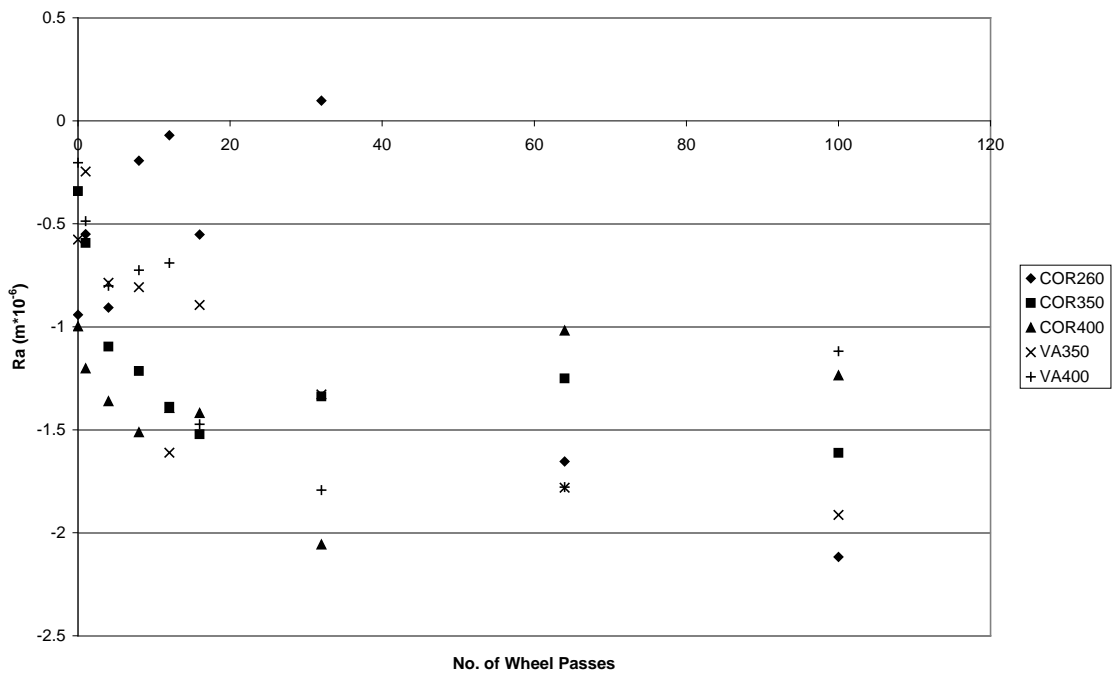


Figure 3.20. Average of Rsk parameter values at all measurement locations plotted against measurement interval for all test samples.

Whilst the averaging of the roughness parameter results gives an overview of the effect of the wheel contact on the roughness of the test sample, it does not represent the extremes of the effect of the contact on roughness. The aim of the tests was to determine

how long the roughness persists at the contact location to affect the propagation rates of Rolling Contact Fatigue cracks, so it is the areas of the contact that experience the highest contact pressures that are of particular interest, since this is where the contact stresses and therefore crack growth rates are highest. The locations that experienced the highest contact stresses can be inferred from the results, as the locations that experienced the greatest change in roughness parameter values. To study the variation in which areas of the test sample experienced the greatest changes in roughness parameter values, the minimum value at each measurement interval of all the measurement locations for each test sample and roughness parameter are plotted in Figures 3.21-3.23 below.

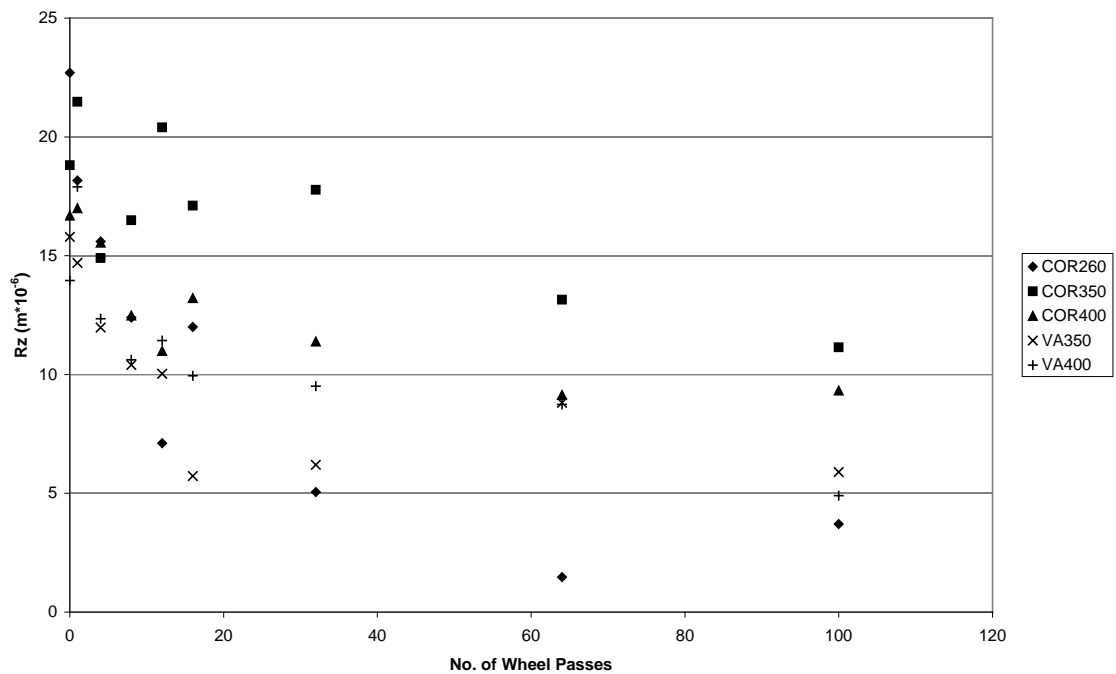


Figure 3.21. Minimum Rz roughness parameter value of all measurement locations for each test sample, plotted against measurement interval.

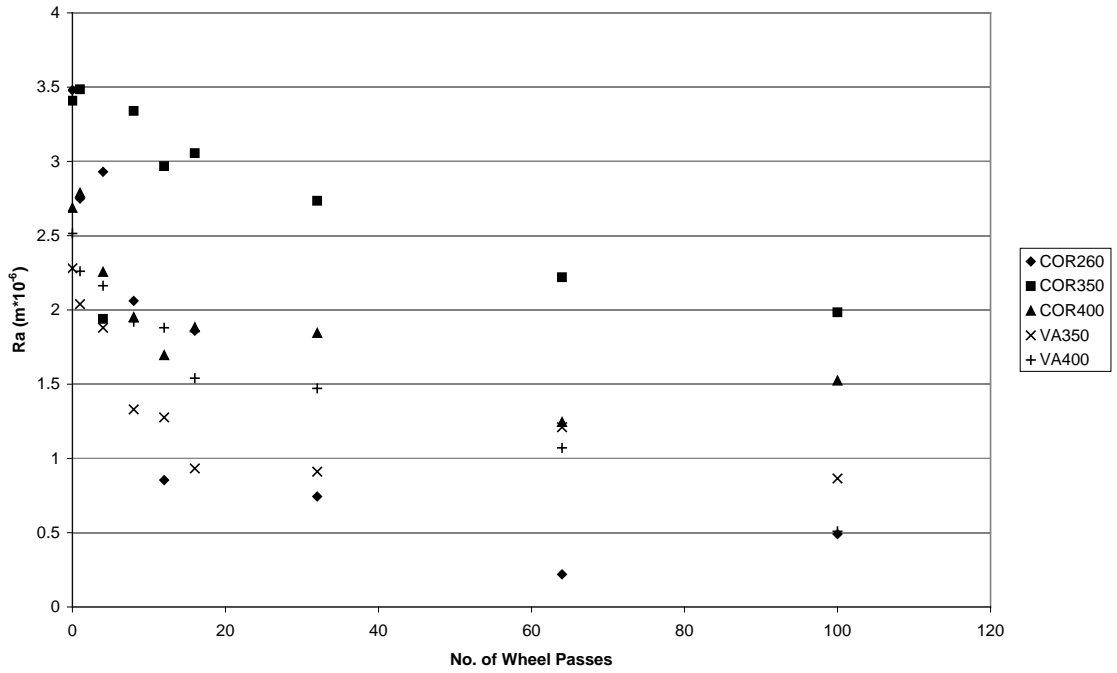


Figure 3.22. Minimum Ra roughness parameter value of all measurement locations for each test sample, plotted against measurement interval.

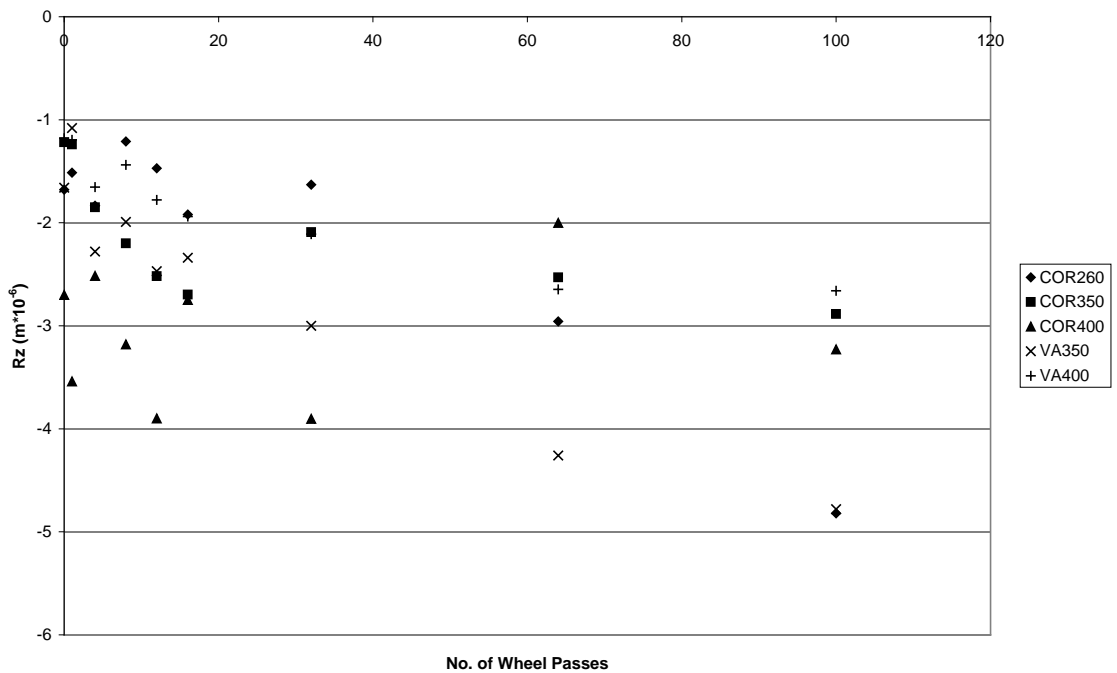


Figure 3.23. Minimum Rsk roughness parameter value of all measurement locations for each test sample, plotted against measurement interval.

The measurement location which exhibited the minimum roughness parameter value at each measurement interval, which are plotted in Figures 3.20-3.23, differed between

measurement intervals. Example plots of where the minimum and maximum roughness parameter values occurred at each measurement interval for selected test samples and roughness parameter are shown in Figures 3.24, 3.26 and 3.27 below. The maximum and minimum Rz values corresponding to the locations in figure 3.24 are plotted in figure 3.25.

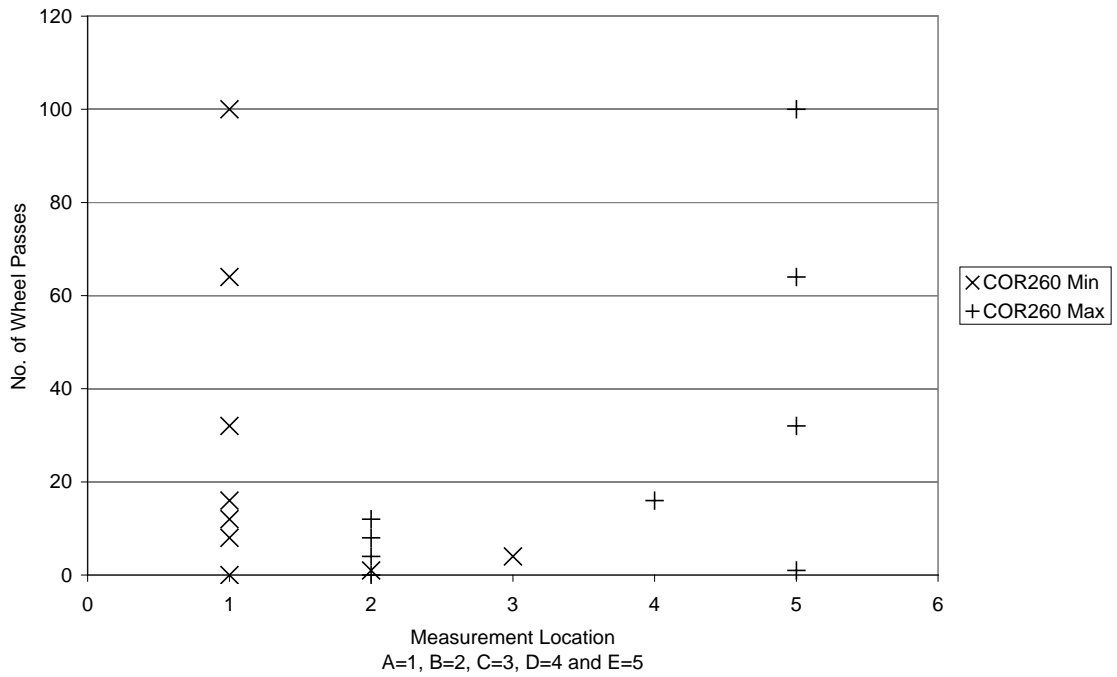


Figure 3.24. Locations of the maximum and minimum Rz roughness parameter values plotted against the measurement interval for the Corus 260 grade test sample.

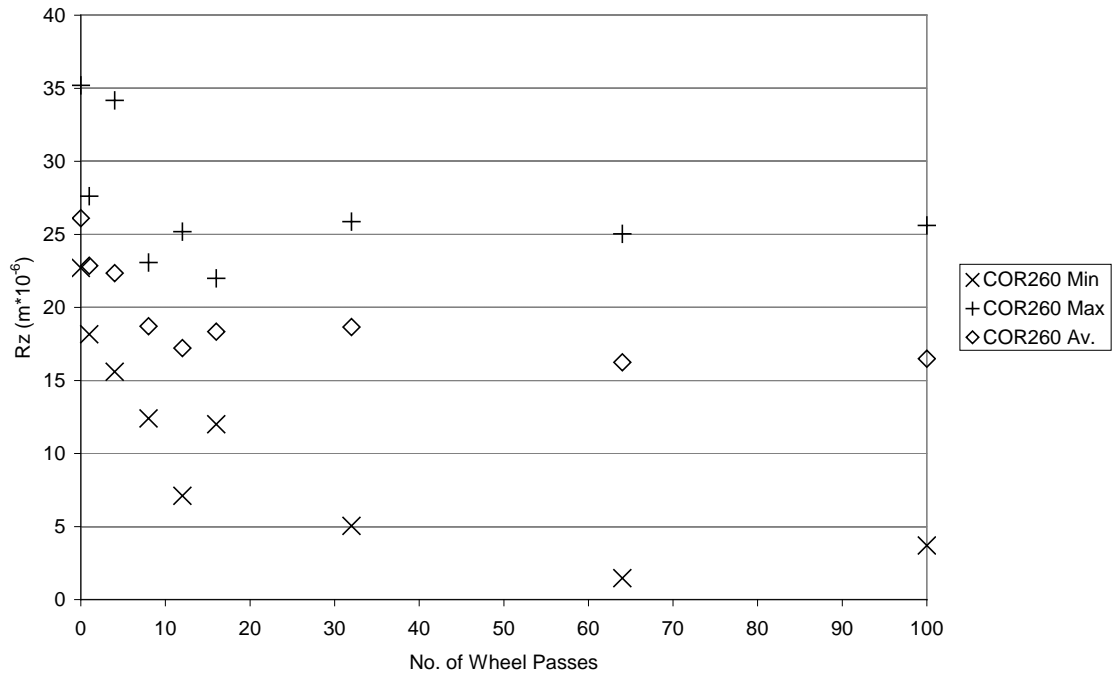


Figure 3.25. The maximum and minimum Rz roughness parameter values plotted (along with the average of the values at all measurement locations) against measurement interval for the Corus 260 test sample. These are the values that correspond to the measurement locations plotted in Figure 3.24.

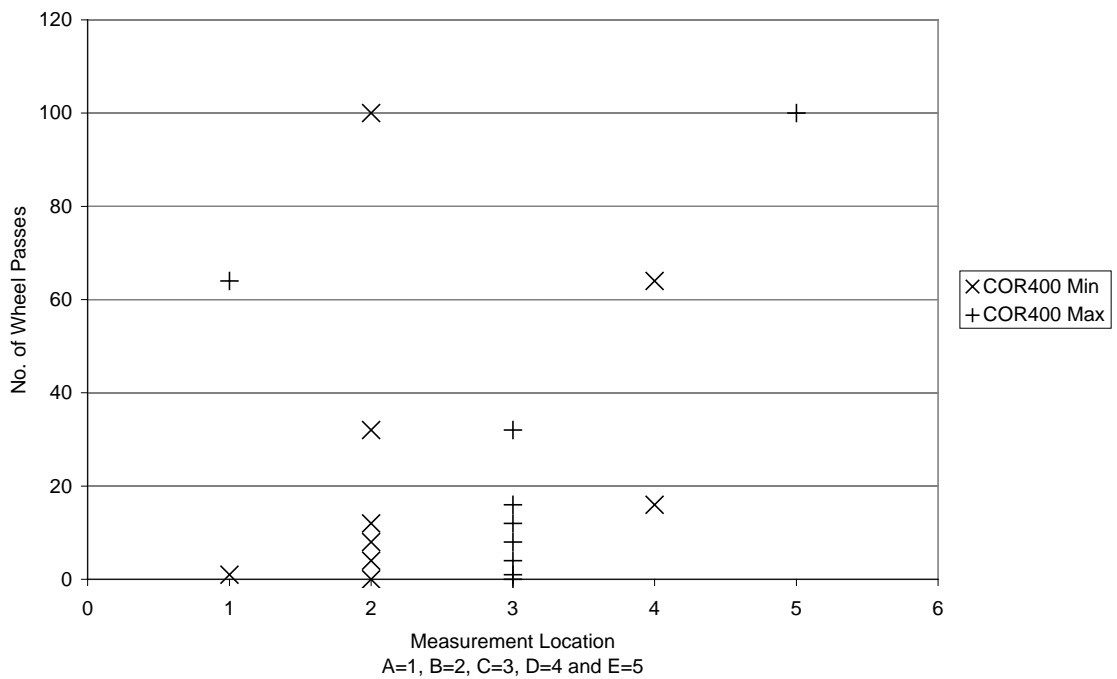


Figure 3.26. Locations of the maximum and minimum Rz roughness parameter values plotted against the measurement interval for the Corus 400 grade test sample.

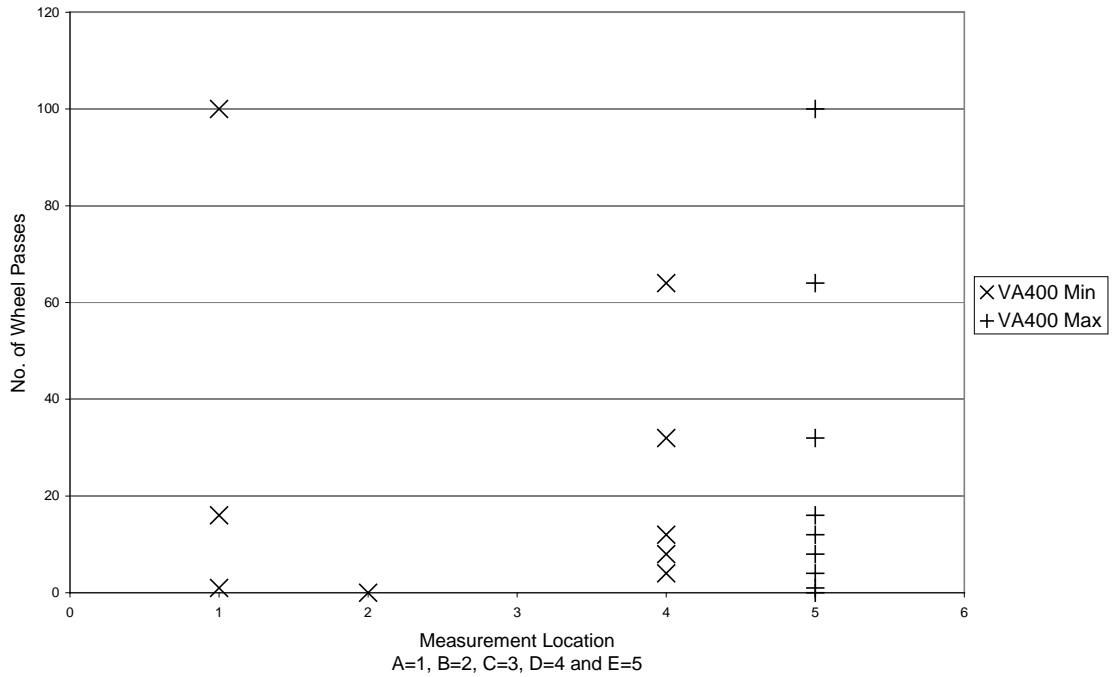


Figure 3.27. Locations of the maximum and minimum Rz roughness parameter values plotted against the measurement interval for the VoestAlpine 400 grade test sample.

### 3.5 Discussion

#### 3.5.1 Scatter

The roughness parameters calculated from the profile for each combination of test sample and location, showed significant scatter about the general trend in roughness parameter values. Possible sources of this scatter are:

- The error in the lateral location of the surface profiler and sample, resulting in measurements taken at the same nominal location at different stages of the tests, being taken on areas that have a different contact load history. This is likely to be more significant if the measurement location coincides with the edge of the contact patch or it is near to the boundary between two grinding facets. These circumstances would result in a rapid change in contact pressures at the contact for only a small lateral difference in the location at which the profile is measured.
- The error in the longitudinal location of the surface profiler support bracket. This will have resulted in the measurements taken at the same nominal location at different stages of the tests having a slight variation in the longitudinal section of the test sample included in the profile measurement. There will also have

been a minor variation in the longitudinal location of the measurement device relative to the support bracket. However this is likely to be insignificant as the measurement device was pressed firmly against the inside of the vertical face of the bracket before each measurement.

- Difference in the location of the test sample in the test site. It is expected that the method of securing the test samples in the test site will have allowed a small amount of movement, particularly as it settled under load after the initial installation. This will have further compounded the error in the lateral alignment of the locations on the test samples at which the profiles were recorded. Also any variation in the test samples position may have altered the wheel-rail contact conditions. This could have resulted in the same location on a test sample being subject to different contact pressures by each wheel contact during the test. Variations in the location of the test sample between wheel contacts mean that the trends in roughness are not as a result of contacts applied in a totally consistent manner.
- Differences in the lateral position of the locomotive wheels relative to the test site, and hence the lateral contact location. Also differences in the longitudinal contacts conditions due to the magnitude and direction of traction or braking forces applied by the wheel. The main reasons for these differences would be random variation in the path of the wheel set over the test site and differences in the locomotives speed of travel, direction of travel and the level of traction or braking applied.

These potential differences in lateral location of the measurement device, test sample and wheel contact, compound the error in the generation of the ideal uniform contact loads and repeatable measurement locations. That is, these potential differences would cause deviation from the ideal case of the contact taking the same path across the test sample each time and the profile being recorded along the same track on the test sample. The combinations of these errors are the most likely cause of the scatter of the results about a general trend. The general trend is similar to that which would be expected if the experimental conditions had matched the ideal case.

The error in the longitudinal location of the test sample during the taking of measurements is likely to be smaller than the lateral error as the test sample was resting

against the test site rail. During each measurement the longitudinal location of the surface profiler was determined from this rail of the test site, as opposed to the rail of the test site which had packing material in between it and the test sample. The error in the longitudinal location of the test sample during the contact is not known. However since the contact rolls over the test sample in the longitudinal direction, this error mainly affects the longitudinal profile presented to the wheel as it passes, that is the longitudinal and vertical gap to be bridged by the wheel mounting the test sample. The measured section being in the middle of the test sample will have been remote from the extremes of this effect. The longitudinal location of the test sample may have affected the lateral location of the contact; however it was not possible to distinguish this effect from the random variation as a result of passing along the test site. The effect on the results of the error in the longitudinal location of the test sample during the taking of measurements, and the longitudinal location of the measurements, is felt to be less significant than that of the errors in the lateral direction. This is because they only affect the determination of, which sections of the test sample are included at the ends of the profile measurement, and the statistical nature of the roughness parameters further reduces their effect. Whereas the lateral location errors affects the determination of the whole section of the test sample that is included in the profile measurement.

### ***3.5.2 Location Dependence***

At different locations on the same test samples, the values of the roughness parameters exhibited different rates of change. This was expected since pressure applied at the contact patch(s) between the wheel and the rail varies across the contact patch(s) according to the load and contact geometry. If the profiles of the test samples and the contact conditions were the same, the locations at which the rate in change of roughness parameters was greatest and least would be expected to be the same. Since these would be the locations at which the contact pressures are greatest and least respectively. Although the absolute roughness parameter values for each of the test samples, at the same measurement location and stage of each test, would be expected to be different, since they are all made from different grade steels.

The test results showed that the locations at which the rate of change of roughness parameters was greatest and least, was different for different test samples. In the early



stages of the test, this could partially be attributable to the variability in the lateral location of the wheel as it passes over the test. However as the tests progressed this variability would have generated a similar average contact history, but the results still exhibited differences at the end of the tests. The reason for the location of the greatest and least rate of change of roughness parameters varying by the end of the test, and part of the reason for it varying in the initial stages of the tests, is the variation in the lateral profile of the test samples. The lateral profile of the test samples was determined by the judgement of the operator of the Rail Profile Grinder, as they attempted to match the profile of the test site, whilst ensuring that that the locomotive wheels would make contact with the test sample. It is not possible to ensure the repeatability profile formed on the test samples using this process. The variability in the test sample profile, results in the conditions at the wheel-rail contact differing between test samples, the contact patch(es) having different shapes and pressure distribution, even when the wheels pass over the test samples in the same lateral alignment.

In addition to the variation in the general profile, the lack of repeatability in the grinding process results in a variation in the distribution of the grinding facets. The ground profile is made up of planes parallel to the longitudinal axis of the rail and orientated about it, these are the grinding facets. They are the result of the single grinding stone in the Rail Profile Grinder, grinding material from the rail in one plane; the combination of multiple passes at different angles about the rail axis forms the profile. Each grinding stone on a Production Rail Grinder also operates in one plane; the setting of the individual stones at different angles forms a similar faceted profile in one pass, dependent upon the amount of material that it is required to remove. The grinding facets produce a local variation in the contact pressure within the contact patch, the intersection between two neighbouring facets experiences higher contact pressures. This is because the wheel makes contact here first and prevents the middle of the flat areas in between edges taking the proportion of the load they would in a smoothly curved profile. The lack of repeatability in forming the test samples profile with a Rail Profile Grinder, results in the profile ground on each test sample having a different distribution of grinding facets.

The variation in the general profile and distribution of the grinding facets between test samples, affects the contact pressures at the measurement locations and thus the rate of

change in the roughness. This affects which measurement location on each test sample exhibits the greatest and least rate of change in the roughness parameter values. The distribution of the grinding facets further affects the roughness parameter results, in that, it results in the possibility of there being a rapid change in the roughness results for only a small lateral offset. This, in combination with the lateral error in the location of the test sample and measurement device, contributes to the scatter of the results about the general trend. A small lateral offset in the measurement location, to a measurement location closer, or further from an intersection of two grinding facets, results in the profile being taken on an location that has had a measurably different contact history, and hence roughness trend.

Figures 3.15-3.17 show that at a single measurement location, location A, most of the roughness trends are similar, showing reducing roughness parameter values with accumulated wheel passes. However the roughness parameter values for the Corus 400 test sample remain almost constant with no definite trend of change in values emerging from the scatter. The averages of the roughness parameter results from all measurement locations plotted in Figures 3.18-3.20, and the minimum roughness parameter values plotted in figures 3.21-3.23 show that the Corus 400 test sample exhibits similar trends to the other test samples, this indicates that the results are location dependent.

Figures 3.24, 3.26 and 3.27 are example plots of which measurement location the maximum and minimum roughness parameter values, indicating lowest and highest contact pressure in later stages respectively. Figure 3.25 shows an example of the maximum and minimum values for one of the test samples, this particular plot corresponds to that of Figure 3.24. Figure 3.24 shows an example where the minimum values reliably occur at location A (nearest to the gauge corner) and the maximum values occur initially at location B then shift to location E in the later stages. This indicates that the contact pressure was highest in the region of measurement location A, and the contact was centred about this location. Whilst the adjacent location, B, roughness at had the highest roughness up to between 16 and 32 wheel passes, when the highest roughness location transferred to location E. This indicates that initially location B is sheltered from the contact by the shape of the profile until the repeated higher pressure contacts at location A modifies the profile so that the contact pressure at

location B increases, leading to the cumulative contact pressure being lower at location E.

Figures 3.26 and 3.27 show different trends in where the maximum and minimum roughness parameter values occurred to that shown in Figure 3.24, illustrating the different contact conditions between test samples. In Figure 3.27 the maximum roughness values consistently occur at location E and the minimum values mainly occur at location D, with some of them occurring at location A. This shows that there are two locations where the contact pressures are highest, separated by two other measurement locations. This indicates that something approaching two-point contact conditions exist on this test sample, that is that whilst the conditions may be similar to a true two-point contact there may not be complete separation between the contact patches in an individual wheel passes. It is not possible from the results to distinguish between, a two-point contact in which each individual wheel pass has two discrete contact patches that the contact areas that might overlap on subsequent wheel passes, a single contact patch with two peak contact pressures, and repeated single point contacts that occur at different locations at successive wheel passes. Given the experimental and grinding variations being the most likely cause of the location dependence of the results, it is not thought that the location dependence is determined by a mechanism related to the material hardness.

### 3.5.3 *Initial Roughness*

The roughness parameters results from the initial measurements of different test samples, before wheel contacts were applied, showed that there was some variation in the initial roughness of the test samples. This could be related to the different responses of the different grades of rail steel that the test samples were made from to the grinding process or the variability in the grinding process. In this section the initial roughness parameter value results are examined to determine if the variation in initial roughness parameter values is due to the response of the different materials to the grinding process or the variability in the grinding process. The individual initial roughness parameter values at each measurement location for the different rail steels are plotted in Figure 3.28 below; also the average initial roughness parameter values for each test sample are given in Table 3.5.

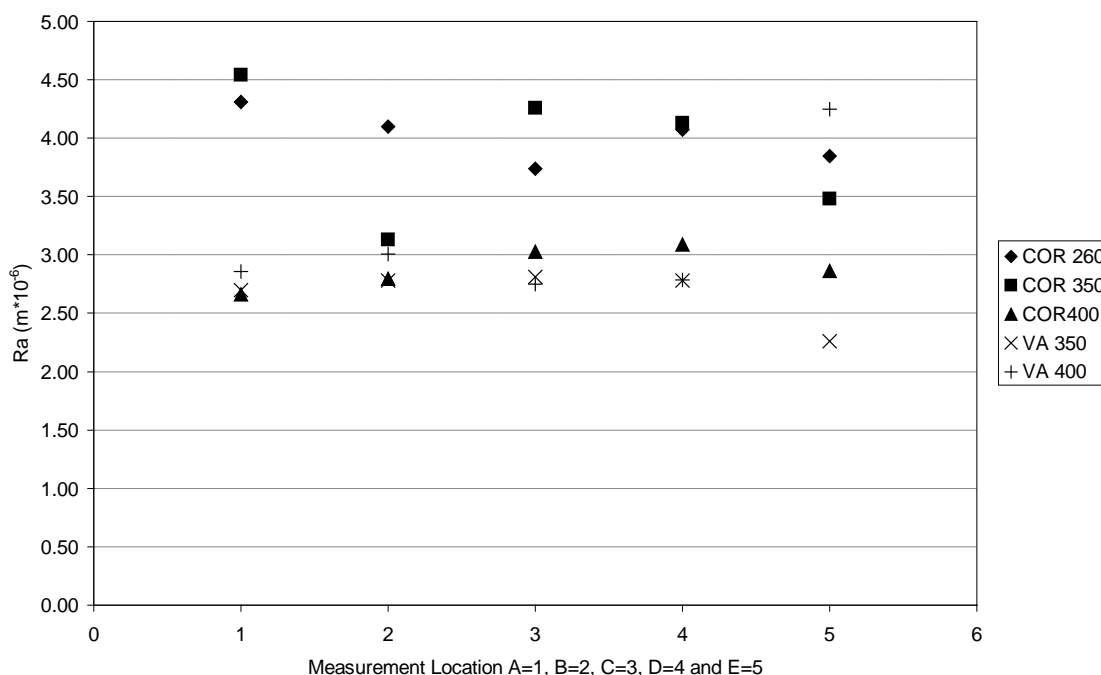


Figure 3.28. The initial Roughness Parameter Values (Ra) plotted against the measurement location for all test samples.

Table 3.5. Initial Roughness Parameter Values (Ra) from all measurement locations averaged for each of the different test sample.

Rail Steel	Average Initial Roughness Value, Ra
COR260	4.207
COR350	4.229
COR400	3.047
VA350	2.549
VA400	2.863

The results show that there was some variation in the initial roughness parameter values between measurement locations for each test sample, but they were mostly within a range approximately 0.5 wide. The values which this range covered was different according to which test sample the values were for. The variation in the results at different measurement locations of the same test sample within this range would appear to be the variation due to the grinding process. There is no discernible link between roughness and measurement location, there are some values that are outside the above range, but these are not associated with any particular location. The occurrence of initial roughness parameter values outside of the general range for each test sample could be

due a significant variation in the grinding procedure, such as contact pressure or grinding stone speed, either rotary or longitudinal, since these were controlled by the judgement of the operator. Alternatively the occurrence of these values could be due to the alignment of the measurement device with features on the profile, such as the boundary between two grinding facets, caused by the combination of, variation in the distribution of the grinding facets and variation in the location of the measurement device.

The differences between the general distribution ranges of initial roughness parameter values for the different test samples, represented by the difference in the average of all measurement locations for each test sample, appears to be attributable to the test sample materials having different responses to the grinding process. The initial roughness parameter values for the Corus grade 400 and the VoestAlpine grades 350 and 400 test samples were similar, furthermore these values were about 75% of those of the Corus grade 350 steel and the Corus grade 260 steel was between those values. That the test samples made of harder grade steels, exhibit lower initial roughness parameter values following the nominally similar grinding process, indicates that the grinding marks on the harder materials are less deep. The most plausible reason for this is that for a grinding stone of the same roughness, and applied at the same contact pressure, the individual grains don't remove material from as far below the mean surface level when grinding the harder steels. The initial values of the Rz roughness parameter, which gives the average of the maximum peak to trough from several sample lengths of the profile, are shown in Table 3.6. The initial Rz values show that the depth of the roughness was less for the Corus grade 400 and the VoestAlpine grades 350 and 400 test samples, than the Corus 260 and 350 grades.

Table 3.6. Initial Roughness Parameter Values (Rz) from all measurement locations averaged for each of the different test sample.

Rail Steel	Average Initial Roughness Value, Rz
COR260	26.109
COR350	25.867
COR400	19.912
VA350	17.554
VA400	18.486

That the initial roughness values for the Corus 260 test sample are higher than those of the VoestAlpine and Corus 400 test samples is expected, as explained above the softer steel would be expected to have a rougher surface from the same grinding process. Also due to the scatter of results being of similar magnitude to the separation between the average initial roughness values of the VoestAlpine and Corus 400 test samples, it is not appropriate to try to differentiate between the roughness response to grinding of these materials. That is, that the variation in results from different locations of the same test sample is greater than the difference between the average initial roughness parameter results. The initial roughness parameter values for the Corus 350 test sample do not comfortably fit with the suggested trend in initial roughness values and the reasons for it, although they are not entirely incompatible. This could be because there were factors that affected the materials response to grinding other than its indicated hardness, or variations in the grinding process.

#### 3.5.4 *Roughness Trends*

The results in figures 3.15-3.20 show general trends (with more or less scatter) that indicate that the overall roughness levels that resulted from the grinding of the test samples was reduced by the passage of locomotive wheels over the samples. The reduction in roughness is indicated by the reduction of the Rz, Ra and Rsk roughness parameter values, as the number of wheel passes applied to the test samples increases. The rate of reduction of the general trends in roughness parameter values from their initial values reduces with increasing numbers of wheel passes indicating that they are an asymptotic trend towards a steady state value or heading towards a local minimum.

The results in the minimum parameter value plots (figures 3.21-3.23) show similar trends to those in the plots of the average of the roughness parameter values across the measurement locations (figures 3.18-3.20). The main difference between the trends for figures 3.21-3.23 being that the values head towards the asymptotic value or local minimum, sooner than the trend for the same respective roughness parameter and test sample in figures 3.18-3.20.

The reduction in Rz values, which averages the maximum peak to trough measurements for several profile sample lengths, as the tests progress, indicates that the repeated wheel contacts, progressively reduces the maximum peak to trough height of the roughness. The initial rate of reduction is high and reduces as the roughness parameter approaches a steady state value. This is thought to be due to the wheel contact plastically deforming the peaks, the material at the peaks failing and being worn away, or a combination of the two. The rate of change reducing, due to the resulting wider, flatter peaks giving a larger contact area that is able to support more load, and requires more work to deform by the same distance.

The Ra parameter is an arithmetic mean of the departure from the mean profile line of a sample of points on the profile. The reducing trend in the values of Ra taken at each measurement interval indicates that the departure from the mean profile line at the points on the profile sampled is reducing, which in turn indicates that the roughness of the profile is reducing. The changes in the surface profile that are responsible for the trends in the Ra values, and the mechanisms by which those changes occur, are thought to be the same as described for the changes in the Rz values.

The Rsk parameter quantifies what proportion of the profile is above and below the mean profile line, in the results the trend for all the test samples is that the Rsk values change from near zero at the start of the tests to negative values at the end. This trend in the Rsk values indicates that the roughness is becoming more skewed, with a greater proportion of the roughness being below the mean surface. It also indicates that the peaks of the grinding roughness marks are being reduced in height by the wheel contacts, at a greater rate than any increase in depth of the troughs. In conjunction with the other parameters that indicate a reduction in the roughness, this shows that the grinding roughness is being reduced by the reduction in height of the peaks either by wear and/or plastic deformation. This is as opposed to the hypothetical situation of the negative trend being due an increase in the depths of the troughs occurring at a greater rate than any increase in the height of the peaks. The observed trend in Rsk values is the expected trend for the initial stages of the roughness response to traffic, it would be expected that at some point in the life of a ground rail the Rsk values would tend back towards zero, or the worn rail's steady state value. This trend would be due to the rail wearing down to below where the bottoms of the troughs of the grinding roughness are,

eliminating the grinding roughness, and a smooth, worn rail surface being established. However the number of wheel passes required for all of the material at the surface after grinding to be removed by the wear process, and thus for the Rsk parameter achieve its steady state value, would be significantly greater than the number applied during these tests.

From the analysis of the results for all the locations it becomes apparent that the trends for each test sample are different at each location, this is due to the lateral range of the measurement locations exceeding the width of the contact patch(s) between the wheels and the test sample. The differences in results at each measurement location for each steel has been interpreted as showing that the contact pressure between the wheel and the rail is different at each measurement location. The variance from the general trend in the results at individual measurement locations on the same test sample, indicating a rate of change in the results between measurement intervals is different from that of the general trend, is thought to be due to the variation in the path of the contact over the test sample resulting in variations in the contact pressure from the average experienced at each location on each test sample. The variance in results from the general trend could also be due to the variation in the lateral location of the measurement device, resulting in the measurement being taken at a location that has experienced a different contact history. The locations that exhibit steeper trend towards lower roughness parameter values, are believed to those where the wheel is making contact (or at least where the contact pressure is highest for the majority of wheel passes) as it passes over the rail. That the steeper trends towards lower roughness are at different measurement locations for different test samples, is believed to be due the variation in the transverse profiles of the rails resulting in the locomotive wheels making contact at different lateral locations for each steel. The differences in lateral profile of the test samples is due to the manual grinding operation not being precisely repeatable and the error in the machining of the test samples to fit the test site.

As well as the analysis of the results showing that the maximum change in roughness parameters occurred at different locations for different steels, it also showed that the location of the maximum and minimum change in roughness parameters for each steel (from the initial roughness value) varied at various stages as the test progressed and the roughness modification developed. This is thought to be due to the processes that affect



the scatter of the results, such as the error in the lateral location of the measurement device and the rigidity of the test sample in the test site. Another reason for the changes in the location of maximum and minimum roughness parameter for each of the test samples is thought to be the variation in the lateral location of the wheel contacts of the locomotive. These occur due to differences in direction, speed, and traction/braking levels, as well as the random variation of the contact location under similar conditions. More gradual changes in the locations of the maximum and minimum could be due to the contacts modifying the profile and altering the distribution of contact presses, resulting in different relative cumulative contact histories.

### *3.5.5 Comparing Test Sample Roughness Trends*

The plotting of the results for the different test samples together on the same graph, as in Figures 3.18-3.23, shows that the general trends in roughness parameter values, with increasing numbers of wheel passes applied, were broadly similar. If we initially discount the results for the Corus 350 test sample, the results for the remaining test samples appear to show that the softer Corus 260 grade test sample has a significantly different response to the passage of wheel over the grinding roughness. The general trend of the Corus 260 test sample starts off with higher Rz and Ra roughness parameter values than the other harder grade test samples, and all of the Corus 260 roughness parameter values reduce at a greater rate compared to the harder grade test samples and tends towards its asymptotic values at the same time or sooner than the harder grade steels. The differences between the general trend of the test samples made from Corus 400 and VoestAlpine 350 and 400 grade rail steels are less than the scatter in the results about the trend, therefore it is not possible to distinguish between the relative responses of the roughness of these test samples with any degree of confidence. However since the nominal hardness of these test samples is similar, it might be that the subtle difference in results that the hardness of the test samples might lead one to expect, are smaller than the resolution obtainable with the test method and might only show up if the tests for each type of rail steel were repeated several times and the results averaged and compared.

The results imply the following relationship between the hardness of the rail steel and the reduction of grinding roughness by wheel contacts. Harder steels exhibit lower

initial grinding roughness (as discussed in the initial roughness section) and that the reduction of that grinding roughness by the subsequent passage of rail vehicle wheels occurs at a reduced rate compared to that of softer rail steels. The roughness of the harder steels reduces at a lower rate is explained by the harder materials requiring more energy to deform the grinding roughness (in the form of more wheel passes), and reducing it by the same amount as the softer materials.

The results for the Corus 350 grade test sample do not correspond exactly with the proposed relationship between hardness and roughness described above. The trend of results for this test sample exhibited characteristics similar to those found in both the Corus 260 grade test sample and the other harder test samples. The Corus 350 grade results started with roughness parameter values similar to the Corus 260 grade test sample, as discussed in the initial roughness section, but the rate of reduction of the roughness parameter values was similar to that of the other harder test samples. There are several possible explanations for the results for the Corus 350 test sample not fitting the relationship. The explanation that is most compatible with the proposed relationship is that the combination of variables in the grinding process, such as the pressure and speed of the grinding stone, for the Corus 350 grade test sample resulted in grinding conditions which were significantly different than those for the other test samples. This in turn resulted in a rougher surface finish than would have been the case, if the grinding conditions had been similar to those for the other test samples. The rate of reduction of the roughness of the Corus 350 grade test sample during the test was consistent with the other harder rail steels, indicating that it was at sample grinding stage at which the most significant variation in the test procedure occurred for this sample. Alternate explanations are that there are other factors involved in the material properties of this steel that make it behave differently, or the difference is due to other experimental errors. That the results for the Corus 350 grade test sample didn't correspond to the proposed relationship, neither proves nor disproves the relationship. That the trend for this test sample doesn't exactly fit the relationship reduces the confidence that a relationship might exist. However there are plausible circumstances that could have caused the results to differ from those that would have fitted the relationship more precisely.

The single set of results for each test sample, combined with the overall variability in the test results, means that the relationship between the hardness of the rail steel and the reduction of grinding roughness by wheel contacts, interpreted from the results, can only be used as an indication and not treated as being definitive. The logical reasoning for the proposed relationship appears sound, however whilst the results support it to some extent, they do not prove it sufficiently to have a high degree of confidence of its accuracy.

### **3.6 Conclusions**

#### **3.6.1 *Conclusions Made from Test Results***

Differences in the locations, and different patterns of variation, of the minimum and maximum roughness parameter values, shows that the contact conditions for the different test samples varied independently of the type of material the test sample was made from. The variability in the contact conditions for each test sample being independent of the test sample material is distinct from the contact varying due to a mechanism related to the test sample material. For example the rate at which initially identical profiles are modified (and hence exhibit different contact conditions) could be dependent upon the material properties; whereas differences in the initial profile could be independent of the material properties through manufacturing process variation.

That there were differences in the contact conditions significant enough to affect the results, means that the trends can only be taken as an indicator of the response of grinding roughness on different materials to wheel contacts. The relative responses of the test samples of different materials, allowed an apparent relationship between test sample hardness and roughness response to be observed, that is that, for similar contact conditions, the grinding roughness on harder rail steels is reduced at a lower rate than on softer steels. However, whilst this allowed theories to be formed that explained the relationship, the results are not sufficiently conclusive to support those theories with a high degree of confidence.

Similarly, whilst the results appear to show, with one explainable exception, that for the same grinding process the resulting initial grinding roughness on harder steels will be

less than that on softer steels, it has not been proved conclusively, and the reasons for the exception to the trend not satisfactorily determined.

### **3.7 Implications of Grinding Roughness Tests for Grinding Model**

The analysis of the test results has shown that whilst they were useful for forming generalised relations between hardness and grinding roughness, both initially and in response to wheel contacts, the results could not be used to prove conclusively define or quantify those relationships. However the main purpose of the tests was to test the validity of the assumption that the effect of increased rail surface roughness resulting from rail grinding on crack growth could be ignored due to its reduction by wheel contacts a short period of time after grinding, relative to the period of time between grinding operations.

The roughness parameter values calculated from the recorded profiles for all of the test samples tested indicated a significant reduction in the grinding roughness during the tests. Also the values appeared to be approaching either an asymptotic, or local minimum, value after the 100 wheel passes that the test samples were subjected to during the tests, which is a small proportion of the several thousands of wheel passes between grinding operations in the grinding model. This increases the confidence that the simplifying assumption to ignore the effect of grinding roughness on crack growth is valid, and can be accounted for with a suitable factor of safety.

### **3.8 References**

- 3.1. Lundmark J., Höglund E., Prakash B. (2006) Running-in Behaviour of Rail and Wheel Contacting Surfaces. *Proceedings from the 5<sup>th</sup> International Conference on Tribology AITC-AIT 2006. Parma, Italy in September 2006.* ISBN: 978-88-902333-0-2.

## **Chapter 4. Grinding Model Investigation: Optimum Grinding Strategies**

### **4.1 Introduction to the Grinding Model Case Studies**

In Chapter 2 the crack growth model was adapted to include the effect of rail grinding on crack size, in Chapter 3 the validity of one of the simplifying assumptions was investigated. In this chapter the grinding model is used to investigate the effects of different grinding strategies on rolling contact fatigue crack development under different traffic conditions, which has implications for the safe life of a rail. Modelling runs have been conducted for several different traffic conditions with the grinding operations varying in both the intervals between grinding operations and the depths of material removed from the rail (i.e. grinding depth) at those operations. These investigations have been conducted with the aim of using the grinding model to find a grinding strategy, for each traffic condition, which meet the criteria of controlling crack length whilst minimising grinding, and hence maximising safe rail life. A specific optimum crack size trend has been specified as an example, the grinding strategy which results in a predicted crack size trend which closely matches the optimum trend is determined as the optimum grinding strategy for those conditions. The term “crack size trend” shall be used in the description of the work that has been carried out, it specifically means the behaviour of the crack size predictions as the modelling run progresses and the number of wheel passes applied to the contact increases. That is the overall trend (including the effect of grinding operations) in the predicted crack size as the number of wheel passes increases. This term is used for this specific meaning in order to maintain clarity when the behaviour of the crack size predictions as the modelling run progresses is described and discussed; particularly when this is done in conjunction with other terms that are used in the same sentence.

There are two main stages involved in determining the ideal grinding strategy for a specific section of track, firstly the criteria by which the grinding strategy will be judged, for example one that gives the maximum rail life, or minimum rail life cycle cost. The second stage is to optimise the grinding strategy to find the one which best meets the criteria for the given set of conditions. Some of the major factors which affect both the determining criteria and the optimisation of the grinding strategy are:

- Grinding increases safe life of rail by controlling RCF defects that would otherwise threaten rail integrity of rail before wear life of rail is reached.
- Removal of rail material by grinding reduces the wear life of rail
- Longer cracks have higher crack growth rate (more frequent and/or deeper grinding required to control)
- Grinding machine efficiency will vary with amount removed per operation.
- Grinding operation will have fixed costs (labour etc.) regardless of the amount of material removed per operation
- Grinding operations are being carried out within a complex system, carrying out the absolute optimum grinding strategy may adversely affect the whole system.
- Initial purchase cost of the rail, different grades of rail steel cost different amounts and behave differently.
- Cost to install replacement rail, including labour, machinery and disruption to system.
- Residual value of the rail after removal from service.
- Error in a strategy to maintaining a tolerable crack size might result in crack size exceeding tolerance and threatening rail integrity, and therefore system safety. The criteria by which the grinding strategy is judged should include a factor of safety.

To investigate the significance of the factors listed above, and apply the grinding model to answer plausible problems, a series of case studies have been carried out whereby an example set of criteria has been selected and the optimum grinding strategy found for different conditions to meet those criteria. The criteria is defined in terms of a specific predicted crack size trend that results from the application of rail vehicle traffic and a grinding strategy to a section of rail. The example criteria for defining the optimum grinding strategy, set out for the investigations in this section, was designed to find the grinding strategy that would give the maximum rail life for a rail containing an existing RCF crack of specified size, with a safety margin. This criteria was applied to the modelling of variety of different rail vehicle traffic patterns and grinding strategy variables, with the aim of investigating the effect of different traffic patterns rail vehicles on the optimum grinding strategy determined with each grinding strategy variable. The grinding strategy determined as the optimum grinding strategy, is only the

predicted optimum for the criteria and constraints as defined for that particular case, it is not a global optimum that considers asset management policy, logistical requirements and cost.

The size of the initial defect used in the case studies is a 1.75mm radius semi-circular crack angled at 30° below the surface, giving it a 3.5mm surface length which is typical of the minimum size reliably detectable by the inspection methods commonly used in practice on the network. The size of the crack being defined as the radius of the crack at its deepest point, that is 1.75mm initially, a simplifying assumption is made that the shape and orientation of the crack remain constant. Whilst a grinding strategy which was just frequent enough to maintain the crack size below a tolerable threshold or its initial size would initially require less material removal than more frequent grinding which would result in the removal of the crack, this would be potentially unstable as if the crack growth rate is even slightly greater than predicted at any point. That is, any slight variation in the conditions, be that the frequency of the grinding or the crack growth rate, could alter the crack size trend away from the stable condition. If an unanticipated increasing crack size trend was detected, it would require extensive grinding to correct and reduce the crack size. Also if an increasing crack size trend remained undetected for a significant period of time, it could result in the crack being uneconomical to control by grinding, requiring the rail to be replaced, and could potentially threaten the integrity of the rail. To add a safety margin and develop a potentially useful grinding strategy, compared to one that maintained the crack below a set size, the criteria selected was that the predicted crack size should tend towards zero after  $3 \times 10^6$  wheel passes, within +/-0.5%. This criteria calls for a prediction of a reducing crack size trend, without the necessity to remove the crack immediately, which would remove rail wear life that can usefully be used to carry rail vehicles. In this manner the grinding operations augment the natural wear caused by the rail vehicle traffic to control the size of, and remove, RCF cracks. Using the same criteria for each case modelled gives a common point for comparison of the optimum grinding strategies determined for different cases.

## **4.2 Grinding Model Optimum Grinding Strategy Investigation Method**

The method of investigation for each combination of traffic pattern and grinding strategy variable was the same and consisted using initial values of the variable and conducting an iterative search. There are two grinding strategy variables which can be altered in the input files to the modelling runs; these are the interval in between grinding operations, expressed as the number of rail vehicle wheel passes and the grinding depth, defined as the vertical depth of material removed from the centreline of the rail. The grinding strategy variable that is altered in the first case study to find the optimum strategy was the interval in between grinding operations with the grinding depth being fixed. Similarly in the second case study the grinding depth was altered to find the optimum strategy, the interval remaining fixed. The fixing of one of the variables for each case study simplified the investigations and could represent an external constraint on the grinding strategy in practice such as operational and machine availability considerations or the capacity of the grinding machine. The stages of the iterative search investigation method to find the optimum grinding strategy are shown below:

1. Initial grinding strategies are modelled, then the values of the grinding strategy variable(s) that resulted in crack size trend either side of that required noted.
2. A grinding strategy variable value between that of the two that resulted in trends either side of the trend required is applied to the model.
3. The grinding strategy variable in stage 1 that produced trend on the same side of that required as the A grinding strategy variable in stage 2 eliminated from investigation.
4. Repeat stages 2 to 3, with the two remaining intervals from stage 3 used in the next iteration of stage 2, until crack size trend approaches required trend.

## **4.3 Train Types and Traffic Patterns**

To investigate the optimum grinding strategy for different traffic conditions, six different traffic data sets are used in this section, as the traffic part of the input to the Grinding Model, the other part of the input being the Grinding Data Configuration file. Each of the traffic input files contains repeating cycles of contact data, each contact data set representing the predicted effect of a wheel pass of a specific rail vehicle on the growth of the crack and the wear of the rail. This allows the overall predicted crack



growth for each wheel pass to be calculated. The order and number of wheel passes for which each set of contact data is applied within the traffic cycle, represents a pattern of vehicles which makes up the traffic which the rail sees. The traffic input files and the traffic patterns which they represent are given below:

- Class 365. Contact data representative of a wheel contact of a Class 365 Electric Multiple Unit (EMU) commuter train is applied 32 times, equivalent to the passage of two units of four vehicles, a cycle.
- Class 365X. As the Class 365 traffic input file except that the wear rate in the contact data is 0.75 times that which represents a Class 365 contact.
- Diesel High Speed Train (DHST), consisting of MkIII coaches and Class 43 locomotives. Contact data for wheel passes of Class 43 locomotives and MkIII coaches is applied in the proportions of 32 MkIII followed by 8 Class 43 per cycle, representing one train set. Although the Class 43 locomotives are marshalled at either end of the train set, it was shown in the model development section (Figure 2.7) that the order of vehicles in cycles of less than 100 wheel passes in total, didn't have a noticeable effect on the overall crack size trend.
- Electric High Speed Train (EHST), consisting of MkIV coaches and Class 91 locomotive. Contact data for wheel passes of MkIV coaches and Class 91 locomotive is applied in the proportions of 36 MkIV followed by 4 Class 91, representing one electric high speed train set per cycle.
- Mixed traffic. Contact data for MkIV coaches, Class 91 locomotive, MkIII coaches, Class 43 locomotive, and Class 365 unit are applied in the respective quantities of 36:4:32:8:32, representing one unit of each type of high speed train and two units of the Class 365 unit
- Mixed (365X) traffic. As the Mixed traffic input file except that the contact wear rate for the Class 365 contact data, is 0.75 times that which represents a Class 365, representing the replacement in the traffic pattern of the Class 365 units with the hypothetical Class 365X units.

#### **4.4 Wear Rates Determined During Optimum Grinding Variable Investigations**

Different combinations of traffic pattern and grinding strategy produce different amounts of wear. In the investigation to find the optimum grinding interval, the effect of the wear rate produced by a traffic pattern, and any grinding strategy applied, has been

considered in terms of whether the crack size trend is dominated by the crack growth rate, and is increasing, or dominated by the wear rate and is decreasing. The wear rate can also be considered in terms of the total cumulative wear which the rail accumulates, the higher the wear rate, the more quickly the rail accumulates wear. The significance of the total cumulative wear is that it is one of the limiting factors on the life of the rail, once a certain limiting amount of material is lost from the rail head it will require replacing. As well as writing the crack size to the output file at each data point it also writes the cumulative vertical wear, which allows the effect of the traffic pattern and grinding strategy on the wear life of the rail to be determined. Since the cumulative wear is a product of the frequently repeating different wear rates of the vehicles in the traffic pattern, and the relatively infrequent (in terms of number of wheel passes) grinding operations, a value referred to as the Effective Continuous Wear Rate is calculated to allow direct comparison between the wear rates for each case modelled.

The Effective Continuous Wear Rate is a continuous wear rate per wheel pass, equivalent to the product of vehicle and grinding wear, it is calculated as the total wear at the first data point in results file after the last grinding operation divided by the number of wheel passes that have occurred at that point. When no grinding is carried out the Effective Continuous Wear Rate is calculated as the cumulative wear divided by the number of wheel passes at the last data point. The reason that it is not calculated using the last data point in cases with grinding, is that the grinding produces a stepped trend to the cumulative wear value, so there would be a discernible difference in the Effective Continuous Wear Rate if the data point at which it was calculated occurred just before or after a grinding operation. Therefore it is calculated from the top of the last step, so if extrapolating the cumulative wear from the Effective Continuous Wear Rate and the number of wheel passes, the value is always greater than or equal to the predicted wear at any point. Calculating it in this way gives the most conservative answer if the wear limit of the rail and Effective Continuous Wear Rates were to be used to predict the wear life of the rail. Data points are created in the output file of a modelling run every 1000 wheel passes, rather than every wheel pass, this is done to save processing time and file space, this resolution of results being sufficient for most purposes. To illustrate how the Effective Continuous Wear Rate relates to the actual cumulative wear values, the cumulative wear results in section 4.6.3 have the

cumulative wear corresponding to the Effective Continuous Wear Rate plotted alongside the actual cumulative wear values.

#### **4.5 Case Study 1: Variable Grinding Interval Investigation**

The first group of investigations concentrate on grinding strategies where the depth of material removed at each grinding operation modelled is fixed both within each modelling run and between modelling runs. The interval between each grinding operation is fixed within the modelling run, but is varied between modelling runs, as per the method of investigation, to find the optimum interval for each of the different traffic patterns. The grinding depth used for each grinding operation in this group of modelling runs is of 0.2mm; this grinding depth is representative of the maximum depth of material which can typically be removed by in a single pass of a large multi-stone production rail grinding machine. All of the modelling in this case study has been carried out with an initial crack size of 1.75mm, and all of the discussion of the results and conclusions drawn from them, are only valid for this initial crack size. The initial size of 1.75 mm has been chosen as it represents a transverse crack length of 3.5mm at the surface of the rail, which represents what is felt to be the smallest crack size which can be reliably detected by visual inspection. The investigation of the effect of different initial crack sizes on the predicted crack size trend and therefore the optimum grinding strategy is discussed in the section on possible further work, section 9.6.

In relation to the maximum grinding capacity of a rail grinding machine, it should be noted, both for consideration in this chapter and subsequent chapters, that the speed of travel of a production rail grinding machine whilst grinding, and the configuration of the grinding stones can be altered. Where the maximum depth of material which can be removed by in a single pass of a grinding machine, grinding capacity, is referred to, this is not generally a specific absolute physical limit to the depth of material a particular production rail grinding machine can remove, but the maximum it can remove whilst operating within certain practical constraints. Such practical constraints would be operating at a speed achieve a certain length of rail ground in a work shift, whilst grinding the rest of the rail to the required profile. Therefore it is useful to set a maximum amount of material which can be removed in a single pass of a grinding machine whilst being operated at the appropriate speed for the grinding undertaken, a

different value to the generic typical value specified here could be used as appropriate to a specific situation.

#### 4.5.1 Variable Grinding Interval Investigation Crack Size Results

##### *Class 365 and Class 365X*

The first traffic pattern investigated was that consisting of just Class 365 Electric Multiple Units (EMUs), the results of modelling runs with no grinding and an initial grinding strategy with a grinding depth of 0.2mm applied at  $1 \times 10^6$  wheel pass interval are plotted in Figure 4.1 below. The scale of the plotted area is maintained the same for all of the results in this group to allow direct comparisons between results.

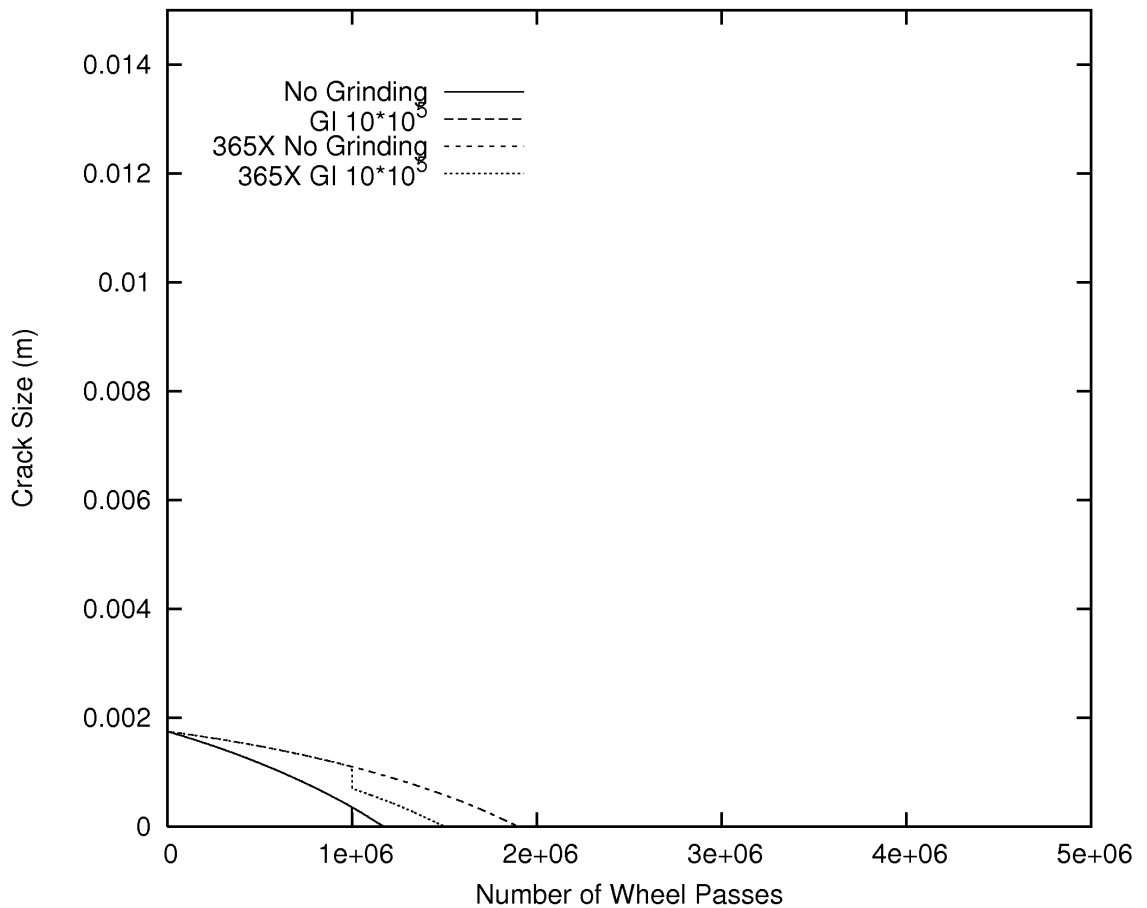


Figure 4.1. Crack size trend results for the Class 365 and Class 365X traffic cases of the Variable Grinding Interval Investigation.

It can be seen from Figure 4.1 that for both the Class 365 and 365X traffic cases with an initial crack size of 1.75mm, the wear rate dominates crack growth rate, therefore the

crack size is predicted to tend towards zero. The lower wear rate associated with the Class 365X case is still enough to dominate the crack growth mechanism and reduce the predicted crack size to zero quicker than the crack growth mechanism can grow it, although it does take more wheel passes for the crack to be predicted to be removed. In both cases the crack size is predicted to tend to zero within the  $3 \times 10^6$  wheel passes specified by the example criteria. The number of wheel passes that it takes for the crack size is predicted to reach zero without grinding is  $1.172 \times 10^6$  wheel passes in the Class 365 case and  $1.902 \times 10^6$  wheel passes in the Class 365X case. Runs of the grinding model with the initial grinding strategy, of 0.2mm of depth at an interval of  $1 \times 10^6$  wheel passes, were carried out for both the Class 365 and Class 365X traffic cases as an example. The results of these modelling runs are also plotted on Figure 4.1, they show that the application of grinding is predicted to remove the crack sooner than without in each case. In these cases applying grinding is predicted to be a waste of the wear life of the rail and grinding resources, as the predicted crack size trends of both traffic cases meet the example criteria without grinding. It should be noted that although it is predicted that grinding appears to be unnecessary for the control of rolling contact fatigue (RCF) cracks, it might still be necessary to carry out grinding for profile control and other RCF defects, such as corrugations. All of the predictions of grinding requirements in this section apply only to that necessary to control RCF cracks, if more frequent grinding is required to treat other RCF defects or maintain the rail profile within specified limits, then that grinding strategy should be adhered to.

### *Diesel High Speed Train*

The predicted crack size trends of a series of modelling runs with the Diesel High Speed Train (DHST) traffic case and various grinding strategies are plotted in Figure 4.2. The figure shows that without grinding the crack size trend for the DHST traffic case is predicted to tend towards a size greater than 10mm, the crack size trend exceeding 10mm after  $1.77 \times 10^6$  wheel passes. The significance of the predicted crack size exceeding 10mm is that it is around this size at which the rail bending crack propagation mechanism (which is not modelled) starts to have a significant effect on crack growth rate. Once the rail bending crack propagation mechanism starts to grow the crack, then it is likely to be propagated by rail bending to a size which would threaten the integrity of the rail. Therefore although the predicted crack size appears from the plot to be

reaching a stable value of about 14mm, this is the result is used as an indication that the crack size is tending towards a size at which other mechanisms would be expected to dominate and grow the crack to failure. This means that it is predicted that applying a grinding strategy would be required to achieve the required crack size trend.

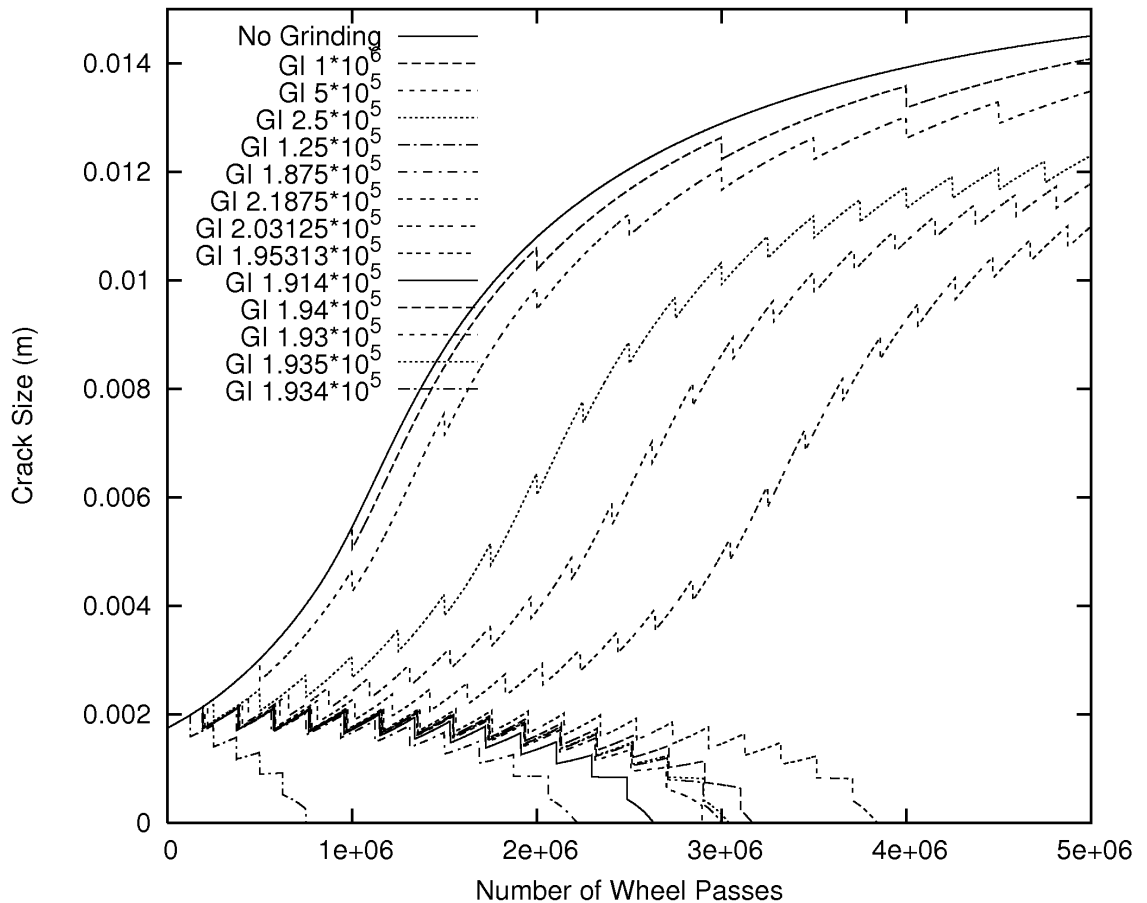


Figure 4.2. Crack size trend results for Diesel High Speed Train traffic case of the Variable Grinding Interval investigation.

Figure 4.2 also shows that when an initial grinding strategy was applied, with the grinding depth used for this investigation of 0.2mm and an interval of  $1 \times 10^6$  wheel passes, then this amount of extra wear was not sufficient to overcome the crack growth rate and prevent it exceeding 10mm. The initial grinding strategy only had a very slight effect on the predicted general crack trend, the number of wheel passes after which it exceeded 10mm being only slightly greater than without grinding. Therefore to find the "optimum" grinding interval further modelling runs were carried out which are also plotted in Figure 4.2, they are listed in the key to the figure in chronological order, identified by their grinding interval. The same chronological convention described here,

regarding the order in which the plots are listed in the key, is followed in the subsequent plots which show an iterative investigation to find an optimum, the individual plots being identified by the significant grinding variable. As the initial grinding strategy was not predicted to produce the required reducing crack size trend, the interval was halved in each successive grinding strategy modelled, which has the effect of doubling the grinding frequency with respect to the traffic pattern, until the crack size was predicted to tend towards zero after  $3 \times 10^6$  wheel passes or less. This was predicted to happen when the grinding interval was  $1.25 \times 10^6$  wheel passes, therefore it was known that the "optimum" interval was between this value and the preceding interval modelled of  $2.5 \times 10^6$  wheel passes. Then further modelling runs were carried out, using the iterative search method described at the beginning of this chapter, section 4.2, until the optimum interval for the traffic pattern and grinding depth were found. The predicted optimum grinding interval was found to be 193400 wheel passes for the DHST case.

#### *Electric High Speed Train*

The predicted crack size tends for the investigation to find the optimum grinding interval for the Electric High Speed Train (EHST) traffic case and a grinding depth of 0.2mm are plotted in Figure 4.3 below. Without grinding the predicted crack size trend exceeds 10mm after  $1.37 \times 10^6$  wheel passes, which is less than for the DHST traffic case, indicating that the balance of the natural wear and crack growth rates is even more dominated by the crack growth rate than for the DHST case. Using the same methodology as for the DHST case, the optimum grinding interval was found to be 244950 wheel passes. This is a longer interval than the DHST case, indicating that the EHST case required less additional wear from grinding, for the balance of the effective wear rate and crack growth rate to be dominated by the wear rate sufficiently for the required reducing predicted crack size trend to be achieved.

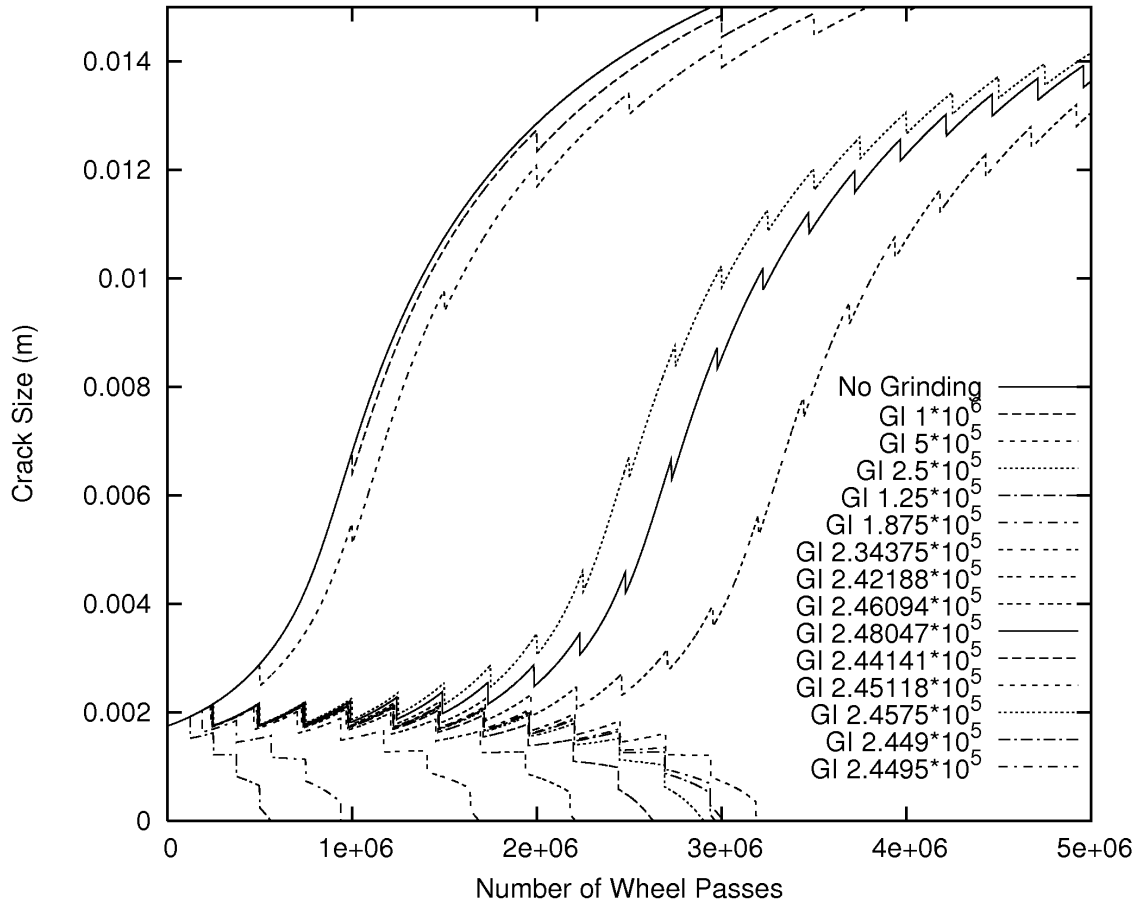


Figure 4.3. Crack size trend results for Electric High Speed Train traffic case of the Variable Grinding Interval investigation.

*Mixed traffic case.*

The predicted crack size trend results for Mixed traffic case optimum grinding interval investigation are plotted in Figure 4.4. The predicted crack size trend for the Mixed traffic case without grinding is shown to be dominated by the crack growth rate, similar to the high speed train traffic cases, however less so as it takes longer to exceed 10mm, not reaching that size until  $2.14 \times 10^6$  wheel passes. Therefore the behaviour of the predicted crack size trend appears to be a combination of the behaviours of the different individual train type traffic cases, the wear dominant Class 365 behaviour reducing the crack growth rate dominance of the crack size trends of the high speed trains. This is reflected in that the result of the iterative investigation method to find the optimum grinding interval, was that the optimum interval is 369700 wheel passes, which is longer than for the individual high speed train cases and is shorter than the Class 365 traffic case which required no grinding, so the interval can be considered infinite.



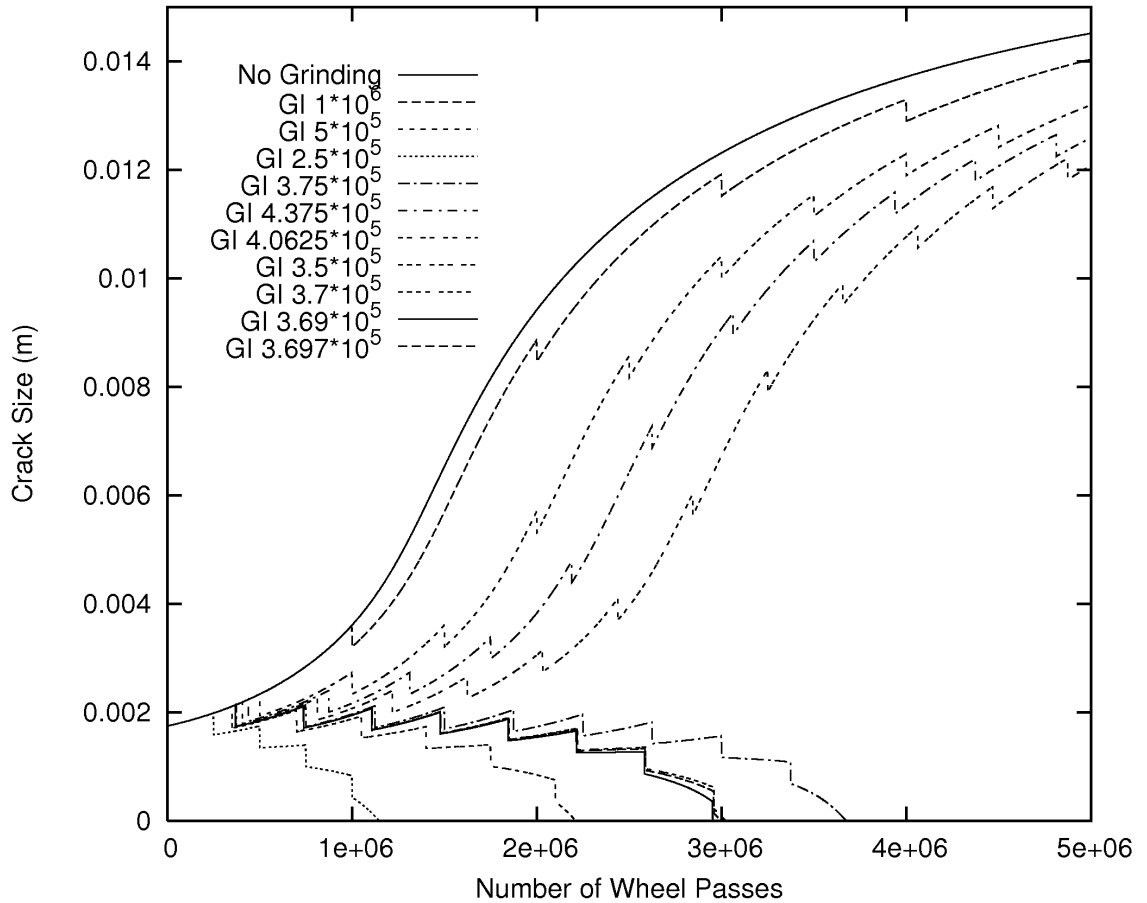


Figure 4.4. Crack size trend results for Mixed traffic case of the Variable Grinding Interval investigation.

#### *Mixed (365X) case*

Figure 4.5 plots the crack size trend results of the optimum grinding interval investigation for the Mixed (365X) traffic case. The result of the Class 365X having a lower wear rate than the Class 365 means that the crack size trend without grinding is slightly more crack growth dominated than the Mixed traffic case, it exceeds 10mm a small number of wheel passes sooner, after  $2.02 \times 10^6$  wheel passes. The optimum grinding interval to produce the required predicted crack size trend was found to be 323500 wheel passes for the Mixed (365) traffic case, which is less than for the Mixed traffic case. This indicates that if grinding is required to control crack size, then reducing the wear rate of one of the vehicles in a traffic pattern means that for the predicted crack size to tend toward the same point, more frequent grinding is required to compensate.

Considering that the Mixed and Mixed (365X) traffic cases were similar, it was expected that the optimum grinding interval for the Mixed (365X) traffic case might be

similar to that for the Mixed traffic case. Therefore to save time with the iterative search for the Mixed (365X) traffic case optimum grinding interval, the Mixed traffic case optimum grinding interval was used as an initiation grinding strategy to the search.

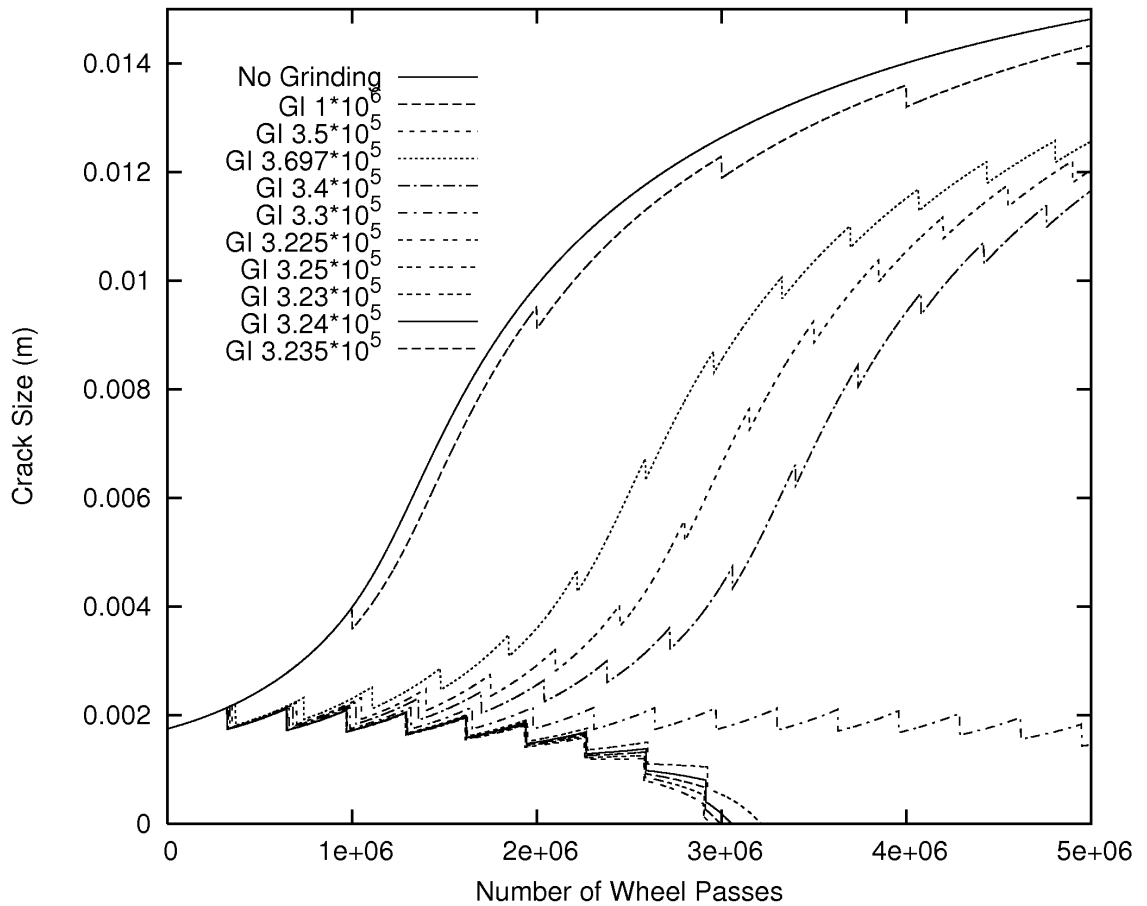


Figure 4.5. Crack size trend results for Mixed (365X) traffic case of the Variable Grinding Interval investigation.

A summary of the results of the optimum grinding interval investigations for each of the traffic cases are presented in Table 4.1, in all cases the grinding depth was fixed at 0.2mm. That the Class 365 and Class 365 traffic cases were found not to need grinding to reduce the 1.75mm initial crack to zero within  $3 \times 10^6$  wheel passes, means that there was no valid optimum grinding interval result.

Table 4.1. Results of the Variable Grinding Interval Investigation, table of optimum grinding interval for each traffic case.

Traffic Pattern	Grinding Depth (mm)	Optimum Grinding interval (Wheel Passes)
365	0.2	N/A #
365X	0.2	N/A #
Mark III and Class 43	0.2	193400
Mark IV and Class 91	0.2	244950
Mixed	0.2	369700
Mixed (365X)	0.2	323500

Notes: # # In these cases the crack size trend was predicted to tend to zero without grinding before the specified number of wheel passes, therefore no grinding should be carried out. Where an example is required a grinding interval of  $1 \times 10^6$  wheel passes is used.

Figure 4.6 plots the predicted crack size trend results of two modelling runs, one of the Mixed traffic case and the other of the Mixed (365X) traffic case, both carried out with the same grinding strategy. The grinding strategy used is that which was determined earlier in this section as optimum for the Mixed traffic case, that is a strategy which uses a 0.2mm grinding depth and a 369700 wheel pass grinding interval for each operation. The results show that for the Mixed traffic case, the crack size trend meet the example criteria, however the for the Mixed (365X) traffic case the crack size trend tends to a value greater than 10mm, indicating a crack that could grow to threaten the integrity of the rail.

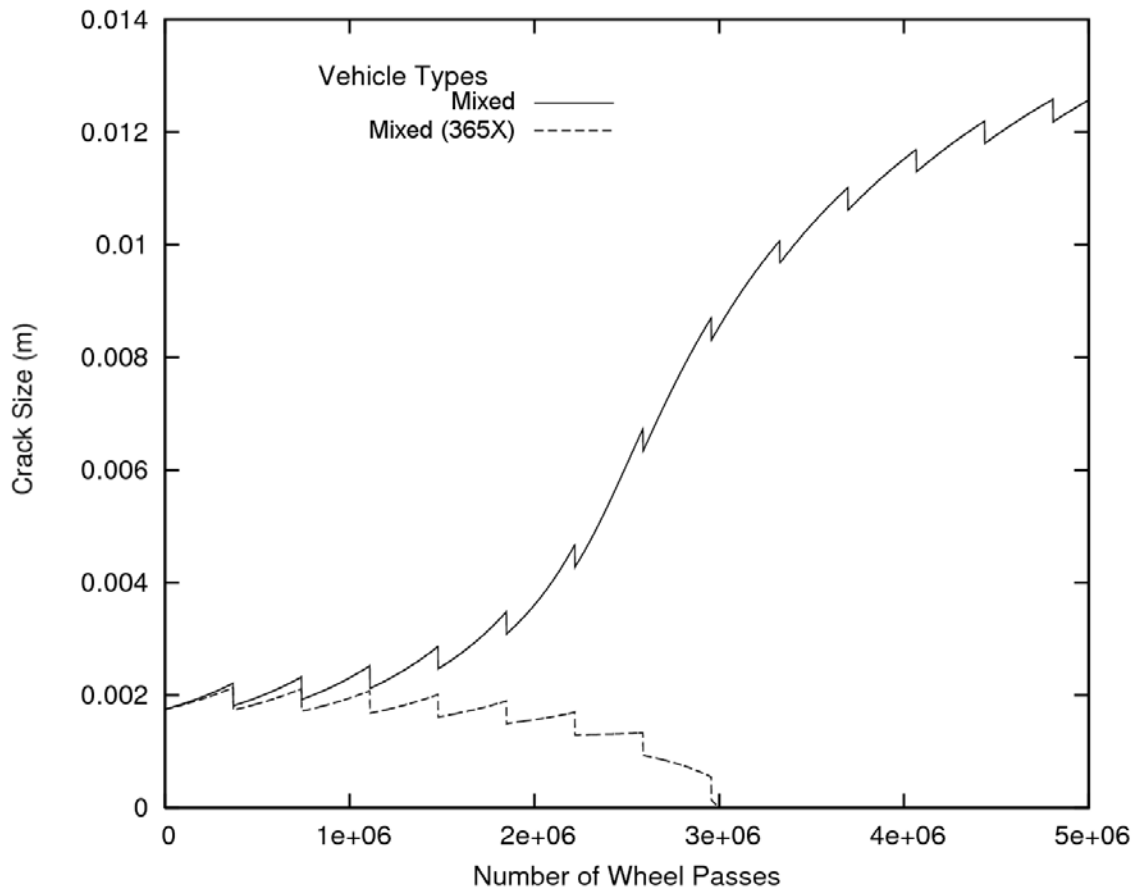


Figure 4.6. Crack size trend results for the Mixed and Mixed (365X) traffic cases of the Variable Grinding Interval investigation both modelled with the optimum grinding determined for the Mixed traffic case.

Table 4.2 summarises the point in the applied traffic pattern at which the crack size trend for each traffic case is predicted to exceed the threshold of 10mm, for an initial crack size of 1.75mm, when no grinding strategy is applied. This value gives an indication of the extent to which the effect of the traffic on crack size is dominated by the crack growth produced by the traffic, increasing the crack size, or it is dominated by the wear produced by the traffic, reducing the crack size. The crack size trend for both the Class 365 and Class 365X results are predicted to tend towards zero without grinding, so these represent a wear dominated traffic case, from Figure 4.1 it can be seen that the crack size trend is predicted to reach zero soonest for the Class 365 case, so this is the most wear dominated traffic case. The crack size trend for Electric High Speed Train is predicted to exceed 10mm soonest, so this is the most crack growth dominated traffic case. The point in the applied traffic pattern at which the threshold is reached is expressed both in terms of the number of wheel passes of traffic that have been applied, which is the unit of measure used in the modelling, and in terms of

Million Gross Tonnes (MGT) of traffic, which is a conventional method of measuring the traffic over a section of track used in the rail industry. The measure of gross tonnes of traffic is the cumulative total of the static weight of the traffic which has passed over a section of track, within a specified period, one MGT being of traffic being when this total reached  $1 \times 10^6$  tonnes. The convention for expressing traffic and quantities such as rail life and maintenance intervals in terms of MGT allows a meaningful common term of reference to life of all track across a network without, including the type of vehicles which constitute the traffic or the time period over which the traffic occurs. It should be noted that one MGT of traffic under one set of circumstances (vehicle type, speed, time frame and weather conditions) will not necessarily have the same effect on the rail life of as one MGT of traffic under another set of circumstances, however it is a useful, simplified, way of expressing the traffic experienced by track which can be determined for all circumstances.

Table 4.2. Point in modelling run at which crack size is predicted to exceed the 10mm size threshold, for each traffic case without grinding applied.

Traffic Pattern	Wheel Passes/MGT	Number of wheel passes after which crack size exceeds 10mm	Amount of traffic after which crack size exceeds 10mm (MGT)
365	99441	N/A	N/A
365X	99441	N/A	N/A
DHST	94073	$1.77 \times 10^6$	18.8
EHST	89266	$1.37 \times 10^6$	15.3
Mixed	93716	$2.14 \times 10^6$	22.8
Mixed (365X)	93716	$2.02 \times 10^6$	21.6

#### 4.5.2 Variable Grinding Interval Investigation Wear Rate Results

##### *Class 365 and Class 365X Wear*

The predicted cumulative wear for the Class 365 and Class 365X traffic cases are plotted, in Figure 4.7, both with and without the initial grinding strategy of 0.2mm depth at  $1 \times 10^6$  wheel pass intervals. The uppermost plot (highest cumulative wear) in the figure is for the Class 365 traffic case with the initial grinding strategy, it exhibits

the stepped trend mentioned above in the description of the calculation of the Effective Continuous Wear Rate (section 4.4). The near vertical portion of the stepped profile is due of the grinding operation occurring between (or at one of) the two data points at the bottom and top of the step, producing a significantly greater change in the cumulative wear than the small regular change between the other data points.

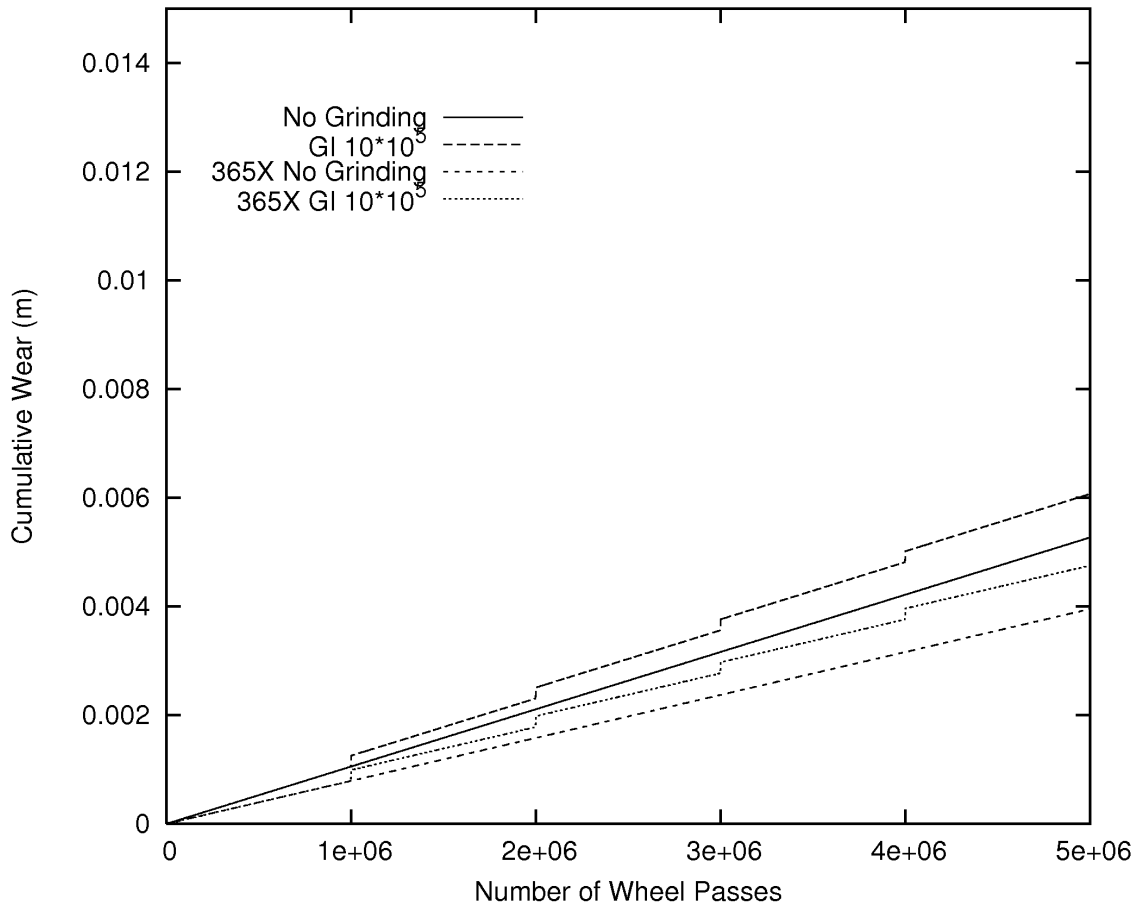


Figure 4.7. Cumulative wear results for the Class 365 and Class 365X traffic cases of the Variable Grinding Interval Investigation.

The Effective Continuous Wear Rate calculated for the Class 365 traffic case is 1.055nm/wheel pass (WP) without grinding and 1.204nm/WP with the initial grinding strategy. Similarly the predicted Effective Continuous Wear Rate for the Class 365X traffic case is 0.791nm/WP without grinding and 0.940nm/WP with the initial grinding strategy. The crack growth predictions for these cases shows that grinding is not necessary to control crack length. Therefore the wear life of the rail, i.e. the number of trains that can be carried before the vertical wear limit of the rail is reached, is reduced unnecessarily by applying grinding. Applying the initial grinding strategy increases the

Effective Continuous Wear Rate by 14% and 18% for the Class 365 and Class 365X traffic cases respectively, this means that applying the initial grinding strategy reduces the wear life of the rail to 88% and 85% respectively compared to that without grinding.

#### *Diesel High Speed Train Wear*

Plotted in Figure 4.8 are the cumulative wear results for the optimum grinding interval investigation for the Diesel High Speed Train traffic case. The cumulative wear for the optimum grinding interval case tends to 0.015m at the end of the  $5 \times 10^6$  wheel passes modelled, as the iterative investigation proceeded, the cumulative wear plots start to cluster around that for the optimum grinding interval. The uppermost plot in the figure is that for the case with the grinding strategy that had the lowest grinding interval, therefore it had more grinding operations during the period modelled, and subsequently had the highest cumulative wear.

The Effective Continuous Wear Rate calculated for the Diesel High Speed Train traffic case is 1.966nm/wheel pass (WP) without grinding and 3.000nm/WP with the optimum grinding strategy. The Effective Continuous Wear Rate for this traffic case with the "optimum" grinding strategy is 50% greater than the natural wear rate for this type of traffic, this means that after  $5 \times 10^6$  wheel passes the cumulative wear with and without grinding is 15.0mm and 9.8mm respectively. However without grinding the initial crack is predicted to grow to 10mm in size (5mm in depth) within  $1.773 \times 10^6$  wheel pass, after which other crack growth mechanisms are predicted to propagate the crack to threaten rail integrity. Therefore although the wear life of the rail is predicted to be reduced by approximately one third by using the optimum grinding strategy to control crack size, without grinding the growth of cracks would be expected to limit the life of the rail to less than the wear life with or without grinding.

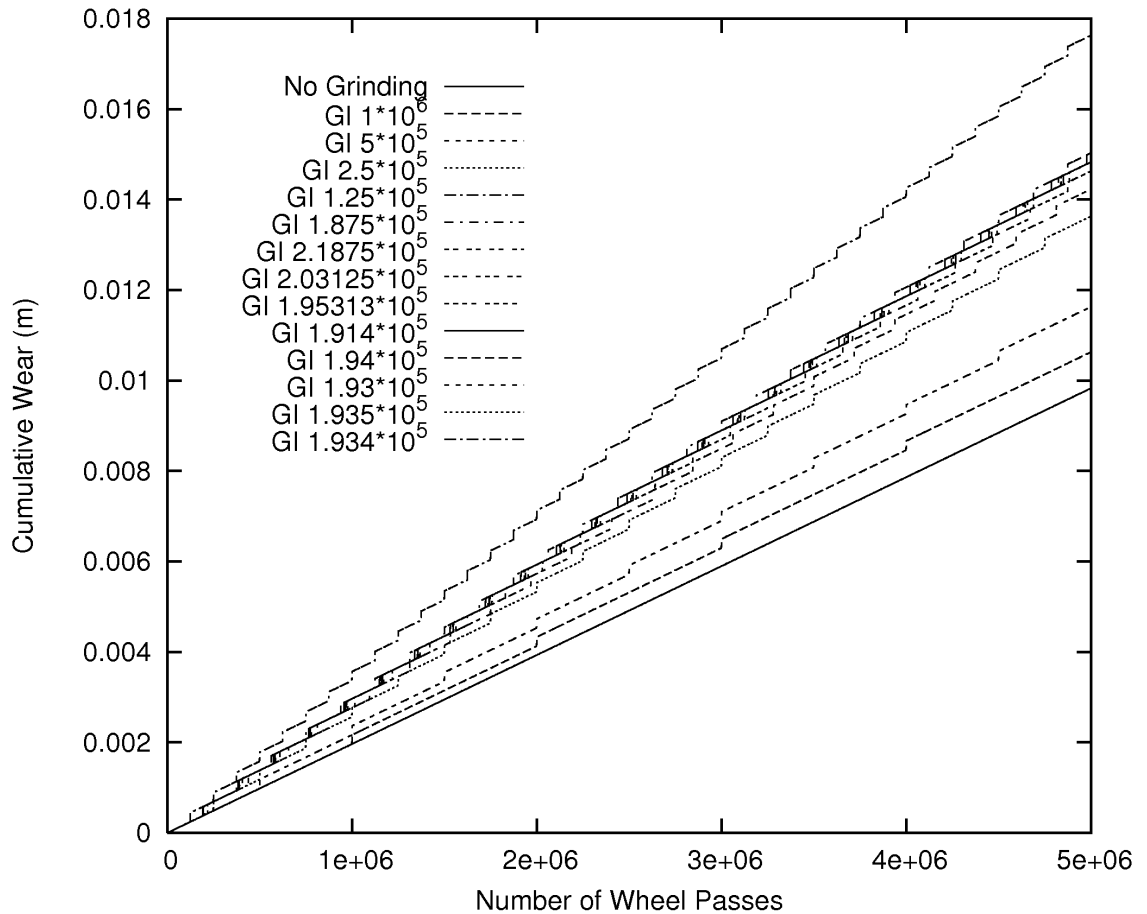


Figure 4.8. Cumulative wear results for the Diesel High Speed Train traffic case of the Variable Grinding Interval Investigation.

*Electric High Speed Train Wear*

The cumulative wear results for the Electric High Speed Train optimum grinding interval investigation are plotted in Figure 4.9. As with the Diesel High Speed Train traffic case, as the plots progress towards the optimum case, they cluster around the plot for the optimum case. For the Electric High Speed Train traffic case the cumulative wear after the  $5 \times 10^6$  wheel passes modelled was 14.5mm with the optimum grinding strategy and 10.4mm without. This corresponds to an Effective Continuous Wear Rate of 2.899nm/WP with the optimum grinding strategy and 2.083nm/WP without grinding.



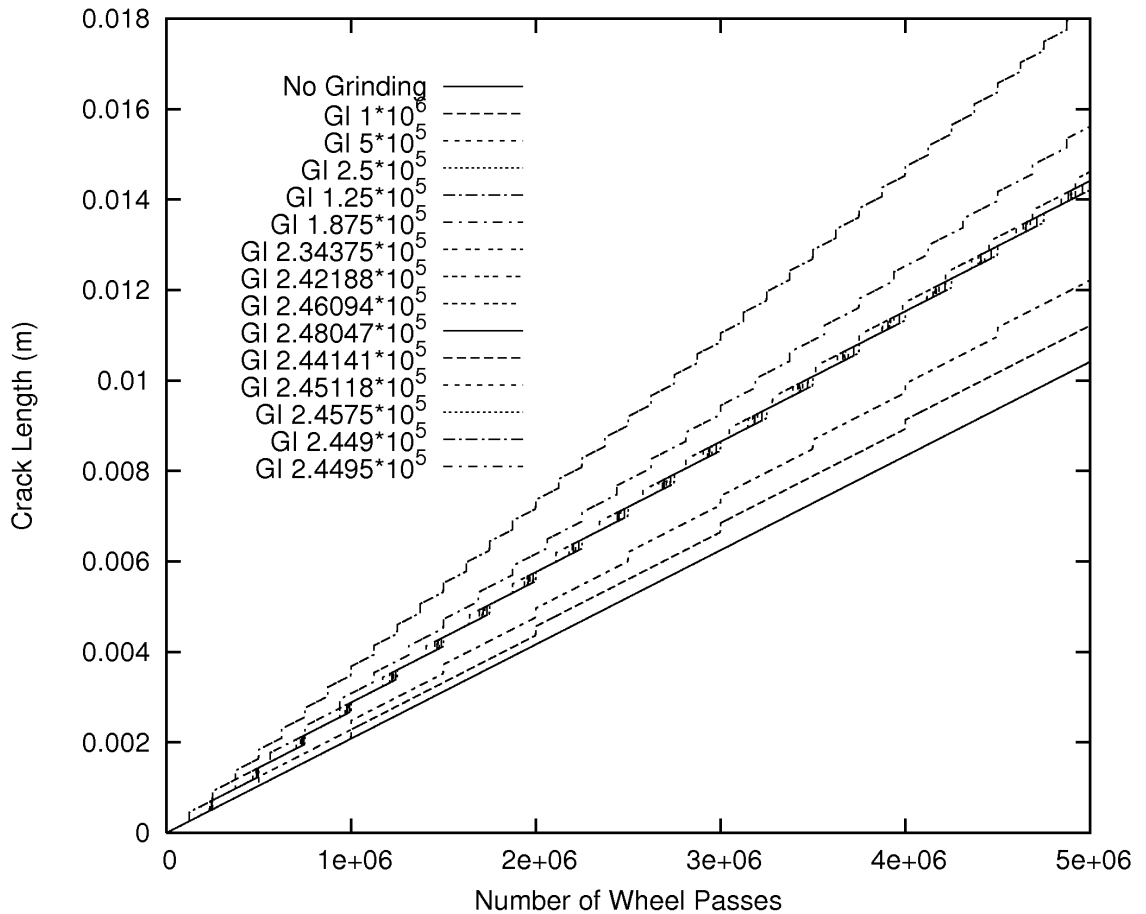


Figure 4.9. Cumulative wear results for the Electric High Speed Train traffic case of the Variable Grinding Interval Investigation.

#### *Mixed Traffic Wear*

The cumulative wear results for the Mixed traffic case, plotted in Figure 4.10, show a similar pattern to those of the individual High Speed Train cases. For the Mixed traffic case after modelling  $5 \times 10^6$  wheel passes the cumulative wear with the optimum grinding interval and without grinding tend towards 11.3mm and 8.7mm respectively. These cumulative wear values correspond to an Effective Continuous Wear Rate of 2.288nm/WP with the optimum grinding strategy and 1.747nm/WP without grinding.

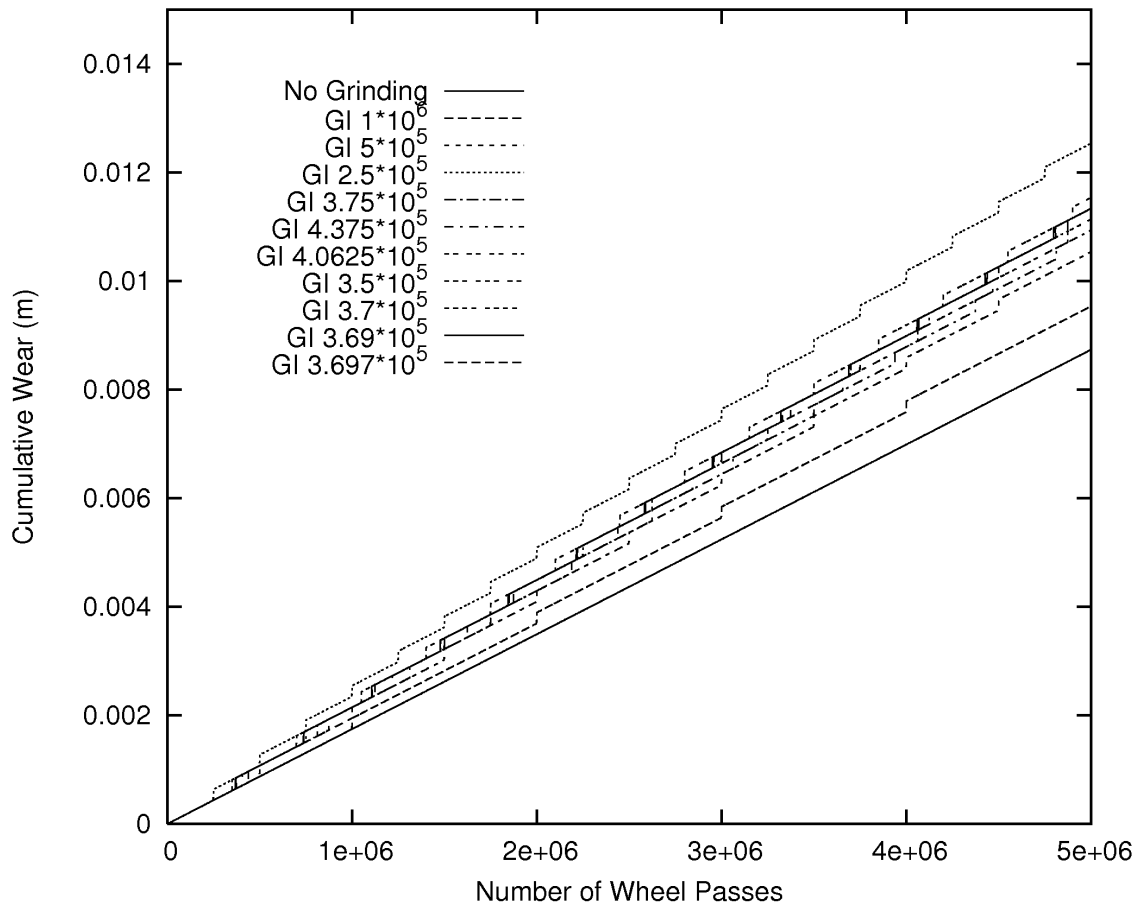


Figure 4.10. Cumulative wear results for the Mixed traffic case of the Variable Grinding Interval Investigation.

*Mixed (365X) traffic Wear*

The cumulative wear results for the optimum grinding interval investigation of the Mixed (365X) traffic case are plotted in Figure 4.11. The cumulative wear plots, other than the no grinding and initial grinding strategy cases, are clustered tightly around the optimum grinding interval case, this is because after the initial grinding strategy was modelled, the optimum grinding interval from the similar Mixed traffic case was used as an initiation point for the iterative search. For the Mixed (365X) traffic case after modelling  $5 \times 10^6$  wheel passes the cumulative wear with the optimum grinding interval and without grinding tend towards 11.4mm and 8.3mm respectively. These cumulative wear values correspond to an Effective Continuous Wear Rate of 2.290nm/WP with the optimum grinding strategy and 1.672nm/WP without grinding.

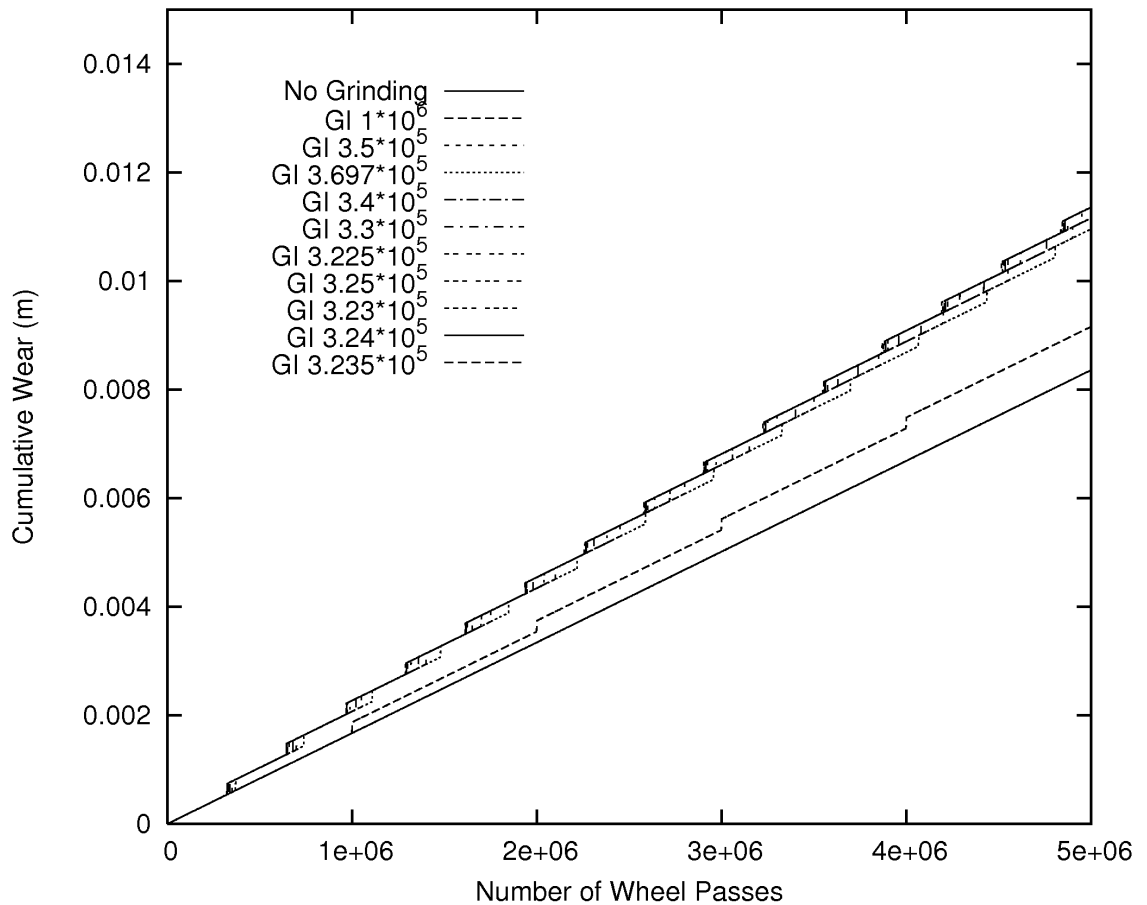


Figure 4.11. Cumulative wear results for the Mixed (365X) traffic case of the Variable Grinding Interval Investigation.

The Effective Continuous Wear Rates for the variable grinding interval investigation are given in Tables 4.3 and 4.4 below. In Table 4.3 the wear rates are expressed in terms of the average amount of wear per wheel pass of the traffic pattern, the number of wheel passes being the unit of measure for the period of the Grinding Model. In Table 4.4 the wear rates are expressed in terms of the amount of wear per Million Gross Tonnes (MGT) of traffic. Taking an example from Table 4.4, the difference in the effect of one MGT of traffic on the rail under different conditions, mentioned earlier with the crack size results, can be seen in the difference in the predicted Effective Continuous Wear Rate without grinding for EHST traffic being almost twice that of Class 365 traffic.

Table 4.3. Effective Continuous Wear Rates for each traffic case, expressed as the average vertical wear in metres per wheel pass, with and without optimum grinding interval strategy determined in the Variable Grinding Interval Investigation.

Traffic Pattern	Effective Continuous Wear Rate - No Grinding (nm/WP)	Effective Continuous Wear Rate - Optimum Grinding (nm/WP)
365	1.055	# 1.204 #
365X	0.791	# 0.940 #
DHST	1.966	3.000
EHST	2.083	2.899
Mixed	1.747	2.288
Mixed (365X)	1.672	2.290

Notes: # # Indicates the Effective Continuous Wear Rate for an example grinding strategy, not the optimum, for cases where crack was predicted to be removed by traffic alone, without grinding.

Table 4.4. Effective Continuous Wear Rates for each traffic case, expressed as metres of vertical wear per Million Gross Tonnes (MGT) of traffic, with and without the application of the optimum grinding interval strategy determined in the Variable Grinding Interval Investigation.

Traffic Pattern	Wheel Passes/MGT	Traffic Wear Rate - No Grinding (mm/MGT)	Effective Continuous Wear Rate - Optimum Grinding (mm/MGT)
365	99441	0.105	# 0.120 #
365X	99441	0.079	# 0.940 #
DHST	94073	0.185	0.282
EHST	89266	0.186	0.256
Mixed	93716	0.164	0.214
Mixed (365X)	93716	0.157	0.215

Notes: # # Indicates the Effective Continuous Wear Rate for an example grinding strategy, not the optimum, for cases where crack was predicted to be removed by traffic alone, without grinding.

#### 4.5.3 Variable Grinding Interval Investigation Discussion

The results of the optimum grinding interval investigation show that for some traffic cases, specifically the Class 365 and Class 365X traffic cases, grinding was not required to control crack size and application of grinding (for the purpose of crack size control)

would represent a waste of grinding resources and rail life. For the other case it was found that applying grinding strategies affected the predicted crack size trend favourably, compared to the predicted trend without grinding, and that the application of grinding strategies with different grinding intervals resulted in different predicted crack size trends. The results illustrate the use of the grinding model to find a grinding strategy which matches a set criterion for a variety of traffic cases.

For the traffic cases which require grinding, i.e. both High Speed Train cases and both Mixed traffic cases, the Effective Continuous Wear Rates are in the range 0.214-0.282mm/MGT with optimum grinding for that traffic case applied. Without any grinding the Effective Continuous Wear Rates for these cases are in the range 0.157-0.186mm/MGT, however without grinding the crack is predicted to exceed 10mm in size within at least 24MGT for all these cases. This figure is derived from the longest period for the crack to exceed 10mm from all of the cases, multiplied by the lightest traffic of all the cases, individual cases take less traffic for the crack to exceed 10mm. At 24MGT of traffic and optimum grinding, with the case which has the highest Effective Continuous Wear Rate, the maximum predicted vertical wear with grinding applied is 6.8mm. The vertical wear limit of UIC 60 section rail is approximately 14mm, dependent upon side wear and situation. Therefore for the cases which required grinding, the application of the optimum grinding strategy effectively doubled life by taking to end of wear life at 50MGT or more, depending upon the specific Effective Continuous Wear Rate. This is as opposed to the crack being predicted to grow to threaten the integrity of the rail within 24MGT of traffic where no grinding is applied to these traffic cases. It should be noted that 50MGT is a relatively short rail life; however the modelling has been carried out for a curve of tight radius for a mainline, where the contact forces driving crack growth and wear are high. The safe rail life of 50MGT with grinding as opposed to 24MGT without the optimum grinding strategy have been determined from the aggregated results of the traffic cases that were predicted to require grinding. That is that 24MGT is the longest rail life that could be expected of all the cases without grinding and 50MGT is the shortest rail life of all the cases with the optimum grinding strategy for that traffic case applied. The difference between the point at which the crack size exceeds 10mm without grinding and the end of the wear life of the rail with the optimum grinding strategy applied will be different in each specific case, but is predicted to be greater than twice the amount of traffic. For the purpose of

this discussion it is sufficient that the results show that applying the respective optimum grinding strategy to the traffic cases modelled which were predicted to require grinding to control crack life, at least doubled the safe life of the rail. That grinding was predicted to extend rail life for some traffic cases, showed that there was potential for regular maintenance grinding to be cost effective in extending the operational life of the rail, the extent of the cost effectiveness would be dependent upon the relative cost of the grinding and the value of the increased rail life, that is, the reduction in the whole life cycle cost of the rail.

The investigation was carried out with the grinding depth set to represent the maximum utilisation of the grinding machine in a single pass. There are practical situations where it could be more effective to operate at a specific grinding interval, rather than at the maximum utilisation of the grinding machine, these are discussed in the next set of case studies where the optimum grinding depth for a fixed grinding interval is investigated.

#### **4.6 Case Study 2: Variable Grinding Depth Investigation:**

In the Variable Grinding Interval investigation the grinding machine was used at its maximum capacity, by comparison considering varying the grinding depth and therefore not using the grinding machine at its maximum capacity might on initial assessment appear to be inefficient. However, if sections of track kilometres in length, composed of segments with different characteristics, such as curve radius, are grouped into maintenance sections, then practical considerations such as grinding machine availability and minimising site transfer movements, dictate that grinding operations are carried out on all the track segments within the maintenance section at the same time. Therefore all the track segments would have the same grinding interval, dictated by that required to control crack size in the section where crack growth dominates the crack size trend, or the grinding frequency required to control rail profile of a determining section. The determining section being that which requires the most frequent grinding attention. Alternatively the grinding interval could be set by operational considerations. Using the same grinding strategy for all the segments within a maintenance section might waste the wear life of those sections where the crack size trend is more wear dominated than the most crack growth dominated section and waste grinding resources.

If the frequency of grinding operations is fixed by either the requirements of other segments of track in a maintenance section or logistical constraints, then it is potentially useful to investigate varying the grinding strategy applied to each track segment by varying the depth of material removed at each grinding operation to obtain the optimum grinding strategy for a given fixed interval. A series of case studies have been carried out to investigate the optimum grinding depth per grinding operation for several traffic cases with a fixed grinding interval. The grinding interval selected to carry out the investigation, was  $2 \times 10^5$  wheel passes. This interval was selected as it was close to the optimum minimum grinding interval determined across all traffic cases in the variable grinding interval investigation to achieve the required predicted crack size trend with a grinding depth which represents the maximum depth of material removable by in a single pass by a typical production grinding machine. Therefore the maximum grinding depth that was expected to be predicted as the optimum for all the traffic cases would be similar to the maximum single pass grinding depth of the grinding machine. This allows all the traffic cases to be investigated with the same conditions whilst keeping the grinding machine operating at near maximum utilisation. The definition of the optimum crack size trend is the same as for the variable grinding interval investigation, that is that a crack of 1.75mm initial size should be predicted to tend towards zero after  $3 \times 10^6$  wheel passes of traffic (to within  $\pm 0.5\%$ ). The investigation was carried out in a similar way, in this instance starting with three initial grinding strategies consisting of grinding depths of 0.2mm and 0.1mm applied every  $2 \times 10^5$  wheel passes in both strategies, and no grinding. Then the grinding depth for the next grinding strategy in the investigation was set at a value between the previous values that produced trends either side of the required trend, until the value for the grinding depth predicted to produce the required predicted crack size trend was found. This process was carried out for the same traffic cases as investigated in the variable grinding interval investigation, to allow the effects of the different traffic pattern compositions on the grinding depth variable of the grinding strategy required to achieve the required crack size trend to be studied.

#### 4.6.1 Variable Grinding Depth Investigation Crack Size Results

##### *Class 365 and Class 365X case*

Figure 4.12 plots the crack size results for the Class 365 and 365X traffic cases together. As with the variable grinding interval (VGI) investigation it can be seen that grinding is not required to control crack size for the initial crack size of 1.75mm used. The crack size trend tends to zero before  $3 \times 10^6$  wheel passes of traffic, without applying grinding, for both traffic cases, the standard Class 365 tending to zero sooner. Applying grinding strategies with the fixed interval and different depths of grinding only serves to waste the wear life of the rail and is therefore counter-productive. Figure 4.12 also shows that for each traffic case, Class 365 or Class 365X, the crack size trend tends towards zero after fewer wheel passes when the grinding depth applied is 0.2mm than when it is 0.1, however both tend towards zero faster than required.

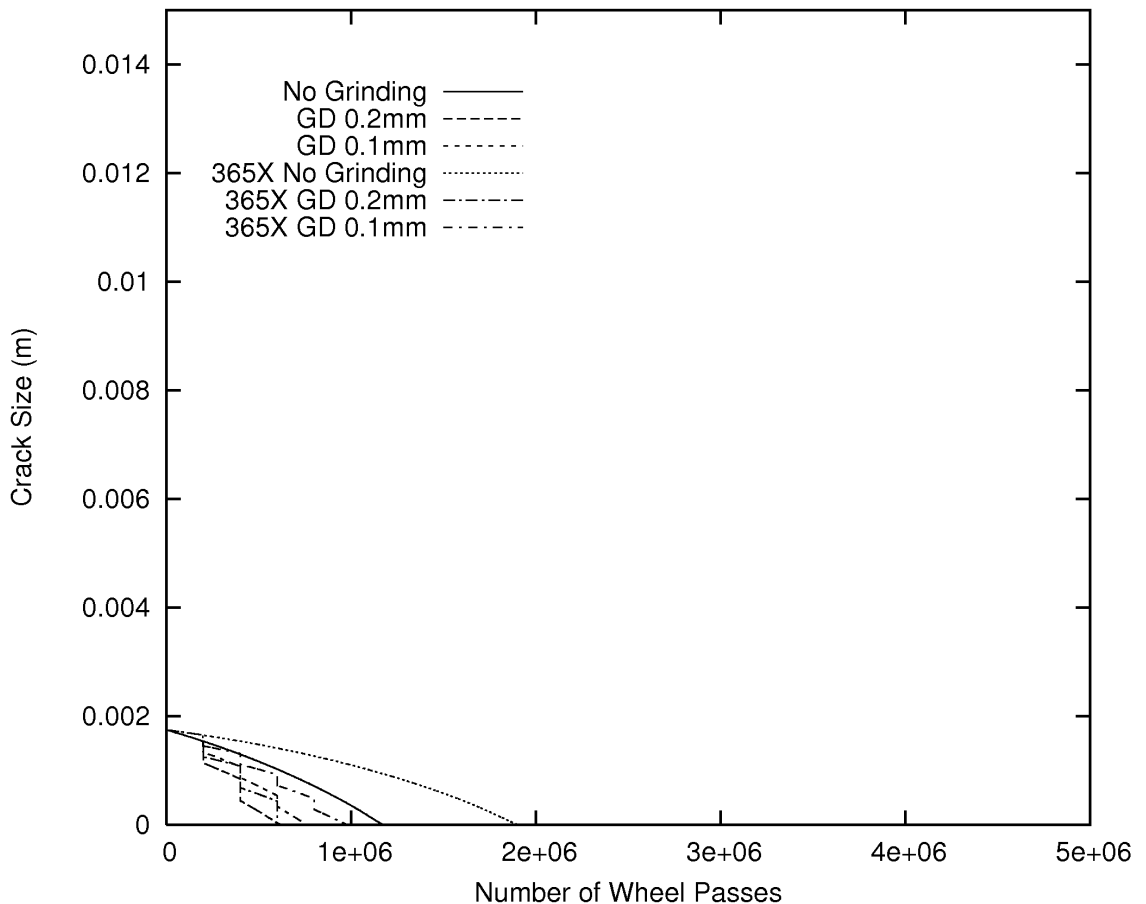


Figure 4.12. Variable Grinding Depth Investigation, crack size trend results for Class 365 and Class 365X traffic cases.



The crack size trends without grinding applied for the Class 365 and Class 365X traffic cases, as well as for all the other traffic cases, are the same as those for each traffic case modelled without grinding for the Variable Grinding Interval Investigation.

#### *Diesel High Speed Train case*

The initial modelling runs for the Diesel High Speed Train traffic case showed that the crack was predicted to exceed 10mm without grinding and that the most severe of the initial grinding strategies was insufficient to control crack size and produce a predicted crack trend that tended towards zero within  $3 \times 10^6$  wheel passes. Therefore an additional initial grinding strategy with a grinding depth of greater than 0.225mm was carried out, which did produce a crack size trend which tended to zero before  $3 \times 10^6$  wheel passes, meaning that the optimum grinding depth was between 0.2mm 0.225mm, so the iterative search was conducted using these grinding depths as the starting point. It was found that a grinding strategy which had a depth of 0.208mm, with the specified interval of  $2 \times 10^5$  wheel passes, produced the required predicted crack size trend, as shown in figure 4.13.

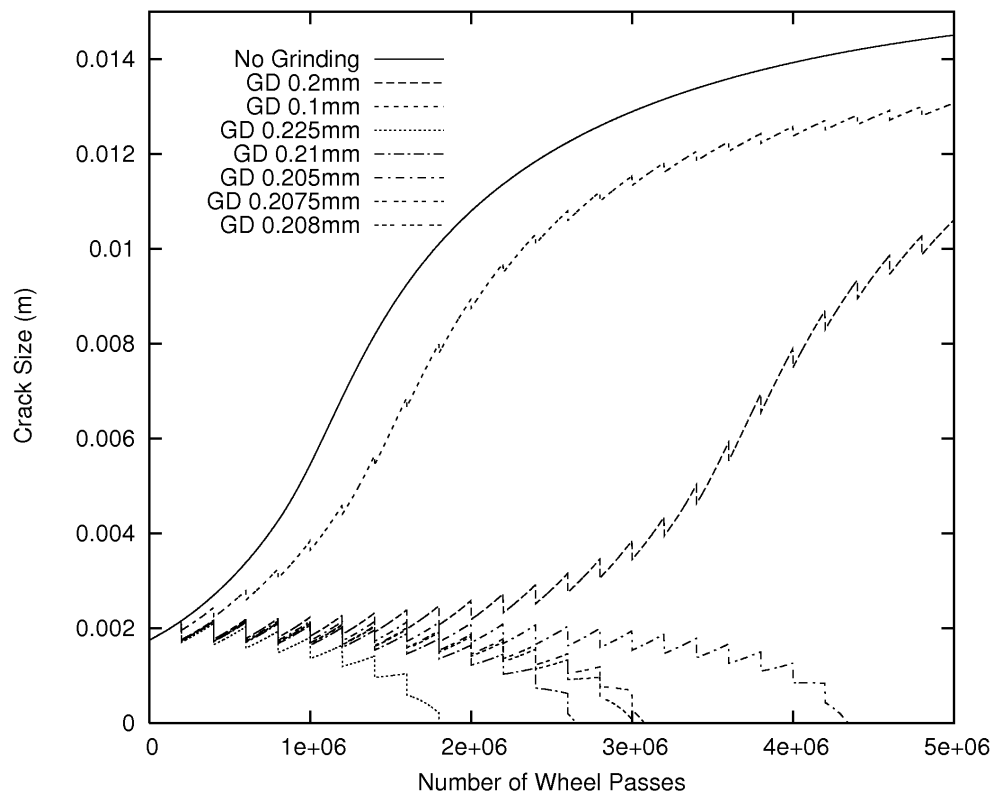


Figure 4.13. Crack size trend results for Diesel High Speed Train traffic case of the Variable Grinding Depth investigation.

### *Electric High Speed Train case*

The results of the investigation to find the optimum grinding depth for the Electric High Speed Train case are shown in figure 4.14; it was found that a grinding depth of 0.154mm was required to produce the required predicted crack size trend for the Electric High Speed Train traffic case with a fixed grinding interval of  $2 \times 10^5$  wheel passes.

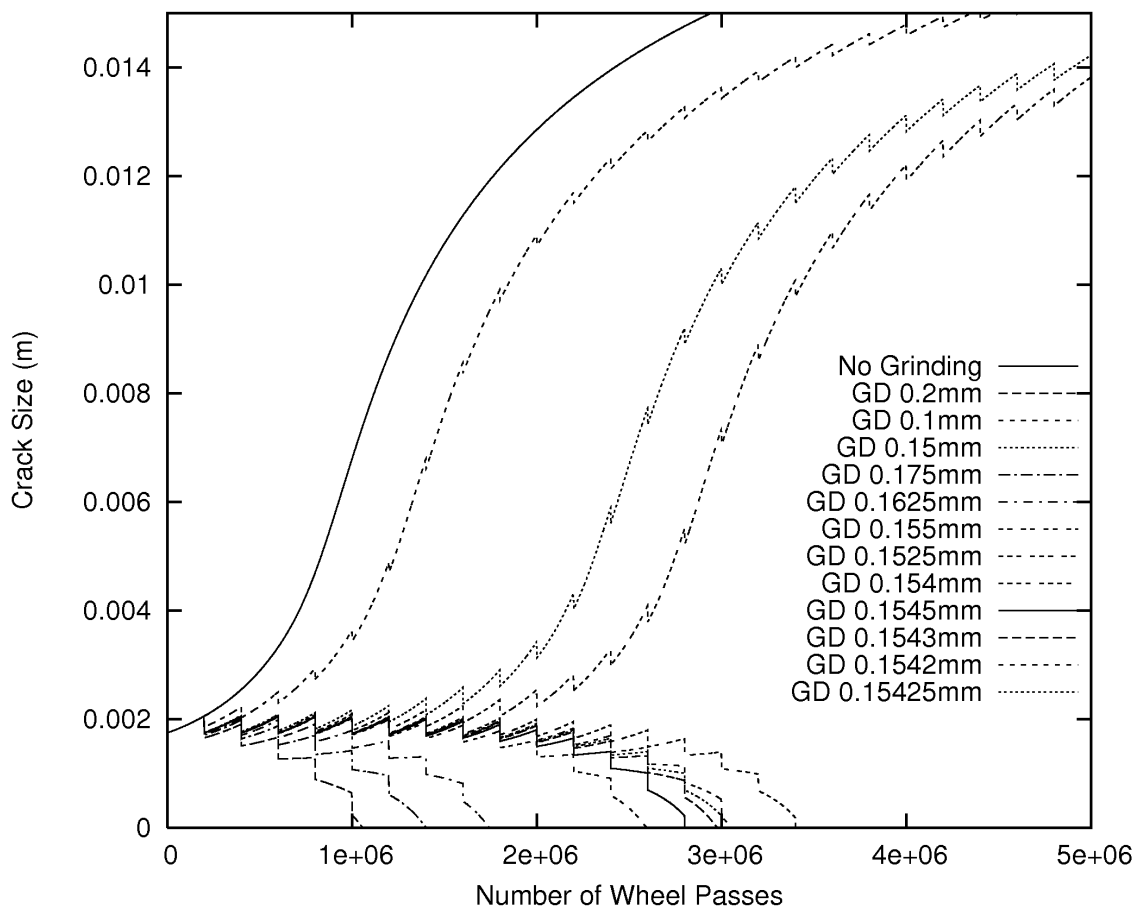


Figure 4.14. Crack size trend results for Electric High Speed Train traffic case of the Variable Grinding Depth investigation.

### *Mixed Traffic Case and Mixed Traffic (365X) case*

The Mixed Traffic case showed that the grinding depth used in the grinding strategy which produced the required crack size trend that was within the range of the optimum grinding depth values for the individual traffic cases. This indicates that not only if the composition of the traffic significant when determining the optimum grinding interval,

as found in the Variable Grinding Interval investigation, it is also significant in determining the optimum grinding depth for a grinding strategy to control crack length. As can be seen from Figure 4.15 the optimum grinding depth corresponding to the fixed grinding interval was 0.094mm for the Mixed Traffic case with the standard Class 365 in the traffic pattern. The crack size trend results for optimum grinding depth investigation with the Mixed (365X) traffic case with the low wear Class 365X replacing the Class 365 in the traffic pattern are shown in Figure 4.16, the optimum grinding depth for this case was found to be 0.1115mm.

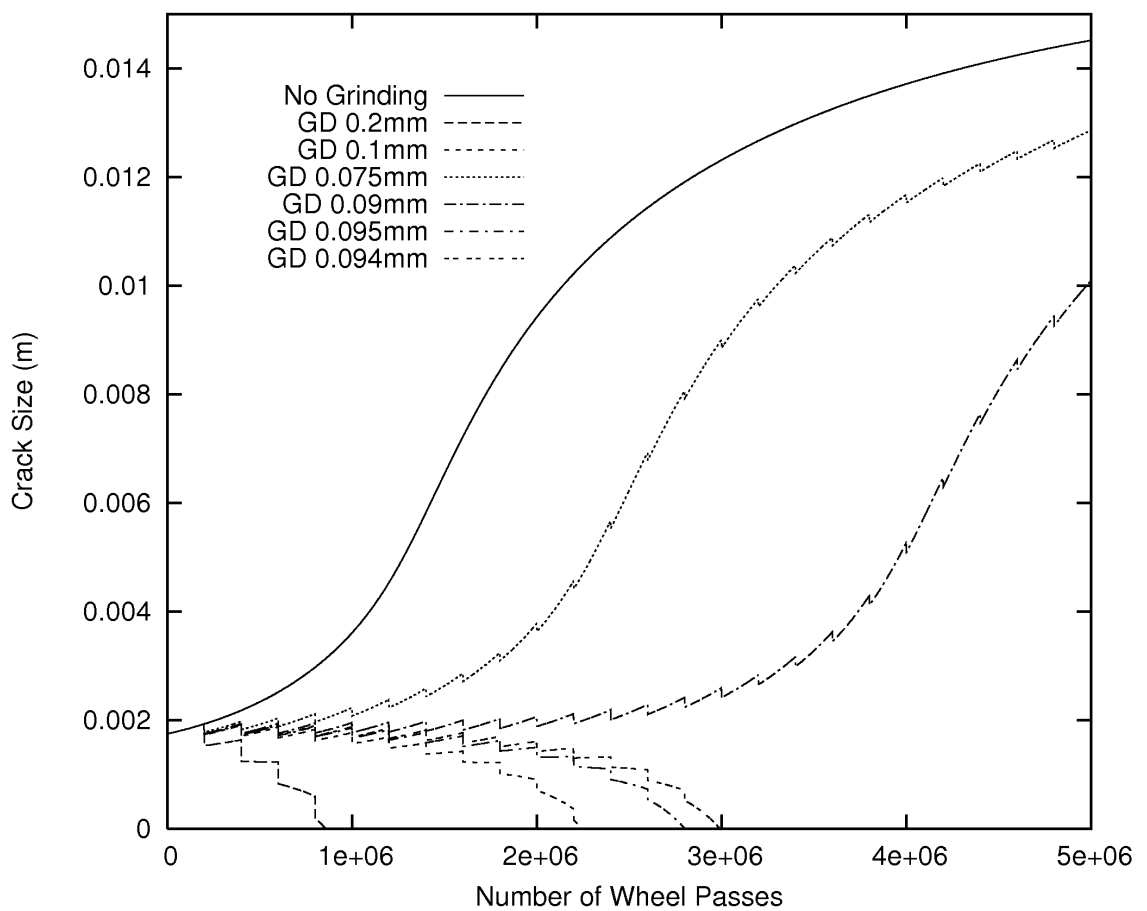


Figure 4.15. Crack size trend results for Mixed traffic case of the Variable Grinding Depth investigation.

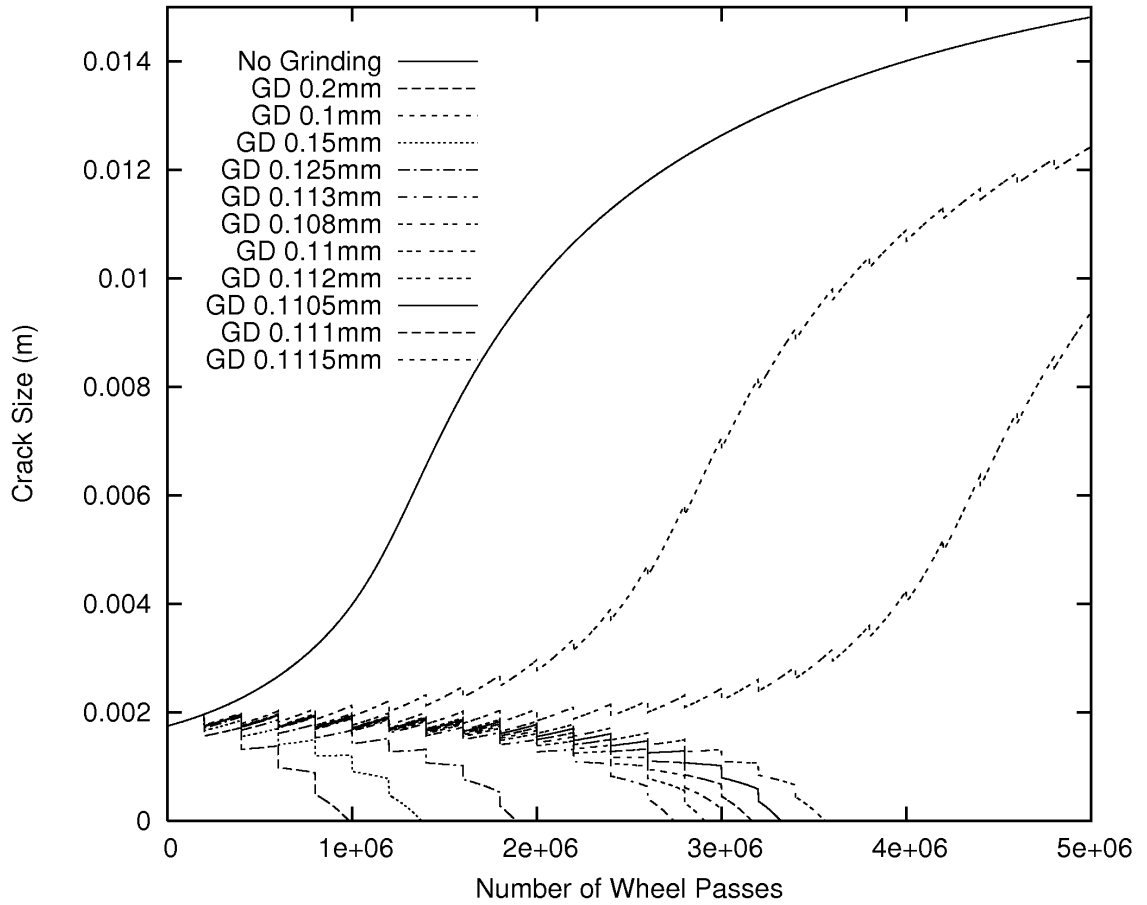


Figure 4.16. Crack size trend results for Mixed (365X) traffic case of the Variable Grinding Depth investigation.

#### 4.6.2 Summary of Variable Grinding Depth Investigation Results

The optimum grinding depths found in the Variable Grinding Depth Investigation for the different traffic cases are summarised in table 4.5.

Table 4.5. Results of the Variable Grinding Depth Investigation, table of optimum grinding depth determined for each traffic case.

Traffic Pattern	Optimum Grinding Depth (mm)	Grinding interval (Wheel Passes)
365	N/A #	200000
365X	N/A #	200000
DHST	0.208	200000
EHST	0.154	200000
Mixed	0.094	200000
Mixed (365X)	0.112	200000

Notes: # In these cases the crack size trend was predicted to tend to zero without grinding before the specified number of wheel passes, therefore no grinding should be carried out. Where an example is required the initial grinding strategy with the grinding depth of 0.1mm will be used.

#### 4.6.3 Variable Grinding Depth Investigation Wear Results

Figure 4.17 plots the cumulative wear results for the Class 365 and 365X traffic cases, as the optimum grinding depth is effectively zero, the wear results for each case with a grinding depth of 0.1mm applied every  $2 \times 10^5$  wheel passes are shown as examples. Figure 4.18 plots the cumulative wear results for the Diesel High Speed Train and Electric High Speed Train traffic cases, the wear results for the optimum grinding depth and no grinding cases are plotted for each traffic case. Figure 4.19 plots the cumulative wear results for the Mixed Traffic cases. In Figures 4.17-4.19 the Effective Continuous Wear Rate of each case with grinding, calculated (as described in section 4.4) to enable comparisons to be made between the numerical wear values for different cases, is plotted alongside the actual cumulative wear values. This illustrates how the Effective Continuous Wear Rate relates to the actual cumulative wear values.

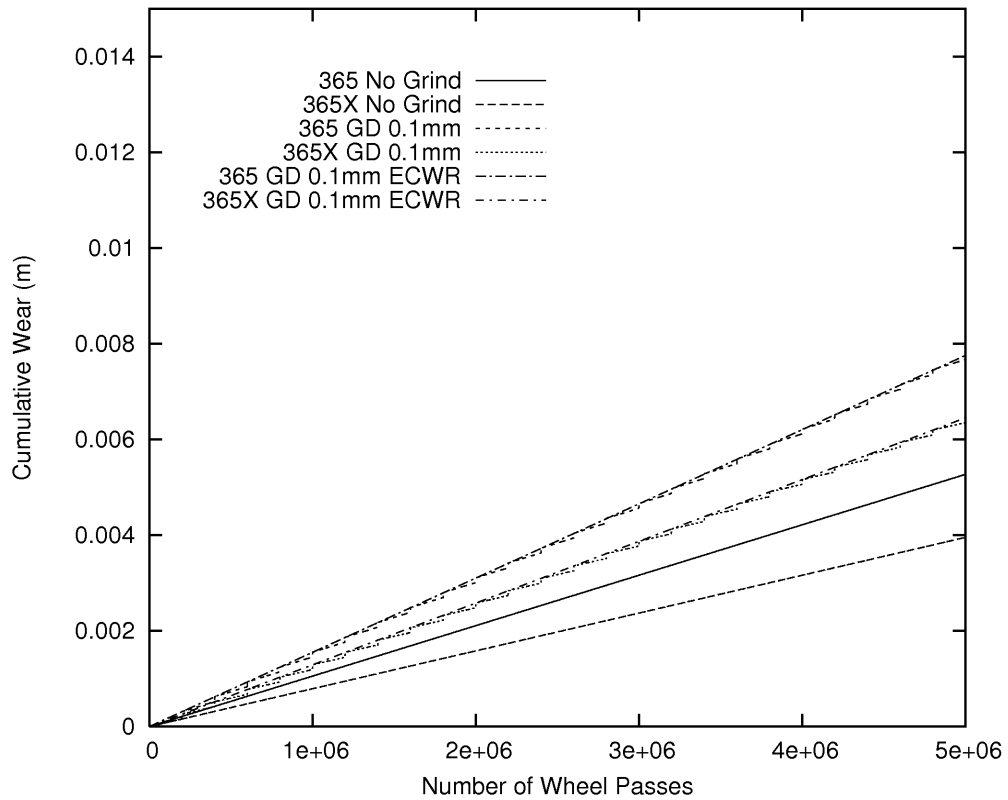


Figure 4.17. Cumulative wear results for the Class 365 and Class 365X traffic cases of the Variable Grinding Depth Investigation, with and without example grinding strategy.

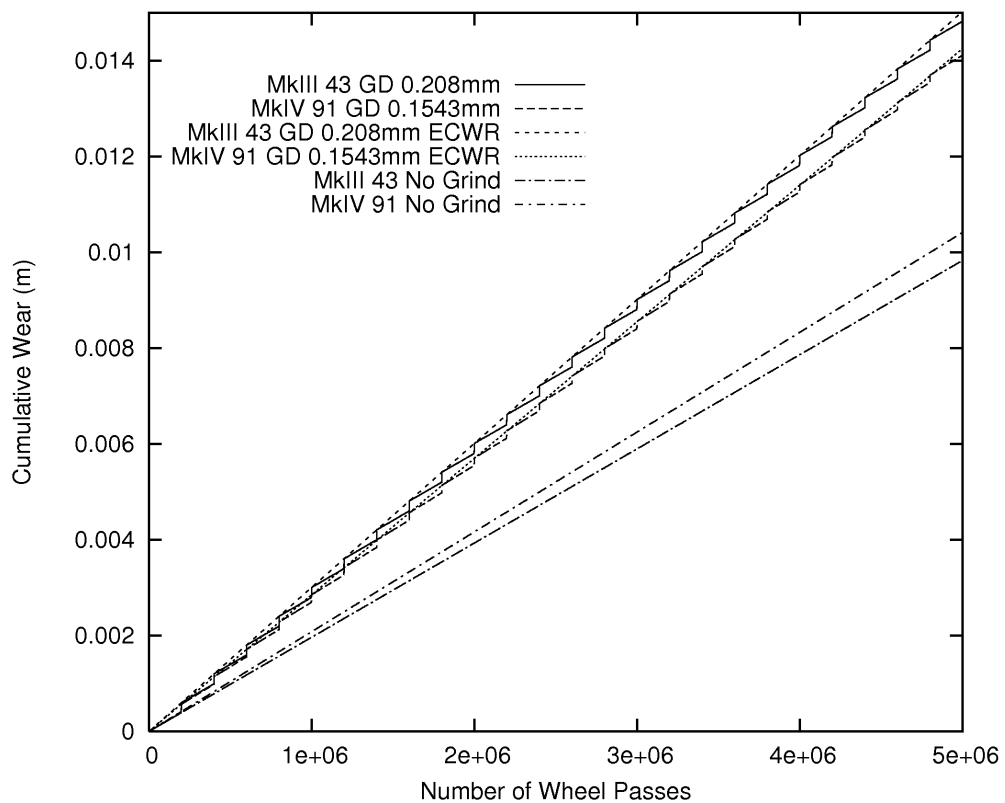


Figure 4.18. Cumulative wear results for the traffic cases of the Variable Grinding Depth Investigation, consisting of only the Diesel or Electric High Speed Train, with and without example grinding strategy.

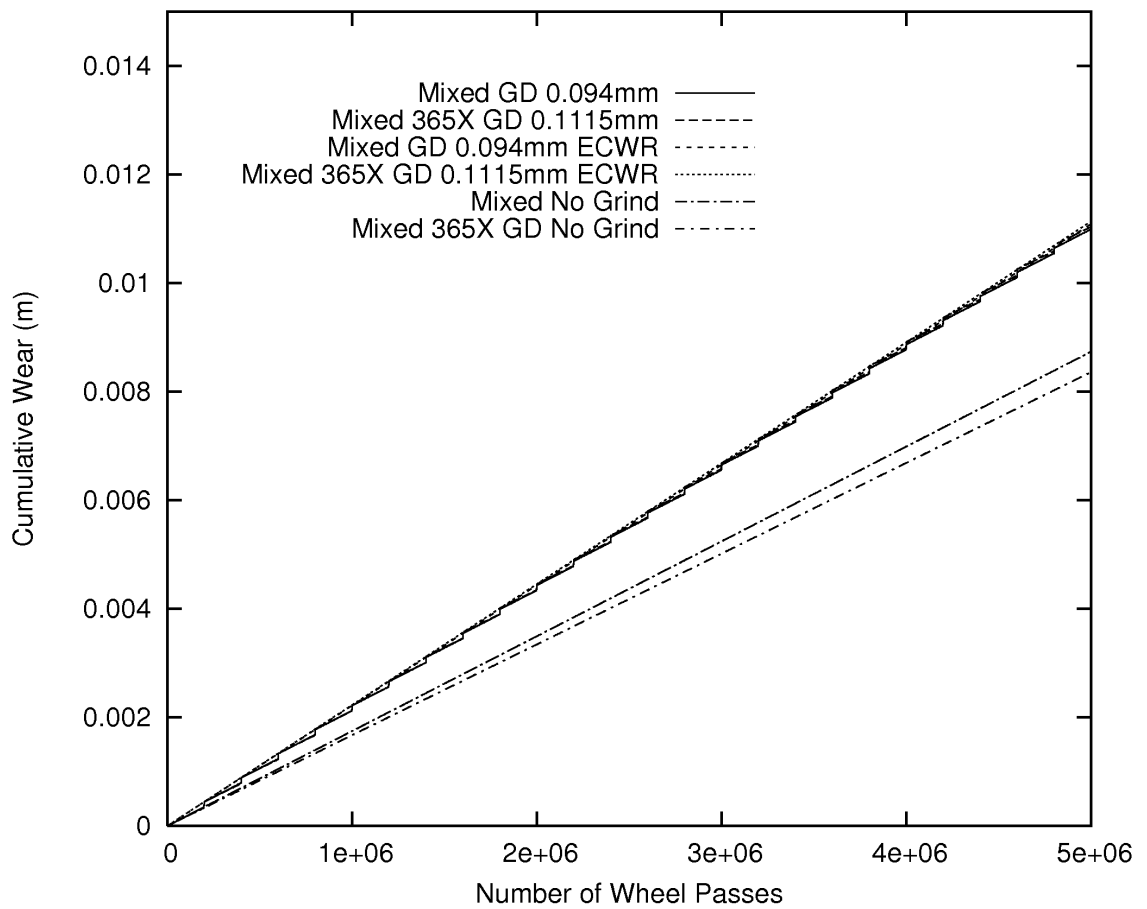


Figure 4.19. Cumulative wear results for the Mixed and Mixed (365X) traffic cases of the Variable Grinding Depth Investigation, with and without their respective optimum grinding strategy.

Tables 4.6 and 4.7 below show the Effective Continuous Wear Rate, with and without optimum grinding depth determined for each traffic case (shown in Table 4.5) grinding strategy for each traffic case.

Table 4.6. Effective Continuous Wear Rates for each traffic case, expressed as the average vertical wear in metres per wheel pass, with and without optimum grinding depth grinding strategy determined in the Variable Grinding Depth Investigation.

Traffic Pattern	Effective Continuous Wear Rate - No Grinding (nm/WP)	Effective Continuous Wear Rate - Optimum Grinding (nm/WP)
365	1.055	# 1.552 #
365X	0.791	# 1.291 #
DHST	1.966	3.006
EHST	2.083	2.854
Mixed	1.747	2.217
Mixed (365X)	1.672	2.229

Notes: # # Indicates the Effective Continuous Wear Rate for an example grinding strategy using a grinding depth of 0.1mm, not the optimum, for cases where crack was predicted to be removed by traffic alone, without grinding.

Table 4.7. Effective Continuous Wear Rates for each traffic case, expressed as metres of vertical wear per Million Gross Tonnes (MGT) of traffic, with and without the application of the optimum grinding depth strategy determined in the Variable Grinding Depth Investigation.

Traffic Pattern	Wheel Passes/MGT	Traffic Wear Rate - No Grinding (mm/MGT)	Effective Continuous Wear Rate - Optimum Grinding (mm/MGT)
365	99441	0.105	# 0.154 #
365X	99441	0.079	# 0.128 #
DHST	94073	0.185	0.283
EHST	89266	0.186	0.255
Mixed	93716	0.164	0.208
Mixed (365X)	93716	0.157	0.209

Notes: # # Indicates the Effective Continuous Wear Rate for an example grinding strategy using a grinding depth of 0.1mm, not the optimum, for cases where crack was predicted to be removed by traffic alone, without grinding.

#### 4.6.4 Variable Grinding Depth Investigation Discussion

The optimum depth of grinding applied at the fixed interval for each of the traffic cases is quoted in millimetres at a precision of up to four decimal places. Whilst it is appreciated that it would not be possible to apply grinding at this level of precision in practice on the railway network, it was found that, the point at which the crack size



trended to zero, was sensitive to small changes in grinding depth. This meant that when the model was run for some traffic cases, with grinding strategies in which the grinding depth was specified to a precision of three decimal places, then two adjacent values could produce predicted crack size trends which straddled the optimum and were outside the +/-0.5% tolerance applied to the optimum trend. This necessitating investigating grinding depth values between the two three decimal place values to find a value that generated a crack size trend that fell within the tolerance applied to the optimum trend. In practice if an optimum grinding depth value determined using the model was to be applied on the network using a production grinding machine, then the first increment of grinding depth that the grinding machine can apply, which is greater than the optimum value should be used. This would ensure that the predicted track size trend would be predicted to tend to zero before the number of wheel passes specified as optimum, this being safer than using the first increment of grinding depth that the grinding machine can apply which is less than the optimum value.

As with the Variable Grinding Interval Investigation, the Class 365 and Class 365X traffic cases do not require grinding for the predicted crack size trend to reach zero within the specified number of wheel passes. Applying any grinding for the removal of RCF cracks would represent a waste of rail wear life and of grinding resources. Similarly both of the high speed train and mixed traffic cases were predicted to require grinding to control the crack size, as these crack trends without grinding are the same as in the Variable Grinding Interval Investigation, then the same prediction for when the crack size is expected to exceed 10mm is true, that is within at least 24MGT for these four traffic cases.

#### **4.7 Comparisons Between Case Studies 1 & 2**

The Class 365 and Class 365X traffic cases do not require grinding for the predicted crack size trend to reach zero within the specified number of wheel passes. Applying any grinding for the removal of RCF cracks would represent a waste of rail wear life and of grinding resources. The only difference is that the initial grinding strategy used, 0.1mm depth removed at  $2 \times 10^5$  wheel pass intervals, produces more wear, than the initial grinding strategy used for the Variable Grinding Interval investigation. For example, the Effective Continuous Wear Rates for the Class 365 case are 1.552nm/WP

for the Variable Grinding Depth Investigation and 1.204nm/WP Variable Grinding Interval Investigation.

Comparison of the results from both case studies show that for the same traffic conditions, the Effective Continuous Wear Rate is lower when the required crack size trend is achieved by removing smaller amounts of material more frequently. For example the optimum grinding strategies determined for the Mixed Traffic case in the Variable Grinding Interval Investigation and the Variable Grinding Depth Investigation produced different effective continuous wear rates. A grinding depth of 0.2mm applied at an interval of 369700 wheel passes determined in the Variable Grinding Interval Investigation which produced an effective continuous wear rate of 0.214mm/MGT, whereas a grinding depth of 0.094mm applied at an interval of 200000 wheel passes determined in the Variable Grinding Depth Investigation produced an effective continuous wear rate of 0.208mm/MGT. Both of these grinding strategies met the optimum grinding strategy criteria, however the grinding strategy with the lower grinding depth and shorter interval produced a lower effective continuous wear rate, in combination with the same traffic pattern. This is because, for the given initial crack size, the crack grows at a higher rate the greater its size, so for grinding strategies that produce the same overall crack size trend (i.e. tend to zero after the same number of wheel passes) a lower grinding depth applied sooner, reduces the crack size sooner and therefore reduces its growth rate in the period up until the larger grinding interval is reached, this means that the crack has grown less and less grinding is required to control it. That is, that from the same size initial crack and grinding strategy start point, a grinding strategy with a lower interval initiates grinding sooner which shortens the crack, which in turn reduces its growth rate. Since the traffic wear rate is considered the same, then to get the crack size to tend to zero after the same period less grinding is required overall, because the crack is growing at a lower rate, this is due to the lower grinding interval resulting in the crack size being reduced by grinding sooner.

Generally for each traffic case, it was the optimum grinding strategy determined in the Variable Grinding Depth Investigation which had a marginally lower predicted Effective Continuous Wear Rate than that determined in the Variable Grinding Interval Investigation, as they generally consist of lower grinding depth applied more frequently. The exception to this general result is results for the Diesel High Speed Train traffic

case, this is because the interval used in the Variable Grinding Depth Investigation is slightly longer than the optimum determined in the Variable Grinding Interval Investigation, and consequently the optimum grinding depth was found to be greater. This is consistent with the observation in the previous paragraph, and shows that the difference in Effective Continuous Wear Rates is not a factor of which investigation the optimum was determined in.

An example of the differences in crack size trend produced by the applying optimum grinding strategy determined from both the Variable Grinding Interval and Variable Grinding Depth investigations, to the same traffic case, the Mixed traffic case, is shown in Figure 4.20. The details of the grinding strategies are a 0.2mm grinding depth with a grinding interval of  $3.697 \times 10^5$  wheel passes determined in the Variable Grinding Interval investigation, and a grinding interval of  $2 \times 10^5$  wheel passes with a grinding depth of 0.094mm determined in the Variable Grinding Interval investigation.

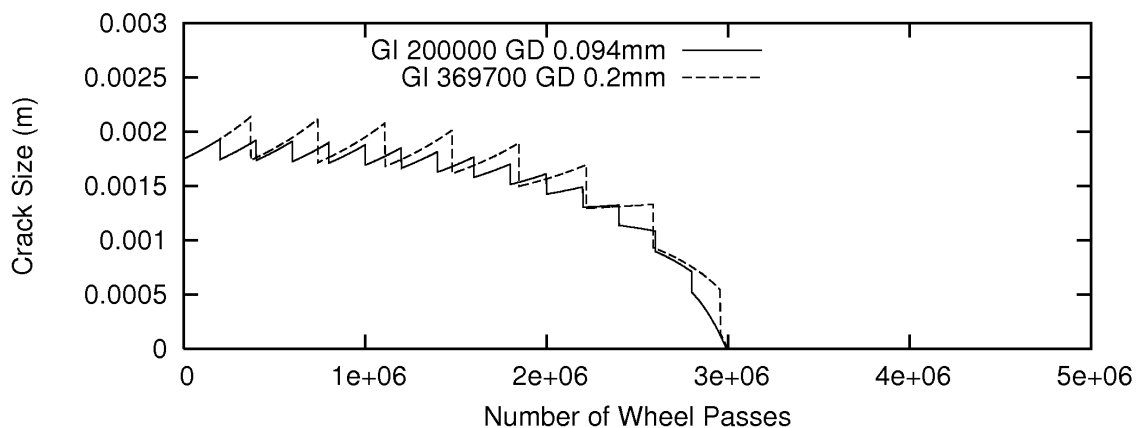


Figure 4.20. Comparison of the predicted crack size trend results with the optimum grinding strategies determined in the Variable Grinding Interval investigation and the Variable Grinding Depth investigation for the Mixed traffic case.

The general crack size trend for shorter interval, lower grinding depth, grinding strategy case can be seen to reduce marginally quicker at the start of the modelling run, and approach zero at the specified point at a lower rate than the longer interval, deeper grinding depth case. The Effective Continuous Wear Rates which corresponding to the crack size trends plotted in Figure 4.20 are 2.217nm/WP for the optimum determined in the variable grinding depth investigation and 2.288nm/WP for the optimum determined in the variable grinding interval investigation. Both grinding strategies produce the required crack size trend for the traffic case, with the Effective Continuous Wear Rate

of the strategy with the shorter interval and lower grinding depth, determined in the Variable Grinding Depth investigation is 3% less than that for the other optimum grinding strategy.

From this it can be deduced that the shorter the grinding interval used, with associated grinding depth, to produce a specified crack size trend, then the lower the Effective Continuous Wear Rate and hence the longer the rail life. However the grinding interval of the optimum from the Variable Grinding Depth Investigation is 54% of that from the Variable Grinding Interval investigation, yet the Effective Continuous Wear Rate is only reduced by 3%, therefore the rail life is only 3% longer. It is unlikely that the higher grinding interval and increase in the number of instances of the fixed grinding costs of each grinding operation would be less than the value of such a small increase in rail life.

#### **4.8 Application of Optimum Grinding Strategies**

That there can be two grinding strategies which meet the technical requirement for the crack size trend shows that various combinations of the grinding depth and interval can produce the required predicted crack size trend for each traffic case. In each of the investigations carried out one of the grinding strategy variables was fixed at an example value, however when considering a specific situation, these fixed values might not be suitable, then a suitable value of one of the variables could be selected and the value of the other variable to produce the required predicted crack size trend found. Alternatively there could be a range of discrete values for one of the grinding strategy variables, such as the grinding frequency being restricted to either annual or bi-annual for scheduling reasons for example, or a requirement that less than 10% of the track in a maintenance section should require more than one grinding pass per grinding operation. In this case for each of the discrete values of one variable, the value of the other variable which gives a grinding strategy that meets the technical requirements for predicted crack size trend could be found. Then the most suitable of these optimum grinding strategies selected for application base on other criteria such as the rail life cycle cost, profile grinding requirements, the logistical arrangements surrounding the allocation of grinding machine time.

The determination of the suitability, and more particularly the safety, of any of the grinding strategies determined in this chapter is theoretical. The investigations carried out illustrate the technique of using the Grinding Model to determine a grinding strategy or strategies which match a set of criteria and some of the practical implications for rail maintenance have been highlighted. Before grinding strategies determined using the Grinding Model should be used specify grinding strategies for application to a railway network, where the integrity of real rails and maintenance budgets are at stake, further development should take place, the predictions of the model should be tested and verified. The use of the Grinding Model to specify grinding strategies for application to a railway network is discussed further in the following sections.

## **Chapter 5. Grinding Strategy Parameter Error and Sensitivity Analysis**

### **5.1 Introduction to Grinding Strategy Parameter Error Case Studies**

In the previous case studies that have been carried out, it has been assumed that the grinding operations have been carried out exactly as specified in the grinding strategy. That is, it has been assumed that each grinding operation was carried out at the exact point in the traffic pattern specified, and the exact vertical depth of material was removed from the rail during it. In practice, when applying a grinding strategy to an operating network, it is to be expected that there will be some variation in the interval at which grinding operations actually take place. Also it is to be expected that there will be some variation in the actual depth of material removed from the surface of the rail compared to the specified value. To investigate the sensitivity of the crack size trends to errors in the point at which each grinding operation is applied and the depth of material removed at each operation, modelling runs have been carried out using as base grinding strategy with different variations applied to the grinding interval and depth. To limit the number of variables to be considered a single traffic pattern, the Mixed Traffic case, was used, the base case being the optimum grinding strategy which was determined in the variable grinding interval investigation.

The optimum grinding strategy determined in that investigation for this traffic pattern consisted of a grinding depth of 0.2mm applied at intervals of 369700 wheel passes. It was decided to investigate the effect of the values applied in the grinding model being between 5% greater or lesser than these originally specified values. A +/- 5% error on the grinding interval represents approximately 660 trains of the various types represented in the mixed traffic case. In real terms if there are assumed to be an average of four trains per hour then 5% of the grinding interval represents 6.9 days of traffic, meaning that the actual grinding operation could occur up to 7 days before or after it was originally specified to take place. A +/-5% error applied to a grinding depth of 0.2mm is represented by applying a grinding depth of between 0.19 and 0.21mm to the grinding model. Discrepancies in the application of the originally specified grinding strategy were modelled by altering the values in the grinding model input file, representing the points at which grinding operations take place in the traffic pattern, and

the depths of those grinding operations, to incorporate errors or variation into the originally specified strategy.

Four different sets of cases were modelled with the errors applied to the originally determined optimum grinding strategy in different ways to represent different circumstances; the details of these cases are given below:

- The first case modelled, Worst Strategy Error case, had the grinding interval and depth set at the value within the error range which was expected to be worst case combination for every grinding operation. That is, every grinding interval was 5% larger than originally specified and the depth of every grinding operation was 5% less than originally specified, this combination has the lowest wear rate per wheel pass and therefore reduces crack length least, representing the worst case scenario within the specified error limits.
- The second case, Worst Grinding Error case, was modelled with the originally specified grinding interval and the depth of every grinding operation was 0.19mm. This represents the grinding operations being carried out at the specified intervals with a systemic worst case error in the depth of grinding applied at each operation.
- Thirdly the Random Depth and Cumulative Random Interval error cases were modelled. In this pair of cases, the originally specified grinding interval and depth for each grinding operation, had a randomly determined value added to them, which was in the range of -5% to +5% of the originally specified value, to determine the actual traffic interval to, and depth of, the next grinding operation. This was carried out with a few different sets of values to establish how sensitive the crack size trend is to different permutations of the random variation in the grinding depth and interval.
- Fourthly the Random Depth and Independent Random Interval error cases set of grinding strategy error cases were modelled. In these cases the random variation of the depth of the grinding depth was determined in the same way as for the previous set of cases, the random depth and cumulative interval error cases, but differed in the determination of when each grinding operation was carried out. In those previous cases the point in the traffic pattern at which grinding was carried out was based on adding the originally specified interval, with the

addition of that operations error value, to the point in the traffic pattern at which the previous operation was carried out, hence the error in the interval was cumulative. In these cases the point at which the grinding operation was carried out was determined by the point at which each operation was originally specified to occur, a randomly determined value, which was in the range of -5% to +5% of the originally specified interval, was then added to the point in the traffic pattern at which the operation occurred. This represents the error being applied to a pre-determined grinding schedule, rather than the error being applied to individual intervals. As with the previous cases the grinding model was run with several different grinding input files, each with different random variations applied to the values to establish how sensitive the crack size trend is to different permutations of the random variation in the grinding depth and interval.

## **5.2 Grinding Strategy Parameter Error Results**

The results of the worst strategy error case and worst grinding error case are plotted in Figure 5.1, as "GI  $3.882 \times 10^5$  GD 0.19mm" and "GI  $3.697 \times 10^5$  GD 0.19mm" respectively, where GI stands for Grinding Interval and GD stands for grinding depth. The crack size trend of the optimum grinding strategy determined in the variable grinding interval investigation is also plotted (GI  $3.697 \times 10^5$  GD 0.2mm) for comparison. These results show that for the worst strategy error case (that is the grinding interval being at the maximum of the error range and the grinding depth being at the minimum) the crack size trend is of a rapid increase in size, to sizes where the crack could grow to threaten the integrity of the rail. This worst strategy error case applies if the error is not random but systemic and repetitive, such as the calibration of the grinding machines depth being wrong every time or grinding operations only initiated within one week of reaching the specified interval from the previous grinding operation. The results of the worst grinding error case, which represents the worst case for a systemic and repetitive error in the depth of grinding operations, showed that the crack size trend shows an increase in crack size from the initial size. This indicates that the crack is predicted to grow to threaten the integrity of the rail.



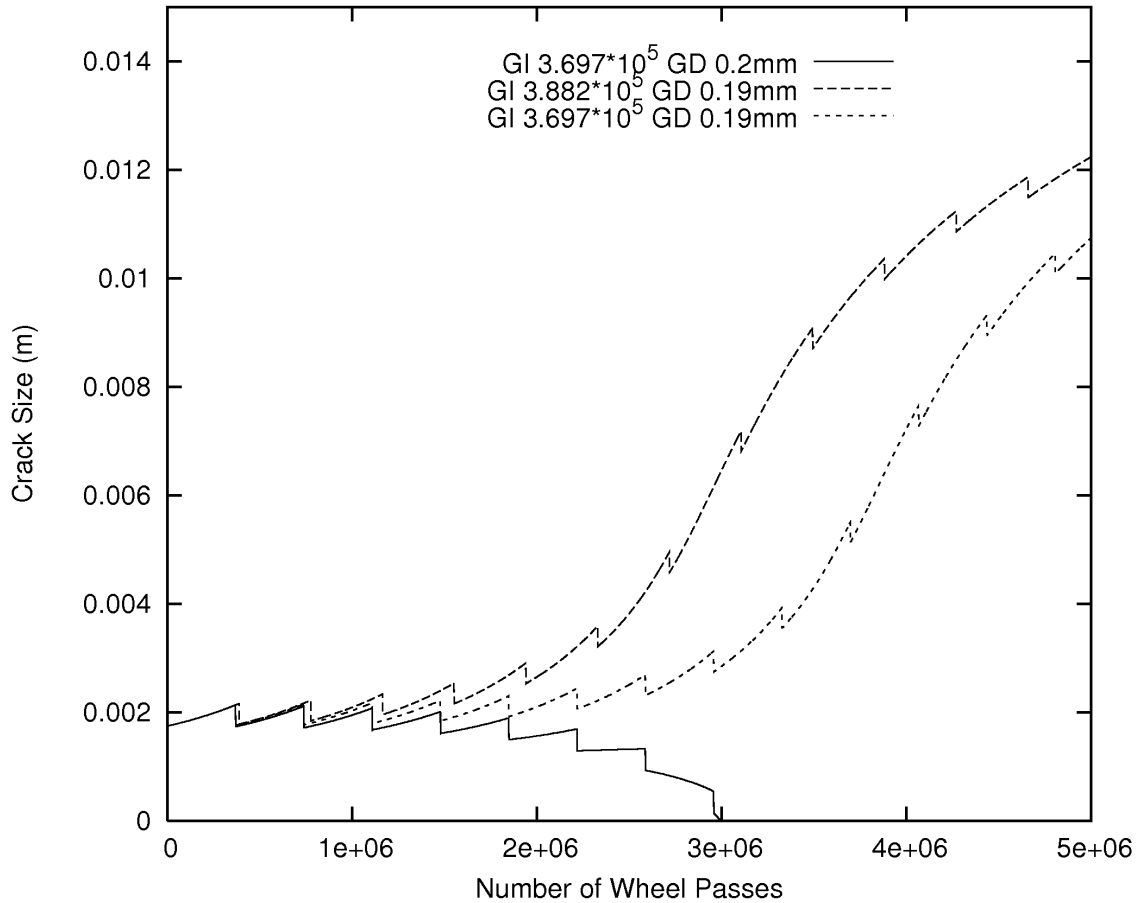


Figure 5.1. Results of the Worst Strategy Error and Worst Grinding Error cases plotted along with the Determined Optimum Grinding Strategy case.

The results of both the worst strategy error case and the worst grinding error case, showed that the ability of the optimum grinding strategy determined to control crack size is sensitive to moderate changes in the interval and depth of grinding operations. Specifically that the crack size trend is predicted to be sensitive to the depth of grinding operations being 5% shallower than the determined optimum both with and without a 5% increase in the grinding interval. The high degree of sensitivity to systemic grinding strategy errors is shown by the fact that in both cases the change in crack size trend was to one that could be expected to grow to threaten the integrity of the rail. This is more severe than the errors having the effect of extending the number of traffic and grinding cycles required to remove the initial defect, which would not be predicted to threaten rail integrity. That the behaviour of the crack trend is so sensitive to errors in the grinding strategy, errors that are representative of the expected operational grinding accuracy, is to be expected since the errors applied are greater than the difference, in grinding strategy values between iterations applied to the grinding model, in the latter

stages of finding the optimum strategy. That is, the error range representing the expected operational grinding accuracy is greater than the range of values which produce a crack size trend which matches the optimum criteria. Therefore it should be expected that the effect of errors in the operational grinding accuracy on the predicted crack size trend, would be that it no longer matches the optimum criteria.

Figure 5.2 shows the results of the random depth and cumulative interval error cases. It shows that these cases are sensitive to the specific cumulative random errors in the grinding interval and random errors in the grinding depth of each case. Different combinations of errors can have different effects on the predicted crack size trend; these combinations of errors can be divided into three different categories based on their effect on the predicted crack size trend. One effect of some combinations of errors is to cause the crack to be predicted to wear out before  $3 \times 10^6$  wheel passes of the traffic pattern have occurred. The second category of combinations have the effect of the crack being predicted to grow to a size which would threaten the integrity of the rail, whilst the third has an effect on the predicted crack size trend which somewhere between the other two, that is the crack size tends to zero after  $3 \times 10^6$  wheel passes of stays below it's initial size. The variation in predicted crack size trends between safe conditions, where the crack size is predicted to tend to zero, and unsafe conditions, where the crack size is predicted to grow to threaten the integrity of the rail, for different combinations of errors, shows that errors of this type and magnitude would have to be taken into account when determining the grinding strategy to be applied to a section of the network.

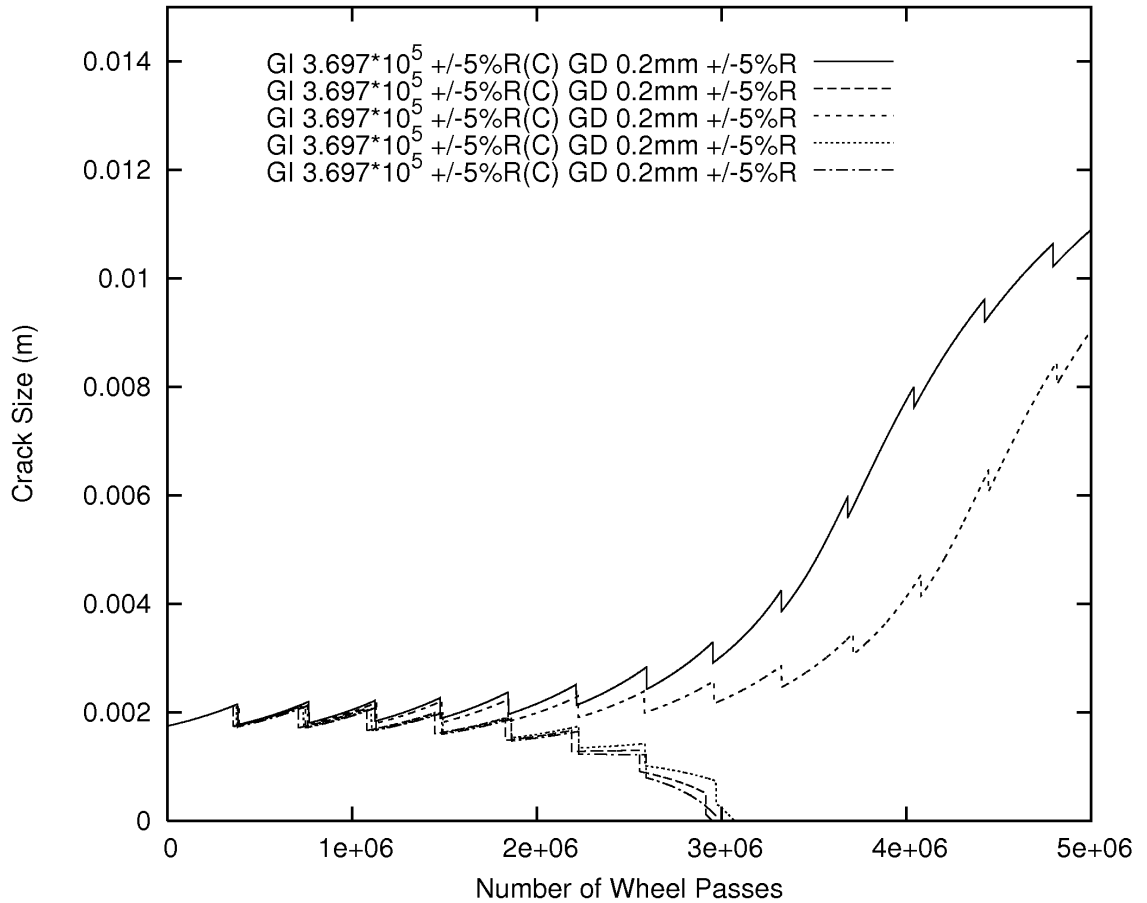


Figure 5.2. Crack size results of the grinding strategy error cases, with random grinding depth error and cumulative random interval error.

The results of the random depth and independent interval error cases are shown in Figure 5.3. They show that for all five cases the crack size trend was noticeably, but not significantly, affected by the random errors in the grinding strategy. This was indicated by the point in the traffic pattern at which the crack was predicted to wear out being altered from the optimum value to somewhere in the range of  $2.8 \times 10^6$  to  $3.6 \times 10^6$  wheel passes. The low significance of the errors is indicated by the effect of the errors being only to alter the number of wheel passes in the traffic pattern after which the crack is predicted to be removed, and that for none of the cases is the crack predicted to grow to a size which might threaten the integrity of the rail. However five cases are not sufficient to fully assess the chances of a combination of grinding errors leading to a crack being predicted to grow to a size to threaten the integrity of the rail, a near worst combination is still a possibility, which would predict the crack growing to a size that could threaten the integrity of the rail. A consequence of this finding is that if it was determined that these are the types of error that are present, it would be up to the

judgement of the persons responsible for the integrity of the track, if the determined optimum grinding strategy should be used, with and appropriate inspection and calibration regime, or a more conservative strategy adopted. It is only in the very unlikely event of all the errors being continuously and consecutively near to the worst case values for the initial grinding operations, that it would be expected that the crack would be predicted to grow to threaten the integrity of the rail. This is assuming that the errors are contained within the limits set down; there are conceivable circumstances, particularly with regard to grinding interval, where the errors might exceed these limits, such as grinding machine break down or personnel being unavailable. In cases of such disruption to the planned grinding strategy then the strategy would have to be reassessed, possibly in combination with out of routine inspections, to achieve the necessary confidence that cracks would not be allowed to grow to threaten the integrity of the rail.

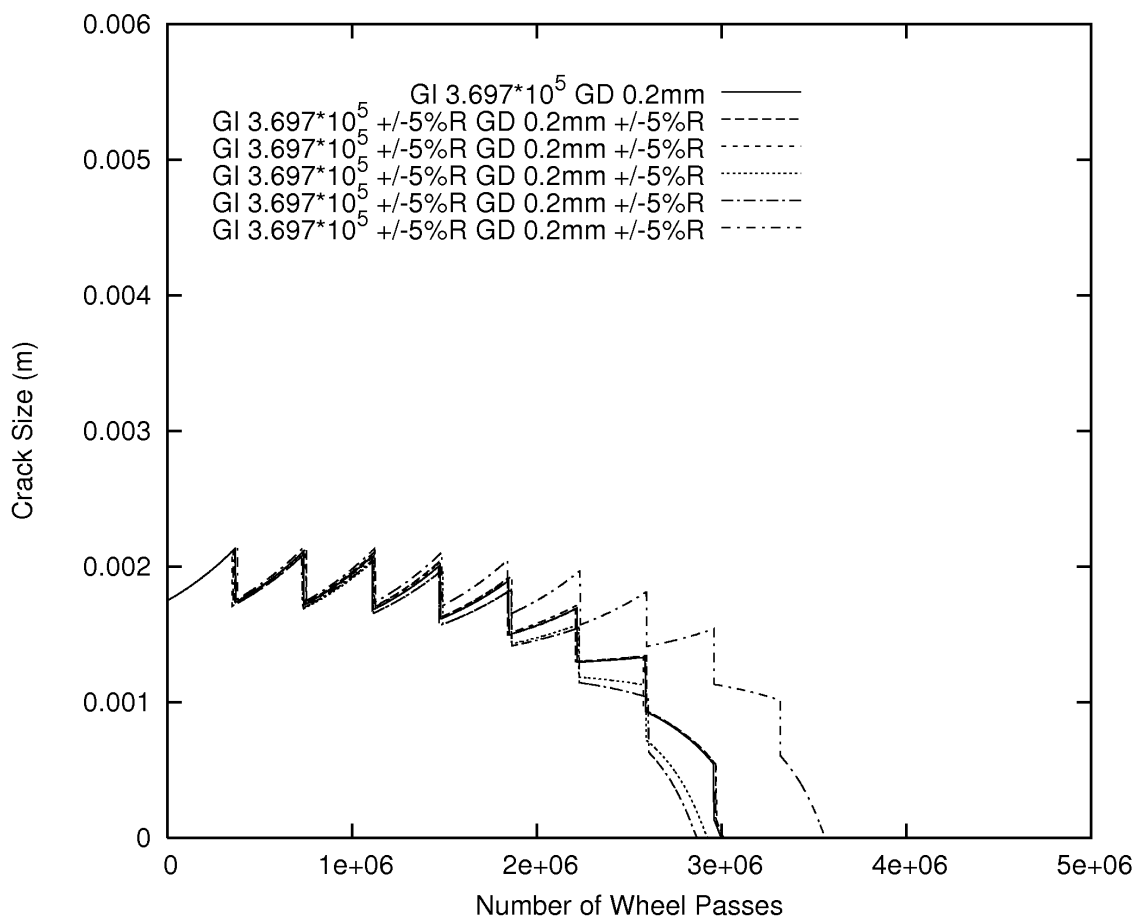


Figure 5.3. Results of the cases with random grinding depth error and independent random interval error.

### 5.2.1 *Grinding Strategy Parameter Error Conclusions*

The results demonstrate that, with grinding strategy errors of a magnitude which could reasonably be expected, then the worst case combination of these errors applied to the optimum grinding strategy result in crack size trends that are predicted to grow to sizes which would be expected to pose a threat to the integrity of the rail. The results also show that random variations of the grinding strategy parameters due to errors can result in crack size trend which predict the crack growing to a size which could threaten the rail if the grinding interval errors are cumulative, as in two of the five cases modelled. Only if the grinding errors at each operation are independent of each other, is there the possibility that the risk of the errors in the determined optimum grinding strategy, leading to the crack being predicted to grow to a size which could threaten the integrity of the rail, could be determined as being acceptable.

Due to the predicted sensitivity of the crack size trend to errors in the grinding strategy, and the potential consequences of these errors, i.e. a crack growing to a size which could threaten the integrity of the rail, then it could be advisable to specify a grinding strategy for which the repeatedly worst case combination of grinding strategy errors, representing a systemic error source, results in a crack size trend that tends towards zero. This could be done by finding the strategy with the worst acceptable crack size trend behaviour, then reducing the specified grinding interval and increasing the specified grinding depth, in the case of the examples used, by 5% for the strategy to be applied. Where it is intended to operate the grinding machine at its maximum grinding depth then the investigation should be carried out at a depth which is half the error range less than the maximum to allow for the errors in this.

## **Chapter 6. Trends of Optimum Grinding Strategy Variable Combinations**

### **6.1 Introduction to Trends of Optimum Grinding Strategy Variable Combinations**

In previous sections analysis has concentrated on situations where one of the two grinding strategy variables of the Grinding Model is fixed, and various conceivable practical situations where this approach would be suitable have been discussed. However whilst there might be reasons for limiting the variable to certain practical values, both grinding strategy variables could theoretically occupy any value across the range from zero to an upper limit. In practical terms the upper limit of the variables which it is reasonable to consider, would be the depth of the initial defect in the case of the grinding depth, and the wear life of the rail without grinding in the case of the grinding interval. The optimum grinding strategies determined in the Variable Grinding Interval and Variable Grinding Depth investigations for each traffic case differed from each other in terms of the values of the grinding strategy variables. This showed that there were at least two grinding strategies for the same traffic case with different values of the variables, which produced predicted crack size trends that matched the optimum criterion. This implies that for every value of one of the grinding strategy variables there is a corresponding value of the other variable which produces a predicted crack size trend that matches the optimum criterion.

The work described in this chapter involves a series of investigations which were carried out with the Grinding Model for each of a range of discrete values of one grinding strategy variable, grinding depth, to find the optimum value for the other grinding strategy variable. The aim of this was to determine the relationship between the two variables, and establish trends of optimum grinding strategy variable combinations. The series of investigations was carried out with both the wheel-rail contact data representing the location considered in the previous chapters and also with data representing a second location. This was done to allow comparisons to be made between the optimum grinding strategy variables combinations determined for different contact conditions. For both locations the contact data representing different types of vehicles at that location were applied in the same traffic pattern, this was the Mixed traffic pattern

described in previous chapters. The use of trends of optimum grinding strategy variable combinations at two locations for quick reference, when determining the grinding strategies to be applied at those locations, if the locations are considered as part of the same maintenance section is discussed.

The contact data, and hence crack growth and wear rate predictions, used in previous chapters as the input to the Grinding Model, was generated in a previous project for a curve at Harringay on the East Coast Mainline. That is, the track geometry data which was fed into the vehicle dynamics software to generate the contact forces, from which the crack growth and wear rate predictions were made, was representative of an actual location, that location being Harringay. Another location that these previous projects studied was Sandy on the same line, therefore the data for a second location was available to this project. Further details about these locations and the previous modelling work carried out can be found in the final report of the previous project to the Railway Safety and Standards Board [6.1]. In the previous project detailed therein measurements were taken at more than one position at each location (also referred to as sites), each measurement position within a location are identified by a number corresponding its distance in metres from a local reference point. In the work described in this thesis the data relating to Harringay position 2188 and Sandy position 880 has been used throughout.

To generate each data point used to establish the relationship between the optimum crack size trend and the grinding strategy variables, an investigation was carried out to find the optimum grinding interval for each of the selected grinding depths across the range 0.04mm-0.4mm. For a fixed grinding depth, the optimum grinding strategy maximises the grinding interval while requiring that the predicted crack size tends to zero within three million wheel passes (the term "crack size zero point" is used, to mean the number of wheel passes after which a crack size trend is predicted by the Grinding Model to tend to zero). Previously a grinding strategy which produced a crack zero point that was within +/-0.5% of the optimum value was considered an optimum grinding strategy. In this chapter the optimum grinding strategy criteria were relaxed such that, a grinding strategy which produced a crack zero point that was within +/-5% of the optimum value was considered an optimum grinding strategy. A grinding depth and grinding interval which produces a predicted crack size trend that matches the

optimum criteria are considered an optimum combination of the grinding strategy variables. This is true whether the optimum grinding interval was determined for a fixed grinding depth or the optimum grinding depth was determined for a fixed grinding interval.

This relaxation of the optimum grinding strategy criteria was made for two reasons, the first was that the wider target range of predicted crack size zero points required for a strategy to meet the optimum criteria, meant that fewer iterations of grinding interval value had to be modelled manually, before a value was found which matched the criteria. With a large number of investigations to carry out, reducing the number of iterations that had to be modelled per investigation saved time. The second reason, and the reason that it was thought to be acceptable to increase the range of the predicted crack size trend optimum zero points, was that the range of the grinding strategy variables which would match the original crack size zero point was impractically small. As the discussion of the sensitivity analysis in Chapter 5 highlighted, the level of precision which the actual grinding strategy variables could be reasonably expected to be applied at, would be outside the range required to produce a crack size trend which matched the original criteria. That is range of the error which could reasonably be expected to occur in the grinding strategy variables when applying the strategy, would be greater than the range of values which would produce grinding strategies that matched the original range of optimum crack zero points. Therefore it was felt that finding grinding strategies which matched the optimum crack size zero point so closely would be of little value, especially as the interest was in finding general trends of optimum grinding strategy variable combinations.

The number of grinding depths and the extent of the range of grinding depths for which the optimum grinding interval was determined for each location was different. The reason that fewer grinding depths across the same range were investigated for the Sandy location was that the trend from the Harringay location was found to be smooth and change gradually. Therefore it was felt that the eleven data points generated over the 0.1mm to 0.2mm grinding depth range for Harringay, were more than was necessary to establish the trend, so fewer data points were generated for the second location modelled.



The reason that the extent of the range of grinding depths investigated for the Sandy location was narrower was because there is a programming limit of 40 grinding operations for the grinding strategy input file. Since for the same grinding depth it was predicted that Sandy would require a lower grinding interval than at Harringay, and subsequently more grinding operations, this limit was reached at a higher grinding depth for the Sandy investigations. That is grinding strategies with depths of less than between 0.06mm and 0.08mm are predicted to require grinding intervals of less than 80,000 wheel passes at Sandy, as opposed to depths of less than 0.04mm at Harringay. For the optimum criteria used, the 40 grinding operation limit translates to limit of grinding interval which can be modelled, of not less than 80,000 wheel passes. This value is the least which allows for a few grinding operations after the  $3 \times 10^6$  wheel pass crack size zero target point, to be sure that no operations are missed before the crack size is predicted to reach zero. If there should be more than 40 grinding operations before the end of the modelling run, at  $5 \times 10^6$  wheel passes, then the Effective Continuous Wear Rate should be calculated from the first data point after the last modelled grinding operation as usual, not the first data point after a missing grinding operation. The use of grinding strategies shorter than the modelling run was considered acceptable, so long as there were no grinding operations missing before the maximum allowable crack zero point, and the Effective Continuous Wear Rate was calculated from the first data point after the last grinding operation modelled. The limit on the number of grinding operations which can be modelled was set in the early stages of the Grinding Model development, it is merely an arbitrary limit determined by the setting of the amount of memory allocated to hold the grinding strategy values. It would be simple to change this limit by modifying the program if required, however it was felt that it was better to be consistent and use the same version of the program throughout the modelling and omit two data points, rather than change the model or repeat all the modelling.

## **6.2 Trends of Optimum Grinding Strategy Combinations Results**

The values across the range of grinding depths for which investigations were carried out at each location are recorded in Table 6.1, along with the optimum grinding interval determined for each investigation, these values have been plotted in figure 6.1. It can be seen that the trends of optimum grinding variables are of similar form, with the optimum grinding interval for any given grinding depth at Harringay being roughly

twice that at Sandy. This shows that the track geometry is predicted to have a significant effect on the optimum grinding strategy; in this case the overall effect of traffic at Harringay is more wear dominant than it is at Sandy.

Table 6.1. Results of the optimum grinding interval investigations for selected grinding depths at two locations, with the Mixed traffic pattern. Optimum grinding intervals are those which produce a crack size trend which tends to zero within 5% of the required number of wheel passes.

Grinding Depth (mm)	Optimum Grinding interval (WP)	
	Harringay	Sandy
0.04	93000	
0.06	135000	
0.08	174000	90500
0.1	211000	111000
0.11	228000	
0.12	246000	
0.13	263000	
0.14	280000	150500
0.15	295000	
0.16	311000	169000
0.17	325000	
0.18	340000	
0.19	356000	
0.2	369700	204000
0.25	435000	246000
0.3	498000	285000
0.35	555000	321000
0.4	600000	355000

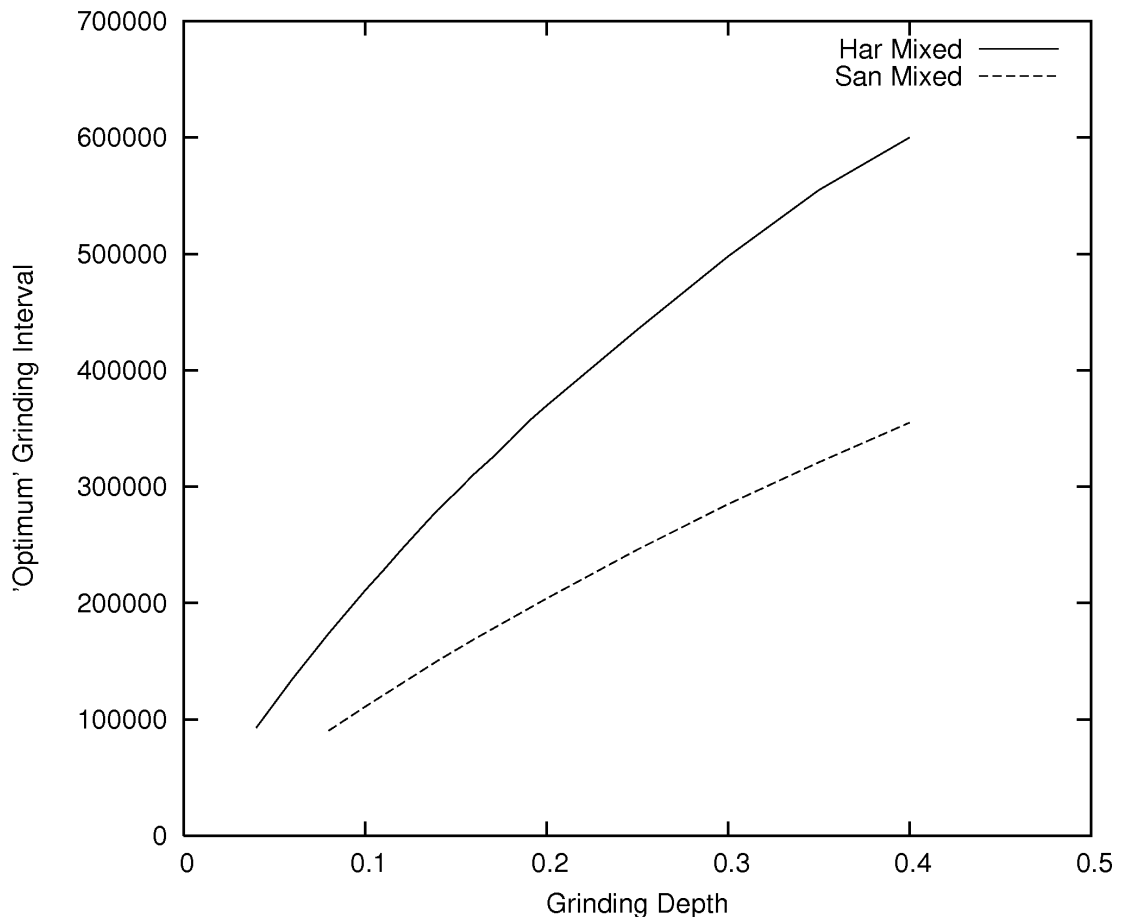


Figure 6.1. Trends of optimum grinding strategy variable combinations for the Harringay and Sandy locations.

### 6.3 Fitting an Equation to the Trends of Optimum Grinding Strategy Variable Combinations

The trends of optimum grinding strategy variable combinations plotted in figure 6.1, both appeared to have similar characteristics that would be describable by the same simple mathematical equation, with different values of constants to fit it to the trend for a specific location. Determining the equation for the trends would assist in interpolating the predicted matching grinding strategy variable for a given value of the other which hasn't been modelled, so it was decided to attempt to fit a mathematical equation to the trends. Both trends appeared to be heading towards zero at the intersection of the axis, and have a shape similar to that where ordinate is the square root of the abscissa. Thus it was thought that a possible equation to describe the trends would include a square root term, a multiplier to scale the ordinate, and a term to control the curve of the ordinate. Since it appeared that both trends tended towards zero at the intersection of the axis, it was thought that the equation that it was attempted to fit to the data should also tend

towards zero at the intersection of the axis. Although the concept of an optimum grinding interval for a grinding depth of zero is not useful, it did seem to be logical that the optimum grinding interval for a very small grinding depth would also be correspondingly very small. The term small has different meanings for grinding depth and interval, as the absolute values of the pairs of variables that are predicted to form an optimum grinding strategy are orders of magnitude different from each other. In this case, small is taken to be relative to the scale the trends of optimum grinding strategy variable combinations are plotted on, that is thousandths of a millimetre and a few thousand wheel passes for the grinding depth and grinding interval respectively. After some experimentation and trial and error an equation which matched these requirements was found, that equation was:

$$I = a(\sqrt{D + b} - \sqrt{b}) \quad \text{Equation 1}$$

In Equation 1,  $I$  represents the grinding interval and  $D$  represents the grinding depth of an optimum grinding strategy variable combination,  $a$  and  $b$  are constants, the appropriate values of which will fit the equation to each of the trends of optimum grinding strategy variable combinations.

For each location values of the constants  $a$  and  $b$  in equation 1 were found by experimentation which produced plots that were of the same order of magnitude and similar shape curve to that particular curve. These values were then used as the initial values to input to the function fitting capability of the Gnuplot graphing utility, which was used to fit Equation 1 to the data for the trends of optimum grinding variable combinations at each location. The values of the constants  $a$  and  $b$  which were determined to produce the best fit of the equation to the data for each location are given in table 6.2. In figure 6.2, Equation 1 is plotted using these values of constants  $a$  and  $b$  found to produce the best fit of Equation 1 for each location, along side the trends of optimum grinding variable combinations at the locations, to examine the fit of the equation to the trends.

Table 6.2. Values of constants  $a$  and  $b$  which produce the best fit of equation 1 to the trends of optimum grinding strategy variable combinations for each location.

Constant of equation 1	Location	
	Harringay	Sandy
$a$	1446780	1000000
$b$	0.071235	0.149571

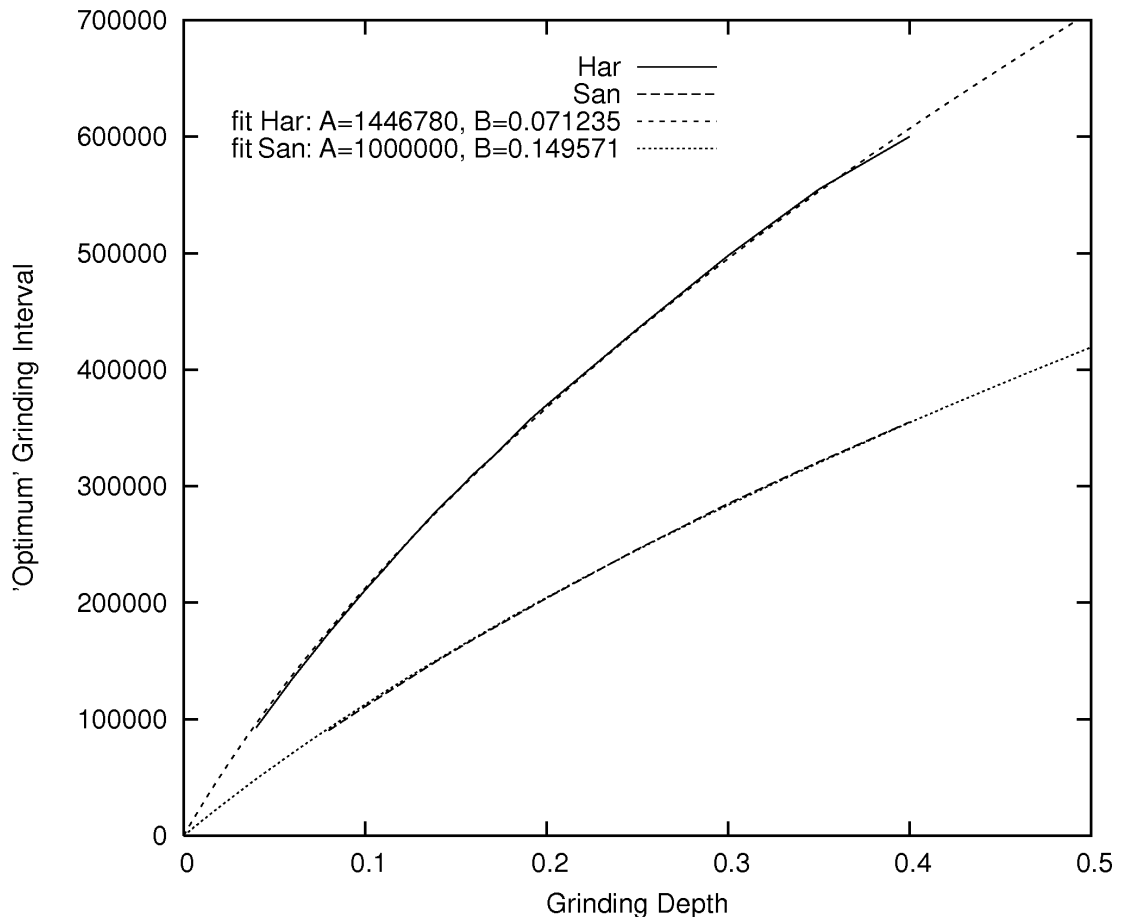


Figure 6.2. Trends of optimum grinding strategy variable combinations plotted along with equation 1 using the values of constants  $a$  and  $b$  which produce the best fit with the data for the trends for each location.

Figure 6.2 shows that the fit between the data and the fitted equation is very good for both locations. To test how useful the fitted equation is for interpolating the optimum value of a grinding strategy variable, for a given value of the other grinding strategy variable which has not been investigated, it was used to predict the outcome of the Variable Grinding Depth Investigation. The results of the Variable Grinding Depth Investigation were not used to develop the trends, and it is therefore independent of the

trend or the equation which describes it. To do this the equation was rearranged to give the inverse equation, that is, equation 2.

$$D = \left( \frac{I}{a} + \sqrt{b} \right)^2 - b \quad \text{Equation 2}$$

The result of the Variable Grinding Depth Investigation for the Mixed traffic case was that for a grinding interval of 200,000 wheel passes, grinding depth which would produce a predicted crack trend which tended to zero within 0.5% of the optimum number of wheel passes was 0.094mm. Putting the values of constants  $a$  and  $b$  from table 6.2 for Harringay and the grinding interval ( $I$ ), of 200,000 wheel passes into equation 2, gives a predicted optimum grinding depth of 0.0929mm. This is very close to the value determined by investigation.

To further test the usefulness of equations 1 and 2 for interpolating between the data points determined to establish the trends of optimum grinding strategy variable combinations, a grinding depth of 0.175mm, which hasn't been investigated to establish the trend for the Sandy location, was selected. This value was entered into equation 1 (as the value of  $D$ ) with the values of  $a$  and  $b$  which best fit the equation to the Sandy data, gave a predicted optimum grinding interval of 182,968 wheel passes. Creating a Grinding Model grinding strategy input file with this grinding depth and grinding interval, and running the model gives a predicted crack size trend which tends to zero after 3,111,000 wheel passes. This is within 5% of the required crack zero point of 3,000,000 wheel passes, and hence within the optimum criteria used to establish the trends of optimum grinding variable combinations. The results of these two test indicates that equations 1 and 2, with the values of the constants  $a$  and  $b$  which produce the best fit to the trend data for a particular location and traffic pattern, are useful for obtaining a predicted optimum value of a grinding strategy variable, which corresponds to any practical value of the other grinding strategy variable.

It should be noted that, whilst the equation fitted to the trends established (equation 1) might be appropriate for fitting to other locations and traffic patterns, the equation and values of  $a$  and  $b$  for each set of conditions, do not relate to any identifiable physical properties. They are simply a fitted equation that describes the trend of optimum grinding variable combinations, and is used to interpolate between the data points

determined to establish the trend. Therefore it is unlikely that the values of  $a$  and  $b$  could be determined without conducting the investigations to establish the trend and fit the equation to those data points. Although if confidence in the suitability of equations 1 and 2 for interpolating between the data points for other conditions was gained from repeating the process for other conditions, the number of data points determined for each set of conditions could be reduced.

## **6.4 Trends of Effective Continuous Wear Rate Relating to the Trends of Optimum Grinding Strategy Variable Combinations**

### **6.4.1 *Effective Continuous Wear Rate Relating to Optimum Grinding Strategy Variable Combinations***

The different optimum grinding strategy variable combinations used to determine the trends of optimum grinding strategy variable combinations in the preceding sections (sections 6.2 and 6.3) have different impacts on the wear life of the rail. When evaluating which combination of optimum grinding strategies should be selected for application to the rail, it is important that relative impact on the wear life of the rail is considered. A rail which is subject to a grinding strategy and traffic pattern combination that has a higher Effective Continuous Wear Rate (ECWR), will reach its wear limit sooner, and hence require replacement sooner. However optimum grinding strategies which result in a lower ECWR have a lower interval, requiring more grinding operations over the same period of time, which has maintenance cost implications. The ECWR have been calculated, as described previously (Chapter 4.4), from the results files of the modelling runs used to determine the trends of optimum grinding strategy variable combinations. This is to enable the evaluation of the impact of selecting grinding strategies from different positions along trends of optimum grinding strategy variable combinations on the rail life. The ECWR values calculated from the results files of the modelling runs used to determine the trends of optimum grinding strategy variable combinations for each location are displayed in table 6.3 and plotted in figure 6.3. These are the ECWR values that correspond to the optimum grinding interval determined for the grinding depths listed.

Table 6.3. Effective Continuous Wear Rate (ECWR) results associated with the optimum grinding strategy variable combinations used to determine the trends of optimum grinding strategy variable combinations.

Grinding Depth (mm)	ECWR (nm/WP)	
	Harringay	Sandy
0.04	2.177	
0.06	2.192	
0.08	2.207	1.000
0.1	2.221	1.017
0.11	2.230	
0.12	2.235	
0.13	2.242	
0.14	2.247	1.046
0.15	2.256	
0.16	2.262	1.063
0.17	2.270	
0.18	2.277	
0.19	2.281	
0.2	2.288	1.096
0.25	2.322	1.132
0.3	2.350	1.169
0.35	2.383	1.206
0.4	2.414	1.243



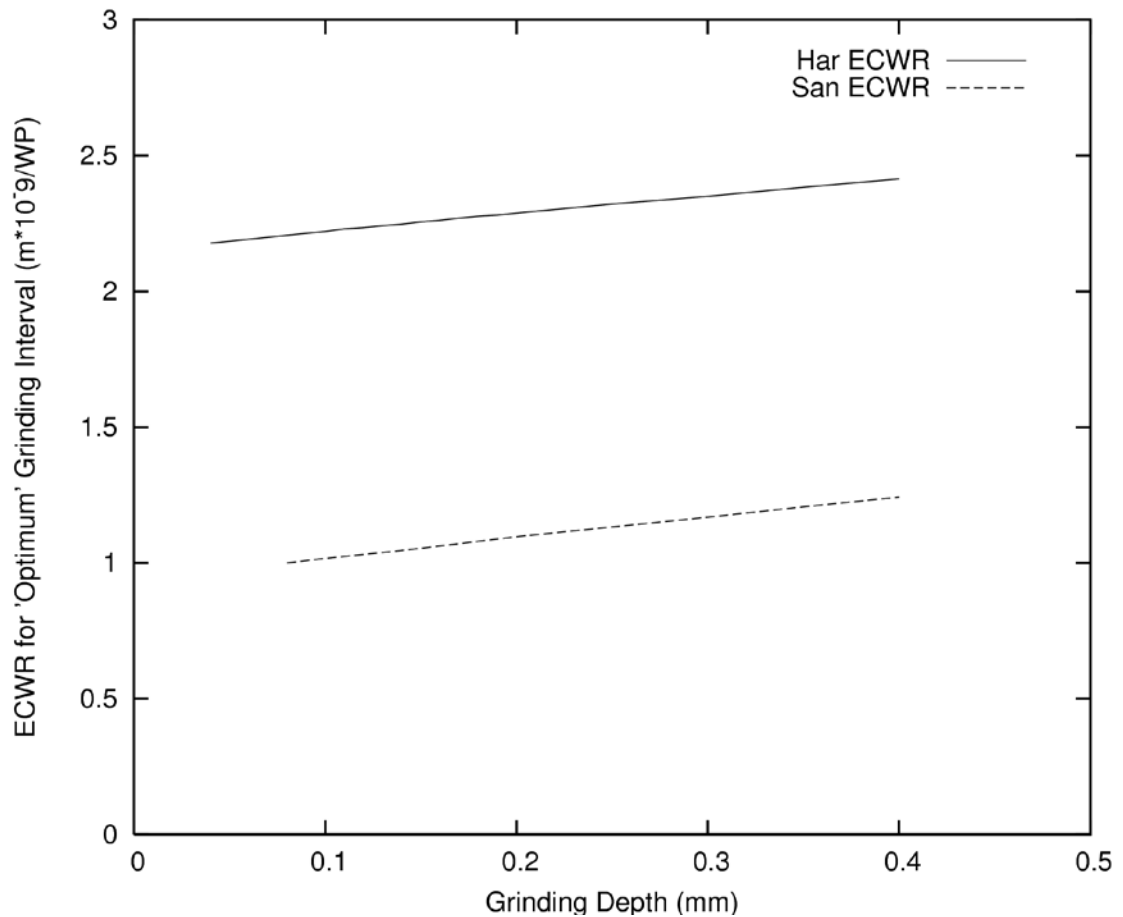


Figure 6.3. Effective Continuous Wear Rate (ECWR) for the optimum grinding strategy variable combinations used to determine the trends of optimum grinding strategy variable combinations.

#### 6.4.2 *Fitting an Equation to Trends of Effective Continuous Wear Rate Relating to Trends of Optimum Grinding Strategy Variable Combinations*

As it is proposed to interpolate from the trends of optimum grinding strategy variable combinations, specific grinding strategies which might be considered for application to a rail, it will be necessary to determine the Effective Continuous Wear Rate (ECWR) for those grinding strategies. It can be seen from figure 6.3 that the trends in the ECWR for the optimum grinding strategy variable combinations at both locations appear to describe a straight line of constant gradient and cross the vertical axis with a positive ECWR value when the grinding depth is zero. Therefore it was decided to fit an equation which describes the trends of the ECWR for the optimum grinding strategy variable combinations, in a similar way as was done for the trends of optimum grinding strategy variable combinations, to interpolate the ECWR for specific optimum grinding strategies interpolated from the trends of optimum grinding strategy variable

combinations. In view of the apparent straight line described by the ECWR trends for the range of grinding depth considered practical to apply, it was decided to fit a simple linear equation, that is, equation 3 shown below, to the trends of ECWR for each location. In equation 3  $D$  represents the grinding depth and  $W_w$  the ECWR. As with trends of optimum grinding strategy variable combinations, the equation was fitted to the data points, in this case those in table 6.4, using the function fitting capability of the Gnuplot graphing utility. There was one distinction from the process of fitting equation 1 to the trends of optimum grinding strategy variable combinations. That distinction was that the initial values of the constants  $c$  and  $d$ , that were input to the function fitting process for each location, were calculated by rearranging equation 3 and using values of grinding depth ( $D$ ) and the ECWR ( $W_w$ ) from two of the data points, to solve for  $c$  and  $d$ . The values of  $c$  and  $d$  which produced the best fit with the ECWR data which relate to the trends of optimum grinding strategy variable combinations for each location are given in table 6.4. Also equation 3 is plotted with the values for each location in figure 6.4 along with the trends of ECWR related to the trends of optimum grinding strategy variable combinations. It can be seen from figure 6.4 that for both locations the fitted equation is a good fit for the ECWR data and that it provides a useful and repeatable means of extrapolating the ECWR for an optimum grinding strategy which has been determined from the trends of optimum grinding strategy variable combinations.

$$W_w = cD + d \quad \text{Equation 3}$$

Table 6.4. Values of constants  $c$  and  $d$  which produce the best fit of equation 3 to the trends of Effective Continuous Wear Rate relating to the optimum grinding strategy variable combinations.

Constant of equation 3	Location	
	Harringay	Sandy
$c$	$0.652472 \times 10^{-9}$	$0.75813 \times 10^{-9}$
$d$	$2.15614 \times 10^{-9}$	$0.941304 \times 10^{-9}$

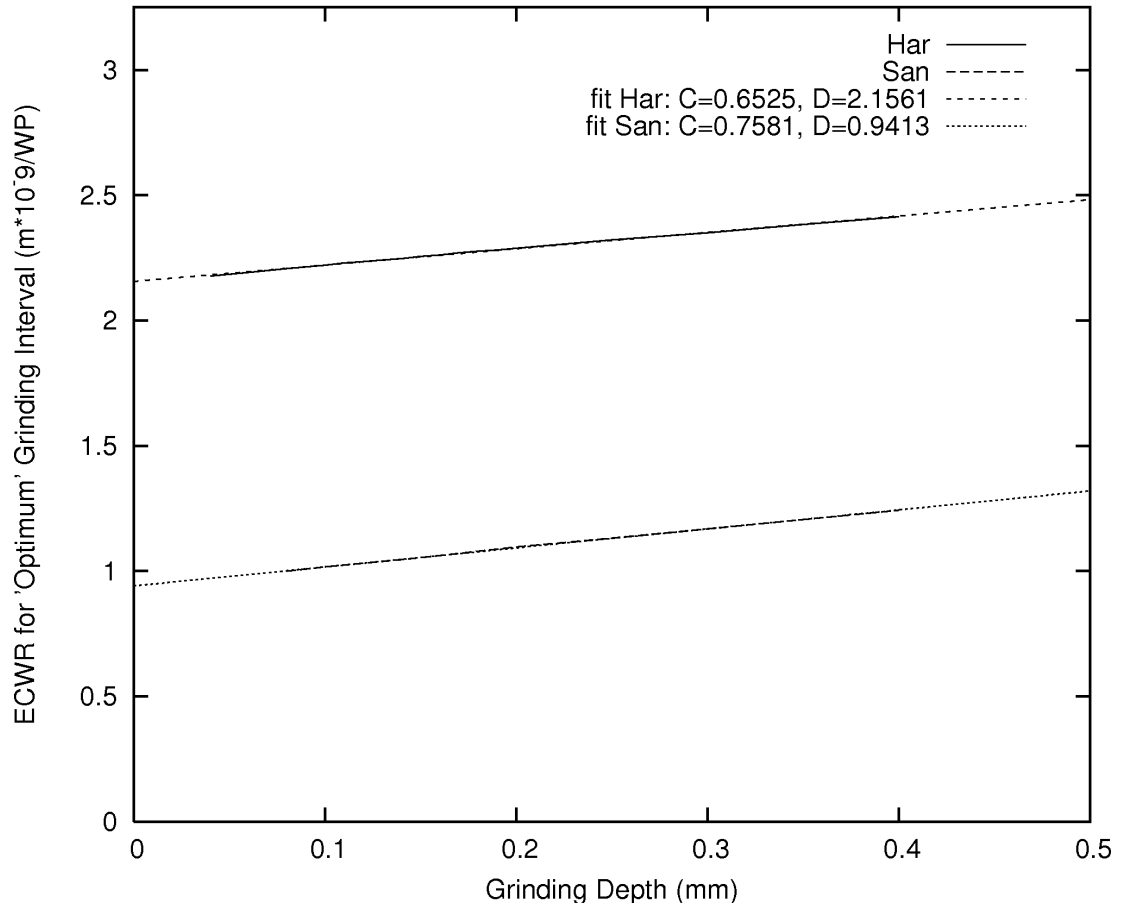


Figure 6.4. Trends of Effective Continuous Wear Rate relating to optimum grinding strategy variable combinations, plotted along with equation 3 using the values of constants  $c$  and  $d$  which produce the best fit with the data for the trends for each location.

To test the use of equation 3 for determining the ECWR of a grinding strategy determined from the trends of optimum grinding strategy variable combinations, the optimum grinding depth determined in the Variable Grinding Depth Investigation for the Mixed traffic case, 0.094mm, was input to equation 3 for the Harringay location. The ECWR at Harringay for an optimum grinding strategy with grinding depth 0.094mm was predicted by equation 3 as 2.2175nm/WP, the result for the Variable Grinding Depth Investigation predicted the ECWR to be 2.2173nm/WP. The results from the Variable Grinding Depth Investigation were not used to determine the trends of optimum grinding strategy variable combinations, so the trends of ECWR are independent of its results. That the equation describing the trend of ECWR related to the trend of optimum grinding strategy variable combinations, predicted the ECWR of an independently conducted optimum grinding strategy investigation, shows that equation 3 is useful as a repeatable method for predicting the ECWR for optimum grinding

strategies determined from the trends of optimum grinding strategy variable combinations.

As with the equation used to interpolate between the data points for the trends of optimum grinding strategy variable combinations, equation 3, and values of constants  $c$  and  $d$  for each set of conditions, do not relate to any identifiable physical properties. The equation only describes the observed trend in Effective Continuous Wear Rate (ECWR) for the trends of optimum grinding variable combinations, allowing the ECWR of a grinding strategy determined from the trends to be predicted without having to carry out the optimum grinding strategy investigation. Furthermore it should be noted that equation 3 and values of constants  $c$  and  $d$  for each location, only predict the ECWR for optimum grinding strategy variable combinations. The ECWR have been expressed in terms of the grinding depths of the optimum grinding strategy which they relate to, grinding operations carried out at non-optimum intervals would have a different ECWR. Equation 3 will be used in subsequent sections and chapters to evaluate the effect the different optimum grinding strategies determined from the trends of optimum grinding strategy variable combinations on the wear life of the rail, when determining the grinding strategy to apply to sections of track.

## **6.5 Using the Trends of Optimum Grinding Strategy Variable Combinations to Determine Grinding Strategies to Apply to a Maintenance Section**

It is considered that the principal advantage of determining the trends of optimum grinding strategy variable combinations is that, when this is carried out for multiple locations within a maintenance section, the trends can be used as a quick reference to see the effect of selecting a grinding strategy which suits a section of track with one set of characteristics has on the grinding strategy for another section of track. That is, if grinding is going to be applied to all of the sections of track in a maintenance section on the same occasion, then the optimum interval to the next grinding operation at a set grinding depth, for example the maximum grinding machine single pass grinding depth, can be determined. This sets the interval for the other sections of track within the maintenance section, and so the optimum grinding depths for those sections at that grinding interval can be determined. The determination of the trends of optimum grinding strategy variable combinations allows the impact of any grinding strategy

variable value set for one location on the optimum grinding strategies for the other locations to be quickly determined, in some cases at a glance. This is as opposed to having to conduct investigations to determine the optimum grinding strategy for all of the locations, when a grinding strategy variable is specified for the first location considered. This is an approach which after trying a few different values could well involve as many individual investigations as would be involved in determining the trends of optimum grinding strategy variable combinations for all locations in the maintenance section. Since either determining the trends of optimum grinding strategy variable combinations or conducting each investigation as required could involve a similar number of investigations. Then it is arguable that having the trends presented up front could allow a human interpreting the trends to spot issues or beneficial combinations more easily, and a more efficient combination of grinding strategy could result.

#### **6.5.1 *Example Maintenance Sections A and B***

To better understand this technique of using the trends of optimum grinding strategy variable combinations to specify grinding strategies for a maintenance section, two example maintenance sections will be considered. Both maintenance sections of track consist entirely of sections with characteristics similar to either Harringay or Sandy, and therefore the appropriate trend of optimum grinding strategy variable combinations applies to that section. Maintenance Section A is made up from sections, 50% of which are similar to Harringay, and 50% are similar to Sandy. Maintenance Section B is made up from sections, 90% of which are similar to Harringay, and 10% are similar to Sandy. The interpolating between the data points for the trends of optimum grinding strategy variable combinations could be done visually from the plots, interpolating mathematically between the data points, or by using the equation which describes the trend. However the interpolation is done in detail, a human considering the problem is likely to at least evaluate approximately visually from the plots, how selecting one optimum grinding variable combination for one type of location might affect another. This is the advantage of establishing the trends as it allows some options to be quickly eliminated and other promising options selected for more precise evaluation. For the precise evaluation conducted in this section, when considering the example maintenance sections described above, the interpolation will be done using the equation which

describes the trend, since the equations fit the respective trends well and it is a precise and repeatable method.

#### *6.5.2 Determining the Most Suitable Grinding Strategy Combinations for the Example Maintenance Sections Considered in Isolation*

To provide a demonstration the use of the trends of optimum grinding strategy variable combinations to specify the grinding strategies for the example maintenance sections, firstly an initial visual assessment of the trends was made. During this visual assessment the proportions of the location types within the example maintenance sections, and their relative grinding requirements was taken into consideration, when looking for combinations of optimum grinding strategy variable for detailed study. The next step was to select a value of one of the grinding strategy variables that was felt to be a reasonably justifiable selection, the value which was selected as the initial step was a grinding depth of 0.19mm. This value was selected as it is close to the maximum single pass grinding depth (0.2mm) that a typical production grinding machine is capable of, so that the strategy should achieve high utilisation of the machines capacity, for the sake of efficiency. The reason the absolute nominal maximum value of grinding depth of the machine was not used is due to the results of the sensitivity analysis, which showed the predicted crack size trend to be sensitive to errors in application of the grinding strategy. Specifying a grinding depth slightly below maximum, leaves a bit of machine capability in reserve to account for errors and ensure, as far as reasonably practicable, that the grinding value specified is the minimum achieved. The selected grinding depth was put into equation 2 for both the Harringay and Sandy type locations, this predicted optimum grinding intervals of 353,000 wheel passes and 196,000 wheel passes respectively. From this starting point, five possible combinations of grinding strategy for the example maintenance sections were developed, and are presented in the following four paragraphs, which are numbered i to v.

(i) The first grinding strategy combination proposes to conduct grinding operations for both types of location within the maintenance section at the same time, both types being ground to the required depth in a single pass. This means adopting the shorter of the two grinding intervals, 196,000 wheel passes, so that the Sandy type locations can be ground in one pass. To avoid wasting the wear life of the rails at the Harringay type locations

when using this grinding interval, the interval was input into equation 1 for Harringay to obtain an optimum grinding depth of 0.09mm. So the combination of grinding strategies specified for the maintenance section would be for the Harringay type sections to be ground at intervals of 196,000 wheel passes with a depth of 0.09mm, and the Sandy type sections to be ground on the same occasions at intervals of 196,000 wheel passes with a depth of 0.19mm.

(ii) The second proposed grinding strategy combination adopts the longer of the two starting point grinding intervals (i.e. 353,000 wheel passes), which is the optimum for the starting grinding depth at the Harringay type locations, and determine the new optimum grinding depth for the Sandy type locations, allowing multiple grinding passes where necessary. Inputting a grinding interval of 353,000 wheel passes to equation 1 for Sandy type locations, gives a predicted optimum grinding depth of 0.4mm. Therefore the combination of grinding strategies specified for the maintenance section would be, for the Harringay type sections to be ground at intervals of 353,000 wheel passes with a depth of 0.19mm, and the Sandy type sections to be ground on the same occasions at intervals of 353,000 wheel passes with a depth of 0.40mm. A grinding depth of 0.4mm would be at the limit of the suggested grinding machines capacity to achieve in two passes, and it would be desirable to avoid a third pass to remove potentially very little or no material.

(iii) In the first grinding strategy combination (i), the grinding interval is set to a value at which the type of location which requires the most grinding, the Sandy type, can be ground in a single pass at about the capacity of the machine. In view of the fact that the predicted optimum grinding depth at the other location was approximately half of the machine's capacity, it is proposed that for the third grinding strategy combination, the other type of location, the Harringay type, would be ground on alternate operations, with the same interval. Therefore the effective grinding interval for the Harringay type locations would be 392,000 wheel passes (i.e. double 196,000 wheel passes). Inputting this interval to equation 1 for Harringay the predicted optimum grinding depth obtained was 0.22mm. So the combination of grinding strategies specified for the maintenance section would be, for the Harringay type sections to be ground at alternate operations at an interval of 392,000 wheel passes, with a depth of 0.22mm, and the Sandy type

sections to be ground at every operation, at intervals of 196,000 wheel passes with a depth of 0.19mm.

(iv) In the third grinding strategy combination (iii) the act of doubling the grinding interval for the type of location which requires the least grinding, the Harringay type, more than doubles the corresponding predicted optimum grinding depth, the result of which is that although grinding is carried out half as often at this type of locations, two grinding passes would be required. Due to this, the fourth combination of grinding strategies proposed is based on the Harringay type location, which is predicted to require the least grinding, being ground at alternate operations. Therefore the effective interval for the Harringay type of location was set as the optimum interval for a grinding depth of 0.19mm, and the Sandy location would ground at every operation for the maintenance section, which would occur at half the effective interval of that for Harringay type location. So from the starting point, the optimum grinding interval for a Harringay type location when the grinding depth is 0.19mm, was predicted to be 353,000 wheel passes, so the grinding interval for the maintenance section was set at half this: 177,000 wheel passes. This maintenance section grinding operation interval was put into equation 2 for the Sandy type location, and the predicted optimum grinding depth was 0.17mm. Therefore the combination of grinding strategies specified for the maintenance section, would be for the Harringay type sections to be ground at alternate operations at an effective interval of 353,000 wheel passes, with a depth of 0.19mm, and the Sandy type sections to be ground at every operation, at intervals of 177,000 wheel passes, with a depth of 0.17mm. This means that the grinding machine is operating at near its maximum capacity for every pass, and that all grinding operations for each of the maintenance section grinding operation intervals can be conducted in a single pass of the maintenance section by the grinding machine.

(v) The fifth grinding strategy combination is a variation on grinding strategy combination (ii), where it was marginal if the Sandy type locations could be ground in two passes. Therefore grinding strategy (v) is similar but determined from the optimum interval for a grinding depth of 0.38mm (two passes at 0.19mm) at a Sandy type location, and the optimum grinding depth at the Harringay type location for that interval. Therefore the combination of grinding strategies specified for the maintenance section would be that both location types would be ground at every maintenance section



grinding operation interval, which would be 341,000 wheel passes. The Harringay type sections would be ground to a depth of 0.18mm, and the Sandy type sections to be ground to a depth of 0.38mm in two passes of the grinding machine.

The combinations of grinding strategies within a maintenance section described above are summarised in table 6.5. The combination of grinding strategies that are most suitable, for a particular maintenance section, would depend upon the types and proportions of locations that the maintenance section is made up of. It is not proposed within the scope of this thesis to make, or suggest, absolute rules to adhere to when determining the combinations of grinding strategies suitable for a particular maintenance section. It is intended to demonstrate how the trends of optimum grinding strategy variable combinations determined with the grinding model could be used to allow informed judgements to be made by someone specifying grinding strategies, whilst considering other factors.

Table 6.5. Summary of the proposed grinding strategy combinations for the different types of location within the example maintenance sections.

Grinding Strategy Combination	Maintenance Section Grinding Operation Interval	Harringay Type Location		Sandy Type Location	
		Effective Grinding Interval (WP)	Grinding Depth (mm)	Effective Grinding Interval (WP)	Grinding Depth (mm)
i	196,000	196,000	0.09	196,000	0.19
ii	353,000	353,000	0.19	353,000	0.40
iii	196,000	392,000	0.22	196,000	0.19
iv	177,000	353,000	0.19	177,000	0.17
v	341,000	341,000	0.18	341,000	0.38

As an example of how a combination of grinding strategies might be more suitable for one example maintenance section than another let us consider the suitability of grinding strategy (i) for application to both example maintenance sections. Grinding strategy combination (i) involves the grinding being carried out at both location types during every maintenance section grinding operation, within a single pass of the grinding machine, the machine being operated at near to its single pass grinding depth capacity

for the location type that requires the most grinding and the other location ground to the optimum depth for that interval. For example maintenance section A, in which the two types of location occur in equal proportion, the grinding machine would be operating at about maximum capacity (and therefore be nearly fully utilised) for half of the pass through the maintenance section, and operating at half capacity for the rest of the pass. For example maintenance section B, in which the Harringay type locations account for 90% of the maintenance section, using grinding strategy combination (i) would result in the grinding machine operating at half its capacity (and hence perhaps under utilised) for 90% of the pass, only being used at near full capacity for the remaining 10% of the pass over sections comprised of Sandy type locations. From this example it can be argued that grinding strategy combination (i) is an acceptable compromise between the grinding requirements of the different location types for example maintenance section A. However applying grinding strategy combination (i) to example maintenance section B, results in low utilisation of the grinding machine for the majority of its pass through the maintenance section. This means that grinding strategy combination (i) is far less of an ideal compromise between the grinding requirements of the different location types. Therefore grinding strategy combination (i) can be said to be less suitable for example maintenance section B, than example maintenance section A.

It should be noted that in the context of this section, the relative suitability of grinding strategy combinations refers to the practical operational considerations of applying a combination of strategies, and their impact on cost. All of the grinding strategy combinations proposed are still predicted to be safe and control cracks, for either example maintenance section. That is in so far as the predictions of the Grinding Model at its current stage of development could be used for determining the grinding strategies to be used on a railway network, which is discussed elsewhere.

Having determined that one grinding strategy combination might be more suitable for a maintenance section than another, arguments will now be put forward as to which of the five grinding strategy combinations proposed would be most suitable for each of the example maintenance sections. This will demonstrate one possible use of the trends of optimum grinding strategy variable combinations to assist in the judgement as to the most suitable and efficient grinding strategy combination to apply to a maintenance section. As has already been discussed, grinding strategy combination (i) could be said

to be reasonably suitable for example maintenance section A, the grinding machine being used at near full capacity for half of the maintenance section, and at half its capacity for the other half. Given this utilisation pattern grinding strategy combination (iii) was created to investigate whether using the grinding machine at full capacity on the sections that required least grinding on alternate grinding operations was feasible. This showed that although the machine was being used at half its capacity on this location type in grinding strategy combination (i), doubling the interval meant that the required grinding depth was predicted to be slightly greater than the full capacity of the grinding machine. This would be due to the crack being allowed to grow longer would be predicted to grow at a slightly higher rate for the second part of the interval. That grinding strategy combination (iii) would require an additional low grinding machine utilisation pass for every operation the Harringay type locations were ground, which would reduce its suitability. However the principal behind grinding strategy combination (iii) appeared sound, so grinding strategy combination (iv) was developed by adjusting the intervals so that the Harringay type locations could be ground in a single pass on alternate maintenance section grinding operations. This achieved good utilisation of the grinding machine across both location types, and since when the grinding machine transits sections that it is not grinding at significantly higher speed and in a short time, than when grinding, then little grinding machine utilisation is lost transiting sections not to be ground, on alternate maintenance section grinding operations. To even up the workload for each maintenance section grinding operation, the sections to be ground on alternate operations could be divided into half, each half being done on one of a pair of grinding operations. Therefore it could be judged that grinding strategy combination (iv) would be the most suitable for example maintenance section A.

Turning to consideration of the most suitable combination of grinding strategies for example maintenance section B, it is perhaps obvious that those considerations would be dominated by the Harringay type locations, since they make up 90% of the maintenance section. Thus grinding strategy combination (i) would be completely unsuitable as the grinding machine would be underutilised for the majority of the grinding operations. So grinding strategy combination (ii) was created to maximise the utilisation of the grinding machine at the Harringay type locations, this resulted in a requirement to grind 0.4mm from the Sandy type locations. This could require up to

three passes of the grinding machine to ensure the required depth of grinding was achieved, as the machine would be at the absolute limit of its capability to grind to that depth in two passes. A grinding strategy combination that has good single pass grinding machine utilisation over the majority of a maintenance section and requires multiple passes over the remaining 10% could be a better compromise, than the grinding machine being underutilised for the majority of the operation. That grinding strategy combination (ii) could require 3 passes of each section of Sandy type location within a maintenance section to achieve the required grinding depth, might not be such a disadvantage as it first appears. This is because the machine might be carrying out work at each location type as it progresses through the maintenance section in one general direction, with reversals for locations that require multiple passes. This in turn means that after carrying out two passes at the machines full capacity, it would have to make a third transit pass anyway to reach the next location, if a very small depth third grinding pass was still required after two passes, this could potentially be carried out at higher speed, reducing the impact of the Sandy locations requiring three passes. As an alternative to grinding strategy combination (ii), grinding strategy combination (v) was created from it, with the grinding intervals adjusted so that the grinding depth required at the Sandy type locations could be achieved reliably within two passes of the grinding machine. The grinding depth for the Harringay type locations was also modified to suit the adjusted interval, the difference between the suitability of grinding strategy combinations (ii) and (v), for application to example maintenance section B, is marginal. The exact determination as to which is the most suitable could depend of the relative speed of the grinding machine when transiting a location and when performing light grinding, and also the relative cost of the two operations. It also depends on the balance between the benefits of two or three passes on a small proportion of the locations and maximising the utilisation of the grinding machine for the majority of the locations. However as grinding strategy combination (v) has more certainties associated with it (in terms of the number of grinding passes required and the speed at which they can be carried out) and has good utilisation of the grinding machine for all of the passes, it is suggested that it would be the most suitable to apply to example maintenance section B.

It should be noted that all of the trends of optimum grinding strategy variable combinations have been determined for grinding strategies which consist of a repeating

pattern of the same grinding interval and depth applied at each location type at each operation. The Grinding Model could be used to find grinding strategies for which the predicted crack size trend matched the optimum criteria, where the interval or grinding depth was not the same on each subsequent grinding operation. An example of such a grinding strategy might be one where grinding to a fixed depth was carried out on two out of three maintenance section grinding operation intervals, resulting in unequal effective intervals between operations at the specified location. However this would introduce a whole new range of possible combinations of grinding strategy variables, and whilst it could be considered for a specific case which proves difficult to fit in with other location types, it is not thought that it would be practical to determine the trends for a larger set of independent variables.

### ***6.5.3 Determining the Most Suitable Grinding Strategy Combinations for Maintenance Sections within a Wider Network***

In the previous section the most suitable grinding strategy combinations were selected whilst considering the example maintenance sections in isolation, without outside operational and organisational constraints on the frequency of grinding operations. This is unlikely to be possible for an operational railway network, as the provision of maintenance resources required to allow the grinding requirements of every maintenance section to be specified independently could counteract any savings in terms of maximising rail life. One possible slight concession to considering maintenance sections as part of a wider network would be to break neighbouring continuous maintenance sections up, and group the types of locations within them that have similar grinding requirements into discontinuous maintenance sections. The appropriate grinding strategy would then be applied to each discontinuous maintenance section. An alternative approach would be to have a global set of grinding operation intervals for the network, each maintenance section being allocated a grinding interval on the basis of which of the global intervals that was most suitable for the location types within it. This being determined from the trends of optimum grinding strategy variable combinations, the optimum grinding depth at that for that grinding operation interval would then be specified for each location type. The principal behind this being that it would be easier from an organisation point of view to have a grinding machine grind one maintenance section each shift, working through the maintenance sections with the

same grinding operation interval in sequence, and then repeating the sequence at the set intervals. This is as opposed to grinding maintenance sections at different intervals which might lead to several maintenance sections becoming due for grinding during the same shift.

To give an example, the effect of the global network grinding operation frequencies being set to values which were equivalent to intervals of 100,000 or 150,000 wheel passes, for the traffic through the example maintenance sections will be considered. The actual interval can be a multiple of the global ones, that is, the maintenance section could be allocated to alternate global grinding operations, and so the local grinding interval would become 200,000, 300,000 or 400,000 wheel passes. These grinding intervals were input into equation 2 for the Harringay and Sandy locations, and the results are presented in table 6.6.

Table 6.6. Predicted optimum grinding depths for grinding intervals set by network grinding practice.

Grinding Operation Interval	Optimum Grinding Depth (mm)	
	Harringay	Sandy
100,000	0.04	0.09
150,000	0.07	0.14
200,000	0.09	0.19
300,000	0.15	0.32
400,000	0.22	0.47

From the results in table 6.6 it would appear that example maintenance section A would be most suitable for inclusion in the 100,000 wheel pass interval grinding operation program, with the grinding operations being carried out at alternate operations. This would make the effective grinding interval 200,000 wheel passes and the grinding depths 0.09mm and 0.19mm at the Harringay and Sandy type locations respectively, this will be known as grinding strategy combination (vi). It is very similar to grinding strategy combination (i) in section 6.4.1, and the same arguments, regarding an average machine capacity utilisation of approximately 75%, apply here. It is not intended that the grinding machine would pass over the maintenance section on the occasion of the global grinding operation interval at which grinding is not scheduled to be carried out,

the intention is that the machine will be allocated elsewhere on these occasions. It also appears that it would be most suitable to include example maintenance section B in the 150,000 wheel pass interval grinding operation program, with the grinding operations on the Harringay type locations being carried out at alternate operations making the effective grinding interval 300,000 wheel passes. Therefore the grinding strategy combination, grinding strategy combination (vii), would be for the Harringay type locations to be ground at 300,000 wheel pass intervals to a depth of 0.15mm, and the Sandy type locations to be ground at 150,000 wheel pass intervals to a depth of 0.14mm. Alternatively the Sandy type locations in example maintenance section B could be ground either in a single pass at every grinding operation interval, or in two passes on the same occasion as the grinding on the Harringay type locations is carried out. This would be grinding strategy combination (viii) and consist of the Harringay type locations to be ground at 300,000 wheel pass intervals to a depth of 0.15mm, and the Sandy type locations also to be ground at 300,000 wheel pass intervals to a depth of 0.32mm. The latter is likely to be more efficient for example maintenance section B as it avoids sending a grinding machine to the maintenance section to make a single grinding pass over 10% of the track on alternate occasions.

It should be noted that the grinding strategies which it has been proposed to apply to track representative of real locations in this chapter, have been proposed for illustrative purposes only. These grinding strategies proposed here have been used as examples to illustrate techniques which could be employed, to use trends of optimum grinding strategy variable combinations determined from the Grinding Model, to specify grinding strategies for real track locations. It is not intended to suggest that the output of the Grinding Model should actually be used to specify grinding strategies in its current state of development. Further work including the determination of suitable factors of safety, field trials and management policy for the use of the model and how it's applied to the specification of grinding strategies, would be required before the Grinding Model could be used in this way.

The selection of grinding strategies to apply to a rail, from the trends of optimum grinding strategy variable combinations that has been presented here, is an objective process. However the judgements as to which combination of these optimum grinding strategies would be the most suitable to use for the different locations in a maintenance

section have been made on a subjective basis. In the next chapter a more objective method for determining the best combinations of optimum grinding strategy to apply will be presented. This is based on estimates of the effect that the costs of the grinding strategies, and the predicted effect of the grinding strategies on the wear life of the rail, have on the life cycle cost of the rail.

## **6.6 References**

- 6.1. Burstow M.C., Fletcher D.I., Franklin F.J., Kapoor A. (2008) Management and Understanding of Rolling Contact Fatigue: WP1 Mechanisms of Crack Initiation - Final Report.

*[http://www.rssb.co.uk/SiteCollectionDocuments/pdf/reports/Research/T355\\_rpt\\_final\\_wp1.pdf](http://www.rssb.co.uk/SiteCollectionDocuments/pdf/reports/Research/T355_rpt_final_wp1.pdf)*



## **Chapter 7. Estimating Grinding Strategy Effect on Rail Life Cost**

The determination of which combination of the optimum grinding strategies would be the most suitable to select from the trends of optimum grinding strategy variable combinations, for application to a maintenance section have so far been made by subjective judgements. A more objective judgement could be made if a common characteristic property is determined, for which the grinding strategies and grinding strategy combinations could be compared against each other. From a railway infrastructure manager's point of view, after safety and performance criteria have been satisfied, perhaps the most useful characteristic of a rail management strategy to consider is their whole life cycle cost of the rail. Therefore, when selecting grinding strategies to apply to a rail, the effect of those different grinding strategies on the whole life cycle cost of the rail would be an important consideration. This means that any tools or techniques which provide information on the likely effect of grinding strategies on the whole life cycle cost of the rail would be useful when selecting grinding strategies to apply. In this chapter a method is presented for estimating the effect of the different combinations of grinding strategy variables on the rail life cost of individual locations types and the average rail life cost of maintenance sections. The method is applied to the estimation of the rail life costs for the combinations of optimum grinding strategies proposed in section 6.5.2 and 6.5.3. Also the same cost calculations have been carried out for grinding strategies which were predicted to be safe, but have not been optimised, this is to allow comparison of the combinations of optimum grinding strategies, with grinding strategies representing those which have been derived from experience.

### **7.1 Method of Estimating Effect of Grinding Strategies on Rail Life Cost**

The method described here is not intended to give a full economic costing for the life cycle cost of the rail, it is intended to provide an estimate of the effect of different grinding strategies on the rail life cost. This is to illustrate a technique for using the trends of optimum grinding strategies to provide an objective means of determining which grinding strategies should be selected. The cost calculations described here are based on the cost of replacing a rail at the end of its life, the cost of applying the grinding strategy over the life of the rail, and effect of the grinding strategy on the wear life of the rail, all shared over the traffic carried by the rail during the life of the rail.

The ultimate unit of the rail life cost calculated, is the cost for each Equivalent Million Gross Tonne of traffic carried by each kilometre of rail. The cost estimation is based on the information which was available; the calculation method used could be adapted to take into account other factors, where the information is available. For example the cost estimation method does not take into account ancillary costs, such as getting the grinding machine to the work site, a cost which might be shared over different amounts of track ground in each operation, depending upon the combinations of grinding strategies for the different location types. The method outlined here is aimed at providing an estimate of the cost for the combinations of optimum grinding strategies determined as described in section 6.5.2 and 6.5.3, however it can be used for other cases.

#### ***7.1.1 Definition of the Parameters for Estimating the Effect of Grinding Strategies on Rail Life Cost***

There are a number of parameters which are required for the estimation of the effect of a grinding strategy on the rail life cost. Some of these are characteristics of the wider railway network. Firstly there is the average cost of a grinding operation, represented by the symbol  $G$ ; this is the average cost of one grinding pass of one kilometre of track at the maximum grinding capacity of the grinding machine. Secondly there is the maximum grinding depth which the grinding machine can reliably achieve in a single pass, represented by the symbol  $M$ . These first two parameters are the basic values from which the cost of applying the grinding depth specified at each grinding operation are calculated from. The third parameter is the cost to replace a kilometre of life expired rail, given the symbol  $R$ , and the fourth is the vertical wear limit of the rail, represented by  $V$ , this is the difference between the height of the new rail and life limiting height. These two parameters relate to the length of the operational life of the rail, in terms of how long it would take for it to be worn to the point it requires replacement, and the investment cost in that life. In order to obtain a value for the life of the rail, it is assumed in these calculations that the rail is replaced because it has reached its vertical wear limit. Rails could be replaced for other reasons before the vertical wear limit is reached, if these cases were to be studied, the rail life cost calculation method could be adapted by entering the rail life, as determined by the other factor, directly. A summary of these parameters and the values used for the cost estimation are given in table 7.1

below, the values are taken from the UK Track Standards [7.1], and the Network Rail Asset Management Policy [7.2], and are therefore representative of UK practice. Other values could be used for estimating the costs for other networks, or to reflect changes to UK practice. Those values could represent the current practice, or planned changes in infrastructure management practice, as part of a process of predicting the effect of those changes on infrastructure management costs.

Table 7.1. Values of the wider railway network parameters used for estimating the effect of grinding strategies on rail life cost.

System Parameter	Value	Symbol
Average Cost of a grinding operation (£/km)	700	<i>G</i>
Maximum grinding depth reliably achievable in a single pass, i.e. capacity of grinding machine (mm)	0.19	<i>M</i>
Rail Replacement Cost (£/km)	150,000	<i>R</i>
Vertical Wear Limit of Rail (mm)	14	<i>V</i>

In addition to the parameters of the wider system used for estimating the effect of grinding strategies on rail life cost, there are the parameters of the specific grinding strategies and maintenance sections for which the costs are being estimated. The rail life cost is estimated separately for each location type within the maintenance section, the calculations being performed on the values of the parameters for each location type separately, to obtain the rail life cost of each kilometre of rail for every MGT of traffic carried during its life. The average rail life cost is then obtained from the respective rail life cost of each type of location, and proportions of each type of location within the maintenance section. The grinding strategy parameters are the grinding interval and grinding depth of the grinding strategy applied at each location type, represented by the symbols *I* and *D* respectively. The interval is the effective grinding interval, i.e. the intervals at which grinding is applied to that type of location, not the operational grinding interval at which grinding is applied to one or more location types within the maintenance section. The symbol *P* is used to represent the proportion of the maintenance section which is made up of that type of location. The final parameter is the number of wheel passes which are equivalent to one million gross tonnes of traffic for the traffic pattern modelled, represented by the symbol *T*. This is used to convert between the measure of traffic used in the Grinding Model, a wheel pass, and the

measure of traffic commonly used on the UK railway network, equivalent million gross tonnes of traffic (MGT). The traffic is assumed to be the same for all locations in the maintenance section, that is that all vehicles pass through the whole maintenance section. The value of  $T$  for the Mixed traffic pattern, which is the only traffic pattern considered in this and the previous chapter is that 93,720 wheel passes are equivalent to a million gross tons of traffic.

### 7.1.2 *Calculation of Rail Replacement Cost of a Kilometre of Rail for Each Million Gross Tonnes of Traffic Carried*

To calculate the rail replacement cost for each million gross tonnes of traffic carried by the rail, an estimate of the rail life is required, this is based on the vertical height of the rail being reduced by wear and grinding to the point at which the rail requires replacement. Therefore to predict the life of the rail,  $L$ , the vertical wear limit of the rail,  $V$ , and the wear produced by traffic and grinding are needed, that is, the Effective Continuous Wear Rate (ECWR), given the symbol  $W_w$ . For the optimum grinding strategies determined from the trends of optimum grinding strategy variable combinations discussed in chapter 6, the ECWR,  $W_w$ , is obtained from equation 3, using the equation fitting constants for that location. Since equation 3 is only suitable for the optimum grinding strategy. To obtain the ECWR for non-optimum grinding strategies, the Grinding Model should be run for the grinding strategy and location for which the cost is being estimated, as described previously, and not interpolated from the trends of ECWR using equation 3. The ECWR values generated in the modelling and from the trends of model results are in the units of the amount of wear per wheel pass (m/WP). This needs to be converted to the amount of wear per million gross tonnes (MGT) of traffic,  $W_T$ , by multiplying the ECWR,  $W_w$ , by the number of wheel passes per MGT,  $T$ , as shown in equation 4 below.

$$W_T = W_w T \quad \text{Equation 4}$$

The vertical wear life of the rail in MGT,  $L$ , can now be found by multiplying the wear per MGT,  $W_T$ , obtained in equation 4, by the vertical wear limit of the rail,  $V$ , as shown in equation 5 below.

$$L = W_T V \quad \text{Equation 5}$$

The replacement cost of each kilometre of rail for every MGT of traffic carried during its life,  $C_R$  can now be calculated by dividing the cost to replace each kilometre of rail, the replacement cost of the rail,  $R$ , by the rail life  $L$ , see equation 6. Since the rail life is based on the wear predicted for the grinding strategy for which the cost is being estimated, then it, and the cost of rail life estimated from it, takes into account the effect of different grinding strategies on the life of the rail, and hence rail life cost.

$$C_R = \frac{R}{L} \quad \text{Equation 6}$$

### 7.1.3 *Calculation of the Cost of Grinding Each Kilometre of Rail for Each Million Gross Tonnes of Traffic Carried*

The estimation of the cost of applying a grinding strategy to each kilometre of rail for each million gross tonnes (MGT) of traffic over the life of the rail is based on the cost of each grinding operation, the number of grinding operations carried out over the life of the rail, and the amount of traffic carried during that life. The first step in the method to estimate the grinding cost is to convert the effective grinding interval for the location type, from a value expressed in wheel passes to a value expressed in MGT,  $I_T$ , where the addition of the subscript,  $T$ , indicates that it is the effective grinding interval for the location expressed in MGT of traffic. The interval in MGT is obtained by dividing the effective interval for the location type,  $I$ , by the by the number of wheel passes per MGT,  $T$ , as shown in equation 7.

$$I_T = \frac{I}{T} \quad \text{Equation 7}$$

The number of grinding operations carried out during the wear life of the rail at each location type,  $N$ , is obtained by dividing the wear life,  $L$ , for that location type, obtained in equation 4, by the effective grinding interval for that location type,  $I_T$ , as shown in equation 8. Only the integer value of the number of grinding operations,  $N$ , is used, the

value being rounded down from the exact result of the division, to obtain the number of grinding operations completed before the rail is removed.

$$N = \left\lfloor \frac{L}{W_T} \right\rfloor \quad \text{Equation 8}$$

The cost of an individual grinding operation at a location type,  $O$ , is determined from the average cost of a single grinding pass over one kilometre of track at the grinding machines maximum grinding capacity,  $G$ , and the maximum grinding depth the grinding machine can reliably achieve in one pass,  $M$ . It has been chosen to represent the cost of each grinding pass as consisting of a fixed cost for the pass and a variable depending on the depth of grinding applied, since grinding at a depth less than the machines capacity is likely to take less time and consume fewer grinding stones, and hence be cheaper. The cost of a single pass could be represented in a different way to reflect different contractual arrangements for charging for grinding. The model used here assumes that the fixed cost is half of the cost of a single pass at the grinding machines capacity, and that the variable cost ranges linearly from zero for a grinding depth of zero, to half of the cost of a pass single pass at the grinding machines capacity, for a grinding depth of the machines capacity. The estimation of the cost of a grinding operation is expressed by equation 9 below.

$$O = D \frac{G}{2M} + \frac{G}{2} \left( 1 + \left\lfloor \frac{D}{M} - 0.001 \right\rfloor \right) \quad \text{Equation 9}$$

The first part of equation 9 represents the variable portion of the cost for the pass or passes of the operation, required to achieve the specified grinding depth,  $D$ , the grinding depth,  $D$ , being multiplied by, the half of the cost of a pass,  $G$ , divided by the capacity of the machine. The second part of equation 9 represents the fixed portion of the cost of the grinding operation, and is determined by the number of grinding passes required to achieve the specified grinding depth multiplied by the fixed cost of one pass (half of the average cost of a pass at full grinding capacity,  $G$ ). The number of grinding passes required, and therefore the number of fixed cost per pass, to be applied, is obtained from one plus the integer of the grinding depth,  $D$ , divided by the capacity of the machine,  $M$ .

One is added so that the fixed cost of a pass at less than capacity, which would be removed by taking the integer, is applied. The subtraction of a small amount, 0.001 which is smaller than the precision to which grinding depths are specified, is to ensure that when all of the grinding passes are at full capacity, the fixed cost of an extra pass is not added.

The cost of applying a grinding strategy to each kilometre of rail for each million gross tonnes (MGT) of traffic over the life of the rail is obtained by multiplying the cost of each grinding operation,  $O$ , by the number of grinding operations required during the life of the rail,  $N$ , and dividing by the life of the rail, in MGT, as shown in equation 10.

$$C_G = \frac{NO}{L} \quad \text{Equation 10}$$

#### 7.1.4 *Calculation of the Rail Life Cost for Individual Locations and Maintenance Sections*

To obtain the estimated rail life cost for each location type,  $C_L$ , the estimated cost of rail replacement,  $C_R$ , and estimated cost of rail grinding,  $C_G$ , for that location, obtained from equations 6 and 10 respectively, should be added together, as shown in equation 11.

$$C_L = C_R + C_G \quad \text{Equation 11}$$

The rail life cost,  $C_L$ , is an estimate of the cost of replacing and grinding one kilometre of rail, for every million gross tonnes of traffic (MGT) carried by the rail, for one location type. Since the grinding strategies and crack growth rate and wear rate will be different at different locations, although with further investigation it might be found that the rail life cost for locations with similar properties could be considered together, the rail life cost for each location type is calculated separately. The average rail life cost for a maintenance section,  $C_{Mj}$ , is the sum of, the rail life cost,  $C_{Li}$ , multiplied by the proportion in which that location type occurs within the maintenance section,  $P_i$ , for each location. Where the suffix,  $i$ , is a variable which represents the location type, and the suffix,  $j$ , is a variable which represents the maintenance section. For the cases

examined here, this is represented by equation 12, the location type specific suffix,  $i$ , being,  $H$ , for Harringay type locations and,  $S$ , for Sandy type locations. Also for the cases examined here, the maintenance section specific suffix,  $j$ , will be either,  $A$ , for maintenance section  $A$ , or,  $B$ , for maintenance section  $B$ . For other cases, the form of equation 12 would be altered with additional terms for each additional location type, and the appropriate suffixes denoting the relevant locations and maintenance section.

$$C_{Mj} = P_H C_{LH} + P_S C_{LS} \quad \text{Equation 12}$$

## 7.2 Rail Life Cost Estimates for Example Grinding Strategies

The calculation method described in section 7.1 was compiled into a spreadsheet to enable automated calculation of the rail life costs for the different optimum grinding strategies applied at the two locations, and the average rail life cost of the example maintenance section to be made. An extract of the spreadsheet showing the calculation of the rail life costs for grinding strategy combination (i), described in section 6.5.2, is shown in table A.1 in appendix A as an example. A variation on the spreadsheet was created to calculate the rail life costs for non-optimised grinding strategies, the difference being that the Effective Continuous Wear Rate (ECWR) had to be calculated from a modelling run of the grinding model with those grinding variable values, and entered manually.

From these spreadsheets the estimated rail life costs, that is the rail life cost at each location, and the average rail life costs of the example maintenance sections, were calculated for the grinding strategy combinations in sections 6.5.2 and 6.5.3. In addition to these grinding strategy combinations, the rail life costs were also calculated for two example cases where the grinding strategies applied had not been optimised. The rail life costs were calculated for these non-optimum cases, including conducting the necessary Grinding Model runs to obtain the ECWR, to allow comparisons to be made between the estimated rail life costs for cases where the grinding strategies had and hadn't been optimised. All of the grinding strategies in the non-optimum grinding strategy cases were predicted to be safe, that is the predicted crack size trend for all of them tended to zero in less than the  $3 \times 10^6$  wheel pass target value of the optimised



values. It might appear biased to compare optimised grinding strategies with grinding strategies that are expected to require more grinding than necessary and hence have a shorter rail life. However, as the grinding sensitivity analysis showed, there would not be much margin within which to select grinding strategies which specified less grinding than the optimum strategies, yet the crack size still tended to zero. As a result the chances of arbitrarily selecting grind strategy values which specified less grinding, yet still produced a crack size which tended to zero, and hence would be safe, would be small, and would probably require an investigation to find. This would in essence be an optimum grinding strategy investigation with a different optimum criterion. Therefore it was felt justifiable to select grinding strategies which would reliably predict a safe crack trend, to represent grinding strategies determined from broad network wide experience, and applied to specific locations.

The first non-optimum example grinding strategy combination (non-optimum grinding strategy combination 1) consisted of a grinding strategy with an interval of 250,000 wheel passes and a depth of 0.19mm applied to the Harringay type locations and a grinding strategy with an interval of 125,000 wheel passes and a depth of 0.19mm applied to the Sandy type locations. This represents grinding operations being carried out with a depth approximately equal to the capacity of the grinding machine, at intervals not too dissimilar to those used by optimised grinding strategies, albeit not necessarily with the grinding machines operating at capacity. The second non-optimum example grinding strategy combination (non-optimum grinding strategy combination 2) consisted of a grinding strategy with an interval of 312,500 wheel passes and a depth of 0.19mm applied to the Harringay type locations and a grinding strategy with an interval of 156,250 wheel passes and a depth of 0.19mm applied to the Sandy type locations, this case being closer to the optimised cases. The grinding depth used for both locations of both non-optimised grinding strategies was maximum grinding depth reliably achievable by the grinding machine, since it was felt that if a board specification of grinding strategy was being applied without a prediction of the exact amount of grinding required, then it would attempt to maximise the utilisation of the grinding machine.

### **7.3 Rail Life Cost Estimate Results for Example Grinding Strategies**

The results of the rail life cost estimation calculations for both the optimised and non-optimised grinding cases are shown in table 7.2. To be clear where the term, non-optimum grinding strategy combination is used it is intended to indicate that it is the grinding strategies at the individual locations which haven't been optimised, not the combination of grinding strategies. The combinations of grinding strategies have not been optimised for any of the grinding strategy combinations described in this thesis, only those combinations judged to be the most suitable for application to a maintenance section selected.

The first thing from table 7.2 to be noted about the rail life cost estimations produced using this method, is that there is relatively little difference between the rail life cost estimates for different optimised grinding strategies at each location where only one grinding pass is required per operation. There is a moderate but distinct difference in the rail life cost between the single pass grinding strategies at each location and those that require two or more passes. That is, for the Harringay location, the optimum grinding strategies with grinding depths in the range achievable in a single pass had grinding depths that ranged from 0.09mm to 0.19mm, and had a rail life costs in the £2,469-£2,471/kmMGT range. Compared to the optimum grinding strategy with a 0.22mm grinding depth which would require two passes of the grinding machine had a rail life cost of £2,564/kmMGT. Similarly for the Sandy location, the optimum grinding strategies with grinding depths in the single pass range had grinding depths that ranged from 0.14mm to 0.19mm, and had a rail life costs in the £1,415-£1,431/kmMGT range. Where as the optimum grinding strategy for Sandy with a 0.38mm grinding depth had a rail life cost of £1,614/kmMGT and the optimum grinding strategy for Sandy with a 0.40mm grinding depth had a rail life cost of £1,711/kmMGT. There appeared to be little variation in the estimated rail life cost for different optimum grinding strategies except where there was a change in the number of grinding passes required.

### **7.4 Rail Life Cost Trends**

It was decided that before the effects of different combinations of grinding strategy on the estimated average rail life cost of a maintenance section was considered in detail, further study should be conducted to understand how the estimated rail life cost varied

with different optimum grinding strategies. Therefore the rail life cost for further optimum grinding strategies, with grinding depths across the range 0.04mm-0.50mm, were calculated for both locations, the results of these, and the rail life cost already calculated are shown in table 7.3 and plotted in figure 7.1. The optimum grinding strategies for which the rail life cost case been calculated, have been characterised by the grinding depth of those strategies, they could also have been characterised by the grinding interval, the grinding depth has been selected as the characteristic value and is used for consistency.

Table 7.2. Rail Life Cost (£/kmMGT) estimations for example grinding strategy combinations.

Grinding Strategy Combination	Harringay Type Location			Sandy Type Location			Average Rail Life Cost	
	Effective Grinding Interval (WP)	Grinding Depth (mm)	Rail Life Cost	Effective Grinding Interval (WP)	Grinding Depth (mm)	Rail Life Cost	E.g. Maintenance Section A, 50% Harringay Type, 50% Sandy Type	E.g. Maintenance Section B, 90% Harringay Type, 10% Sandy Type
i	196,000	0.09	£2,469	196,000	0.19	£1,420	£1,945	£2,364
ii	353,000	0.19	£2,471	353,000	0.4	£1,711	£2,091	£2,395
iii	392,000	0.22	£2,564	196,000	0.19	£1,420	£1,992	£2,450
iv	353,000	0.19	£2,471	177,000	0.17	£1,421	£1,946	£2,366
v	341,000	0.18	£2,470	341,000	0.38	£1,614	£2,042	£2,384
vi	200,000	0.09	£2,461	200,000	0.19	£1,415	£1,938	£2,356
vii	300,000	0.15	£2,452	150,000	0.14	£1,431	£1,942	£2,350
viii	300,000	0.15	£2,452	300,000	0.32	£1,587	£2,020	£2,366
Non-opt Comb. 1	250,000	0.19	£2,776	125,000	0.19	£2,164	£2,470	£2,715
Non-opt Comb. 2	312,500	0.19	£2,575	156,250	0.19	£1,755	£2,165	£2,493
ix	250,000	0.12	£2,457	125,000	0.11	£1,442	£1,950	£2,356

Table 7.3. Rail life cost estimates for optimum grinding strategies for Haringay and Sandy type locations with grinding depths in the range 0.04mm-0.50mm

Grinding Depth of Optimum Grinding Strategy (mm)	Rail Life Cost	
	Haringay Type Locations	Sandy Type Locations
0.04	£2,587	£1,791
0.07	£2,507	£1,547
0.09	£2,469	£1,484
0.1	£2,461	£1,461
0.12	£2,457	£1,439
0.14	£2,458	£1,431
0.15	£2,462	
0.17		£1,421
0.18	£2,470	£1,422
0.19	£2,471	£1,420
0.2	£2,558	£1,582
0.22	£2,564	£1,580
0.25	£2,563	£1,575
0.28	£2,577	£1,581
0.32	£2,599	£1,587
0.35	£2,609	£1,603
0.38	£2,617	£1,615
0.4	£2,687	£1,711
0.44	£2,697	£1,725
0.47	£2,726	£1,736
0.5	£2,722	£1,761

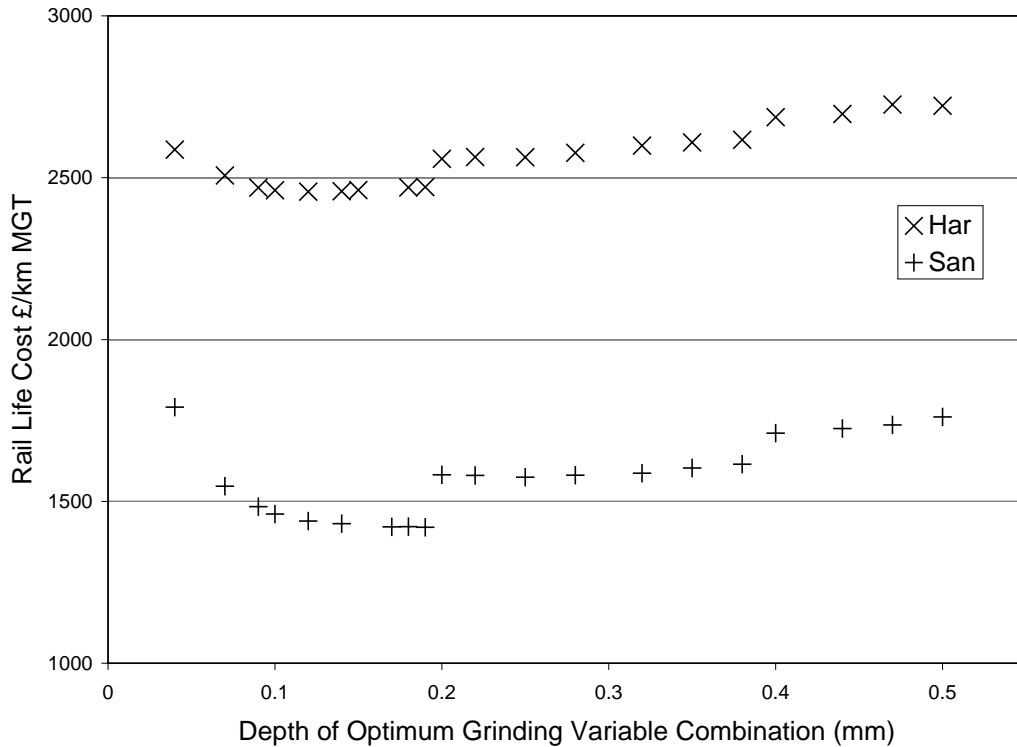


Figure 7.1. Rail life cost estimates for optimum grinding strategies for Harringay and Sandy type locations with grinding depths in the range 0.04mm-0.50mm.

It should be noted that the scale on which the rail life cost is displayed in figure 7.1 starts at £1000/kmMGT, this is to increase the spread of the values across the range which is of interest, to enable the small variations in rail life cost between some grinding strategies to be seen more clearly. The trends of cost in figure 7.1 show that the trends at both locations follow a very similar pattern, in which, the rail life cost for optimum grinding strategies which require the same number of grinding passes are broadly similar. This is except for an initial phase when the grinding depth of the optimum grinding strategies is less than half the machine capacity, where the rail life cost reduces significantly as the grinding depth increases to half the grinding machines capacity. As was noted from the results in table 7.2, when the number of grinding passes required for a grinding strategy goes up, there is a corresponding distinct increase in the rail life cost. This is shown in Figure 7.1 by the steps in the rail life cost trend which occur when the number of grinding machine passes required to achieve the grinding depth specified increases. The number of grinding machine passes can only be increased in integer steps,

therefore the addition of the fixed costs for the extra grinding pass causes a step in the rail life cost at the point where the increase in grinding depth requires an additional pass of the grinding machine. It should be noted that the increase in rail life cost when the number of grinding passes increases is relatively small compared to the total rail life cost. This is thought to be because, as can be seen from the example cost calculation in table A.1 in appendix A, the rail replacement cost is the major factor of the rail life cost, and the number of grinding passes per grinding operation doesn't affect the rail life directly, only the grinding depth applied during the operation. The stepped profile to the rail life cost trend is a result of the way that the cost of grinding operations has been determined, from the average cost of a grinding pass at full grinding machine capacity. This represents one possible way of accounting for the charging of the rail grinding, to rail life cost, there are other possible models for charging the rail grinding carried out, to rail life cost, which could reflect other contractual grinding arrangements. However the model used was selected as it was thought that this would be the most likely to be able to differentiate between strategies which make efficient use of the grinding machine, as with it the logistical implications of the efficient use of the grinding machine, i.e. the number of passes required, have some effect on the cost. This could be an important consideration as, even if number of grinding passes isn't taken into account by the charging structure, the cost of inefficient use of grinding machines is likely to be passed on by contractors to network operators through higher general rates. The model for charging the rail grinding carried out to rail life cost used might not take into account the cost impact of the efficient use of grinding machine in the most effective way possible, but its selection does recognise the potential significance of the efficient use of grinding machines on rail life cost.

It could be argued that there is potentially a discernible trend in the rail life cost plots between the steps in trend indicating a local minimum, however any such trend which might exist is barely discernible from the scatter in values. The scatter in the values plotted in figure 7.1 is thought to be due to rounding errors in the calculations. Also if these local minima could be found, it would be impractical to apply the grinding strategies to a high enough precision to take advantage of them.

As mentioned in the previous paragraph, the source of the scatter in the trends in figure 7.1 was thought to be due to rounding errors in the calculation method. The source of the rounding errors was investigated, and it was found that rounding error from the interpolation of the optimum grinding strategy variable value, which corresponded to the value of the other grinding strategy variable, could affect the rail life cost determined by up to £10/kmMGT. The rounding error arises because the grinding interval is quoted to more significant figures, than the grinding depth. Therefore there is a range of grinding intervals, which produce the same value of grinding depth (when rounded to two decimal places) when entered into the inverse of trends of optimum grinding variable combination interpolation equation, equation 2. Taking the Harringay location as an example and using equation 1, the optimum grinding interval for a 0.145mm grinding depth was determined as 286,624 wheel passes. Similarly the optimum grinding interval for a grinding depth of 0.1549mm was determined as 301,852 wheel passes. These grinding intervals are at the limits of the range which when entered into equation 2 for Harringay to determine the optimum grinding depth, give a value which rounds to 0.15mm. Performing the rail life cost calculations for these grinding intervals and a grinding depth of 0.15mm, gives estimated rail life cost of £2,452/kmMGT with the 301,852 wheel pass interval, and £2,462/kmMGT with the 286,624 wheel pass interval. It is not useful to find the lowest rail life cost to the nearest £1/kmMGT, since this is less than the effect of the rounding error on rail life cost. Also it is not useful to specify the grinding depth to a degree of precision which the grinding machine is unlikely to be able to apply reliably. In addition there is likely to be some variation in the general trend between the steps relating to the number of grinding passes, due to the rounding of the number of grinding operations carried out over the life of the rail to an integer value. It would be expected that there would be a small step in the trend, each time the calculation of the number of grinding operations required over the life of the rail crosses the integer threshold, and the cost of another grinding operation is added.



## **7.5 Determining the Most Suitable Grinding Strategy Combinations to Apply from the Estimated Rail Life Cost Results**

Turning back to the consideration of the use of the effects of different grinding strategies have on estimated rail life cost effects for determining the most suitable grinding strategy to apply to sections of track and maintenances sections, and the results presented in table 7.2. As previously stated there is relatively little difference between the rail life cost estimates for different optimised grinding strategies at each location where only one grinding pass is required per operation. There is a moderate but distinct difference in the rail life cost between the single pass grinding strategies at each location and those that require two or more. Figure 7.1 shows the full extent of this stepped profile in the rail life cost trends, including the increasing rail life costs for optimum grinding strategies as the grinding depth reduces below half the capacity of the machine. From these observations it can be inferred that generally the most suitable optimum grinding strategy to apply at a location, or combination of optimum grinding strategies to apply to a maintenance section, would be those where the grinding depth is greater than half the full grinding capacity of the grinding machine, and can be ground in one pass. Furthermore it indicates that if this point is observed there is very little to distinguish between which is the most suitable of the grinding strategies or grinding strategy combinations to select. Therefore as the cost estimates shown are unproven and there are no guarantees that the predicted cost difference would be achieved, it would be unlikely that extensive measures to implement one of these strategies, or combinations thereof, over another would be of benefit. Especially when there are other factors affecting the whole life cycle cost of the rail which are not included in the rail life cost estimate.

Of the first five proposed grinding strategy combinations, developed for maintenance sections considered in isolation from the network. It was optimum grinding strategy combination (i) which turned out to have the lowest rail life cost, for maintenance section A, not grinding strategy combination (vi) which had been considered more suitable. Similarly of the first five optimum grinding strategy combinations it was grinding strategy combination (i) which turned out to have the lowest rail life cost, for

maintenance section B as opposed to grinding strategy combination (v), even though grinding strategy combination (i) had been expected to be unsuitable. As it turned out an optimum grinding strategy with a grinding depth of 0.09mm was nearer to the optimum grinding depth which gave the lowest rail life cost for the Harringay type locations, which make up 90% of maintenance section B, than the other grinding depths considered. It appears that maximising the utilisation of the grinding machines grinding capacity is not as important as first thought, at least for the grinding operation cost model used. Although the average rail life cost of grinding strategy combination (iv), which was designed to maximise the utilisation of the grinding machine in maintenance section B, was estimated to only cost £2/kmMGT more. If an objective judgement was being made as to which of the first five grinding strategy combinations to apply to a maintenance section, on the basis of the one with the lowest estimated average rail life cost, then this selection would be contrary to the subjective judgements made in section 6.5.2. That is grinding strategy combination (i) would be selected for both maintenance sections, as in both cases it had the lowest estimated average rail life cost of the first five grinding strategy combinations.

Of all the grinding strategy combinations for which the average rail life cost was calculated, it was grinding strategy combinations (vi) and (vii) which gave the lowest estimated rail life cost for example maintenance sections A and B respectively. Hence if selecting which grinding strategy combination to apply to a maintenance section, on the basis of the one with the lowest estimated average rail life cost then of the combinations for which the rail life costs were estimated, these would be selected for their respective maintenance section. When grinding strategy combinations (vi), (vii) and (viii) were created from a list of pre-determined optimum grinding strategies in section 6.5.3 the subjective judgement was that of them, (vi) and (viii) would be the most suitable for maintenance sections A and B respectively. Since grinding strategy combinations (vi) has been determined by the least rail life cost objective criteria as the most suitable of all the combinations calculated for maintenance section A, then in this case the subjective and objective judgements agree. For maintenance section B, it was unclear at the time whether grinding strategy combinations (vii) or (viii) would be most suitable, by the

objective criteria (vii) would be judged the most suitable of the three, (viii) was estimated to cost £16/kmMGT more. The subjective judgement between grinding strategy combinations (vii) and (viii) was made on the basis that it would be more economical to grind a small proportion of locations twice at double the interval. Whilst the objective judgement might be correct and it does take into account some effect of multiple grinding passes, it does not take into account other considerations like the time a grinding machine availability and the time it spends transiting between locations, which the subjective judgement did as well. Since the estimated rail life cost for grinding strategy combinations (vii) and (viii) applied to maintenance section B were similar, the subjectively selected grinding strategy combinations could still be the more suitable. The point here is that for the selection of grinding strategy combinations the subjective judgement of section 6.5 and the objective judgement of this section might not agree, however both are useful, particularly when the techniques are used together, for making the final judgement as to which grinding strategy combination to apply.

As has been discussed earlier in this chapter, there were slight to moderate differences between the average rail life cost estimates for the grinding strategy combinations which use optimised grinding strategies, all of them being within 8 or 4 percent of the one with the lowest rail life cost estimate. However it can be seen from the rail life cost results in table 7.2 that for both maintenance sections, there was a significant difference between the average rail life cost estimates for the grinding strategy combinations with the lowest value, and the ones using non-optimised grinding strategies. This was particularly true in the case of non-optimum grinding strategy combination 1, where the estimated rail life cost was 27% higher than the lowest case for maintenance section A, and 15% higher than the lowest case for maintenance section B. The grinding strategy variables of non-optimum grinding strategy combination 2 were deliberately chosen to be closer to the optimum values, indeed the intervals are not much different from grinding strategy combination (vii). However the non-optimum grinding depths significantly increase the estimated average rail life cost for both maintenance sections, to levels which are noticeably higher than those of the grinding strategy cases using optimised grinding strategies which had the highest estimated average rail life cost.

To illustrate the effect of optimising the grinding strategies applied on the estimated rail life cost, even when one of the grinding strategy variables has been arbitrarily ascribed, another grinding strategy combination was looked at. This is grinding strategy combination (ix), which can be found on the last line of table 7.2, it is essentially the same as non-optimum grinding strategy combination 1, except that the grinding depths applied at each operation have been reduced from the grinding machines capacity, to the optimum depths for the interval at each location. The effect on the estimated rail life cost of optimising the grinding strategy, by simply reducing the grinding depth applied, is shown by the difference between non-optimum grinding strategy combination 1 and grinding strategy combination (ix) results. Where the estimated rail life cost was reduced by 21% and 13% for maintenance sections A and B respectively, when the grinding depth applied was reduced. Although it should be remembered that the non-optimum grinding strategy combinations were created with a knowledge of the optimum grinding strategy variable combinations, and it was anticipated that they could have a higher estimated rail life cost.

Having established the rail life cost trends in section 7.4 it was decided to use them to select a grinding strategy combination, by selecting the optimum grinding strategies for each location with the lowest rail life cost as given in table 7.3. This gave a grinding strategy combination which had a grinding strategy of 0.12mm depth applied at 246,540 wheel pass intervals at the Harringay type locations, and a grinding strategy of 0.19mm depth applied at 195984 wheel pass intervals at the Sandy type locations. The average rail life costs estimated for these grinding strategy combinations was £1,939/kmMGT and £2,354/kmMGT for example maintenance sections A and B respectively, both of these rail life cost values are within the rounding error of the lowest rail life costs estimated for their respective maintenance sections. This shows that selecting the grinding strategy combination from the optimum grinding strategies which have the lowest rail life cost at each location is not expected to result in noticeably lower rail life cost estimates for the maintenance sections, than using optimised grinding strategies

which can be carried out in a single pass, and have a grinding depth between half and the full capacity of the grinding machine.

## **7.6 Summary of the Use of Estimations of Rail Life Cost for Specifying Grinding Strategies**

The shape of the rail life cost trend, that the rail life cost estimates for grinding strategy combination (ix) happen to be close to the lowest value for the rail life cost from the other grinding strategy combinations, and that there appears to little advantage in selecting the optimum grinding strategies with the lowest rail life cost estimates, all serves to highlight one thing. That is, that the rail life cost results indicate that the important consideration when selecting combinations of optimum grinding strategies to apply to a maintenance section, is that where possible the grinding strategies should require only one grinding machine pass to apply, and the grinding machine should be operating at least half its grinding depth capacity. This is if the lowest rail life cost estimated by this method is being used as an objective criterion to select the grinding strategy combination to apply. It has already been mentioned that the method used to calculate the rail life cost, does not take into account all of the factors which affect the life cycle cost of the rail, also different models of the cost per grinding operation might produce different results. The conclusions drawn from the results are for the calculations carried out for the conditions and values of the parameters specified, this method can be used to calculate equivalent values for other conditions, and the same techniques used to asses the results. For the selection of grinding strategy combinations, the use of the lowest rail life cost estimated by this method as an objective criterion, might not agree with the subjective judgements discussed in section 6.5, which takes into account more factors. However both could be useful together for making the final judgement as to which grinding strategy combination to apply.

The calculations and method presented here and the conclusions drawn from them are intended to serve as an illustration of the techniques which could be used to select grinding strategies to apply. They are based on cost estimates which do not take into account all factors which affect the whole life cycle cost of a rail. Furthermore they are

based on the trends of optimum grinding strategy variable combinations derived from the Grinding Model, and the previously stated caveats regarding their use to actually specify grinding operations on a railway network apply here.

## **7.7 References**

- 7.1. Business Process Document. Inspection and Maintenance of Permanent Way (2005). Ref: NR/SP/TRK/001. Issue 02. October 2005
- 7.2. Network Rail October 2007 Strategic Business Plan Supporting document Asset management (2007)

## **Chapter 8. Comparing Grinding Model Predictions and Rail Life Cost Estimates with UK Railway Network Practice.**

### **8.1 Introduction to the Comparison of the Grinding Model Predictions and Rail Life Cost Estimates with UK Railway Network Practice.**

In previous chapters, the characteristics of the predictions of the Grinding Model and the rail life cost estimates have been discussed on their own merits without reference to the current, detailed grinding practice on the UK railway network. In this chapter, the grinding strategies determined using the Grinding Model and suggested as being the most suitable for application to the rail for the given conditions, will be compared with what is actually applied to the UK network, and the observations regarding the effectiveness of the policy at the locations represented in the modelling. Also the rail life cost of the current UK network grinding practice will be estimated using the same technique as was used for the grinding strategies determined with the trends derived with the Grinding Model, and the estimated rail life cost for the different cases compared and discussed.

#### ***8.1.1 Current UK Rail Grinding Policy for Rolling Contact Fatigue Damage Management.***

The current UK policy for grinding rails to manage the damage caused by rolling contact fatigue (RCF), specifically the cracking of rails, is to carry out grinding on a preventative basis. That is, the rails are ground on a regular basis with the aim of preventing RCF initiated cracks from developing to threaten the integrity of the rail or significantly reduce its performance. Through experience it has been found that overall a policy of grinding curves of 2500m radius or less, to a depth of approximately 0.2mm at intervals of 15 million gross tonnes (MGT) of traffic carried by the rail, is effective at preventing significant RCF cracks developing in the majority of these curves and extending the safe rail life. Similarly the policy for straight track is to grind to a depth of approximately 0.2mm at intervals of 45MGT of traffic, this being extended from 25-30MGT intervals used on straight track previously. This policy is applied to principal

routes, where the traffic levels justify the level of investment in the maintenance of the rail to extend its safe operational life. Both of the locations modelled in this thesis are at different points along the same route which fits into the category of a principal mixed traffic route. Meeting the grinding criteria for managing RCF cracking is not the only circumstances under which the rail is ground; grinding is applied in order to manage other rail head defects and for profile maintenance, as well as in specific cases where it is found necessary to apply additional grinding to manage the RCF cracking of rails. The curve at Harringay has a radius of 1250m, so is in the 15MGT interval grinding category, and the curve at Sandy has a 3000m radius, so is in the 45MGT interval grinding category.

## **8.2 Comparison of UK Rail Grinding Policy with the Variable Grinding Interval Investigation Results**

The optimum grinding interval determined for the Mixed traffic case in the Optimum Grinding Interval Investigation conducted with the Grinding Model in Chapter 3 was, 369,700 wheel passes. This is equivalent to a grinding interval of 3.95MGT for the Mixed Traffic case that is being compared with current practice as it is the traffic case that is most representative of the traffic seen at the Harringay location. Therefore the grinding interval determined with the Grinding Model for a grinding depth of 0.2mm, with the aim of optimising the interval to minimise grinding and maximise rail life was nearly a quarter of that which is applied in practice. That is the grinding strategy determined with the Grinding Model specified grinding to be carried out nearly four times more often than the current practice for those conditions, hence it would produce more wear and shorten the vertical wear life of the rail. However, it should be noted that it was reported in the previous project, for which the contact data used in this project were generated for [8.1], that during the monitoring of the site at Harringay, RCF cracks of up to 14mm surface length were observed at this site. In the Grinding Model cracks of 14mm surface length would be represented by a crack size of 7mm. The actual shape of the cracks observed, and hence their actual size and depth, was not determined, although semi-ellipses of approximately semi-circular shape at an angle of approximately 30



degrees to the surface would be typical. However other crack configurations, such as those that turn back towards the surface and result in spalling would be a possibility.

It is perhaps useful at this point to clarify what is meant when one grinding strategy is said to represent more, or less, grinding than another, or that more, or less, grinding is required to meet a certain predicted crack size trend criteria (such as the optimum crack zero point). Where more, or less, grinding is referred to, it is used to indicate that on average, for the same amount of traffic, the combination of grinding strategy variables of the grinding strategies being compared to the base or current case would remove more, or less, material from the rail by grinding respectively. There is a qualification in that, although a grinding strategy which consists of grinding at half the interval of a base case and with a depth half of that base case, would remove the same amount of material from the rail by grinding over the period of several intervals, and they would have the same Effective Continuous Wear Rate, their effect on the predicted crack size trend would not be the same. This is because where a crack is of a size that it is predicted to grow, grinding half as much at half the interval reduces the crack length during the interval of the reference grinding strategy, reducing its length and therefore the crack growth rate so the crack grows less than it does during the second half of the reference interval. That is, grinding half the depth at half the interval has more impact on the crack size, therefore optimum grinding strategies which have lower interval and depth have lower ECWR, as shown in Figure 6.4. In general the terms, more or less grinding, are only used when the difference in the amount of material removed from the rail on average, for the same amount of traffic, is more than twice or less than half that for the compared strategy, elsewhere more specific terms have been used. In all cases, applying more grinding would refer to a grinding strategy that had a greater impact on the predicted crack size and visa versa.

### **8.3 Comparison of UK Rail Grinding Policy and Grinding Strategies Suggested from the Trends of Optimum Grinding Strategy Variable Combination Results**

The sensitivity analysis having shown how sensitive the crack size predictions were to errors in the application of the grinding strategy, it was deemed appropriate to use 0.19mm as the maximum grinding machine capacity to ensure that the specified grinding depth could be applied. It is thought reasonable to compare the 0.19mm depth (maximum reliably achievable single pass grinding depth) with the typical depth of 0.2mm applied in the UK network policy, as 0.2mm is only stated as the typical grinding depth, so it is single pass grinding strategies at the maximum capacity of the grinding machine which are compared rather than exactly the same grinding depth. This is so that the grinding costs are comparable, as a 0.2mm grinding depth is considered to require two grinding passes from Chapter 5 onwards.

The interpolation of the trends of optimum grinding strategy variable combinations for the Haringay and Sandy locations, predicted optimum grinding intervals of 353,322 wheel passes and 195,984 wheel passes respectively, for a 0.19mm grinding depth. This optimum grinding interval for a 0.19mm grinding depth at the Haringay location given by the trend, represents an interval of 3.8MGT. Grinding the Haringay location at this interval would result in grinding being carried out nearly four times more often than for the current policy. However as mentioned in the previous section, cracks of 14mm surface length, that is, 7mm in terms of the model crack size, were observed at the Haringay site. For the Sandy location the optimum interval given for a 0.19mm grinding depth by the trend represents an interval of 2.1MGT of traffic, grinding the Sandy location at this interval would result in grinding being carried out over 21 times more often than the current policy. In addition the observations carried out at this site, reported in the previous project already mentioned, did not report any cracks visible at this location.

That RCF cracks occur at the actual Haringay location indicates that more grinding than the network policy specifies for this location would be required to control crack size.

Therefore it could be argued that the grinding strategy determined as the optimum using the Grinding Model in the Variable Grinding Interval Investigation, and from the trends of optimum grinding variable combinations, would be an improvement on the policy as it specifies more grinding for this site. However it could be that the grinding strategy specified from the Grinding Model specifies significantly more grinding than the minimum necessary to prevent the RCF cracks observed developing, removing the early stages of the crack much sooner than the optimum criteria and wasting the wear life of the rail. Alternatively it could be that the grinding strategy specified from the Grinding Model specifies less grinding than the minimum necessary to prevent the RCF cracks observed developing and would only reduce the rate at which cracks develop. All that can be said with any degree of certainty in comparison of the observations and predictions at Harringay, is that more grinding than was being applied at the time of the observations was required to control RCF cracks, and that grinding strategies specified on the basis of the Grinding Model predictions specified more grinding than the network policy.

The Grinding Model specifies grinding to be carried out 21 times more often at the Sandy location than the network policy and no cracks were detected. Therefore the Grinding Model could be interpreted as significantly over specifying the grinding to apply at the Sandy location, that is, specifying more grinding than required to control the RCF cracks which might actually occur at the location. The extension of this interpretation would be that applying the grinding strategies derived from the Grinding Model to the Sandy location would result in the waste of grinding resources and rail wear life.

The difference in whether the grinding strategies specified using the results of the Grinding Model could be interpreted as an improvement over those specified by the network policy for the Harringay and Sandy locations, could be explained by the fact that the philosophy behind the Grinding Model and the national policy are fundamentally different. The philosophy of the network policy is that a single grinding strategy is applied to a wide range of conditions, there being only two categories of

conditions, which from experience it has been found prevent the initiation and/or growth of RCF cracks for the majority of cases. The grinding strategy specified for the category being a compromise which attempts to suit all of the conditions within the category. The philosophy behind the Grinding Model is that a grinding strategy to suit a very specific set of conditions is specified such that a crack of a size at the threshold of detection, which is assumed to exist, is predicted to be worn away by the wear from grinding and traffic, in spite of the crack growth generated by the traffic, within a specified period. The Grinding Model assumes the existence of cracks of a much larger size than those at the initiation stage considered by the preventative policy.

One possible reason for the apparent unsuitability of the grinding strategy specified for the Sandy location by the Grinding Model could be that there is no initial crack, and the conditions do not exist, in conjunction with, or in spite of, the current grinding policy for an RCF crack to initiate and/or grow. The Grinding Model predicts that Sandy location would require approximately twice the grinding of the Harringay location to remove the same size initial crack by the same point in the traffic pattern. The wear from traffic at Sandy is predicted to be less than 10% of that predicted for Harringay. These two facts indicate that the factors driving crack growth are predicted to be lower at Sandy than Harringay, but in conjunction with the lower wear, the Grinding Model predicts that for the initial crack size, the crack size trend would be crack growth dominated and therefore require more grinding. However, even though the Sandy location is predicted by the Grinding Model to be more crack growth dominated than the Harringay location for the initial crack size used, the factors driving crack growth being lower, could mean that the conditions for cracks to initiate or grow from very small sizes (less than 1mm) do not exist when taken in conjunction with the current grinding policy. Therefore there is no crack of the initial size which would be predicted to require the grinding strategy specified by the Grinding Model to control it, so no cracks are observed at the site. It is possible that if there was an initial crack of the size specified in the Grinding Model it would grow with the current grinding policy to a size which could threaten the integrity of the rail. However it is not suggested that the Grinding Model should be used to specify grinding strategies to control cracks which are not expected to exist, whether the

expectation that the cracks won't initiate comes from experience or crack initiation predictions.

The situation regarding RCF crack initiation and growth at Sandy discussed above appears to be in opposition to that at Harringay, where the conditions for RCF crack initiation and growth appear to exist since cracks were observed. The Grinding Model predicted that cracks of the initial crack size of 1.75mm would be predicted to grow to sizes which could threaten the integrity of the rail, with grinding strategies which applied less grinding than the optimum case, but more grinding than the network policy for this location. An example from the mixed traffic case of the Variable Grinding Interval Investigation, is that with an grinding strategy of 0.2mm depth being applied at intervals of  $5 \times 10^6$  wheel passes, that is, 5.3MGT (just over one third of the network policy interval), an initial crack of 1.75mm (3.5mm surface length) was predicted to exceed 10mm (20mm surface length) after  $2.9 \times 10^6$  wheel passes, that is 31MGT. The crack size trend for this modelling run is plotted in figure 4.4, it is the third trend from the top, marked "GI  $5 \times 10^5$ " in the key. From the fact that a crack of the initial size was predicted to grow to a size which could be propagated to threaten the integrity of the rail with a grinding strategy which applied more grinding than the network grinding policy, it can be inferred that a smaller crack would be predicted to grow to the initial crack size and beyond with the network grinding policy. Comparison of the Grinding Model predictions with the Harringay site appears to indicate that the Grinding model prediction could be of the correct order of magnitude to represent the actual conditions at this site where RCF cracks are expected to develop.

It is not claimed, on the basis of one case which is not fully understood, that is the actual life of the rail is not available, that where RCF crack initiation and development is expected to take place, the Grinding Model in its current state of development is able to predict the crack size trend accurately, or is suitable for specifying grinding strategies that maximise rail life. However that the observations for this case and the predictions of the Grinding Model do not contradict each other, could indicate that the predictions of the Grinding Model for cases where the cracks are expected to grow are close to

representing real situations. This indicates that the Grinding Model could be developed to provide a useful tool for predicting the effect of grinding on the growth of RCF cracks and for specifying grinding strategies which maximise the safe rail life.

It should be noted that the actual traffic pattern at reported at Harringay and Sandy, obtained from the network traffic database, are not the same as each other, and are not the same as the Mixed Traffic case. The traffic patterns at Harringay and Sandy are dominated by the types of vehicles included in the Mixed Traffic case, which represented 80% and 70% of the vehicles, but did include a proportion of other vehicle types. The mixed traffic case was designed as a general case to study the effects of different combinations of vehicles, using those vehicles for which the data was available, that might represent a primary route with a mix of high speed and commuter trains. The modelling of the Mixed Traffic case with the hypothetical Class 365X type vehicles substituted for the Class 365 vehicles carried out in the early stages of the investigations with the Grinding Model showed the predictions of the optimum grinding strategy were sensitive to such changes, to the extent that they changed the predicted optimum interval by 12.5%. Further study of mixed traffic cases could be conducted to find out the effect of different traffic patterns, and if one traffic pattern could reliably be used to represent other similar traffic cases. It can not be judged from the limited data available how well the Mixed Traffic pattern represents the crack size trends for the traffic at the locations modelled, only that the predictions appear to be of the correct order of magnitude compared to the Harringay case. It can not be determined if the crack growth predictions of the Grinding Model with the Mixed traffic case, are accurate for the Sandy location, as the Grinding Model does not currently have the ability to predict the initiation and early stage development of RCF cracks. This combined with the prediction from the previous project [8.1] that cracks of the initial size would not be initiated at the Sandy location, means that it would not be expected that there were any RCF cracks of the initial crack size for the Grinding Model to predict the development of.

That cracks at locations such as Sandy were RCF cracks are not thought to initiate, are predicted to grow to threaten the integrity of the rail if they did initiate and grow beyond the early stages, should serve as a warning that it is important to understand the effect of a grinding policy or strategy on the initiation and early stages of development. Making changes to the grinding applied, might allow cracks to initiate at sites which were just below the initiation threshold with the previous grinding policy, and the new grinding policy might not be sufficient to prevent the RCF cracks, which now potentially have the conditions to initiate, from developing.

#### **8.4 Comparison of Cost Estimates for UK Rail Grinding Policy and Grinding Strategies Suggested from Modelling**

To compare the rail life costs for a rail maintained with the UK rail grinding policy and those for the grinding strategies suggested from the modelling, the rail life costs for the rails when using the UK network policy were estimated for each location. To do this the rail life cost estimation method described in chapter 7 was applied to the locations with the grinding interval and depth specified by the policy being entered directly. Also the Effective Continuous Wear Rate (ECWR), with and without the grinding specified by the policy, was calculated and entered directly, rather than interpolated, since the interpolation of ECWR only applied to optimum grinding strategies. In addition the cost of a grinding operation was fixed at £700/km for these calculations as this is the average cost given for a typical grinding operation of 0.2mm depth. The input values and results of the calculations are shown in table 8.1.

Table 8.1. Rail life cost estimation method applied to national network grinding policy to estimate rail life cost at example locations.

	Location type	Radius of 2500m or less, Harringay	More than 2500m Radius, Sandy
No Grinding	ECWR no grinding (mm/MGT)	0.164	0.0109
	Wear Life (MGT)	85.4	1286
	Rail Life cost (£/kmMGT)	£1,756	£117
Network Policy Grinding	Grinding interval (MGT)	15	45
	ECWR 0.2mm grinding (mm/MGT)	0.177	0.0153
	Wear Life (MGT)	79	915
	Rail Replacement Cost (£/kmMGT)	£1899	£164
	Grinding Cost (£/kmMGT)	£44	£15
	Rail Life Cost (£/kmMGT)	£1,943	£179

The first difference to note is that the estimated rail life costs for the Harringay and Sandy locations are very different, both with and without the application of the network grinding policy, the estimated rail life costs for Harringay are at least 10 times those for Sandy. This is because the wear caused by the traffic is over ten times greater at the Harringay location than the Sandy location, the rail life cost being dominated by the rail replacement cost, which is determined by the wear life of the rail, and the wear caused by the traffic is the dominant factor in the wear life. The network policy, [8.2], states that typical service life of track on primary routes is 750MGT, with the RCF control grinding policy being aimed at preventing RCF cracks from reducing this life. If rail replacement is carried out on the basis of the rail reaching its vertical wear limit and not for other factors, the rail at Sandy is predicted to exceed this typical life, where as the rail at Harringay is predicted to have one tenth of the typical life. It is highly doubtful that the rail at Harringay would have a life of 750MGT if it did the estimated rail life cost would be £247/kmMGT. It would be typical to expect a curve in the under 2500m radius category on a primary route to have a life of 300MGT without grinding, in this instance the rail life cost would be £500/kmMGT, if this rail life was attained at



Harringay with the network grinding policy applied, the rail life cost would be £547/kmMGT. However these expected rail lives are for typical rails in curves of radius less than 2500m, Harringay does not appear to be typical, and was selected in the previous project as a site to investigate because of the particular RCF issues there, so the wear rates predicted bring above the typical and reducing the life is not unexpected. Therefore further discussion will centre around the rail life being determined by the predicted rail life and the subsequent rail life cost. Although the rail life predicted at Sandy is greater than the typical, it was selected for examination in the previous project on the basis that it was site for which there were no known or apparent issues. Therefore it would not be inappropriate to accept the life based on the wear life predicted, and use the rail life cost associated with this longer life, for comparison with the rail life costs estimated for the grinding strategies derived from the Grinding Model cases. For completeness the estimated rail life cost, estimated using the method described in Chapter 7, for the Sandy location having the typical rail life of 750MGT, without and with the network grinding policy, would be £200/kmMGT and £215/kmMGT respectively.

Comparing the estimated rail life costs for the rails with the network grinding policy applied, with the rail life costs in Chapter 7, it is clear that the rail life costs estimated for the current network policy are significantly lower than those estimated for the combinations of optimum grinding strategies and the example combinations of non-optimised grinding strategies. The difference in the estimated rail life cost between the cases using grinding strategies derived from the Grinding Model and the cases using the network grinding policy is particularly pronounced at the Sandy location. The lowest rail life cost estimated at the Sandy location for the optimised grinding strategies and non-optimised grinding strategies were 8 and 10 times the rail life cost estimated for the network grinding policy, respectively. The reason for such a marked difference is that the grinding strategies determined from the grinding model on the basis removing a pre-existing crack, and hence produce an Effective Continuous Wear Rate (ECWR) approximately ten times that of the traffic in order that it is predicted that such a crack would be controlled. This increased ECWR drastically reduces the wear life of the rail;

the reduction in wear life with the Grinding Model determined grinding strategies being the dominant factor in the increased rail life cost over that using the network grinding policy. As discussed in section 8.3 the fact that no RCF cracks were observed at the Sandy site indicates that the network grinding policy is sufficient to control and RCF cracks which might develop. Therefore implementing the Grinding Model derived grinding strategies would drastically and unnecessarily increase the rail life cost. That the Grinding Model over specifies grinding in this case, is thought to be because the conditions at Sandy do not exist for cracks of the initial size modelled to develop. As stated previously it would not be expected to apply the grinding strategies derived from the Grinding Model where experience or crack initiation predictions dictate that cracks are not expected to develop, and hence not increase the rail life cost.

The situation with regard to making direct comparisons between the rail life cost estimates at the Harringay location is less clear. The rail life cost estimate for this location when using the network grinding policy is lower than the lowest value found when using grinding strategies determined from the Grinding Model, although they are of the same order of magnitude, £1,943 compared to £2,452 respectively. However there is reason to suspect that the rail life at this location would not be defined by the predicted rail wear life, as significant RCF cracks were observed to have developed which might require the rails replacement before the predicted wear life is reached. Depending upon the difference in rail life between the predicted wear rail life and the actual rail life could dramatically alter the rail life cost estimate. Replacement of the rail before the 79MGT rail wear life predicted with the application of the network grinding policy due to rolling contact fatigue cracking would significantly increase the rail life cost. Working back, if the rail required replacement before a life of 62-63MGT then the rail life cost would be similar to that when using the rail grinding strategy determined with the Grinding Model which had the lowest rail life cost. If the rail required replacement sooner than 62MGT, then the estimated rail life cost of the rail using the network grinding policy would be higher than if the rail grinding strategy determined with the Grinding Model which had the lowest rail life cost was used. The information as to what the actual rail life of the rail at Harringay was is not available at this time, the

RCF cracks could have been developing late in its life, which could have already been longer than the 79MGT predicted from the predicted wear rate, in which case the estimated rail life cost would have been lower.

In a similar way to the discussion of the comparison of the grinding strategies derived from the Grinding Model and network policy in section 8.3, it is not claimed that on the basis of one case that the Grinding Model and rail life cost estimation technique in their current state of development are able to predict the rail life cost of different grinding strategies accurately. However the situation at the Harringay location could indicate that the rail life could be limited by RCF cracks and not wear, therefore the actual rail life cost could be higher than the estimated rail life for this case. This indicates that since the rail life costs are of a similar order of magnitude, the Grinding Model and rail life cost estimation techniques could, with further developments, provide a useful tool for specifying grinding strategies which minimise the rail life cost. The situation at Sandy indicates that specifying grinding strategies based on the predictions Grinding Model and rail life cost estimation techniques, where cracks are not expected to initiate or develop, would result in drastically and unnecessarily increased rail life costs. This indicates crack initiation and early stage growth predictions should be carried out before Grinding Modelling runs, or preferably the Grinding Model developed to include these predictions as the next stage in its development towards a useful tool for specifying grinding strategies at locations similar to Sandy.

It should be noted that there could be additional benefits where grinding is carried out more often as a result in the change in the grinding specification policy, which are not directly related to the control of rolling contact fatigue cracks. One of these is that the grinding carried out would not be limited removing material vertically from the top of the rail to the specified depth, profile maintenance would be carried out at the same time. Therefore the profile could be maintained closer to the ideal profile, rather than just being maintained when it approaches a limit, improved profiles could reduce contact stress and improve wear life of the rail, both vertical and side wear, which might be the rail life limiting factor. Also better profile management would not only be of benefit to

the control of RCF cracks, but could lead to a reduction in the rate of deterioration of other elements involved in the wheel-rail contact, and a reduction in the noise generated by the contact and railway system. This serves to re-emphasise that grinding to manage RCF crack is only a part of wider maintenance programme that deals with other factors, such as rail profile and corrugation. The specification of grinding targeted at one of these other factors might be the reason for the grinding to control RCF being carried out at an interval where the optimum depth is less than the grinding machine capacity. It should also be noted that the modelling has been carried out for one set of conditions, that is, of the data available, only the contact data for representative rail profile with averagely worn wheel profiles used to determine crack growth and wear in the modelling conducted. If profile maintenance was improved as a result of more frequent grinding, there could be a feedback loop, in that the better profiles reduces the crack driving forces and wear rates, this might have implications for the balance of predicted the wear or crack growth, the event of such changes, different profiles rail and wheel profiles could be chosen to represent the rail and traffic.

## **8.5 References**

- 8.1. Burstow M.C., Fletcher D.I., Franklin F.J., Kapoor A. (2008) Management and Understanding of Rolling Contact Fatigue: WP1 Mechanisms of Crack Initiation - Final Report.  
*[http://www.rssb.co.uk/SiteCollectionDocuments/pdf/reports/Research/T355\\_rpt\\_final\\_wp1.pdf](http://www.rssb.co.uk/SiteCollectionDocuments/pdf/reports/Research/T355_rpt_final_wp1.pdf)*
- 8.2. Network Rail October 2007 Strategic Business Plan Supporting document Asset management (2007)

## **Chapter 9. Conclusions and Further Work**

### **9.1 Conclusions from the Initial Stages of Developing the Grinding Model and Investigating the Effects of Different Grinding strategies on Crack Growth**

The first stage of the work described in this thesis was to adapt an existing model for predicting the growth of cracks in rails with traffic patterns of frequently changing train types to make it suitable for including the effects of occasional rail grinding operations. The aim of this modification was to allow the modified model, the Grinding Model, to be used to study the effects of different grinding strategies on the crack size. It was concluded that modifications of the pre-existing Crack Growth Model to create the Grinding Model overcame the limitations of the former which prevented it from being suitable for representing crack growth with traffic patterns of frequently changing train types with occasional rail grinding operations.

The second stage of the work involved the testing of the simplifying assumption made in the modelling process that the rail surface roughness produced by the grinding process did not last long enough, relative to the interval between grinding operations, to significantly affect the crack size predictions. The validity of this assumption was tested by conducting a test program using full scale railway equipment, in which rail samples of different grades (15mm long) were ground, installed in turn into a test site and a rail vehicle passed over them, the surface roughness of the samples being measured at intervals. It was found that the roughness values characteristic of grinding calculated from the longitudinal surface profiles, reduced sooner for the softer grade samples than the harder grade samples for the same number of wheels passing over them. It also appeared that the initial surface roughness caused by grinding was lower for the test samples of harder grade. The inference being that harder grades are more difficult for the grit of the grinding stone to dig into, so the roughness created is less, and they are less easily deformed by wheel contacts to reduce the roughness after grinding than the samples of softer grades. For all the grades of test samples, the roughness calculated from the longitudinal surface profiles was found to tend from the initial roughness characteristic of grinding at the start of the test, towards steady state values within the

100 wheel passes of the test program. This increased the confidence that the simplifying assumption made in the Grinding Model to ignore the effect of grinding roughness on crack growth is valid, considering that the grinding intervals are orders of magnitude larger than the number of wheel passes of the test program in which the roughness values tended towards steady state values.

The third stage of the work involved carrying out investigations with the Grinding Model to investigate the effect of different grinding strategies on the crack size trends of various vehicles and combinations of vehicles. In this process, an example optimum criteria was defined to assess the crack trends predicted for different grinding strategies. The aim of these optimum criteria was to specify a crack size trend which would represent the control of the predicted lengths of cracks within safe limits, whilst removing the least material from the rail. The optimum criteria used in at this and the next stage was that the initial crack should be predicted to be removed (i.e. the point at which the crack size becomes zero) within  $\pm 0.5\%$  of 3 million wheel passes for the grinding strategy to be considered an optimum grinding strategy. An investigative technique was developed for determining grinding strategies which produced a crack size trend which matched the optimum criteria. It was found that the crack size predictions for different vehicles and different combinations of vehicles were dominated by crack growth or wear to different extents for the initial crack size used, and therefore different grinding strategies were required to control crack size. It was also found that having established an optimum grinding strategy for one set of conditions, changing the conditions altered the predicted crack size trend. In the example conducted, the conditions were changed by reducing the wear produced by one of the vehicles in the traffic pattern, by replacing it with another vehicle which had a wear rate of 75% the original vehicle but was the same in all other respects. The effect of this change was to change the predicted crack size trend from one which matched the optimum criteria, to one which predicted the crack to grow to a size which could propagate to threaten the integrity of the rail.

The fourth stage of the work was to conduct a sensitivity analysis on the crack size predictions of the Grinding Model. Specifically the sensitivity of the predicted crack size trend for a traffic pattern and grinding strategy combination which matched the optimum criteria, to variations in the grinding strategy variables representative of errors in the application of the grinding strategy on a rail network. It was found that sensitivity of the crack size predictions to these variations in the grinding strategy was such that they were predicted to deviate from the optimum trend. In some cases the extent of this deviation from a trend which matched the optimum criteria, was such that the crack was predicted to grow to sizes which could threaten the integrity of the rail. Therefore it is suggested that the values of the grinding strategy variables specified at the point of application should be altered by at least the size of half the precision with which it would be expected to be applied from the optimum value. That is, for expected errors in the grinding strategy variables of +/-5%, the grinding depth specified should be 5% of the grinding machine's capacity more than the optimum value, and the grinding interval specified should be 5% less. An alternative would be to change the optimum criteria to one where the sensitivity of the predicted crack size trend to variations in the grinding strategy equivalent to the anticipated error in applying the grinding strategy, was such that the crack size trends were predicted to tend to zero with the worst combination of errors.

## **9.2 Conclusions from the Trends of Optimum Grinding Strategy Variable Combinations**

Optimum grinding strategy investigations have been carried out for a range of selected grinding depths to investigate and establish the trend in the values of pairs of grinding strategy variable the values of which form a combination that produce a predicted optimum crack size trend. The optimum criteria used in at this and the following stages was less precise than that used in previous stages, requiring that the initial crack should be predicted to be removed (i.e. the point at which the crack size becomes zero) within +/-5% of 3 million wheel passes for the grinding strategy to be considered an optimum grinding strategy. This was conducted with data input to the Grinding Model representing two locations and the Mixed traffic case. Taking into account the

experience gained with the sensitivity analysis, these investigations were carried out with the optimum specified to a lower level of precision.

With the trends of optimum grinding strategy variable combinations it was concluded that, for each location, each combination of grinding strategy variables which produced a trend which matched the optimum criteria formed an exclusive pair. That is that for a value of one of the variables, there was one "optimum" value of the other variable which made an optimum combination, and that the converse was true, that the value of the initial variable was the "optimum" value for the second variable. Therefore it was decided that the trends of optimum grinding strategy variable combinations were suitable for interpolation to give optimum grinding strategy variable combinations across the full range of useful values of the grinding variables, i.e. those values which might be considered for use in a grinding strategy. An equation was determined which described the trends of optimum grinding strategy variable combinations, with the different constants to fit the equation to the data for each location found. This equation was used subsequently as a repeatable method to interpolate between the data points of the trend to predict optimum grinding strategy variable combinations. Testing determined that this method of predicting optimum grinding strategy variable combination, successfully predicted the optimum values for investigations not used in establishing the trends.

It was also found that the trends of Effective Continuous Wear Rate (ECWR) corresponding to the optimum grinding strategy variable combinations appeared suitable for interpolation. This would enable the ECWR to be quickly found for the grinding strategies selected from the trends for analysis, which would be useful in predicting the life of the rail until the rails wear limit was reached, with the grinding strategies selected from the trends of optimum grinding strategy combinations. An equation with constants fitting it to the ECWR data for the two locations was found as a repeatable method to interpolate between the ECWR data points. Techniques for using these trends to specify combinations of grinding strategies within a maintenance section were developed and the issues surrounding the use of these techniques has been discussed with examples.



### **9.3 Conclusions from the Rail life Cost**

A method for estimating the cost of each kilometre of rail throughout its life for the amount of traffic carried, termed the rail life cost, has been developed. This rail life cost estimation method was applied to the example optimum grinding strategies and combinations of optimum grinding strategies determined from the trends of optimum grinding strategy variable combinations, and to example non-optimised grinding strategy combinations. Techniques for using the lowest estimation of rail life cost as an objective criterion for specifying combinations of grinding strategies within a maintenance section trends were developed and the issues surrounding the use of these techniques discussed with examples. Estimated average rail life costs for two hypothetical example maintenance sections made up of different proportions of the two locations modelled, were calculated for the grinding strategies combinations with optimum grinding strategies and the grinding strategies combinations with non-optimum grinding strategies. The average rail life cost estimated for the combinations of non-optimum grinding strategies was found to be 27% and 15% higher, than the average rail life cost estimate for the combinations of optimum grinding strategies which had the lowest rail life cost for that maintenance section.

In addition the estimated rail life cost for the optimum grinding strategy variable combinations at each location were found for a range of characteristic values of the optimum grinding strategy variable combinations (the grinding depth was selected as the characteristic value). These values were plotted and the general conclusions drawn from the trends of rail life cost were that the minimum rail life costs at each location which were close to the minimum were obtained when the optimised grinding strategy specified, required the grinding machine to operate at a grinding depth between one half of and the full grinding depth capacity of the machine, in a single grinding pass.

#### **9.4 Conclusions Derived from the Comparison of Grinding Strategies Developed using the Grinding Model and those of the UK Network Policy**

The grinding strategies developed and their estimated rail life cost were compared with those of the UK network grinding policy for the locations modelled, as well as to site observations relating to the performance of the networks grinding policy in controlling rolling contact fatigue (RCF) cracks at those locations. It was found that at both locations the grinding strategies determined using the Grinding Model specified more grinding than the network grinding policy. However at the first site there were RCF cracks were present indicating that more grinding than the network grinding policy was required, as predicted by the Grinding Model. At the other site there were no RCF cracks observed indicating that the national network grinding policy was adequate for controlling RCF cracks. Therefore for the second site the Grinding Model over specified grinding for this site and applying the grinding strategies determined using the Grinding Model would have wasted rail life and grinding resources. However RCF cracks were not predicted to initiate at this location and the Grinding Model does not have the ability to predict the initiation or occurrence of cracks of the initial size used in the modelling. Therefore predictions of crack initiation or experience should be used before applying grinding strategies determined using a model which assumes a certain crack size to exist. This means that the comparison of the predictions of the Grinding Model and the limited observations were inconclusive as to whether, if there had been initial cracks of the size assumed by the Grinding Model, these would have grown in spite of the network grinding programme as predicted by the Grinding Model.

With respect to the comparisons of the estimations of rail life cost it was found that in cases where RCF cracks were predicted to, and did, develop the estimated rail life cost of the grinding strategy determined from the Grinding Model could be lower depending on the actual rail life at the site before replacement would be required. That is if the grinding strategy determined from the Grinding Model would actually control the RCF cracks that developed if it were applied. Where RCF cracks were not predicted to, and did not, develop it was concluded that switching to the grinding strategy determined from the Grinding Model would waste rail life and increase rail life costs dramatically,

therefore it should be determined if RCF cracks would be expected to initiate before applying grinding strategy determined from the Grinding Model aimed at reducing rail life costs.

### **9.5 Conclusions Regarding the Suitability of the Grinding Model for Investigating Effects of Rail Grinding on Crack Growth and Specification of Railway Network Grinding Strategies**

The Grinding Model developed from the pre-existing model for predicting the growth of crack in rails has had one of its simplifying assumptions tests and has been compared against the real situations which it is intended to represent. From this work it appears that the Grinding Model is suitable for investigating the effects of rail grinding on crack growth, and that the result would be expected to have relevance to the real situations represented in the modelling. Also that it would be suitable for further investigations to understand how the relationships between the crack growth for various different conditions, such as traffic patterns, wheel and rail profiles, rail grades, and grinding techniques, affects the rail grinding required to meet a set of criteria.

The results of the modelling using the Grinding Model and their comparison with a limited number of real situations have shown that the Grinding Model predictions were not contradicted by the circumstances and observations at the real location where rolling contact fatigue (RCF) cracks are expected to initiate and develop. However at locations where RCF cracks are not expected to develop, the implicit assumption in the Grinding Model that cracks of a size up to the detection limit is flawed and its predictions for a crack of the initial size can't be verified. As a result of these factors the Grinding Model would not be suitable for the specification of grinding strategies to apply to a railway network in its current state of development. The suggested future developments required to make the Grinding Model suitable for the specification of grinding strategies to apply to a railway network are discussed in the next section.

The development of the rail life cost estimation method is intended as a useful tool to compare grinding strategies and objectively comment on their relative suitability.

However whilst the values have been calculated for the real situations modelled, they have not been compared against the real life cycle costs of rails as this information was not available, also it does not include all cost applicable to a rail life and grinding. Therefore it is useful as a guide to how different conditions and grinding strategies might affect rail life cost, and as an illustration of the use of a rail life cost estimation techniques for making judgements about the relative suitability of different grinding strategies.

## **9.6 Further Work**

There are perceived to be two major potential areas for further work involving the Grinding Model and the techniques for the use of its output. The first of these areas of work surrounds the use of the Grinding Model to investigate the effects of grinding on the crack growth predictions for different, rail, vehicle, and traffic conditions. The second is the development of the capability of the Grinding Model and its applicability to a railway network. In addition to these there is considered to be an additional potential area of work surrounding the measurement of grinding roughness. The discussion of each of these potential areas for further work has been divided into separate subsections; however, they are generally all interrelated. In particular, the implementation of the suggested further work related to the development of the grinding model, would enhance the scope of the investigations and the applicability of their results to a rail network. Also each of the individual conditions investigated could be investigated in conjunction with another condition. There is a general theme in that the investigations and model development could be targeted towards the finding of general cases which represent the behaviour of specific locations of a railway network. The aim would be that this would improve the suitability of the Grinding Model for informing and specifying the improvement of the use of grinding to manage RCF cracks.

### **9.6.1 *Investigations with the Grinding Model***

There are several potential topics surrounding use of the Grinding Model to investigate the effects of grinding on the crack growth predictions for different rail, vehicle, and

traffic conditions. The investigation of the effect of grinding on the crack size predictions for different traffic conditions could involve the modelling of both widely differing traffic conditions and similar traffic conditions. The modelling of widely differing conditions would give an understanding across a range of traffic conditions, and the modelling of similar traffic conditions would indicate how representative the predictions for one traffic pattern are of those for other similar patterns. This understanding of the effect of traffic patterns on the grinding requirement could be used in the specification of desirable vehicle properties and the prediction of the effect of a change in vehicles; it could also be used in the formation of general traffic cases for a route which would represent the traffic parts of the route.

The investigation of the effect of grinding on the crack size predictions for different locations would give an understanding across a range of locations, it would also be useful to investigate locations with a nominally similar characteristic such as curve radius, but that differ in a more subtle way such as the rail profile or the traction conditions, i.e. whether the traffic is rolling, applying traction driving forces or braking. Again one aim of this could be to characterise locations so that locations which would require similar grinding treatment for the same traffic case could be identified to simplify the study and specification of grinding at those locations.

The crack face friction parameter  $\mu$  is set at 0.18 throughout the work presented here, investigations could be carried out with different values, to examine the sensitivity of the crack growth and grinding requirement predictions to variations in crack face friction. Additionally investigations could be carried out by varying the crack face friction levels to represent changes in conditions, for example due to occasional rainfall penetrating and lubricating the crack face.

The effects of different rail grades on the grinding required to control crack size could be investigated, to better understand the whole life cost implications of each rail grade in a given situation. This could lead to the Grinding Model being part of the process of selecting rail grades for a location which have the nearest to ideal response to the

conditions, which in turn would have the lowest rail life cycle cost when combined with the grinding strategy to protect the rail from RFC cracks.

#### *9.6.2 Further Development of the Grinding Model*

The current Grinding Model is most suitable for predicting the growth of cracks across the size range of 1-10mm. Outside this range, other crack initiation and propagation mechanisms, which are not currently included in the model, start to exert a significant effect on crack size behaviour and the crack growth model on which the Grinding Model is based becomes progressively less accurate. The work has shown that an understanding of when RCF cracks are likely to occur is important when considering the appropriate grinding to apply. Also if the initiation and early stages of development of cracks can be modelled effectively, the same approach as has been applied to cracks of the initial size of 1.75mm which were assumed to exist could be applied to predicted cracks of a smaller size. The advantage of this is that the grinding strategies to control smaller cracks would be expected to require the removal of less material and have less impact on the wear life. This development would allow grinding strategies to be specified using the Grinding Model on the basis of preventing significant RCF cracks developing, rather than correcting ones that are assumed or observed to exist.

The improvement, development and verification of the rail life cost estimation technique applied would allow the various studies suggested to be targeted towards finding the most cost effective grinding strategy. It would also contribute towards fully understanding how all of the factors affecting the whole life cycle cost of the rail affect each other, including grinding.

As part of the process of developing and assessing the performance of the Grinding Model, modelling could be carried out for specific locations with characteristics of interest to the particular investigations. This would allow comparison of the Grinding Model outputs with the observations for the locations they are intended to represent. This in turn would place the conclusions of each investigation into context with regard to its accuracy in predicting both the relationship between the factors considered, and the

accuracy of the values predicted. This would also form part of the process of developing suitable factors of safety to use when using the output of the Grinding Model to specify grinding strategies to apply to a railway network.

### 9.6.3 *Further Grinding Roughness Testing*

It was concluded from the tests on grinding roughness conducted as part of this project, described in chapter 3, that the simplifying assumption to ignore the effect of grinding roughness on crack growth in the Grinding Model in its current state of development was valid. However if the grinding model was to be developed further, further work to provide a more detailed analysis of the persistence of grinding roughness, and consideration of its effects on the crack growth rate and wear rate might be appropriate. An incremental improvement to grinding roughness test procedure has been considered, the proposed improvements intended to reduce the scatter in the results from the experimental procedure and are described in appendix B. Additionally a step change to the grinding roughness test procedure could be carried out with larger test site with longer lengths of samples, 1m or more, installed. This would give wheel contact conditions more representative of continuous rail, avoiding the edge effects of samples, and allow a production grinding machine to be used.

## Appendix A. Rail Life Cost Estimate Calculation

Table A.1. Extract from spreadsheet used to calculate Rail Life Cost illustrating calculation for Grinding Strategy Combination (i) as an example.

<b>Grinding Strategy Parameters</b>			<b>Symbol</b>
Average Cost of a grinding operation (£/km)	700		<i>G</i>
Maximum reliably achievable single pass grinding depth (mm)	0.19		<i>M</i>
Rail Replacement Cost (£/km)	150000		<i>R</i>
Vertical Wear Limit of Rail (m)	0.014		<i>V</i>
<b>Location Type</b>	<b>Harringay</b>	<b>Sandy</b>	
<b>Grinding Strategy and Maintenance Section Variables</b>			
Effective Interval	196000	196000	<i>I<sub>i</sub></i>
Grinding Depth	0.09	0.19	<i>D<sub>i</sub></i>
Proportion of Location Type in Maintenance Section	0.5	0.5	<i>P<sub>i</sub></i>
WP/MGT For Traffic Pattern	93720	93720	<i>T</i>
<b>Calculation of Rail Replacement Cost for each MGT of traffic carried</b>			
	$W_w = cD + d$		
ECWR, Input Grinding Depth to Equation 3	2.215E-09	1.085E-09	<i>W<sub>w</sub></i>
	$W_T = W_w * T$		
Wear per MGT of traffic	0.0002076	0.0001017	<i>W<sub>T</sub></i>
	$L = V / W_w$		
Wear Life of Rail (MGT)	67.444881	137.63423	<i>L</i>
	$C_R = R / L$		
<b>Replacement Cost/kmMGT of Traffic (£/kmMGT)</b>	<b>£2,224</b>	<b>£1,090</b>	<i>C<sub>R</sub></i>
<b>Calculation of Cost of Grinding Strategy over the life of the rail for each MGT of traffic carried</b>			
	$I_T = I / T$		
Grinding Interval in MGT	2.0913359	2.0913359	<i>I<sub>T</sub></i>
	$N = \lfloor L / I_T \rfloor$		
No. Grind Ops/Life	32.249664	65.811634	
Round Down to Integer	32	65	<i>N</i>
	$O = (D * (G / (2 * M))) + (G / 2) * (1 + ((D / M) - 0.001))$		
Grinding Operation Cost (£/km)	515.78947	700	<i>O</i>
	$C_G = O N / L$		
<b>Grinding Strategy Cost over life of Rail (£/kmMGT)</b>	<b>£245</b>	<b>£331</b>	<i>C<sub>G</sub></i>
<b>Calculation of Total cost of rail over its lifetime for each MGT of traffic carried</b>			
	$C_L = C_R + C_G$		
<b>Rail Life Cost (£/kmMGT) (By location type)</b>	<b>£2,469</b>	<b>£1,420</b>	<i>C<sub>L</sub></i>
	$C_S = P_i C_{Li} + P_{i+1} C_{Li+1}$		
<b>Average Rail Life Cost for Maintenance Section (£/kmMGT)</b>	<b>£1,945</b>		<i>C<sub>S</sub></i>



## **Appendix B. Proposed Modifications to Grinding Roughness Test Procedure**

### **B.1 Introduction to Proposed Modifications to Grinding Roughness Test Procedure**

After the completion of the grinding test and analysis of the results, attention turned to the possibility of modifying the test method to improve the results. A fundamental change in the test method, such as installing several meters of each type of rail steel and using a process grinding machine, was not practical. However it was felt that with some modifications to a test site and the sample preparation procedure could achieve a reduction in the scatter of the results. This scatter is thought to be due to the lack of constraint of sample, and lack of consistency in sample preparation which could be achieved with the original test procedure. It was also felt that improving the accuracy and repeatability of test sample grinding would allow better comparison between the results for different test samples by reducing the influence of the grinding process on the results. The proposed alterations to the Grinding Roughness test method are described here; it was found that whilst alterations to a test site to improve the constraint of the sample would be feasible, it proved difficult to source the manufacture of the test samples to the required specification. Therefore it was decided not to proceed with a test program with the modifications to a test site alone, as it was felt that the aimed for reduction in the scatter of results due to the test method, would not be achieved and the improvement which might be attained did not justify proceeding with the tests.

### **B.2 Proposed Modifications to Test Procedure**

A different test site has been selected for the modified tests; this consists of a standard fishplated rail joint which had been formed by cutting a rail to allow different sections of rail to be inserted. It is proposed that the end of one of the rails of the joint has a small section cut from the end of it to increase the distance between the ends of the rails at the joint from the standard gap, to one which is just sufficient to have the test samples inserted. The new test site has more modern rails of larger cross section which is closer

to that of the test samples as provided by the manufacturer. Whilst the new test site rails are of a cross section which is closer to that of the test samples, they are heavily worn so that the test samples still require a portion of the underside of their head removing before being ground to a matching profile which slightly exceeds that of the test site rails. The ends of the rails at the new test site have experienced very little rail vehicle traffic since being cut to length, so the profiles of the rails leading up to the joint gap are uniform. They do not exhibit the downwards taper and the tongue of material projecting beyond the vertical end of the rail which are present in the original test site rails. These features of the original test site rails give them a "battered down" appearance and results from the running surface of these rails being plastically deformed towards the unsupported free surface at the ends of the rail by a very large number of rail vehicle contacts.

In addition to selecting a different joint for the test site, it was proposed to manufacture new special fishplates for the test site. These would feature extra holes, on the same axis as those for bolting the plates to the rails, but offset so as to be opposite the gap between rail ends. These extra holes would be threaded to allow screws to be used clamp test samples into position in the test site and restrict their movement. There would also be another hole in each plate below the clamping hole, with a recess to allow a transverse spacer to be installed and bolted into position across the lower portion of the rail gap. The design for the special fishplates, transverse spacer and test sample and the test site selected for the modified tests are shown in figures B.1 and B.2 respectively.

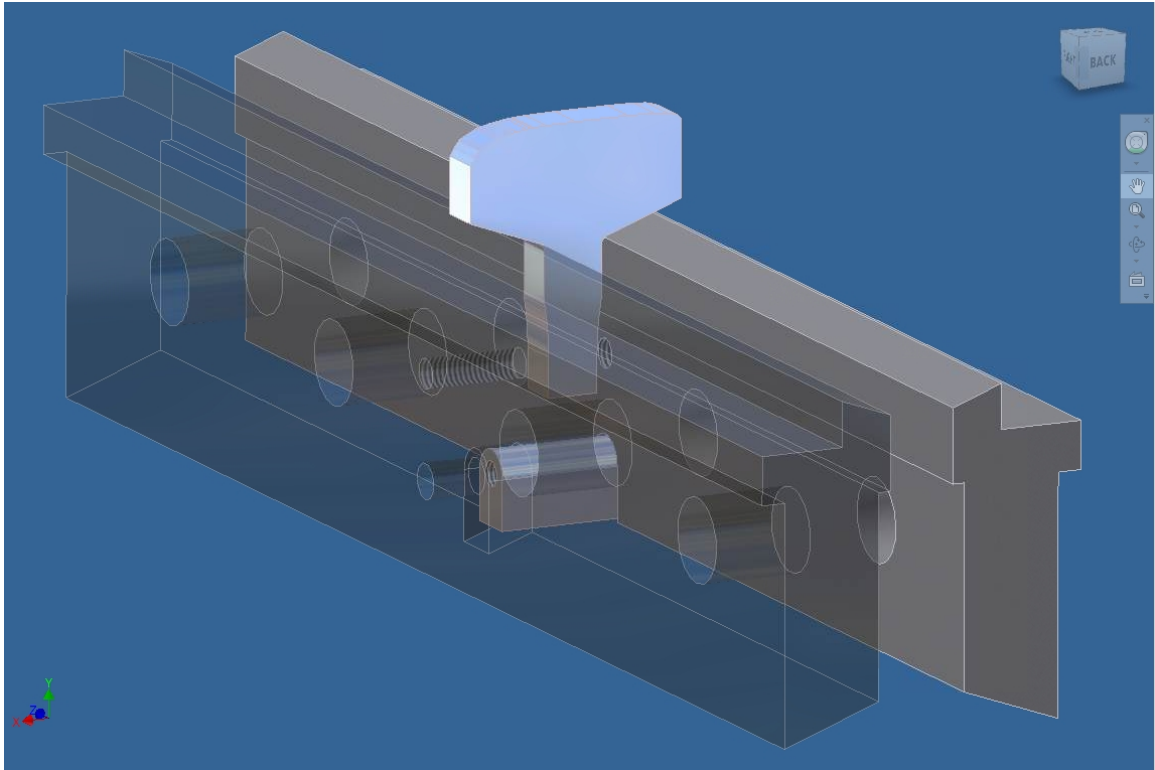


Figure B.1. CAD design for the special fishplates, transverse spacer and test sample shown assembled, the vertical web of the test site rail fits between the two plates.



Figure B.2. Photographs showing the side and end view of the standard fishplates at the selected test site selected for the modified test procedure, the square cut ends of the rail can be seen in the side view.

The change to a specially adapted test site fitted with specially designed fishplates was intended to have the following advantages over the original test procedure:

1. The clamping of tests samples would restrict their lateral movement ensuring consistent contact conditions both through each test and between tests, reducing the variation in the results attributable to variations in the contact position due to sample mounting.
2. The rail gap can be cut so as to be only 1mm longer than the test samples; this reduces both the potential for longitudinal movement of the test samples, and any tendency for the samples to rotate about a lateral axis, as they are loaded. The reduction of the potential of the sample to move about when installed in the test site makes the contact conditions more consistent throughout the test program, and more representative of longer lengths of rail.
3. The insertion of a transverse spacer maintains the rail gap and prevents the thermal expansion of the rails from closing the gap which in turn could prevent the installation of the sample on the test day. Therefore the advantages of having the sample closely constrained could be obtained, without the potential for the gap being too small to insert the test sample. This would be necessary since it would be impractical to ensure that site preparation and testing were carried out at the same rail temperature, or predict the rail temperature sufficiently accurately in advance.
4. The square cut rail ends means that it is possible to reduce amount by which the test sample profile exceeds the test site rail profile when installed. It is necessary that the test sample profile exceeds that of the test site, to ensure that the wheel of passing vehicles makes full contact with the sample, rather than bridging over it. The less the step between the test site and the test sample, the more representative the contact conditions on the measured portion of the test sample are of those on longer lengths of rail.

### **B.3 Proposed Test samples Specifications**

For the modified test method, as was the case for the original test method, the preparation of the test samples would be in two stages; these would consist of a machining stage and a grinding stage. The machining stage would be broadly similar to that carried out for the original test method, with detail differences in the dimensions to account for the different rail profiles of the test sites and the different amount of wear they have experienced. The rail of the site selected for the modified tests was manufactured to a cross section, which is more similar to that which the specimens from which the test samples would be manufactured from, than that the rail of the original test site. However the rail at the site for the modified test had been installed at a mainline

location for an extended period of time, before being removed from mainline service and installed in its current location, this means that it has experienced significant wear. As a result of this wear, there is a difference of several millimetres in the height of the rail head of the test site rail and the rail specimens. The majority of this difference in head height is removed by machining rather than grinding to reduce the amount of heat put into the test sample, grinding several millimetres would heat the specimens if not done gradually. Also machining the majority of the excess head height from the underside of the rail maintains the material properties at the surface of the test sample as near to their as rolled and heat treated state as possible, as only the depth of material necessary to produce the specified profile is removed from the surface.

The major difference in the preparation of the samples for the two test methods would be the method of grinding the test samples to the required profile, and thus also giving the surface of the test samples a ground surface finish required for the test. The modified method would use a CNC controlled grinding machine to form the profile on the running surface of the test sample. The specification would include the distribution of the grinding facets, which would be specified to represent those produced by a production grinding machine with a series of grinding stones set at different angles around the axis of the rail. This is as opposed to the first test method manual application of a series of passes of a single stone held at different angles by judgement. This resulted in an almost random distribution of grinding facets, sometimes several close together, at other times one facet forming a large portion of the profile, and this varied between samples. Also another advantage of using CNC grinding would be that the pressure with which the grinding stone is applied to the test sample would be the same between samples. Potential differences in the as ground surface roughness would therefore be a factor of the materials response to grinding, which would also be present with a production grinding machine (although the difference in response might not be the same), and not a factor of the variable pressure and order in which the operator made the grinding facets with the rail profile grinder.

Having the test samples manufactured so that the surfaces are uniform, including the grinding marks, would allow more direct comparisons between the roughness trends observed during the tests for each of the different materials. Specifically the increase in uniformity of the samples profile and grinding facet locations would mean that the initial roughness and contact conditions at each measurement location would be more similar for each sample. Therefore there could be greater confidence that any differences in the grinding roughness measurement trends between samples were due to the response of the material to contact with the vehicles wheels.

#### **B.4 Proposed Roughness Measurement Procedure Modifications**

The locating of the roughness measurement device at the designated measurement locations for the previous test method was done by eye against marks on the test site rail. This level of precision in the locating of the roughness measurements was considered appropriate when it was compared to the degree of restraint of the test samples and the repeatability of the grinding of the samples. This was because both the amount of possible transverse movement of the samples, and the difference in the grinding pattern between samples, means that it is difficult to justify making direct comparisons between the roughness measurements taken at the same location on each test sample, even if the measurement device was in exactly the same location relative to the test site, as the contact conditions would not be the same for each test sample. The increases in the constraint of the samples and the repeatability of the sample grinding process, expected of the modified test method, would make it feasible to take roughness measurements at equivalent locations on each test sample. That is the roughness measurements could be taken in the centre or on the boundary of specific grinding facets on each test sample, which will have experience similar contact conditions, and compare the grinding roughness results for each material directly

The more precise alignment of the roughness measurement device could be achieved either through aligning it with marks scribed onto the vertical faces of the test samples at the measurement locations, rather than the marker pen marks on the test site used in the initial test method, or indexing the measurement device support bracket to restrain the

device at specific locations. The former method is likely to be the more precise with respect to locating the track of the measurement device probe on the test sample. Allowance would still have to be made for uncontrollable variations, such as the transverse location of the wheel applying the loads and there will still be some variation between samples both in the location of the sample and the distribution of the grinding faces. However these variations between samples should be greatly reduced, making direct comparison of the results for the different materials more useful since it is more likely to be attributable to the way the ground material responds to rolling contact loading.

### **B.5 Issues Affecting Implementation of Modified Grinding Roughness Test Procedure**

The modifications to the test procedure having been decided upon, the test development moved on to the stage of sourcing the test samples and fishplates, also making the adaptations to a test site. Whilst it was found to be feasible to have the fishplates (including spacer piece) manufactured and to adapt a suitable test site which had been located, it proved difficult to have the grinding stage of the test sample preparation carried out to the specification. This was mainly due to the unusual nature of the work, outside that normally carried out by the grinding firms consulted, and the difference between the grades of grinding stone usually used in CNC grinding compared to those used on production grinding trains and rail profile grinders. The nearest grade of grinding stone that one firm could find from their usual suppliers, to fit their machine was a 40 grit stone, compared to the 16 and 20 grit stones commonly used for rail grinding. Both the unusual nature of the job and the requirement for non standard grinding stones resulted in all of the firms who were asked to provide a quote expressing little interest and none giving a firm quote. It was felt that, whilst obtaining quotes for the grinding of the samples could have been pursued further, given the lack of enthusiasm it would be doubtful whether the required specification could be matched at a reasonable cost. This lack of confidence in getting the test samples manufactured to the specification, made it difficult to justify risking committing to the expenditure required for the whole modified test program, while there was uncertainty about the test samples.

It was also felt that using the previous method of grinding the samples, with the other features of the modified test method, would not eliminate enough of the variations in the results, and thereby improve the results sufficiently, to justify the expenditure on a second test program. If there were additional pressures to conduct further tests, such as a requirement to test more specimens of rail or conduct multiple tests on samples from the same specimen, then it could be considered worthwhile proceeding with the modified test method, and use the grinding method from the original test method.